

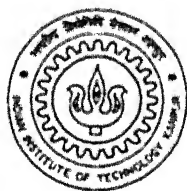
*AB INITIO* AND EXPERIMENTAL STUDIES IN  
 $\pi$ - FACIAL SELECTIVITY AND SYNTHESIS OF  
2,6-DIOXA-3-OXO-BICYCLO[3.3.0]OCTANES

A Thesis Submitted  
in Partial Fulfilment of the Requirements  
for the Degree of

DOCTOR OF PHILOSOPHY

*by*

D. A. JEYARAJ



*to the*

DEPARTMENT OF CHEMISTRY  
INDIAN INSTITUTE OF TECHNOLOGY KANPUR

April, 1998

20 JUL 1999/CAB

CENTRAL LIBRARY  
I. I. T., KANPUR

---

Inv. No. **A** 128580

TH  
20/12/95/5

3535





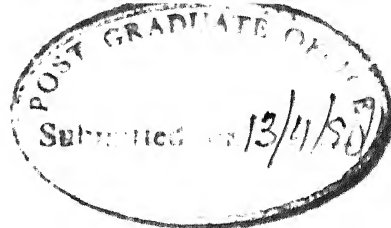
## STATEMENT

I hereby declare that the matter embodied in this thesis entitled "*AB INITIO* AND EXPERIMENTAL STUDIES IN  $\pi$ - FACIAL SELECTIVITY AND SYNTHESIS OF 2,6-DIOXA-3-OXO-BICYCLO[3.3.0]OCTANES", is the result of investigation carried out by me in the Department of Chemistry at Indian Institute of Technology Kanpur, India, under the supervision of Dr. Veejendra K. Yadav.

In keeping with the general practice of reporting scientific observations, due acknowledgement has been made wherever the work described is based on the finding of other investigations.

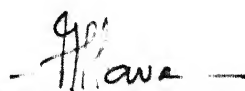
  
D. A. JEYARAJ

April, 1998



## CERTIFICATE - I

It is certified that the work contained in the thesis entitled "*AB INITIO* AND EXPERIMENTAL STUDIES IN  $\pi$ - FACIAL SELECTIVITY AND SYNTHESIS OF 2,6-DIOXA-3-OXO-BICYCLO[3.3.0]OCTANES", by D. A. Jeyaraj, has been carried out under my supervision and that this work has not been submitted elsewhere for a degree.

  
Dr. VEEJENDRA. K. YADAV  
Associate Professor  
Department of Chemistry  
I.I.T. Kanpur

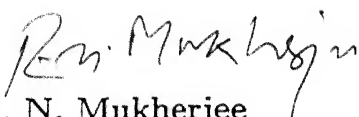
April, 1998

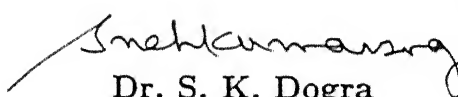
DEPARTMENT OF CHEMISTRY  
INDIAN INSTITUTE OF TECHNOLOGY KANPUR  
CERTIFICATE - II

This is to certify that Mr. D. A. Jeyaraj has satisfactorily completed all the courses required for the Ph. D. programme at our department. These courses include:

CHM605 Principles of Organic Chemistry  
CHM611 Physical Organic Chemistry  
CHM612 Frontiers in Organic Chemistry  
CHM625 Principles of Physical Chemistry  
CHM645 Principles of Inorganic Chemistry  
CHM664 Modern Physical Methods  
CHM800 General Seminar  
CHM801 Graduate Seminar  
CHM900 Ph. D. Thesis

Mr. D. A. Jeyaraj has successfully completed the written and oral qualifying examinations in September, 1994. He delivered his **State of Art** seminar in January, 1995.

  
Dr. R. N. Mukherjee  
Convenor, DPGC  
Department of Chemistry  
I.I.T. Kanpur

  
Dr. S. K. Dogra  
Professor and Head  
Department of Chemistry  
I.I.T. Kanpur

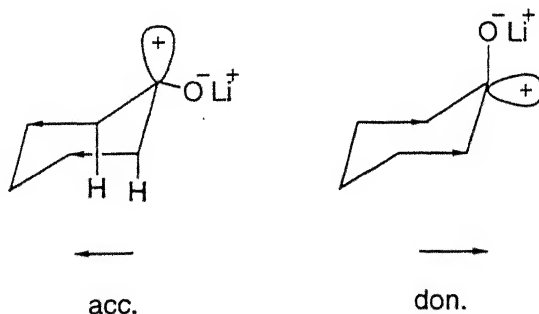
April, 1998.

## SYNOPSIS

$\pi$ -Facial diastereoselectivity in addition reactions to trigonal carbons, Diels-Alder additions, and sigmatropic shifts has been of great interest, both experimentally and theoretically, in recent years in the development of modern organic chemistry. How does a substituent, a hetero atom in particular, transmit its influence to the reaction site has been a subject of much controversy. As a consequence, several models have been proposed. The debate continues. We have ventured into this area and studied, both theoretically and experimentally, systems of substance. The present work is organized into three chapters as described below:

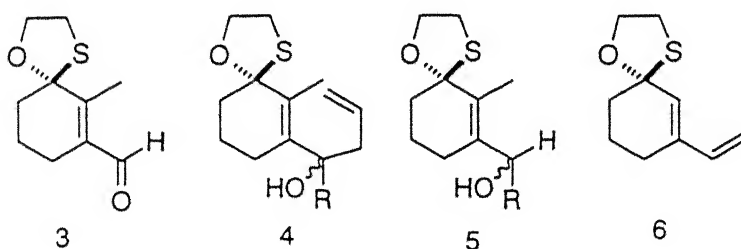
### Chapter 1:

In this chapter we describe a stereoelectronically supported *ab initio* model to explain the diastereofacial selectivity of additions to substituted cyclohexanones. This model is based on the premise that an attack by a nucleophile must generally be preceded by a complexation of a cation with the carbonyl oxygen and that this complexation must occur in the carbonyl  $\sigma$  plane. This complexation will reduce the carbonyl bond order and, hence, affect the torsional angles of its oxygen with the ring positions 3 and 5 in the process of the ensued pyramidalization at the carbonyl carbon. The resultant axial and equatorial orientations of the electron depleted  $p$  orbital on the carbonyl carbon will determine, in turn, the axial and equatorial preference, respectively, of a nucleophilic attack. The geometrical changes were calculated using *ab-initio* MO methods at HF/6-31G and HF/6-31G\* levels. Whether an increase or decrease in the said torsion angles on the axial face is explained by stereoelectronic effects. The electron poor  $p$  orbital on the carbonyl carbon must orient, respectively, antiperiplanar and orthogonal to an electron-donating and an electron-attracting  $\sigma$  bond on the adjacent carbon.



## Chapter 2:

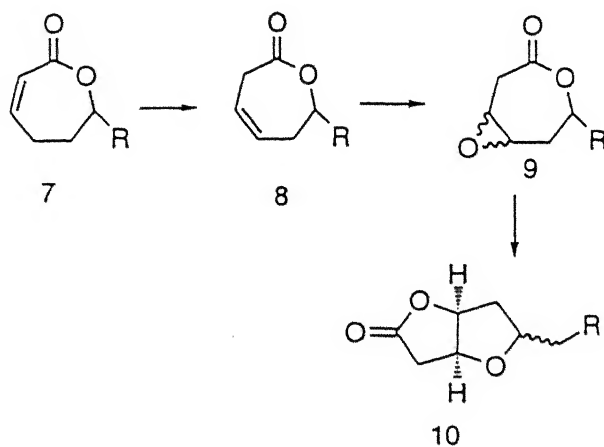
The study of diastereoface selection due to a strategically located heteroatom is of much current interest. It has been shown that a nucleophile attacks *syn* to an oxygen and *anti* to a sulfur; the heteroatom being placed on a carbon adjacent to the centre of nucleophilic attack. Our study has focused on substrates wherein both the oxygen and sulfur atoms are placed on a single carbon with fixed stereodispositions. In particular, we have studied the substrate **3** in reactions with nucleophiles, **4** (R=Ph, H) in oxy-Cope rearrangements, **5** (R=Ph, CH<sub>3</sub>, H) in orthoester Claisen rearrangement, and **6** in Diels-Alder additions. Whereas the reaction of **3** with sp<sup>3</sup> nucleophiles was only in marginal favour of attack *anti* to sulfur (thus violating the vinylogous effect proposed by Wipf), the reactions with sp<sup>2</sup> and sp nucleophiles exhibited relatively highly improved but reversed, *i.e.*, *syn* to S. facial selection. The sp<sup>2</sup>/sp hybridization state of the attacking nucleophile is deemed to play a role in a certain settled manner (at present not understood) to influence the diastereofacial selectivity. Substrates **4** and **5** undergo highly selective oxy-Cope and orthoester Claisen rearrangements, respectively. The observed results are interpreted by steric and electronic effects. The Diels-Alder additions of **5** with dienophiles such as N-phenylmaleimide, N-methyl triazolidinedione, and tetracyanoethylene are almost nonselective. These results are at variance from those reported in the literature. The relative stereochemical assignments were made from X-ray analysis and NMR spectroscopic data such as ROESY, NOESY, TOCSY, <sup>13</sup>C NMR and 1D nOe.



## Chapter 3:

4,5-Didehydro oxepanones **8** were considered precursors to the bicyclic lactones **10**. The stereochemistry of epoxidation of the  $\pi$  bond may be related to the stereochemistry of the R-bearing carbon and the conformational profile of these systems. Prior to our study, there was virtually no information available on the conformational behaviour of species like **8**. The isomerisation of **7** into **8** could not be achieved by several common traditional

methods. In this chapter, we describe the successful utilization of DBU and DBN to achieve this isomerisation, the diastereofacial selectivity of epoxidation of **8** ( $R=CH_3$ ,  $Bu^t$ ,  $CH_2Ph$ ,  $CH_2CH_2Ph$ ), and the transformation of **8** ( $R=CH_2Ph$ ) into a bicyclo[3.3.0] skeleton **10**. The stereochemical determination of epoxidation of the 4,5-didehydro oxepanones was made from an XRD analysis and ROESY of one of its bicyclic derivatives. During the study of isomerisation of the 3,4-didehydro-2-oxepanones **7** into the related 4,5-didehydro derivatives **8**, we have made a theoretically as well as experimentally interesting observation of equilibration between these two species. This equilibration was found dependent on the nature of the C7-substituent and occurred only when this was benzyl-like. Moreover, there was deuterium incorporation in the 7-ring substrates at positions 3 and 5 when the isomerizations were conducted in  $CDCl_3$ . We have conclusively proved the  $CDCl_3$  as the source of deuterium. The significance of the  $\pi$  bond in DBU in these isomerization is also demonstrated. The skeleton **10** is of much current significance as it is present in a class of natural products which exhibit diverse biological activities.



## ACKNOWLEDGEMENTS

It is a great opportunity for me to express my sincere indebtedness to my thesis supervisor, Prof. Veejendra Kumar Yadav, for his excellent guidance, immense help, and useful advices in both academic and personal lives. It was a real pleasure to work with him. His constant unfailing advices and critical comments throughout the programme made me learn the subject, especially synthetic and physical organic chemistry. His hard work inspired me to do research.

I am also grateful to Dr.(Mrs.) Arpita Yadav for her moral support and help.

I wish to express my gratitude to Dr. M. Parvez, Department of Chemistry, The University of Calgary, Canada, for his timely help in providing X-ray structures, which I needed the most for the structural and stereochemical evidence for the work described in this thesis.

Help by Mr. H.M. Gauniyal, CDRI, Lucknow and Dr. R. Yamdagni, Department of Chemistry, The University of Calgary, Canada, in recording 1D and 2D NMRs is gratefully acknowledged.

I am thankful to Prof. N. Sathyamurthy for providing me the Gaussian 94 software for my studies. I am very thankful to Prof. S. Manogaran for teaching me how to use the Gaussian 94 software. I am thankful to Professors V.K. Singh, J. Iqbal, Y.D. Vankar, S. Sarkar, T.K. Chandrasekar, P.K. Bharadwaj and A.J. Elias for allowing me to use their lab facilities.

I thank Professors P. Rajathirumani and P. Krishnan for their encouragement at graduate level which motivated me to take up higher studies.

I thank my labmates Dr. Kamal K. Kapoor, Mr. A. Sanyal, Ms. Joyti Yadav, Mr. G. Senthil, and Mr. R. Balamurugan for their understanding and help whenever I needed.

It is my pleasure to acknowledge all my friends, especially the core lab friends, for their timely help on many occasions.

Sincere thanks are due to Kuppi, Ravi, Puns, Vivek, Siva, Ponds, Sushil, Venkat, Srini, JP, Sudhir, Dilip, Kumaresh, Swadesh, Apurva and Debalina for their wonderful company which made my stay at IITK a memorable and enjoyable one. I thank my sister Simi for her help in the final stages.

I feel thankful to Kuppi, Ravi, Siva, Gomes, Dhanabal, Srini, Bala and Senthil for their help in thesis preparations.

Acknowledgement is also due to Mr Nayab Ahemad for recording IR and NMR spectra.

I am very thankful to computer center staff, IIT Kanpur for generous allocation of computer time on HP-9000 series mini supercomputers.

I am very much thankful to IIT, Kanpur for the financial assistance. Otherwise, my Ph.D. would have been only a life time dream.

I wish to pay my tribute to my parents and brothers for their understanding, encouragement and sacrifice. I am thankful for their encouraging words like "where there is a will, there is a way".

Finally I thank the one above all, The God, who has driven me from childhood. I am thankful to Him for directing me even in dreams and allowing me to finish smoothly.

D.A. Jeyaraj.



*DEDICATED  
TO  
MY PARENTS*

# Contents

## List of Tables

xiii

1	Face Selection of Nucleophilic Additions to Substituted Cyclohexanone. An <i>ab initio</i> study	1
1.1	Introduction	1
1.1.1	Face Selection in Acyclic System	2
1.1.2	Face Selection in Cyclic System	7
1.1.3	Face Selection of Nucleophilic Additions to 3- and 3,5-Heteroatoms Substituted Cyclohexanones	19
1.1.4	Face Selection of Nucleophilic Additions to 3-Substituted Cyclohex- anones	21
1.1.5	Face Selection of Nucleophilic Additions to 4-Substituted Cyclohex- anones	24
1.1.6	Face Selection of Nucleophilic Additions to 2-Substituted Cyclohex- anones	29
1.2	Present Work	33
1.2.1	Face Selection of Nucleophilic Additions to 3-oxa-, 3-thia- and 3,5- dioxo Substituted Cyclohexanones	34
1.2.2	Face Selection of Nucleophilic Reactions to 3-Substituted Cyclohex- anones	39
1.2.3	Face Selection of Nucleophilic Reactions to 4-Substituted Cyclohex- anones <b>119</b>	44
1.2.4	Face Selection of Nucleophilic Reactions to 2-Substituted Cyclohex- anones <b>127</b>	53
1.2.5	Acyclic system	60
1.2.6	Evidence	61

1.3	Conclusion . . . . .	66
1.4	Experimental . . . . .	67
	References . . . . .	69
2	<b>Allylic Substituted Hemithio Acetal in Face Selection: An Experimental Study</b>	<b>74</b>
2.1	Introduction . . . . .	74
2.1.1	1,2-Diastereoselectivity . . . . .	74
2.1.2	1,4-Diastereofacial Selectivity . . . . .	74
2.1.3	Sigmatropic Rearrangements . . . . .	80
2.2	Facial Selectivity in Diels-Alder Reactions . . . . .	81
2.3	Present Study . . . . .	89
2.3.1	Diastereofacial Selectivity of Nucleophilic Additions to 6-Methyl-1-oxa-4-thiaspiro[4.5]dec-6-en-7-carbaldehyde. . . . .	89
2.3.2	Orthoester Claisen Rearrangements of Substituted 6-Methyl-1-oxa-4-thiaspiro[4.5.]dec-6-en-7-carbinol. . . . .	103
2.3.3	Diels-Alder Reaction of 1-Oxa-4-thia-7-vinylspiro[4.5.]dec-6-ene . . .	110
2.3.4	Oxy-Cope Rearrangement . . . . .	113
2.4	Conclusion . . . . .	118
2.5	Experimental . . . . .	118
	References . . . . .	134
3	<b>Synthesis of 2,6-Dioxá-3-oxo-bicyclo[3.3.0]octanes</b>	<b>206</b>
3.1	Introduction . . . . .	206
3.2	Present Study . . . . .	210
3.2.1	Preparation of Starting Materials . . . . .	211
3.2.2	Reaction Monitoring . . . . .	213
3.2.3	Deconjugative Isomerization . . . . .	213
3.2.4	Deuterium Incorporation . . . . .	215
3.2.5	Significance of the Imine Double bond . . . . .	217
3.2.6	Attempted Deconjugation of systems other than the 7-ring lactones: A comparison . . . . .	218
3.2.7	Application to the synthesis of a pharmacophore . . . . .	220
3	Conclusion . . . . .	229
4	Experimental . . . . .	230

References . . . . .	243
----------------------	-----

# List of Tables

1.1	Percentage of <i>syn</i> and <i>anti</i> addition to <b>27</b> . . . . .	11
1.2	Product ratios in NaBH <sub>4</sub> reduction of <b>34</b> . . . . .	12
1.3	Percentage of <i>syn</i> <b>39</b> and <i>anti</i> <b>38</b> addition to <b>37</b> . . . . .	13
1.4	Comparisons of experimental and calculated isomers ratios of ketones <b>40-46</b>	15
1.5	Percentage of axial:equatorial addition to <b>45</b> and <b>49</b> . . . . .	20
1.6	Percentage of axial attack in nucleophilic additions to <b>52</b> . . . . .	22
1.7	Percentage of product formed on reduction to <b>55</b> . . . . .	23
1.8	Percentage of ax and eq attack from NaBH <sub>4</sub> reduction of <b>60</b> abd <b>61</b> . . . .	25
1.9	Product ratios in NaBH <sub>4</sub> reduction of <b>62</b> . . . . .	27
1.10	Percentage of ax and eq attack of hydride to <b>72</b> and <b>73</b> . . . . .	31
1.11	Facial selectivity in nucleophilic addition to <b>80</b> and <b>81</b> . . . . .	32
1.12	Angles and Torsion angles in <b>84-89</b> . . . . .	35
1.13	Angles and Torsion angles in <b>90</b> and <b>91</b> . . . . .	36
1.14	Angles and Torsion angles in <b>92-96</b> . . . . .	38
1.15	Angles and Torsion angles in <b>97-101</b> . . . . .	40
1.16	Angles and Torsion angles in <b>102- 106</b> . . . . .	40
1.17	Angles and Torsion angles in <b>107-111</b> . . . . .	41
1.18	Angles and Torsion angles in <b>112-116</b> . . . . .	42
1.19	Angles and Torsion angles in <b>117</b> . . . . .	45
1.20	Net Mulliken atomic charges on selected atoms in <b>117</b> . . . . .	48
1.21	Bond lengths in <b>117</b> . . . . .	52
1.22	Angles and Torsion Angles in <b>125</b> . . . . .	55
1.23	Net atomic charges in <b>125</b> . . . . .	58
1.24	$\pi$ -Facial selectivity of <b>129</b> . . . . .	62
1.25	Product Distribution from the hydrochlorination of <b>132<sup>a</sup></b> . . . . .	63
1.26	Product Distribution from the hydrofluorination of <b>132<sup>a</sup></b> . . . . .	64
1.27	Product Distribution from the Reduction of <b>138<sup>a</sup></b> . . . . .	65

2.1	Nucleophilic additions to <b>15-17</b> . . . . .	78
2.2	Reduction of <b>21</b> . . . . .	79
2.3	Diels-Alder additions to <b>30</b> . . . . .	82
2.4	Diels-Alder additions to <b>33</b> . . . . .	84
2.5	Copper(I) catalyzed conjugate addition of RMgX to <b>50</b> . . . . .	86
2.6	Diels-Alder additions to <b>56</b> and <b>59</b> . . . . .	88
2.7	Crystal data . . . . .	94
2.8	Nucleophilic additions to 6-methyl-1-oxa-4-thiaspiro[4.5]dec-6-en-7-carbaldehyde <b>66</b> and ketone <b>67</b> . . . . .	96
2.9	Selected $^1\text{H}$ and $^{13}\text{C}$ chemical shifts in the products <b>82</b> , <b>84</b> and <b>86</b> . . . .	108
2.10	Oxy-Cope rearrangement of alcohls <b>70-72</b> . . . . .	115
3.1	Deconjugative isomerization of the 7-ring lactones . . . . .	214
3.2	Epoxidation of 7-substituted-4,5-dehydro-2-oxepanones <b>15</b> . . . . .	221

# Chapter 1

## Face Selection of Nucleophilic Additions to Substituted Cyclohexanone. An *ab initio* study

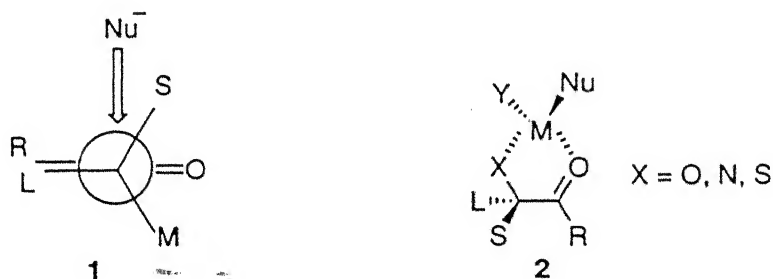
### 1.1 Introduction

Addition of nucleophiles to carbonyl compounds is one of the most common methods to generate a new C-C bond in organic synthesis. On the trigonal carbon, e.g. in ketones, there are two faces from where a nucleophile can attack. It is known that one can make the two faces electronically different by introducing a group or a chiral center in the molecule. Such a facial differentiation may also be possible due to specific ring geometry of a substrate. From such a differentiation of the two faces, one can achieve a face-favored product. It is a matter of great interest to be able to explain how substituents transmit their influence to the reaction site. Consequent to this, numerous theoretical models have been proposed<sup>1-24</sup> to help understand the stereochemistry of the addition to substituted carbonyls. We present below first an account of some of the prominent theoretical models and then discuss a new approach to the prediction of diastereoselectivity in substituted cyclohexanones.

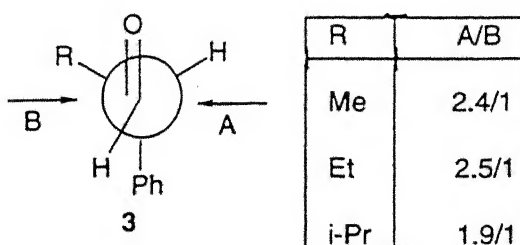
### 1.1.1 Face Selection in Acyclic System

#### Cram model

In 1952, Cram<sup>2</sup> was the first to propose a model to explain the stereoselectivity observed in acyclic systems. Accordingly, the carbonyl is flanked by the two least bulky groups and the nucleophile attacks from *syn* to the smallest substituent as shown in 1. When an oxygen, nitrogen, or sulfur is attached to the carbon  $\alpha$  to the carbonyl, the metal of the hydride can coordinate to both the heteroatom and the carbonyl oxygen, and the nucleophile delivered from the less hindered face as shown in 2. This model which predicts the correct diastereoselectivity is more commonly called 'Cram chelation model'.



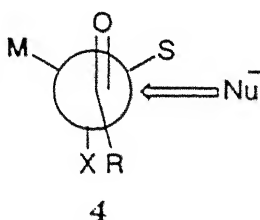
The Cram open chain model failed to predict the correct diastereoselectivity for many acyclic molecules that contain heteroatom substituents.<sup>4, 5</sup> This model also failed to predict the correct diastereomer when the difference of the steric bulk between S and M was not much. For example, the diastereomeric product ratio A/B as in 3 decreased with R varying from methyl to isopropyl as if the effective size of the isopropyl was smaller than that of methyl.





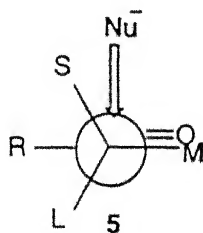
## Conforth model

When the  $\alpha$  substituent is a halogen, neither the open chain model nor the chelation model predicts the correct results. So, Conforth<sup>25</sup> described a model to explain the facial selectivity of  $\alpha$ -halo carbonyl materials. The carbonyl and the chlorine point *anti* as in **4** to avoid the unwanted dipolar interactions and the nucleophile attacks *syn* to the smaller of the remaining two substituents.



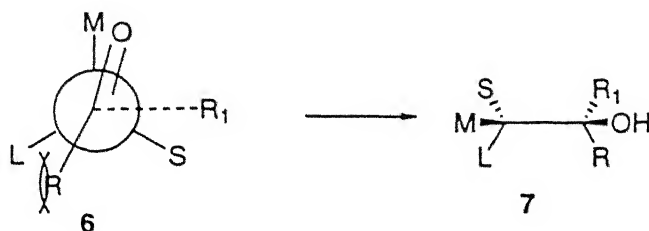
## Karabatsos model

In 1967, Karabatsos<sup>4</sup> modified Cram's model. The carbonyl is eclipsed with the medium sized substituent and the attack of the nucleophile is from *syn* to the smallest group as in **5**.

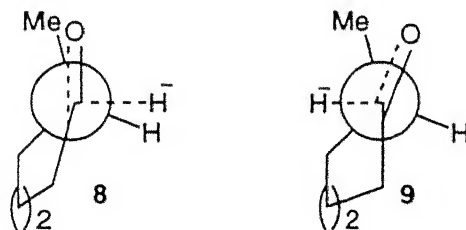


This model did not adequately explain the problems when R was large or when applied to cyclic molecules.<sup>5</sup> For example, the bulkier the R in **5**, the less stereoselective the reaction should be for its steric interactions with the substituent L as shown in **6**. However, experimentally observed results were opposite. For example, for L=Ph, M=Me and S=H, the diastereoselectivity increased from 2.8:1 to 3.2:1, 5:1 and 49:1 when R was changed

from Me to Et,  $\text{Pr}^i$ , and  $\text{Bu}^t$ , respectively. When R was  $\text{Bu}^t$  **7** was formed as the major product.

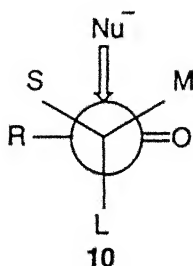


Also, the reduction of 2-methylcyclohexanone led preferentially to *trans*-2-methylcyclohexanol through the TS **9** whereas it would have been expected to lead preferentially to the *cis* isomer by Karabatsos model through the TS **8**.



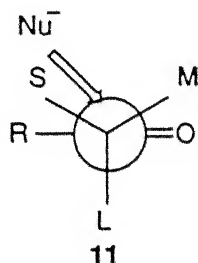
## Felkin model

Since both the Cram model and its Karabatsos modification could not account for the effect of varying the size of the R group, Felkin<sup>5</sup> modified it further to consider the flanking of the carbonyl by the medium and the large substituents. The nucleophile attacks from the direction *syn* to the small substituent as shown in **10**.



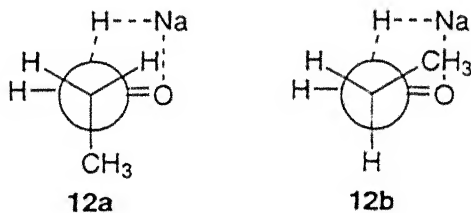
## Anh model

Anh modified the Felkin model further. Anh *et al.*'s<sup>6, 26, 27</sup> *ab initio* calculations of transition state energies for nucleophilic attacks on the carbonyl group supported the Felkin model. However, the reason for this preference is the favorable consequence of achieving antiperiplanarity between the new bond being formed and a bond present on the carbon  $\alpha$  to the carbonyl group. The attack of the nucleophile is at Burgi-Dunitz angle<sup>28</sup> as shown in 11. Felkin model coupled with the Anh model is now referred to as Felkin-Anh model.



## Houk model

Houk's<sup>29</sup> calculation supports the Felkin-Anh model. Large group takes the sterically least hindered position.



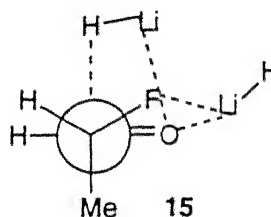
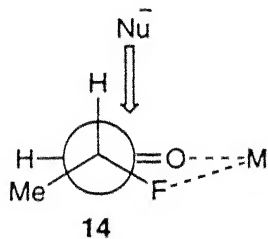
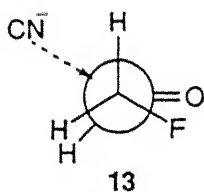
Calculation of transition state structures for the addition of NaH to propanaldehyde showed that the transition state **12a** was disfavored over the transition state **12b** since the C-CH<sub>3</sub> bond is antiperiplanar (app) to the incoming nucleophile in **12a** which destabilizes

it. In **12b** the nucleophile adds *anti* to the less electron donor C-H bond, which stabilizes it. The two assumptions made in the development of this model were

- a) the TS is electron rich, and
- b) a C-H bond is less electron-donating than a C-CH<sub>3</sub> bond.

## Paddon-Row model

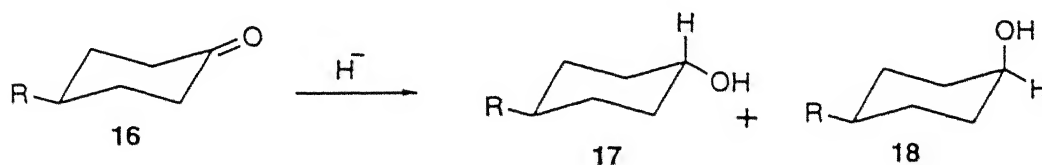
In support of Houk's above TS model, Paddon-Row and coworkers<sup>30</sup> have computed the nucleophile to attack *app* to the more electron withdrawing group on the  $\alpha$  carbon. The lowest energy TS structure for the CN<sup>-</sup> attack on 2-fluoroacetaldehyde is shown in **13**. In the preferred ground state conformer, the C=O was to eclipse the C-F bond. The C=O was, however, orthogonal to one of the two C-H bonds.



Natural population analysis showed larger charge transfer from the cyanide to the aldehyde so that the attack is *anti* to the electron withdrawing group. Gas phase calculation of transition state structure for the addition of LiH to 2-fluoropropanaldehyde has shown that there could as well be some electrostatic interaction between the fluorine and lithium as shown in **14** and **15**.

### 1.1.2 Face selection in cyclic system

Addition of nucleophiles, specifically hydride ion, to cyclohexanones and bicyclic ketones has been studied extensively. The theoretical basis for the stereochemical outcome in the irreversible addition to the conformationally locked cyclohexanones has been controversial for a long time. There appears to be an intrinsic preference for nucleophiles with relatively small bulk to approach from the axial face<sup>31, 32</sup> which is sterically more hindered in cyclohexanones **16** than the alternate equatorial face.

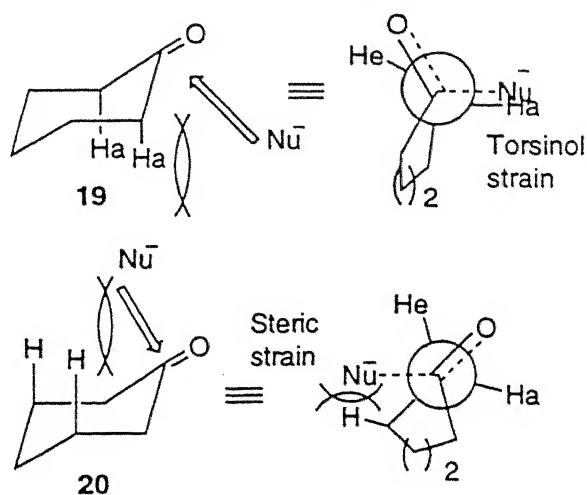


The facial selectivity in additions to cyclohexanones depends on various factors such as (i) the nature of the reagent, (ii) the nature, location, and orientation of the substituent, and (iii) the reaction conditions.

This topic has been reviewed many a times.<sup>14, 24, 31, 33, 34</sup> A short account of the often used models for the rationalization of the observed diastereoselectivities is given below.

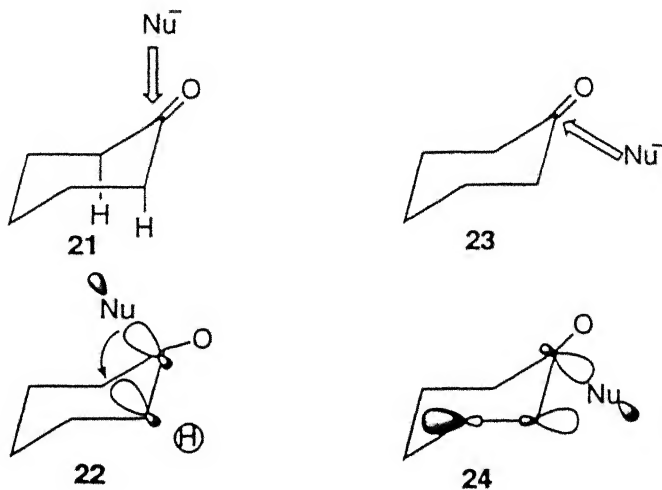
#### Felkin model

According to Felkin,<sup>5</sup> the formation of the axial alcohol emanating from an equatorial attack involves a partially eclipsed TS with some degree of torsional strain as shown in **19**. On the contrary, the formation of an equatorial alcohol from an axial attack involves an essentially staggered TS with some degree of steric strain as shown in **20**. In consideration of the the above torsional factor, Felkin suggested the nucleophilic reactions of cyclohexanones to proceed via reactant-like transition states. The steric outcome is determined by the relative magnitudes of torsional strain in the transition states.



## Anh model

The calculation of transition state energies for nucleophilic attacks on a carbonyl group by Anh<sup>26, 27</sup> *et al.* supported Felkin model for cyclohexanone systems. In cyclohexanones, C2 and C6 axial hydrogens are antiperiplanar to the incoming nucleophile as shown in structures 21 and 22 if the attack is on the axial face. Since this antiperiplanarity is not possible in the alternate equatorial attack as shown in structures 23 and 24, this mode is not favored.



## Klein model

Klein<sup>8, 9</sup> reported a new hypothesis concerning the stereoselectivity of alkylation and hydride reduction of cyclohexanones. For the interaction of the C2-C3  $\sigma$  bond with the  $\pi$ -orbital, two bonding and two antibonding orbitals develop. Of the bonding orbitals, the HOMO has larger coefficient on the equatorial face whereas the LUMO has larger coefficient on the axial face. Consequent to this, the molecule must react with electrophiles and nucleophiles on the equatorial and axial face, respectively. However, electrophiles are reported to attack axial.<sup>35, 36</sup>

## Cieplak model

According to Cieplak,<sup>17</sup> the stereochemistry of nucleophilic addition to cyclohexanone is determined by two factors: (i) steric hindrance which favors the equatorial approach, and (ii) electron donation from the vicinal C-C and C-H  $\sigma$  bonds into the  $\sigma^*$  orbital of the bond being formed. This favors the axial approach since the axial C-H bond is better electron donor than the C2-C3  $\sigma$  bond. The order of the donor abilities of common atom combinations are C-S > C-H > C-C > C-N > C-O.



Cieplak postulated that the above  $\sigma$ - $\sigma^*$  interaction is the dominant conjugative interaction in the bond forming process because the incipient bond is intrinsically electron deficient. The incipient bond is to be considered as a very stretched and polarized covalent bond that is stabilized by strong coulombic interactions.

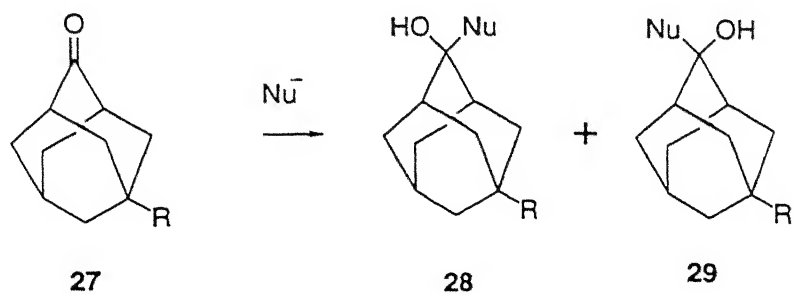
The axial approach is preferred in the hydride reduction of 4-Bu<sup>t</sup>-cyclohexanone because the stabilization energy arising from electron donation from the axial C2-H and C6-H (25) bonds to the incipient  $\sigma^*$  orbital is greater than the stabilization energy arising from the corresponding interaction with the C2-C3 and C5-C6  $\sigma$  bonds (26) which would occur in the equatorial approach of the hydride.

Cieplak model has numerous consequences which can be clearly spelled out and readily verified. For instance, a variation in the electron donating power of the cyclohexanone  $\sigma$ -bonds must result in a corresponding change in diastereoselectivity. Likewise, a variation in the transition state electron affinity must also result in a corresponding change in the diastereoselectivity of the reaction. Thus, substitution of the nucleophile by electron attracting atoms or groups must favor axial attack. Conversely, electron donating substituents on the nucleophile will be expected to favor equatorial attack.

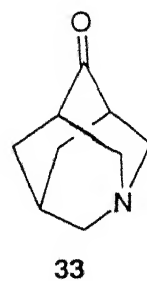
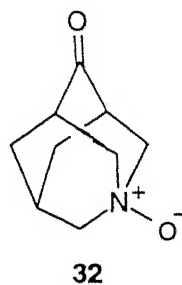
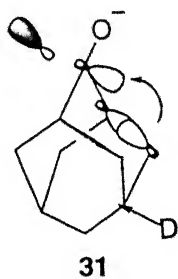
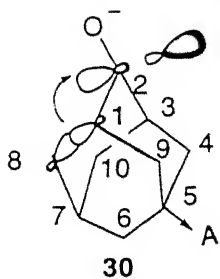
This theory has received wide acceptance as it has served to explain a large number of experimental observations. le Noble *et al.*<sup>37-59</sup> designed substituted adamantanones 27, 32, and 33 as probes to study the Cieplak effect. These adamantanones are sterically unbiased and rigid systems. The C1-C9 and C3-C4 bonds are rendered somewhat electron-deficient because of their antiperiplanarity with the C5-A bond (30). This leaves the C1-C8 and C3-C10 bonds as better electron donating and, hence, an attack *anti* to C8 and C10, as shown in 30, must be favored to give products having the general structure 28. A similar argument for adamantanones bearing an electron donating substituent D (31) will favor an attack *anti* to C4 and C9 and, hence, 29 must predominate.

The results of both nucleophilic and electrophilic additions were in full agreement with the Cieplak theory. The results of some nucleophilic additions are collected in the Table 1.1.



Table 1.1: Percentage of *syn* and *anti* addition to **27**

R	Nucleophile	Condition	% <b>28</b>	% <b>29</b>
C <sub>6</sub> H <sub>5</sub>	LiAlH <sub>4</sub>	Et <sub>2</sub> O, rt	56	44
C <sub>6</sub> H <sub>5</sub>	LiAl(OBu <sup>t</sup> ) <sub>3</sub> H	Et <sub>2</sub> O, rt	49	51
Bu <sup>t</sup>	LiAlH <sub>4</sub>	Et <sub>2</sub> O, rt	50	50
Bu <sup>t</sup>	LiAl(OBu <sup>t</sup> ) <sub>3</sub> H	Et <sub>2</sub> O, rt	42	58
<i>p</i> -C <sub>6</sub> H <sub>4</sub> NO <sub>2</sub>	NaBH <sub>4</sub>	Me <sub>2</sub> CHOH, rt	65	35
<i>p</i> -C <sub>6</sub> H <sub>4</sub> Cl	NaBH <sub>4</sub>	Me <sub>2</sub> CHOH, rt	60	40
C <sub>6</sub> H <sub>5</sub>	NaBH <sub>4</sub>	Me <sub>2</sub> CHOH, rt	58	42
<i>p</i> -C <sub>6</sub> H <sub>4</sub> OMe	NaBH <sub>4</sub>	Me <sub>2</sub> CHOH, rt	48	52
<i>p</i> -C <sub>6</sub> H <sub>4</sub> OH	NaBH <sub>4</sub>	Me <sub>2</sub> CHOH, rt	44	56
F	NaBH <sub>4</sub>	Me <sub>2</sub> CHOH, rt	62	38
Cl	NaBH <sub>4</sub>	Me <sub>2</sub> CHOH, rt	59	41
Br	NaBH <sub>4</sub>	MeOH, 0°C	59	41
F	MeLi	Et <sub>2</sub> O, 0°C	70	30
OH	NaBH <sub>4</sub>	MeOH, 0°C	57	43
CF <sub>3</sub>	NaBH <sub>4</sub>	Me <sub>2</sub> CHOH, 0°C	59	41
CF <sub>3</sub>	MeLi	Et <sub>2</sub> O, 0°C	72	28



Reduction of **32** gave good *syn* selectivity (96%). This high selectivity was viewed as an excellent example of the Cieplak model. The addition of MeLi to **33** gave a mild excess of *anti* addition. It seemed conceivable that the electron pair on nitrogen might interact with the C1-C9 and C3-C4 bonds so as to promote their donor abilities. NaBH<sub>4</sub> reduction in MeOH produced an excess of the *syn* addition. A hydrogen-bonded amine center is possibly responsible for this unprecedented reversal of stereochemistry.

Halterman and McEvoy<sup>36, 60</sup> studied the NaBH<sub>4</sub> reduction of 2,2-diarylcyclopentanones **34**. The results are collected in the Table 1.2. When X is electron-donating, the reduction is from *anti* to the substituted aryl and the product **35** predominates. When X is electron-withdrawing the selectivity is reversed and the product **36** is formed in major amounts. According to these researchers, the diastereoselective reduction of these 2,2-diarylcyclopentanones provides strong evidence for the involvement of stereoelectronic control in carbonyl reduction as proposed by Cieplak.

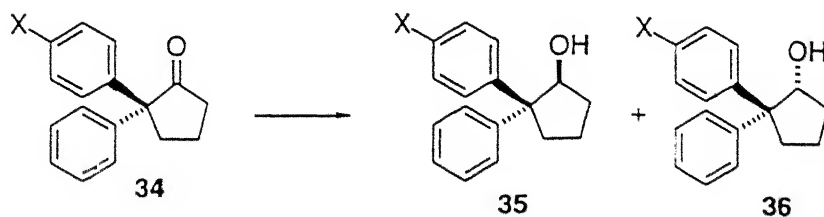


Table 1.2: Product ratios in NaBH<sub>4</sub> reduction of **34**

X	% <b>35</b>	% <b>36</b>
NO <sub>2</sub>	21	79
Cl	37	63
Br	37	63
H	50	50
OMe	57	43
O	70	30
NH <sub>2</sub>	64	36

Mehta and coworkers<sup>61-66</sup> have studied reactions of 2,3-disubstituted-7-norbornanones

37. The observed diastereoselectivities are given in the Table 1.3. As it can be easily seen, all but the species with methoxymethyl and vinyl substituents obeyed the Cieplak model. In a joint publication,<sup>67</sup> Mehta and le Noble deplored further the roles of methoxymethyl and vinyl and concluded that the conformational freedom of these substituents were responsible for the observed anamoly.

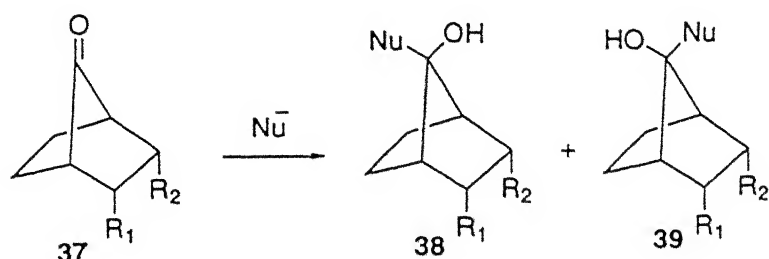


Table 1.3: Percentage of *syn* 39 and *anti* 38 addition to 37

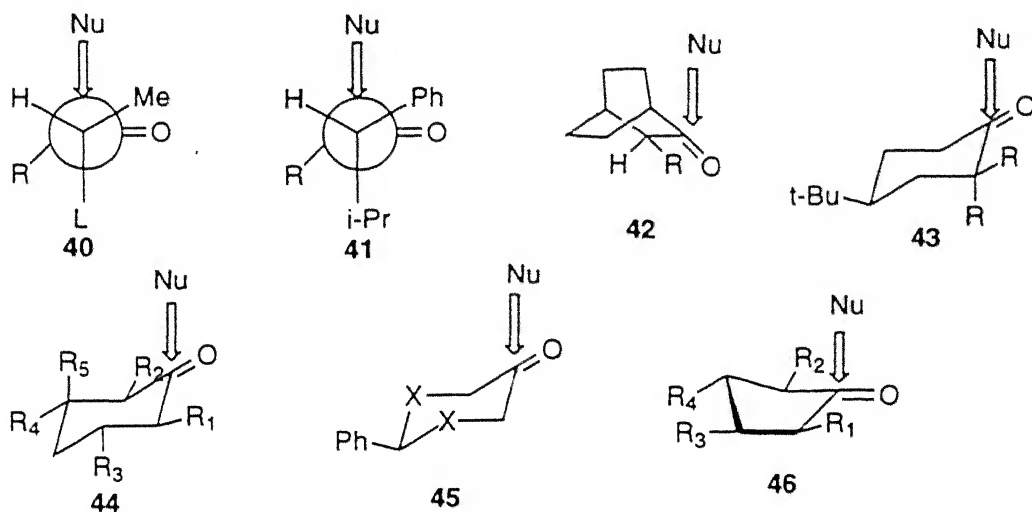
substituent	NaBH <sub>4</sub>	LiAlH <sub>4</sub>	(Bu <sup>t</sup> O) <sub>3</sub> LiAlH	MeLi
R1=R2=CO <sub>2</sub> Me	84:16	87:13	77:23	> 90 : < 10
R1=R2=CH <sub>2</sub> OMe	40:60			34:66
R1=R2=vinyl	36:64	35:65	34:66	27:73
R1=vinyl, R2=ethyl	25:75			
R1=R2=ethyl	20:80	21:79	29:71	17:83

Instead of great success with a very large number of experimental examples, the Cieplak model has failed to interpret several other instances.<sup>34, 68-70</sup> These will be discussed in the following sections.

## Houk model

In 1982, Houk<sup>29</sup> supported the Felkin model for the acyclic and cyclic carbonyl compounds. Transition structures for nucleophilic reactions were calculated by *ab initio* methods using

3-21G and 6-31G\* basis sets. In cyclohexanone, transition structure for axial attack is favored over the one for equatorial attack. This was explained by the torsional strain in the transition structure for equatorial attack. However, the axial attack can be achieved without any significant ring strain. Accordingly, the reduction of 4-substituted cyclohexanones produced the equatorial alcohol. Houk has quantified the selectivity as shown in the Table 1.4. The correspondence with the experimental values is good to excellent for the species 40-46.



## Frenking model

Frenking and coworkers<sup>20</sup> have considered the Cieplak explanation for the reduction of cyclohexanones based on rather "paradoxical assumption" and even "dubious" for FMO reasons. In nucleophilic reactions, there should be some orbital interaction between the reagent and the carbonyl carbon. Calculation of the TS structures for axial and equatorial addition of LiH to cyclohexanone was performed by *ab initio* quantum chemical methods.

The relative energies without LiH but with frozen geometry of the substrate showed that the energy difference is very small, even favoring slightly the equatorial attack. This is

Table 1.4: Comparisons of experimental and calculated isomers ratios of ketones 40-46

Compound	substituents	Reagent	Expt.	Calc.
40a	L=C <sub>6</sub> H <sub>11</sub> , R=Me	LAH	62:38	69:31
40b	L=C <sub>6</sub> H <sub>11</sub> , R=Et	LAH	67:33	72:28
40c	L=C <sub>6</sub> H <sub>11</sub> , R=Pr <sup>i</sup>	LAH	80:20	79:21
40d	L=C <sub>6</sub> H <sub>11</sub> , R=Bu <sup>t</sup>	LAH	62:38	80:20
40e	L=Ph, R=Me	LAH	74:26	60:40
40f	L=Ph, R=Et	LAH	76:24	67:33
40g	L=Ph, R=Pr <sup>i</sup>	LAH	87:13	79:21
40h	L=Ph, R=Bu <sup>t</sup>	LAH	98:2	94:6
41a	R=Me	LAH	97:3	93:7
41b	R=H	MeMgBr	45:55	36:64
43a	R=Me	LAH	50:50	35:65
43b	R=Et	LAH	68:32	46:54
43c	R=Pr <sup>i</sup>	LAH	72:28	58:42
43d	R=Bu <sup>t</sup>	LAH	15:85	30:70
43e	R=Ph	LAH	5:95	7:93
44a	R=H	LAH	88-91:12-9	88:12
44b	R=Me	LAH	95:5	90:10
44a	R <sub>1</sub> =Me, R <sub>2</sub> =R <sub>3</sub> =R <sub>4</sub> =R <sub>5</sub> =H	LAH	60-82:40-18	82:18
44b	R <sub>1</sub> =R <sub>2</sub> =Me, R <sub>3</sub> =R <sub>4</sub> =R <sub>5</sub> =H	LAH	62:38	73:27
44c	R <sub>3</sub> =Me, R <sub>1</sub> =R <sub>2</sub> =R <sub>4</sub> =R <sub>5</sub> =H	LAH	84-87:16-13	88:12
44d	R <sub>3</sub> =R <sub>4</sub> =R <sub>5</sub> =Me, R <sub>1</sub> =R <sub>2</sub> =H	LAH	20-48:80-52	30:70
45a	X=CH <sub>2</sub>	LAH	91:9	89:11
45b	X=O	LAH	94:6	96:4
45c	X=S	LAH	15:85	9:91
45a	X=CH <sub>2</sub>	MeMgI	45:55	68:32
45b	X=O	MeMgI	98:2	94:6
45c	X=S	MeMgI	7:93	3:97
46a	R <sub>1</sub> =Me, R <sub>2</sub> =R <sub>3</sub> =R <sub>4</sub> =H	LAH	74-84:26-16	70:30
46b	R <sub>3</sub> =Me, R <sub>1</sub> =R <sub>2</sub> =R <sub>4</sub> =H	LAH	40-27:60-73	46:54
46c	R <sub>1</sub> =R <sub>2</sub> =Me, R <sub>3</sub> =R <sub>4</sub> =H	LAH	....	93:7
46d	R <sub>3</sub> =R <sub>4</sub> =Me, R <sub>1</sub> =R <sub>2</sub> =H	LAH	90:10	73:27

against the hypothesis of Houk where the transition structure for axial attack was favored because it involved less ring strain. It followed that the stability differences must have been due to the interaction between the substrate and LiH.

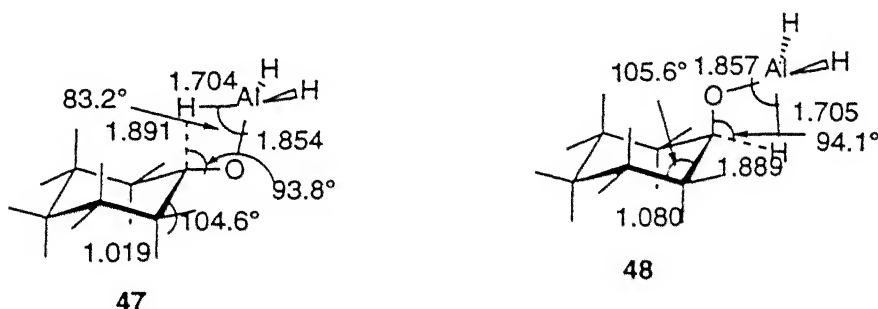
The energy differences of the transition structures calculated without  $\text{Li}^+$  but with frozen geometry of the anionic fragment predicted that axial attack was favored over the equatorial attack by 3.2 kcal/mol. The preference was due to the better interaction of the ketone with the hydride anion. With the help of FMO theory, Frenking explained the interactions responsible for the differences between the axial and equatorial attacks. In general, the addition of a nucleophile to a carbonyl should be controlled by the orbital interaction between the HOMO of the nucleophile and LUMO of the cyclohexanone. For the nonequivalent distribution of LUMO of the carbonyl  $\pi$ -bond on axial and equatorial faces, the axial and equatorial attacks of a nucleophile are different. The size of the LUMO is larger on the axial face than that on the equatorial face in cyclohexanone.

The nonequivalence of  $\pi^*$ -LUMO was determined by the contribution of the 2S orbitals of the C and O atoms of the carbonyl group. The contribution of the 2S atomic orbitals (0.26) was significant and indicated a clear preference for axial attack. The natural bond orbital (NBO) analysis also showed that the  $\pi_{\text{CO}}^*$  orbital interacted more strongly with the C2-H<sub>ax</sub> orbital than with the C2-C3 orbital.

## Coxon model

Coxon and Luibrand<sup>22</sup> have examined the gas phase addition of  $\text{AlH}_3$  to cyclohexanone using *ab initio* and semiempirical calculations. The four centered *ab initio* 3-21G\* transition states for axial (47) and equatorial (48) attacks of hydride showed the incipient H-C bond distances 1.891 and 1.889 Å, respectively, to be somewhat shorter than those for LiH reduction (2.057 and 2.628 Å, respectively).<sup>20, 71, 72</sup> This is indicative of a late transition state for  $\text{AlH}_3$ . The dihedral angles of the adjacent C-H and C-C bonds with

the forming C-H bond are significant since they provide a measure of the ability of these bonds to participate in hyperconjugation. For axial attack, an almost perfect antiperiplanar relationship was calculated. Whereas the  $H_{Nu}-C-C-H_{ax}$  dihedral angle was  $179^\circ$  for axial attack, the  $H_{Nu}-C-C-C$  dihedral angle for equatorial attack was  $170^\circ$ . The ring is flattened to  $140^\circ$  at the transition state for axial attack and puckered to  $119^\circ$  for equatorial attack.



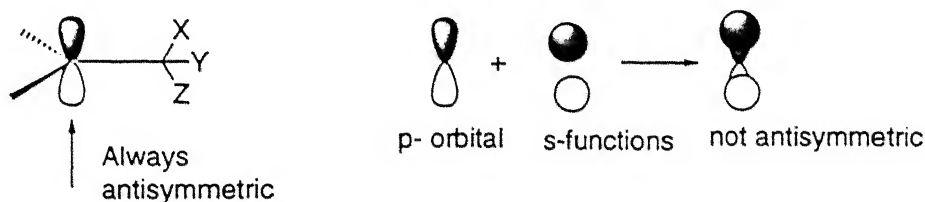
In each transition state, the bonds which are antiperiplanar to the forming  $H_{Nu}-C$  bond are elongated: axial C-H bonds for the axial attack and the C-C bonds for equatorial attack. For axial attack the elongation in axial C-H bond was 0.37 %, but no change in C-C bond lengths. For the equatorial transition state, C-C bond was elongated by 0.84 % with no elongation in axial C-H bonds. Also, the C2-C<sub>co</sub> bond length shortened in both the axial and equatorial transition structures compared to that in cyclohexanone.

The better antiperiplanar orientation of the nucleophile with the adjacent C-H bond in axial attack compared to the poor antiperiplanarism with the C2-C3 bond in equatorial attack supports the suggestion that orbital alignment is important.

Calculated structural changes in the transition state and their molecular orbitals are consistent with hyperconjugative delocalization of the C2-H<sub>ax</sub> bond for the axial and the C2-C3 bond for the equatorial attack.

## $\pi$ -Polarized Frontier Molecular Orbital Theory (PPFMO)

Dannenberg and coworkers<sup>21</sup> have explained the facial selectivity through desymmetrization of p orbitals using PPFMO theory. Since the atomic p orbitals used in simple molecular orbital treatments are rigorously antisymmetric, one can not use the coefficients of these orbitals to predict the diastereofacial selectivity in a manner similar to that employed in the FMO theory to predict regioselectivity. A modification of the same was envisaged to explain the experimental observations.



The basic construct is the superposition of two new basis functions, one upon each lobe of an atomic p function. The p orbital would then be constructed from a linear combination of these three functions. The original antisymmetry of the p function will be tempered by these two additional functions which can differ in magnitude. The difference in magnitude between these functions will indicate the extent to which the  $\pi$ -orbital is polarized at each particular atomic site. The polarization ( $\rho$ ), in turn, can be used to predict the diastereofacial selectivity according to approximations normally associated with the FMO theory. In case of nucleophilic attacks on carbonyl compounds, the polarization of the LUMO of the reactant should be the focus of interest. The direction of attack expected for  $\rho > 0$  is indicated. Calculation of cyclohexanone and protonated cyclohexanone (to mimic reaction of a cyclohexanone that is precoordinated to a cation such as  $\text{Li}^+$  or  $\text{Na}^+$ ) showed that for cyclohexanone the LUMO is highly polarized towards the direction of the observed axial attack on the carbonyl carbon. Protonation of the carbonyl slightly

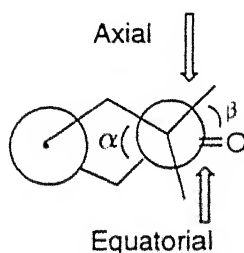


increases the polarization from 0.166 to 0.171 which is in good agreement with Frenking's suggestions.

## Boyd model

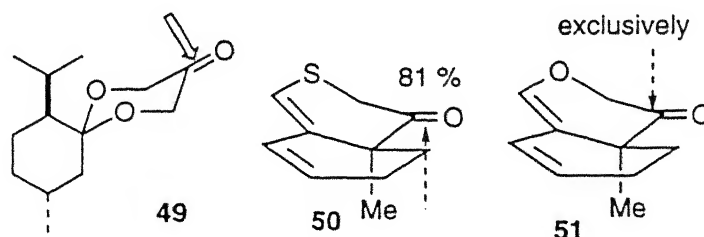
Boyd and Shi<sup>23</sup> have carried out a systematic study of the structure and the distribution of electrons. They used Laplacian of the charge density to reveal the distribution of electrons. This provides direct information about where in space the charge is concentrated and depleted. It has been suggested that  $\nabla^2\rho$  can be used to study the directions of electrophilic and nucleophilic attacks.

Electrophilic attack will occur where the charge is concentrated. Likewise, nucleophilic attack will occur where the charge is depleted. Regions of charge depletion and concentration can be located by the calculation of the critical points of  $\nabla^2\rho$  in the valence shell charge concentration (VSCC). A positive value indicates the charge depletion whereas a negative value indicates the charge concentration.



### 1.1.1.3 Face Selection of Nucleophilic Additions to 3- and 3,5-Heteroatoms Substituted Cyclohexanones

It is known that the Grignard reaction on 3-heteroatom substituted cyclohexanones<sup>73-76</sup> showed different selectivity depending upon the heteroatom. For example, Grignard reaction on 2-phenyl-1,3-dioxan-5-one<sup>73</sup> **45**,  $X=O$  gave the product of axial face addition (Table 1.5).

Table 1.5: Percentage of axial:equatorial addition to **45** and **49**

Nu	<b>45</b> , X=O	<b>49</b>	<b>45</b> , X=S
LAH	94:6	87:13	15:85
DIBAL-H		>94:<6	
MeMgI	99.7:0.3	>96:<4	7:93
MeCH <sub>2</sub> MgI	98:2		11:89
Me <sub>2</sub> MgI	96:4		9:91
Me <sub>3</sub> MgCl	no rxn	>96:<4	
PhMgBr		>96:<4	

The introduction of sulfur into cyclohexanone ring at the  $\beta$  position (**45**, X=S) results in a nucleophilic attack from the equatorial face which is opposite to that observed from the reaction on 2-phenyl-1,3-dioxo-5-one **45**, X=O.

According to Cieplak,<sup>17</sup> C-O bond is less electron donating than a C-H bond. So, in the case of **45**, X=O the attack is antiperiplanar to the electron rich axial C-H bonds. On the contrary, since a C-S bond is more electron donating than a C-H bond and since the trajectory of an equatorial attack is antiparallel to the C-S ring bond, the attack in the thia derivative **45**, X=S is from the equatorial direction.

Houk and coworkers<sup>29, 72</sup> explained the above selectivity on the basis of torsional strain. Since C-O bond is shorter than a C-C bond, the torsional strain in the transition structure for equatorial attack is even more significant relative to that for axial attack. That is, the short ring C-O bonds make the six membered ring significantly flatter than cyclohexanone.

But, since a C-S bond is longer than a C-C bond, the torsional problems are absent in the transition structure for equatorial attack. The long C-S bonds make the ring puckered.

When there are two oxygen atoms in the ring<sup>23</sup> the dihedral angle  $\beta$  is increased to  $37.88^\circ$  from  $2.97^\circ$ . On the contrary, S-atoms flatten the ring and the sign of  $\beta$  is changed from  $-8.7$  to  $2.97$ . Although the electron density along the C2-H2(a) bond is higher for a system with two S atoms in the ring, the ring is quite puckered and the torsional strain for axial attack is more severe than that for an equatorial attack. The equatorial attack, therefore, is favored.

#### 1.1.4 Face Selection of Nucleophilic Additions to 3-Substituted Cyclohexanones

It has been observed that the axial attack is favored when the cyclohexanone is substituted by an electron withdrawing group at C3.<sup>77, 78</sup> Since there was no systematic study for the 3-substituted cyclohexanone **52**, Cieplak and coworkers<sup>79</sup> studied this system in detail to delineate the stereochemical outcome. It is clear from the Table 1.6 that an electron releasing group decreased the % of axial attack as compared to the parent cyclohexanone. However, the axial selectivity was enhanced by an electron-attracting substituents. Noble<sup>80</sup> has shown that the C4-axial substituents in adamantanones **55a** affect the face selectivity sterically. However, the equatorial substituents (**55b**) do not have such effects. It is clear from the Table 1.7 that both **55a-F** and **55a-Br** direct the reagent completely to the remote face of the ketone. The steric factor evidently dominates the electronic factor even in the case of the small fluorine atom.

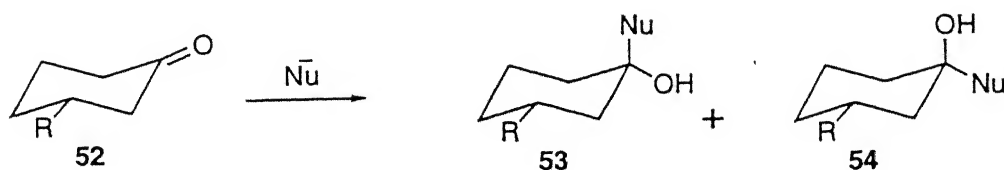
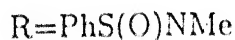
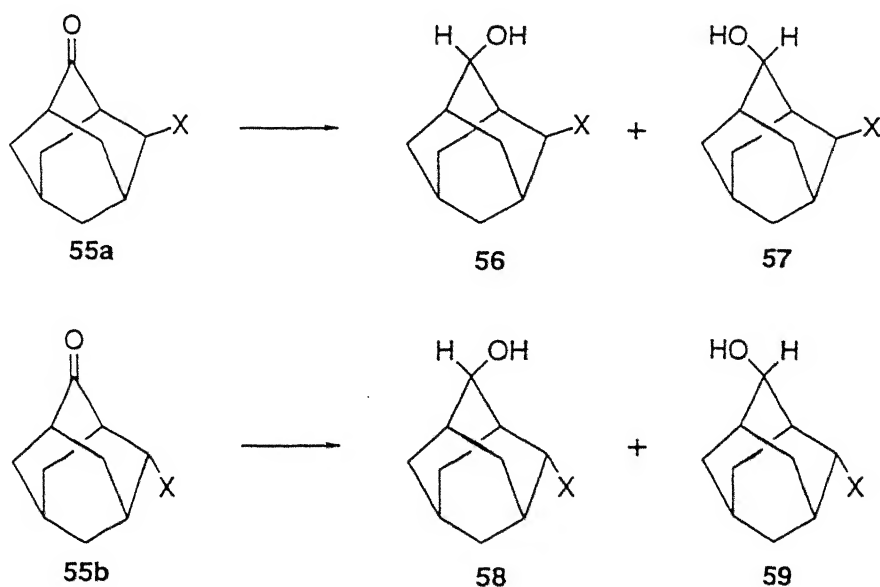


Table 1.6: Percentage of axial attack in nucleophilic additions to **52**

R	CH <sub>3</sub> Li Ether -78°C	Li <sub>2</sub> (CH <sub>3</sub> ) <sub>3</sub> Cu Ether -78°C	CH <sub>3</sub> Li THF -78°C	PhSCH <sub>2</sub> Li THF -78°C	RCH <sub>2</sub> Li THF -78°C	Me <sub>2</sub> S=CH <sub>2</sub> DMSO 0°C
SiMe <sub>3</sub>	15	2	22	10	55	44
Bu <sup>t</sup>	19	3	27	11	56	48
H	21	6		17		80
<i>p</i> -MeOC <sub>6</sub> H <sub>4</sub>	24	8	30	16	66	44
<i>p</i> -MeC <sub>6</sub> H <sub>4</sub>	23	8	30	19	65	48
C <sub>6</sub> H <sub>5</sub>	25	7	30	15	65	45
<i>p</i> -F <sub>3</sub> CC <sub>6</sub> H <sub>4</sub>	28	10	36	24	72	46
C <sub>6</sub> F <sub>5</sub>	34	21	50	28	70	58
CF <sub>3</sub>	50	42	58	53	83	69



Cieplak<sup>79</sup> accounted the diastereoselectivity by stabilization of the transition state by donating electrons from the more electron donating bonds. As a consequence, whether an electron withdrawing group at C3 is axial or equatorial, this model would predict axial attack for both for the C2-C3 bond in both is rendered electron deficient. However, this is at variance from what has been predicted by the TS models of both Houk and Frenking (*vide infra*). Both these models predict axial attack for 3-eq-F-cyclohexanone and equatorial attack for the 3-ax-F-cyclohexanone. In contrast, when cyclohexanone is substituted by an equatorial electron releasing group such as Bu<sup>t</sup>- and SiMe<sub>3</sub>, the C2-C3 bond becomes more electron donating than the axial C2-H and C6-H bonds. As a result, the attack is on the equatorial face.

Table 1.7: Percentage of product formed on reduction to **55**

X	Reagent	56	57	58	59
55a-OH	LAH	95	5		
55b-OH	LAH			30	70
55a-F	Zn(BH <sub>4</sub> ) <sub>2</sub>	33	67		
55a-F	NaBH <sub>4</sub>	100			
55b-F	Zn(BH <sub>4</sub> ) <sub>2</sub>			33	67
55b-F	NaBH <sub>4</sub>			33	67
55a-Br	NaBH <sub>4</sub>	99			
55b-Br	NaBH <sub>4</sub>			24	76

Frenking<sup>20</sup> explained the experimental observations on 3-*eq*-F-cyclohexanone by FMO theory. Calculation of the transition state structures for axial and equatorial additions of LiH to cyclohexanone and 3-*eq*-F-cyclohexanone using *ab initio* quantum chemical methods showed long interatomic distances between the carbonyl carbon and the attacking hydride indicating early transition states. He observed that the axial addition of LiH to

3-eq-F-cyclohexanone was 2.7 kcal/mol more favored than the equatorial addition. This calculation agreed well with the experimental observations. Only the axial addition of nucleophiles is observed.<sup>79</sup>

The contribution of the 2S(C) atomic orbital in the  $\pi$ -orbital is larger in the case of 3-eq-F-cyclohexanone than in the case of cyclohexanone. So the axial attack is increased if there is any electron withdrawing group in the 3-eq-position. For 3-ax-F-cyclohexanone, calculations predicted a clear reversal in favor of equatorial addition of LiH. The energy difference from the axial addition was 1.2 kcal/mol. The transition state for axial attack may additionally be disfavored for the steric interactions between F and the nucleophilic hydride ion.

Dannenberg and Huang<sup>21</sup> explained the observed selectivity by PPFMO theory. The polarization is higher on the axial face in cyclohexanones bearing 3-eq-electron withdrawing substituents than in cyclohexanone itself. The percentage of axial attack is, therefore, increased. Also, the PPFMO calculations of the reagent showed the same trend as  $P/E_{LUMO}$  increased from 0.861 for cyclohexanone to 1.107 for 3-eq-F-cyclohexanone. Thus, at least some of the increased selectivity appeared inherent in the reagent as well.

The dihedral angles did not change much when the cyclohexanone is C3-substituted. VSCC calculations<sup>23</sup> showed that the equatorial attack is slightly favored for 3-eq-substituted cyclohexanones which is in contradiction to the experimental observations.<sup>79</sup> The charge density at bond critical points showed that as the charge density at C2-H(a) increased, the axial attack increased as well; the increase, however, was very small.

### 1.1.5 Face Selection of Nucleophilic Addition to 4-Substituted Cyclohexanones

It is well known that the reduction of 4-Bu<sup>t</sup>-cyclohexanone gives mostly the equatorial alcohol which is a product of axial attack of the hydride ion and, hence, sterically less

avored. In the axial attack, the nucleophile has to encounter the two C3- and C5-axial hydrogens and the 4-eq-Bu<sup>t</sup> group.

Conformational analysis<sup>81, 82</sup> has shown that the axial isomer is more stable than the equatorial isomer if the cyclohexanone is substituted by an electron withdrawing group at C4. Since there is conformational flexibility in substituted cyclohexanones, Monson<sup>83</sup> chose decalone system with polar groups at position 4 to study the true effect of polar groups in facial determination. The parent decalone **60**, X=H itself gave 96% axial attack. When the system was substituted by a CO<sub>2</sub>Me group (**60**, X=CO<sub>2</sub>Me), the axial attack was increased to almost 100%. On the contrary, an equatorial electron-withdrawing **61**, X=CO<sub>2</sub>H group decreased the axial attack in comparison to that for the parent decalone **61**, X=H.

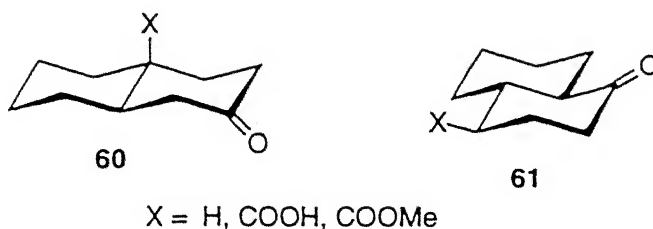


Table 1.8: Percentage of ax and eq attack from NaBH<sub>4</sub> reduction of **60** and **61**

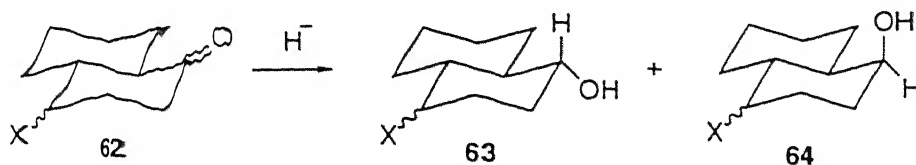
X	<b>60</b>	<b>61</b>
X = H	96:24	68:32
X = CO <sub>2</sub> H	92:8	56:44
X = CO <sub>2</sub> Me	100:0	

The ratio  $k_{ax}/k_{eq}$  increased with the increase in electronegativity of the substituent under all reaction conditions. This data suggested that the MO phase amplitude of  $\pi_{co}$  is highly distorted toward the axial face under the effect of axial chlorine on the other side of the molecule. A number of explanations have been given to explain the experimental observations. A precise account is given below:

According to Cieplak,<sup>17</sup> if there is any effect of polar substituents on C4 on the rate and stereoselectivity of nucleophilic additions to cyclohexanone, that is to be controlled by  $n, \sigma_{nn}^*$  orbital overlap that must lead to a predominance of axial attack for both the axial and the equatorial C4-substituents. Since the substituents enhanced the absolute reaction rate of  $\text{NaBH}_4$  reduction and since the ground state effects of such remote substituents are negligible, it appears that the stereochemical effects result indeed from a selective stabilization. However, several examples of anomalous behavior suggested that the quantitative assessment of the overlap magnitudes did not provide sufficient criterion to predict the selectivity of these systems.

Since there was no systematic study to explain the influence of C4-polar substituents on the stereoselectivity, Houk<sup>71</sup> chose 4-substituted decalones **62** as the probe. Decalone **62** ( $X=\text{H}$ ) itself favored axial attack. When it was substituted by an electron-withdrawing group at C4, the axial attack generally increased. The percentage of axial attack increased little when the substituent was in equatorial position. In contrast, the percentage of axial attack increased considerably when the substituent was in axial position. Since the equatorial  $\sigma_{C-X}^*$  is aligned to overlap with  $\sigma_{2,3}$  and  $\sigma_{9,10}$ , they should interact strongly. Such an interaction is absent for the axial  $\sigma_{C-X}^*$  for the lack of suitable alignment. Consequently, the C2-C3 and C9-C10 bonds of the equatorially substituted isomers should be poorer donors than those of the axial isomers. If nucleophilic addition occurs *anti* to the better donor group (Cieplak model), the equatorial isomers should have considerably more axial attack than the parent species. The axial isomers, on the contrary, should have only slight increase in the axial attack. These predictions are opposite to those observed from experiments. In order to understand these substituent effects, Houk calculated the energies of the axial and equatorial transition structures of substituted cyclohexanones with 3-21G basis set.



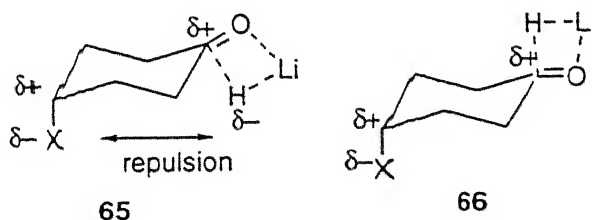
Table 1.9: Product ratios in NaBH<sub>4</sub> reduction of 62

X	%ax	%eq
H	60	40
eqOH	61	39
eqOAc	71	29
eqBr	66	34
eqCl	71	29
axOH	85	15
axOAc	83	17
axCl	88	12
axF	87	13

When the substituent was equatorial, very small variation in stereoselectivity was predicted. The preference for the axial transition structure was computed to have increased for F and Cl substituents by about 0.3 kcal/mol and for OH and NH<sub>2</sub> substituents by 0.6 and 0.2 kcal/mol, respectively, as compared to that for cyclohexanone. The equatorial and axial transition structures for 4-eq-F-cyclohexanone showed the axial transition structure 1.2 kcal/mol more stable than the equatorial transition structure.

When the substituent was axial, the calculations indicated a significant additional stabilization for the axial transition structure in every case. These results are quantitatively in agreement with the experimental observations. The conformers with one lone pair orbital inside the ring are less stable than the conformers with the lone pair orbital outside the ring because of the repulsive electrostatic interactions between the nucleophile and the inside electron pair orbital in the equatorial TS as shown in 65.

The introduction of a substituent on C4 in cyclohexanone computed for a small geometrical distortion of the cyclohexane ring. The geometrical distortion was indicated by dihedral angles. The  $\text{O}=\text{C}-\text{C}_2-\text{H}_{\text{eq}}$  out of plane dihedral angle increased from  $3^\circ$  in cyclohexanone to  $5^\circ$  in 4-eq-F-cyclohexanone. The 4-ax-F substituent had almost no such effect on the geometry. The  $\text{C}-\text{C}_{\text{sp}^2}-\text{C}-\text{C}$  angles are also indicative of ring distortion. This angle changes from  $54.4^\circ$  in cyclohexanone to  $52.9^\circ$  and  $53.8^\circ$  in 4-eq- and 4-ax-F-cyclohexanones, respectively. Accompanying this ring distortion, a small pyramidalization at the carbonyl carbon is also introduced by the fluoro substituent.



The C-C bonds geminal to the C-F bond are shorter than a normal C-C bond by  $0.015^\circ\text{A}$ . These C-C bonds become longer when the substituent is electron-donating. Houk concluded that electron-attracting substituents can increase axial addition and electron-donating substituents can reduce axial addition merely by geometrical distortions. The electrostatic or dipole effects are responsible for the larger increase in axial  $\text{NaBH}_4$  addition to decalones possessing axial electron-withdrawing substituents on C4. As shown in 65 and 66, the equatorial attack by a nucleophile is destabilized by electrostatic repulsive interactions with the axial substituent while the axial attack is favored for dipole interactions.

The calculated polarization<sup>21</sup> of substituted cyclohexanones are in full agreement with the *ab initio* calculation for the addition of LiH as reported by both Houk and Frenking. Calculations showed that the polarization is always positive which indicates a larger lobe on the axial face that leads to the predominant axial attack.

Boyd<sup>23</sup> has explained the experimental observations by the dihedral angle changes and charge density analysis. For 4-substituted cyclohexanones, there was no flattening of the ring. To determine whether or not the unsymmetrical distribution of electrons around a carbonyl group played a role in stereoselectivity, Boyd studied valence shell charge concentration (VSCC) of the carbonyl carbon. The electrophilic attack will occur where the charge is concentrated and the nucleophilic attack will occur where the charge is depleted. The charge density at VSCC did not change significantly for different substituents and was quite similar on the two sides of the carbonyl  $\sigma$  plane. An equatorial attack would be predicted to be slightly favored which is in contradiction to the experimental results. Therefore, the charge density arguments were considered less significant.

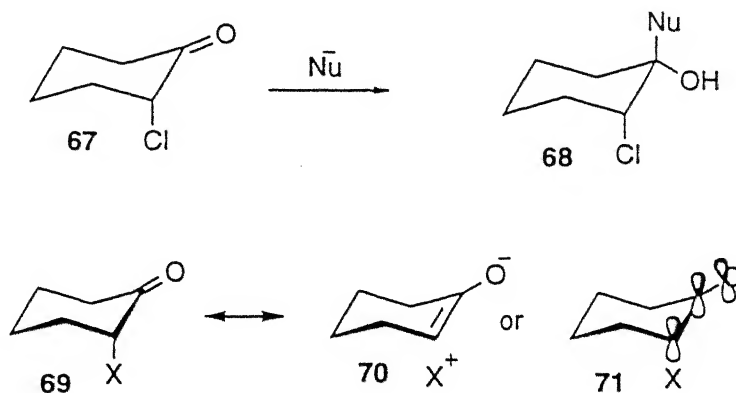
Study of the complex and transition structures for the nucleophilic additions of LiH to 4-substituted cyclohexanones showed that the energy barrier for axial and equatorial attack was the largest for 4-axially substituted cyclohexanones which is consistent with the experimentally observed increased preference for axial attack in the axially substituted systems.

Fully optimized structures of the complexes of 4-eq-F- and 4-eq-Cl-cyclohexanones showed that LiH lay on the axial side. This nonsymmetric alignment indicated the large energy barrier for equatorial attack. Also, the dipole-dipole interaction made the equatorial attack more difficult.

### 1.1.6 Face Selection of Nucleophilic Addition to 2-Substituted Cyclohexanones

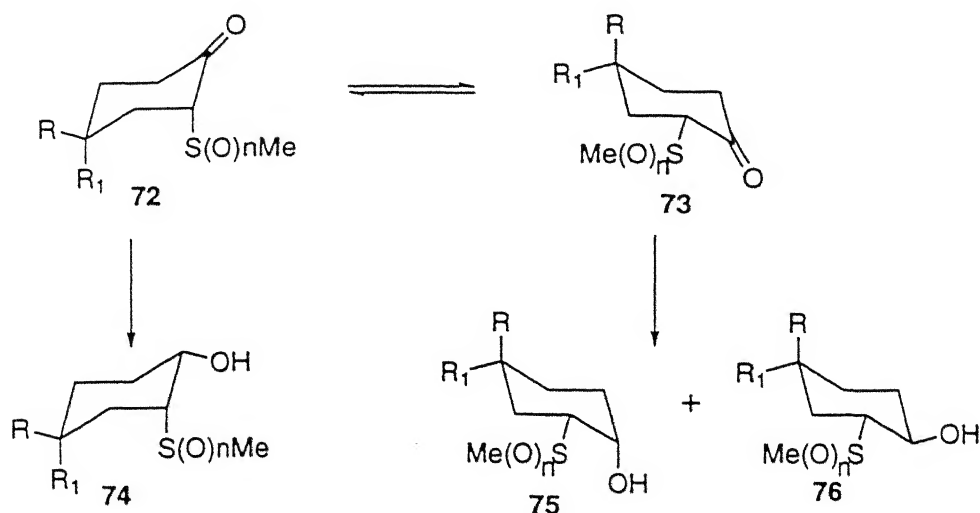
It has been observed<sup>84</sup> that reduction and nucleophilic reactions of 2-Cl-cyclohexanone **67** gives *cis*-chlorohydrin **68**. The addition occurred from axial side since 2-Cl-cyclohexanone is reported by Corey<sup>85</sup> to possess the Cl predominantly axial. The stabilization is derived from the hyperconjugative interaction of the C-Cl bond with the carbonyl  $\pi$ -orbital as

shown. Cieplak model would predict equatorial attack for 2-ax-Cl-cyclohexanone.



Carreno and coworkers<sup>86</sup> have studied the reduction of 2-X- cyclohexanones and *cis*- and *trans*-4-Bu<sup>t</sup>-2-X-cyclohexanones (X=Me, SO<sub>2</sub>Me) with different hydrides. The results of reduction of 4-Bu<sup>t</sup>-2-X-cyclohexanone are collected in the Table 1.10. It is clear that when the sulfur functions adopt the axial disposition, the cyclohexanols resulting from the axial approach of the hydride were the only products obtained even when bulky hydrides were used. However, when the sulfur functions adopted the equatorial disposition, mixtures of diastereomers were obtained.

In the 2-ax-SMe-substituted cyclohexanone **72**(n=0), the unshared electron pairs make the equatorial attack very difficult for the repulsion between the occupied nonbonding orbitals on S and the hydride as shown in **77**. In the equatorially substituted cyclohexanone **73**(n=0), axial attack is rendered for a similar reason as shown in **78**. The spatial arrangement of the  $\sigma_{\text{C-S}}$  equatorial bond with respect to the  $\sigma_{\text{C-H}}$  orbitals in the transition state resulting from the axial or equatorial hydride approach is not suitable for giving a stabilizing interaction. Cieplak theory, therefore, can not be applied to justify the stereochemical results observed from 2-eq-SMe-cyclohexanone **73**(n=0).



a : R = R<sub>1</sub> = H, n = 0  
 b : R = t-Bu, R<sub>1</sub> = H, n = 0  
 c : R = R<sub>1</sub> = H, n = 2  
 d : R = t-Bu, R<sub>1</sub> = H, n = 2

a : R = R<sub>1</sub> = H, n = 0  
 b : R = H, R<sub>1</sub> = t-Bu, n = 0  
 c : R = R<sub>1</sub> = H, n = 2  
 d : R = H, R<sub>1</sub> = t-Bu, n = 2

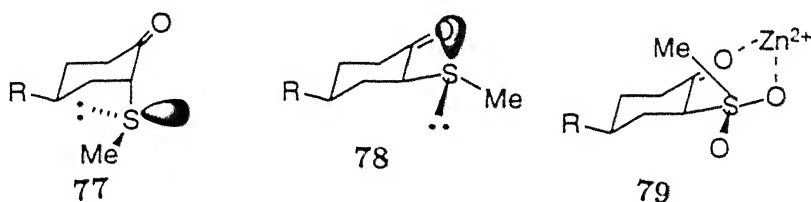
Table 1.10: Percentage of ax and eq attack of hydride to **72** and **73**

Substrate	A	B	C	D	E	F
<b>72</b> (n=0)	100:0			100:0		100:0
<b>73</b> (n=0)	56:44	28:72		46:54	100:0	
<b>72</b> (n=2)	100:0		100:0	100:0		100:0
<b>73</b> (n=2)	34:66	57:43	59:41	75:25	0:100	

A = NaBH<sub>4</sub>, B = NaBH<sub>4</sub>/ZnCl<sub>2</sub>, C = LiAlH<sub>4</sub>,

D = (Bu<sup>t</sup>)<sub>2</sub>AlH, E = (Bu<sup>t</sup>)<sub>2</sub>AlH/ZnCl<sub>2</sub>, F = Li(Et)<sub>3</sub>BH

In the case of 2-ax-sulfonyl-substituted cyclohexanone **72**(n=2), repulsive effect between the hydride and the unshared electron pairs on the sulfonyl oxygen during the equatorial attack led to the more favored axial attack. But in the case of 2-eq-sulfonyl-substituted cyclohexanone **73**(n=2), the complexation of Zn<sup>2+</sup> with both the C=O and one of the sulfonyl oxygens as shown in **79** favored the axial attack. The above results showed that the substituent effects on face selectivity follow neither the theory of Cieplak nor that of Anh.



Yamamoto<sup>87</sup> and Paquette<sup>88</sup> have studied 2-alkoxy cyclohexanones. Grignard reagents added predominantly equatorial with chelation controlled selectivity irrespective of the orientation of the alkoxy group. The results obtained from the reactions of *trans*- and *cis*-4-*t*-Bu-2-methoxycyclohexanones (80 and 81, respectively) are collected in the Table 1.11.

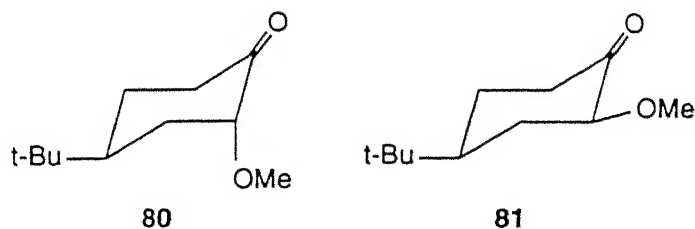
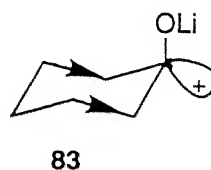
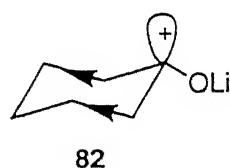


Table 1.11: Facial selectivity in nucleophilic addition to 80 and 81

Substrate	Nucleophile	Solvent and conditions	% eq : % ax
80	$\text{CH}_2=\text{CHCH}_2\text{MgBr}$ , $\text{CrCl}_2$	THF, 0 °C	92:8
80	$\text{ClMgO}(\text{CH}_2)_3\text{MgCl}$	THF, 0 °C	77:23
80	$\text{CH}_2=\text{CHCH}_2\text{MgBr}$ , In	THF, 25 °C	92:8
80	$\text{CH}_2=\text{CHCH}_2\text{MgBr}$ , In	THF: $\text{H}_2\text{O}$ (1:1), 25 °C	92:8
80	$\text{CH}_2=\text{CHCH}_2\text{MgBr}$ , In	$\text{H}_2\text{O}$ , 25 °C	92:8
81	$\text{CH}_2=\text{CHCH}_2\text{MgCl}$	THF, 0 °C	>97:3
81	$\text{CH}_2=\text{CHCH}_2\text{MgCl}$ , $\text{CeCl}_3$	THF, 0 °C	> 97:3
81	$\text{CH}_2=\text{CHCH}_2\text{MgCl}$ , $\text{CrCl}_2$	THF, 0 °C	>90:10
81	$\text{ClMgO}(\text{CH}_2)_3\text{MgCl}$	THF, 0 °C	>97:3
81	$\text{CH}_2=\text{CHCH}_2\text{MgBr}$ , In	THF, 25 °C	92:8
81	$\text{CH}_2=\text{CHCH}_2\text{MgBr}$ , In	THF: $\text{H}_2\text{O}$ (1:1), 25 °C	>97:3
81	$\text{CH}_2=\text{CHCH}_2\text{MgBr}$ , In	$\text{H}_2\text{O}$ , 25 °C	>97:3

## 1.2 Present Work

The nucleophilic attack on a carbonyl carbon must generally be preceded by a complexation of the carbonyl oxygen with a cation and that this complexation must occur in the carbonyl  $\sigma$  plane. This finds ample support in the literature.<sup>89</sup> Reaction mechanism and kinetic studies have shown that reductions take place after the complexation of the metal cation with the carbonyl.<sup>32, 87, 90-106</sup> The TS models proposed to explain the stereoselectivity do not take this complexation into account. It must be noted that the reductions are, in general, exothermic in nature. This suggests, on application of Hammond postulate, a TS that resembles the reactants. This complexation will reduce the C=O bond order and, hence, affect the torsional angles of the carbonyl oxygen with the ring positions 3 and 5 in the process of the ensued pyramidalization at the carbonyl carbon. The direction of pyramidalization must be reflected in these torsion angles which must either increase or decrease in respect of those in the parent uncomplexed species.



The empty p orbital on the carbonyl carbon, whose coefficient is enlarged on cation complexation, must orient *anti* to the more electron-releasing adjacent bond. From the theory of stereoelectronic effects, a situation entailing an electron pair orbital antiparallel to a polar electron-attracting  $\sigma$ -bond on an adjacent atom is more stable than a situation where the same spatial relationship does not exist. The higher stability is ascribed to a donor-acceptor kind of interaction between the two. The interaction is the greatest when the two participating orbitals are antiperiplanar and the least when the same are orthogonal. If we extend this notion to the relative orientation of an electron-attracting

polar  $\sigma$ -orbital and an empty p orbital, both must be orthogonal as in 82. The empty p orbital, however, will orient antiperiplanar to an electron-releasing  $\sigma$ -bond as in 83.

In cyclohexanones, this p orbital may go either axial or equatorial depending upon the nature, location, and orientation of the ring substituents. Remote substituents may also be expected to influence this orientation. An axial p orbital orientation means an equatorial inclination of the carbonyl C-O bond. This shall result in an increase in the torsion angle,  $D1 = OC1C2C3$  and  $D2 = OC1C6C5$ . Likewise, an equatorial p orbital orientation shall correspond to a decrease in the above torsion angles. Electrostatic attraction of this p orbital for the nucleophile must then determine the ax/eq facial selectivity. For the examples studied below, this premise works elegantly on qualitative basis. the order of electron donation for common atom combinations is the same as that reported by Cieplak, *i.e.*,  $C-S > C-H > C-C > C-N > C-O$ .

### 1.2.1 Face selection of Nucleophilic additions to 3-oxa-, 3-thia- and 3,5-dioxa substituted cyclohexanones

We have performed *ab initio* MO calculations at 6-31G level of theory<sup>107</sup> and determined the ground state geometry after complexation with typical cations such as  $H^+$  and  $Li^+$  for computational simplicity. From the changes in  $D1$  and  $D2$ , we explain below the diastereoselectivity of several variously substituted cyclohexanones in reaction with nucleophiles.<sup>108</sup>

The dihedral angles and the bond angles obtained for 3-oxacyclohexanone 84 and its complexed derivatives 85-87 are given in the Table 1.12.

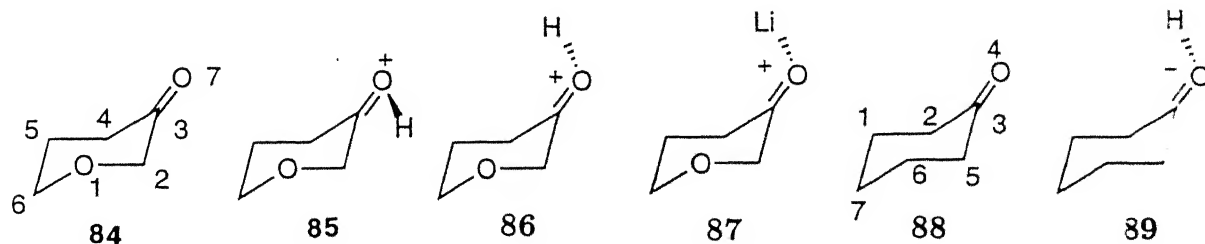




Table 1.12: Angles and Torsion angles in 84-89.

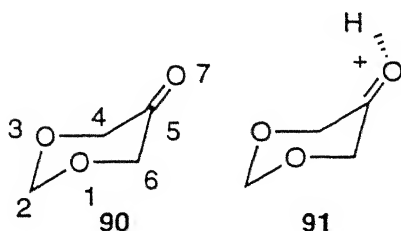
Angles	84	85	86	87	88	89
D1	147.66	157.05	159.97	150.22	132.09	132.94
D2	147.22	153.56	156.41	147.51	132.22	132.96
A1	122.11	116.72	122.43	121.40	121.89	122.36
A2	120.42	121.64	115.33	119.83	121.90	116.74

D1=O7C3C4C5, D2=O7C3C2O1

A1=O7C3C4, A2=O7C3C2

The two torsion angles, D1 and D2, represent the angles on the axial face, their signs have, therefore, been omitted. The site selectivity of complexation was also considered and, hence, the pair 85 and 86 emerged. The energy difference of the pair was small (0.8 kcal/mol) and 86 was more stable than 85. A comparison of 85 and 86 with 84 brings out the following points: (a) the differential changes in the two designated angles A1 and A2 signify the further desymmetrization of the carbonyl, and (b) the increase in the torsion angles D1 and D2 indicates the p orbital tending to orient axial and, thus, pushing the C-O bond equatorial. An attacking nucleophile shall naturally be electrostatically drawn to the axial face of the carbonyl. It is indeed found so from experiments.

For comparison the parameters for cyclohexanone 88 and its protonated derivative 89 are also collected in the Table 1.12. Table 1.13 shows data on 3,5-dioxacyclohexanone 90 and its protonated derivative 91. The combined effect of the two ring oxygens must be the even more pronounced axial orientation of the p orbital than that in 3-oxacyclohexanone. The torsion angles D1 and D2 must, therefore, be larger and lead to a further enhanced preference for axial attack. These stereoelectronic arguments are in excellent accord with the experimental results.<sup>73, 75</sup> The dioxa species 90 itself showed almost 13° larger the torsion angles D1 and D2 than in the monooxa species 84.

Table 1.13: Angles and Torsion angles in **90** and **91**.

Angles	<b>90</b>	<b>91</b>
D1	160.20	165.63
D2	160.10	165.21
A1	120.62	122.40
A2	120.64	115.82

D1=O7C5C4O3, D2=O7C5C6O1

A1=O7C5C4, A2=O7C5C6

Further, a higher Lewis acid strength of a cation will be expected to contribute to the observed face selection through a greater polarization of the carbonyl and, hence, its enhanced desymmetrization. Conversely, the cation remaining the same, the selectivity must not vary significantly for the small changes in the steric requirements of the actual nucleophile. In agreement with this, the ax:eq selectivity varied from 7.7:1 to 16:1 to >25:1 in reactions of a 3,5-dioxacyclohexanone derivative with LAH, DIBALH and a Grignard reagent, respectively.<sup>76</sup> The quality of the complexation will be expected to improve in that order. Moreover, in keeping with the expectation, the diastereoselectivity remained at >25:1 when the nucleophile was varied from Me<sup>-</sup> to n-Bu<sup>-</sup> to Ph<sup>-</sup> derived from the respective Grignard reagents.<sup>76</sup> The 3D structures of the selected species, both before and after protonation, are collected in the Fig. 1.1 .

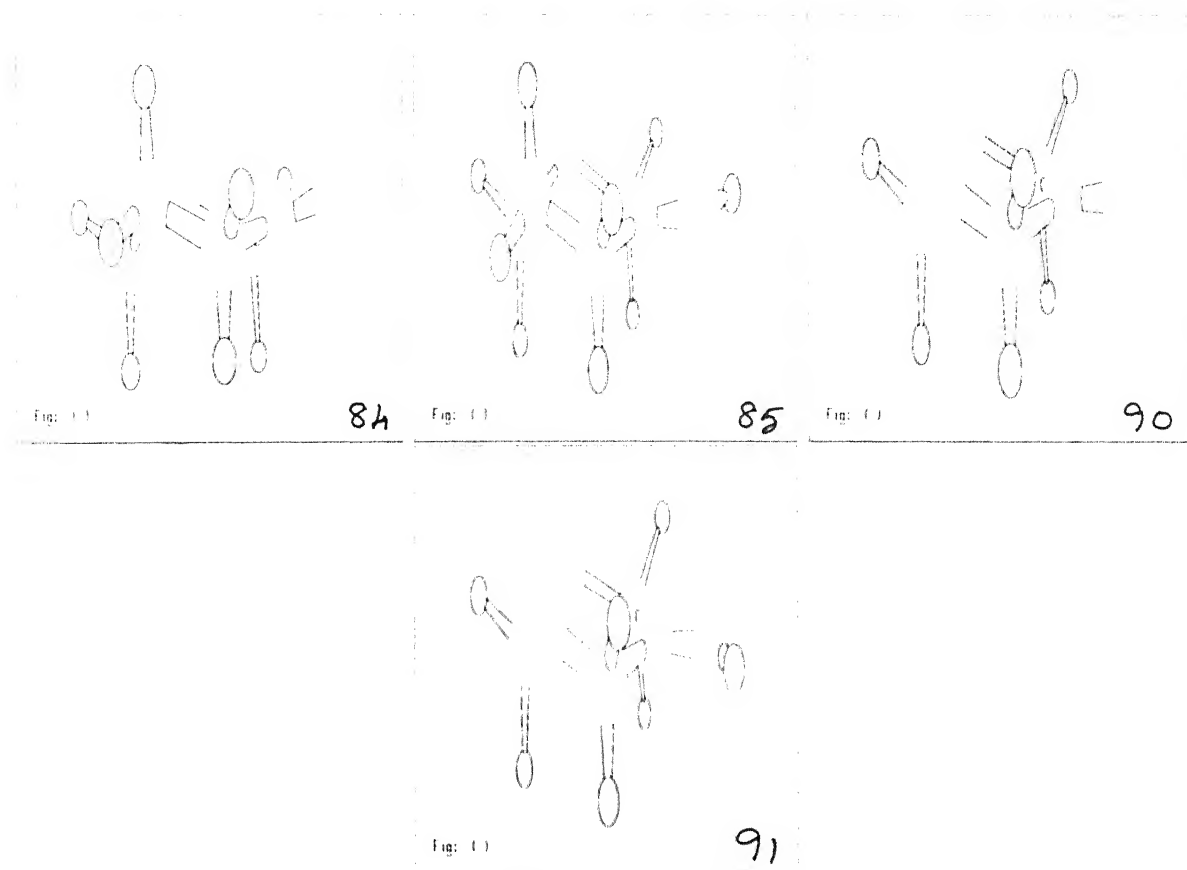


Figure 1.1: 3D structures of 84, 85, 90 and 91

In the event of the cation possessing poor complexing ability, the level of selection must be low for reasons of less carbonyl polarization and, hence, less defined ax/eq disposition of the p orbital. A comparison of 86 and 87 (Table 1.12) brings out these features very clearly. In the complex with  $\text{Li}^+$ , the enhancements in the torsion angles D1 and D2 are 9-10° less than those in the complex with  $\text{H}^+$ . In agreement with this, the relative yield of the equatorial approach of  $\text{AlH}_4^-$  is 10% in the presence of  $\text{Li}^+$  and 15% in the presence of tri-n-octyl-n-propylammonium ion.<sup>32</sup> The ammonium ion has less Lewis acid character than  $\text{Li}^+$ . Again, the high 88% and 80.5% equatorial selectivities observed in the reduction of 4-methylcyclohexanone by, respectively, K-selectride and Li-selectride are necessarily

due to the very high steric interactions involved in the transition state for axial attack; the marginally higher equatorial selectivity observed with K-selectride may be due to the inferior complexing ability of  $K^+$  over that of  $Li^+$ .<sup>109</sup>

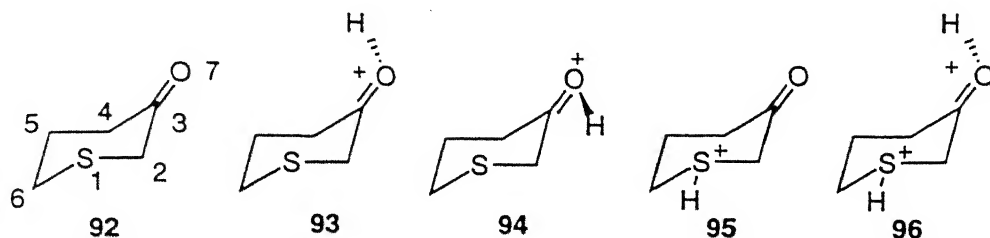


Table 1.14: Angles and Torsion angles in 92-96

Angles	92	93	94	95	96
D1	122.69	105.30	102.21	126.14	151.45
D2	122.91	111.86	107.52	121.71	146.23
A1	120.96	116.46	122.72	118.03	111.59
A2	121.73	122.60	116.46	123.53	122.90

D1=O7C3C2S1, D2=O7C3C4C5

A1=O7C3C2, A2=O7C3C4

We next calculated 3-thiacyclohexanone **92** to see how does the present approach account for the observed equatorial preference of attack by nucleophiles. The stereoelectronic effects and the electron-donating nature of a S-C bond would require the p orbital on the carbonyl carbon to orient antiperiplanar to the S-C bond to constitute an arrangement which will be preferred over that which has them orthogonal. This line of argument is fully supported by the substantial lowering (11-20°) of the torsion angles D1 and D2 on protonation as in **93**, **94**. To reaffirm these observations, we considered imparting electron-withdrawing character to the S-C bond by complexation of S with  $H^+$  as in **95** and studied

the effect of complexation with  $H^+$  on D1 and D2. Sure enough, both the torsion angles enlarged considerably ( $24\text{--}27^\circ$ ). This behavior is similar to that of 3-oxacyclohexanone. The 3D structures of the selected species, before and after protonation are collected in the Fig. 1.2.

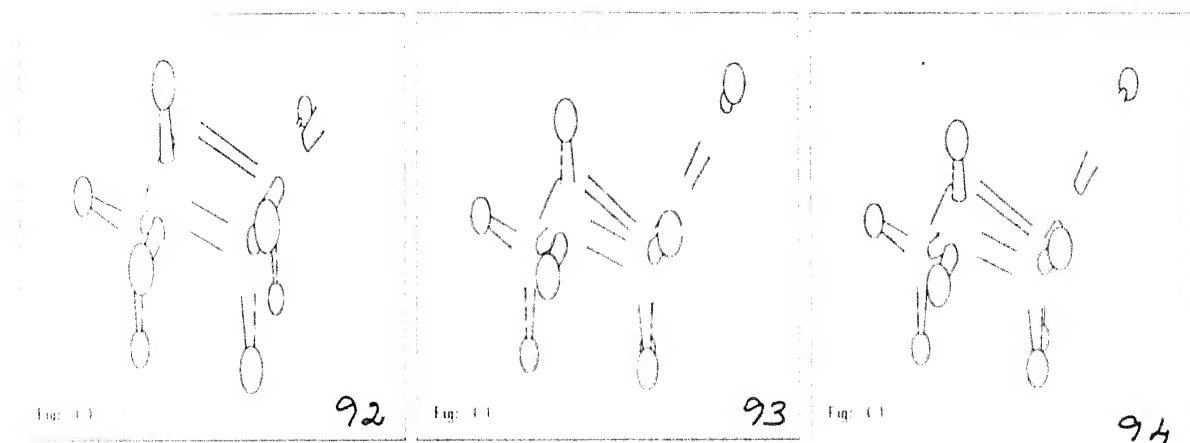


Figure 1.2: 3D structures of **92** to **94**

### 1.2.2 Face Selection of Nucleophilic Reactions to 3-Substituted Cyclohexanones

We have studied 3-Cl- and 3-F-cyclohexanones. The carbonyl oxygen was allowed to complex with  $H^+$  and  $Li^+$  in its  $\sigma$  plane. Again, because there are two distinct sites available for complexation, both were studied.

In Tables 1.15 and 1.16, we have collected D1-D3 parameters for the 3-ax- and 3-eq-Cl-cyclohexanones, respectively. The angles O7C1C6 (=A1) and O7C1C2 (=A2) are also given. The reductions in D1 and D2 in **98** suggest equatorial attack. Although the changes in **100** and **101** are identical, the subtle decreases in the torsion angles support equatorial

attack.

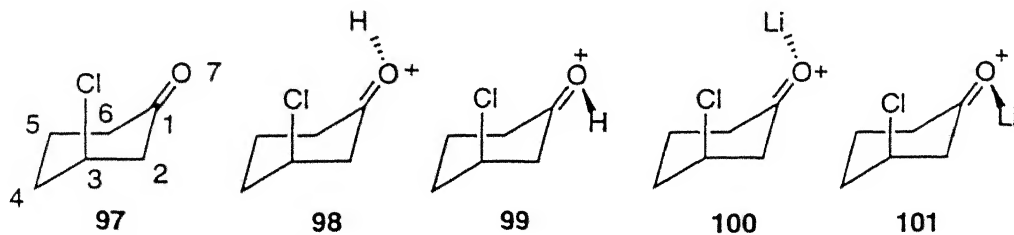


Table 1.15: Angles and Torsion angles in 97-101

Angles	97	98	99	100	101
D1	138.27	135.62	140.72	138.16	138.16
D2	140.47	133.93	138.54	137.56	137.56
A1	122.15	117.21	122.71	121.42	121.42
A2	120.90	122.22	116.00	120.23	120.23

D1=O7C1C6C5, D2=O7C1C2C3

A1=O7C1C6, A2=O7C1C2

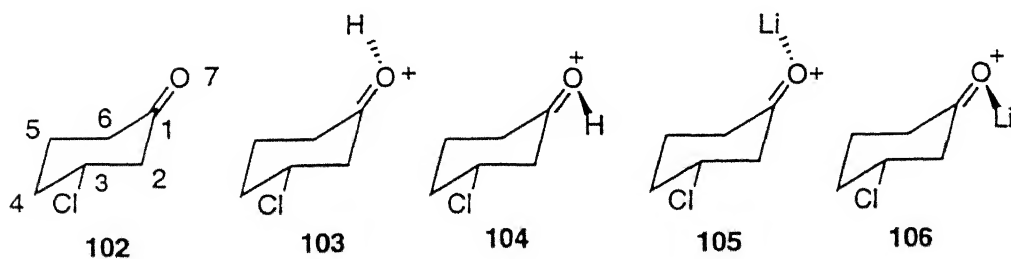


Table 1.16: Angles and Torsion angles in 102- 106

Angles	102	103	104	105	106
D1	134.18	144.89	148.04	141.82	140.74
D2	134.33	145.64	147.80	141.63	141.11
A1	122.32	122.27	116.34	121.07	121.12
A2	121.21	115.73	121.40	120.10	120.14

D1=O7C1C6C5, D2=O7C1C2C3

A1=O7C1C6, A2=O7C1C2

On the contrary, 3-eq-Cl-cyclohexanone (**102**) must prefer axial attack. The torsion angles D1 and D2 are enlarged by  $>10^\circ$  in complexes with  $\text{H}^+$  and  $>6^\circ$  in complexes with  $\text{Li}^+$ . It is interesting to note that the enhancements in D1 and D2 in the complexes of the 3-equatorial derivative are considerably larger than the reductions in the same in the 3-axial counterparts. Consequently, 3-eq-Cl-cyclohexanone may be predicted to display improved  $\pi$ -facial selection in comparison to the 3-ax-Cl-cyclohexanone.

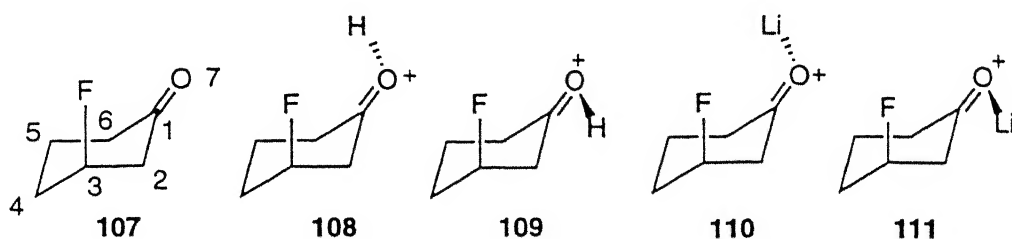


Table 1.17: Angles and Torsion angles in **107-111**

Angles	<b>107</b>	<b>108</b>	<b>109</b>	<b>110</b>	<b>111</b>
D1	138.07	139.44	127.88	130.94	129.38
D2	139.77	136.68	125.92	129.22	127.96
A1	122.08	122.73	117.50	121.77	121.78
A2	121.07	116.13	122.52	120.74	120.86

D1=O7C1C6C5. D2=O7C1C2C3

A1=O7C1C6. A2=O7C1C2

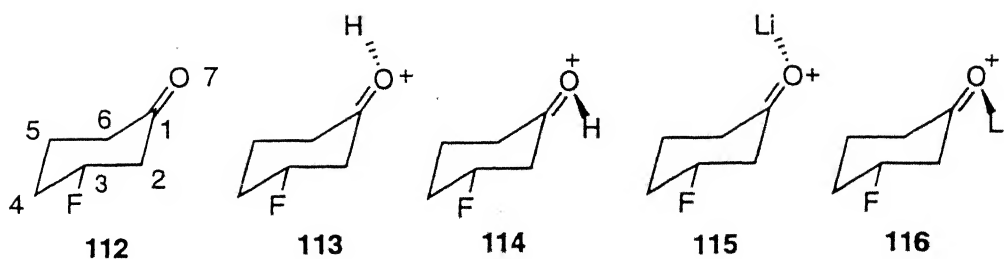


Table 1.18: Angles and Torsion angles in 112-116

Angles	112	113	114	115	116
D1	133.58	147.04	147.13	140.84	142.55
D2	134.59	149.67	149.71	142.26	144.50
A1	122.17	122.05	116.38	121.09	120.93
A2	121.44	115.67	121.39	120.24	120.13

D1=O7C1C6C5, D2=O7C1C2C3

A1=O7C1C6, A2=O7C1C2

Tables 1.17 and 1.18 comprise the results on 3-ax- and 3-eq-F-cyclohexanones, respectively. Analyzed on the patterns of the 3-Cl-cyclohexanones, 3-ax-F-cyclohexanone must undergo equatorial attack and the 3-eq-F-cyclohexanone the axial attack. Looking at the magnitudes of the changes in D1 and D2, an ax-F will be predicted to be a better director for equatorial attack than an ax-Cl atom. A similar observation can be made for the two 3-eq-species where, again, the fluorine appears a better facial control element than chlorine. The present facial selectivity predictions are in excellent accord of the reported predictions of Frenking which are based upon tenuous differential transition state energies. It is known (*vide supra*) from experiments that cyclohexanones bearing 3-equatorial electron-attracting substituents undergo attack by nucleophiles on the axial face.<sup>79</sup> The 3D structures of the selected species, before and after protonation are collected in the Fig. 1.3.

The axial attack on the 3-eq-species can be explained by stereoelectronic effects. The substituent imparts electron-withdrawing character to the C2-C3 bond which, in turn, controls the pyramidalization of the carbonyl carbon and ensures, as much as possible, the arrangement of the enlarged electron-depleted p orbital orthogonal to it.



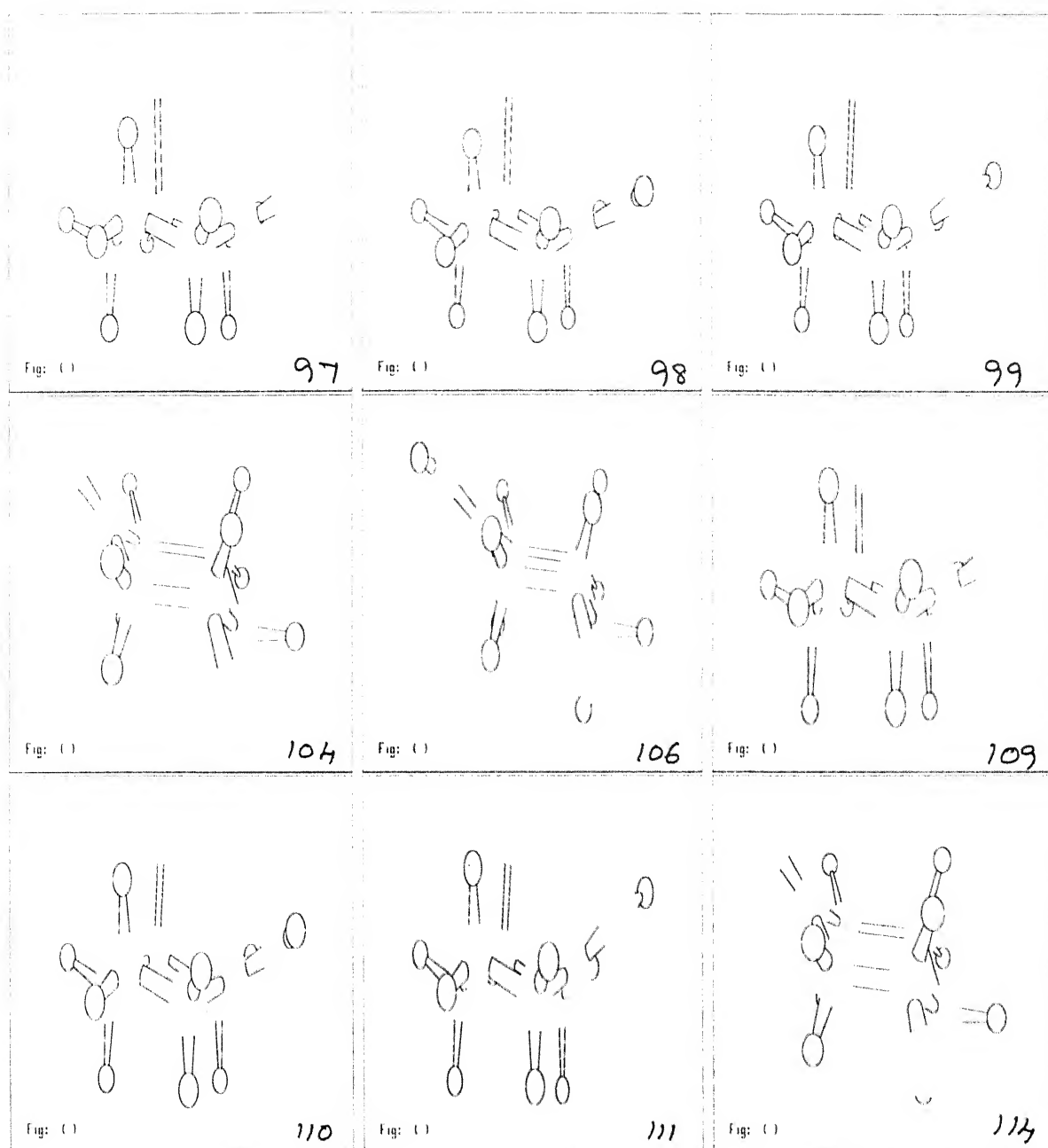


Figure 1.3: 3D structures of 97, 98, 99, 104, 106, 109, 110, 111 and 114

This amounts to axial disposition and, hence, the axial attack by a nucleophile. If these arguments were to hold for the 3-ax-species, as one may like to expect, only axial attack will be predicted. However, the axial orientation of the p orbital will result in a 1,3-dipolar

interaction with the C-F bond. It would, therefore, appear that this dipolar interaction is more important than the stereoelectronic effects arising from the electron-attracting axial substituent. This causes the carbonyl pyramidalization to occur in such a way that the p orbital is oriented equatorial and thus its preferred capture on the equatorial face.<sup>110</sup>

### 1.2.3 Face selection of Nucleophilic Reactions to 4-Substituted Cyclohexanones 117

The relevant geometrical parameters, both before and after complexation with selected cations such as  $H^+$  and  $Li^+$ , are collected in the Table 1.19. It is important to note that all the derivatives retained their chair structures on complexation as well. Whereas the enlargements in the torsion angles D1 and D2 on carbonyl protonation are some  $17^\circ$  at 6-31G level and  $13^\circ$  at 6-31G\* level for the 4-ax-Cl-derivative, the related 4-eq-Cl-derivative computed, on protonation, for much smaller  $5$  and  $6.4^\circ$  changes, respectively. Likewise, whereas the 4-ax-F-cyclohexanone shows an enlargement of about  $15^\circ$  at 6-31G level and  $11^\circ$  at 6-31G\* level in D1 and D2 on carbonyl protonation, these enlargements in the protonated 4-eq-F-cyclohexanone are about  $9$  and  $6^\circ$ , respectively. Both the 4-ax-Cl- and 4-ax-F-cyclohexanones must, therefore, exhibit larger axial selectivity than the corresponding 4-eq-derivatives. The slightly smaller D1 and D2 changes in the protonated 4-ax-F-cyclohexanone in comparison to the protonated 4-ax-Cl-cyclohexanone indicate that an axial chlorine may be a slightly better axial-director than an axial fluorine. All these observations are in excellent accord of the experimental results.<sup>71</sup>

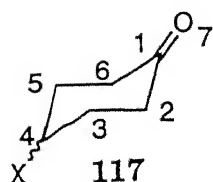
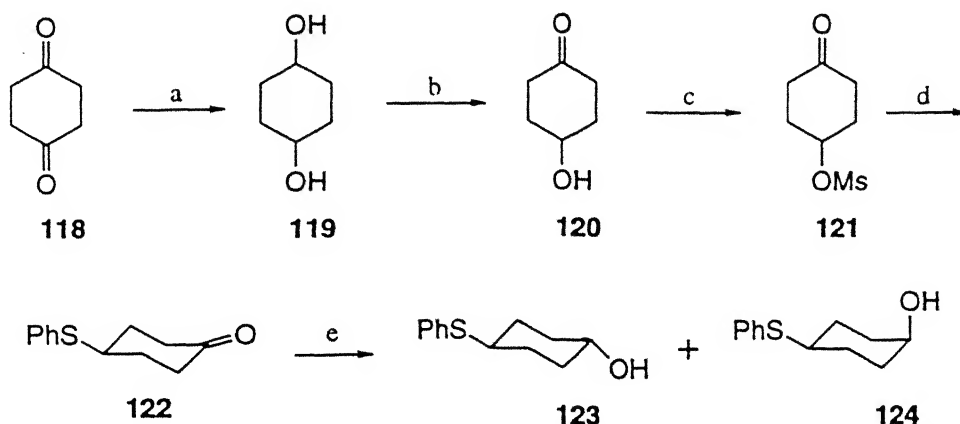


Table 1.19: Angles and Torsion angles in 117

4-X	D1	D2	D3	A1	A2
H	132.22	132.09	180.75	121.89	121.90
	131.53	131.53	179.47	122.31	122.31*
H-H <sup>+</sup>	132.96	132.94	179.60	122.36	121.90
	132.77	132.88	179.94	122.51	117.18*
Cl(a)	132.16	131.92	180.72	121.92	121.94
	132.42	132.42	179.16	122.28	122.28*
Cl(a)-H <sup>+</sup>	148.92	148.40	183.54	115.92	121.68
	145.36	145.12	176.73	116.60	121.98*
Cl(a)-Li <sup>+</sup>	141.76	141.80	182.93	120.55	120.59
Cl(e)	132.13	132.03	180.57	122.00	122.00
	132.52	132.52	179.03	122.39	122.39*
Cl(e)-H <sup>+</sup>	138.51	138.42	181.48	116.62	122.45
	137.48	137.53	178.38	117.14	122.59*
Cl(e)-Li <sup>+</sup>	133.65	133.78	180.86	121.20	121.20
F(a)	132.17	132.45	180.96	121.96	121.93
	131.52	131.52	179.31	122.39	121.39*
F(a)-H <sup>+</sup>	147.51	146.72	183.56	116.03	121.80
	142.92	142.59	177.06	116.78	122.16*
F(a)-Li <sup>+</sup>	143.79	143.93	183.78	120.45	120.46
F(e)	133.00	132.85	180.94	121.97	121.98
	133.04	133.03	178.96	122.34	122.34*
F(e)-H <sup>+</sup>	142.14	142.32	182.60	116.47	122.26
	139.17	139.22	177.80	117.06	122.50*
F(e)-Li <sup>+</sup>	134.37	134.07	181.04	121.18	121.18
OH(a)	132.60	132.54	180.84	121.72	122.12
OH(a)-H <sup>+</sup>	147.13	145.71	183.06	116.03	121.76
OH(e)	132.16	132.20	180.68	122.01	122.00
OH(e)-H <sup>+</sup>	142.73	140.95	182.08	116.41	122.20
SH(a)	132.53	132.15	180.74	121.90	121.91
	132.33	132.35	179.21	121.35	121.25*
SH(a)-H <sup>+</sup>	146.80	146.54	182.85	116.07	121.69
	143.66	143.86	177.12	112.25	121.97*
SH(e)	131.95	132.06	180.62	122.01	122.00
	131.60	131.60	179.42	122.43	122.43*
SH(e)-H <sup>+</sup>	133.00	133.20	179.53	116.82	122.56
	135.96	135.89	179.05	117.18	122.55

D1=O7C1C2C3, D2=O7C1C6C5, D3=C6C1O7C2

Further, the relatively larger torsion angle changes in the 4-eq-F-derivative in comparison to the 4-eq-Cl-species may be predictive of slightly better axial diastereoselection with the former. Unfortunately, no such experimental results are reported to allow us to confirm this prediction. The 3D structures of the selected species, before and after protonation, are collected in the Fig. 1.4. Since good experimental results are reported for the 4-OH-*trans*-1-decalones,<sup>71</sup> we have computed 4-OH-cyclohexanones as well. The results are revealing. Better axial diastereoselectivity must be predicted for 4-ax-OH-cyclohexanone than that for the corresponding equatorial derivative. Accordingly, *trans*-1-decalone exhibits 85% and 61% axial diastereoselection for the 4-ax- and 4-eq-OH substituents, respectively. The related SH-derivatives were also computed. For both the ax- and eq-4-SH-derivatives, axial nucleophilic attack appears to be favored for the enhancements in the said torsion angles. These selectivities appear to be slightly lower than those for the respective Cl-derivatives for the slightly smaller torsion angle changes. We ourselves have determined the selectivity of 4-eq-SPh-cyclohexanone **122** in reductions with LAH in Et<sub>2</sub>O, NaBH<sub>4</sub> in methanol, and Na(CN)BH<sub>4</sub> in MeOH at pH 1.0. The axial attacks, computed from <sup>1</sup>H NMR integrals, were 55, 61, and 64%, respectively. As against the 61% axial selectivity of 4-eq-SPh-cyclohexanone in reduction with NaBH<sub>4</sub> in MeOH, the axial selectivity of *trans*-4-eq-Cl-*trans*-1-decalone is reported at 71%.<sup>71, 83</sup> The slightly larger selectivity with Na(CN)BH<sub>4</sub> may be a consequence of tighter cation-carbonyl complexation, protonation in this case. Otherwise symmetric to a plane, the molecules must lose this symmetry on cation-complexation and, hence, the differences in the bond angles A1 and A2. The 4-eq-SPh-cyclohexanone **122** was prepared from cyclohexane-1,4-dione **118** as shown in the scheme below.



Reagents: a. LAH, Et<sub>2</sub>O; b. Jones' reagent; c. MsCl, Et<sub>3</sub>N, CH<sub>2</sub>Cl<sub>2</sub>, 0 °C;  
d. PhSNa, THF, 0 °C to rt, 4h; e. reducing reagent, solvent, 0 °C to rt

The spectral characteristics of the diol 119 and the ketoalcohol 120 were in accord of the literature.<sup>111</sup> The oxidation of 119 to 120 was accomplished following the literature.<sup>111</sup> The mesylate 121 was reacted with the sodium salt of thiophenol in THF at 0° to rt for 4 h to furnish the desired 4-eq-SPh-cyclohexanone 122 whose <sup>1</sup>H characteristics were as those reported in the literature.<sup>112</sup> The hydrogen on the carbinol carbon in the reduced products 123 and 124 resonated at  $\delta$  3.70-3.62 (well resolved heptet) and 3.87-3.84 (illresolved multiplet), respectively. Likewise, the C4-H resonated, respectively, at  $\delta$  3.07-2.98 (m) and 3.30-3.25 (m).

The net atomic charges on selected atoms are collected in the Table 1.20. Four points become immediately obvious: (i) the carbonyl carbon becomes more electron-deficient on complexation, its magnitude being more or less the same irrespective of whether the substituent is axial or equatorial. (ii) C4 in all  $\pm F$ -derivatives is moderately positively charged whereas the same in the 4-Cl-derivatives carries appreciable negative charge, (iii) the fluorine atom in all the fluorinated derivatives is substantially negatively charged whereas the respective chlorine atom is either very poorly negatively charged or it is near neutral, and (iv) the charge distribution for the C-S bond is similar to that of the C-Cl bond.

Table 1.20: Net Mulliken atomic charges on selected atoms in 117.

X	O	C1	C2	C3	C4	X
H	-0.545	0.496	-0.394	-0.315	-0.310	
	-0.530	0.536	-0.410	-0.332	-0.321*	
H-H <sup>+</sup>	-0.630	0.653	-0.460	-0.323	-0.335	
	-0.559	0.600	-0.459	-0.349	-0.347*	
F(a)	-0.541	0.488	-0.396	-0.352	0.245	-0.479
	-0.527	0.532	-0.419	-0.373	0.264	-0.430*
F(a)-H <sup>+</sup>	-0.634	0.653	-0.468	-0.352	0.223	-0.461
	-0.562	0.599	-0.449	-0.389	0.241	-0.412*
F(e)	-0.533	0.499	-0.417	-0.352	0.279	-0.475
	-0.522	0.542	-0.432	-0.379	0.302	-0.425*
F(e)-H <sup>+</sup>	-0.628	0.662	-0.485	-0.358	0.279	-0.437
	-0.556	0.607	-0.462	-0.403	0.304	-0.388*
Cl(a)	-0.537	0.491	-0.398	-0.315	-0.312	-0.117
	-0.525	0.535	-0.418	-0.335	-0.248	-0.118*
Cl(a)-H <sup>+</sup>	-0.633	0.659	-0.475	-0.308	-0.367	-0.029
	-0.561	0.604	-0.451	-0.349	-0.284	-0.048*
Cl(e)	-0.531	0.498	-0.407	-0.297	-0.343	-0.074
	-0.520	0.540	-0.423	-0.324	-0.262	-0.090*
Cl(e)-H <sup>+</sup>	-0.627	0.658	-0.470	-0.297	-0.406	0.054
	-0.556	0.604	-0.451	-0.345	-0.296	0.011*
SH(a)	-0.542	0.496	-0.395	-0.302	-0.420	-0.024
	-0.528	0.538	-0.414	-0.330	-0.317	-0.069*
SH(a)-H <sup>+</sup>	-0.634	0.661	-0.446	-0.306	-0.465	-0.054
	-0.562	0.606	-0.446	-0.345	-0.350	-0.039*
SH(e)	-0.537	0.496	-0.400	-0.289	-0.449	-0.058
	-0.524	0.538	-0.416	-0.319	-0.339	-0.042*
SH(e)-H <sup>+</sup>	-0.628	0.654	-0.444	-0.300	-0.496	0.162
	-0.558	0.602	-0.445	-0.339	-0.370	0.045*

\* From calculation at 6-31G\* level

The magnitudes of the charges on C4 and the heteroatom on it clearly indicate that the polarity of the C-Cl and C-S bonds are opposite to that of the C-F bond. That the C-Cl bond is electron-donating finds support from a recent report of Alkorta *et al.*<sup>113</sup> Thus, the electron-donating Cl(a)-C4 bond may be expected to raise the electron density on the face axial for the carbonyl. This may further stabilize, by interaction through space, the axially oriented p orbital on the carbonyl carbon. Though this interaction is likely to be weak for the long distance between the two interacting orbitals, a somewhat enhanced axial selectivity from 4-ax-Cl-cyclohexanone in comparison to that from 4-ax-F-cyclohexanone may, however, be predicted. This finds decent experimental support.<sup>71</sup> The electron-attracting C-F bond in the 4-eq-F-cyclohexanone renders the C2-C3 and C5-C6 ring bonds electron-deficient which, in turn and in cooperation with the electron-donating C2-H(a) and C6-H(a) bonds, would enhance further the axial orientating ability of the p orbital on the carbonyl carbon. On the contrary, the electron-donating character of the C-Cl bond in 4-eq-Cl-cyclohexanone would render the C2-C3 and C5-C6 bonds slightly more electron-rich than those in the parent unsubstituted cyclohexanone and reduce, thereby, the axial orienting propensity of the carbonyl p orbital. A reduction in the level of axial attack in 4-eq-Cl-cyclohexanone in comparison to the 4-eq-F-cyclohexanone may, therefore, result. This is in line with the larger torsion angle changes in the former on protonation. The contribution of sulfur is fairly similar to that of Cl. The differential C-F vs C-Cl polarity features are likely to contribute significantly to the facial discrimination in 2-ax-halocyclohexanones. A reversal in facial selectivity in such cases appears imminent (*vide infra*).

The study of C2-H and C3-H bond lengths (Table 1.21), both before and after protonation, is also revealing. Whereas both the C3-H(a) and C3-H(e) bonds have shortened on protonation, on one hand, both the C2-H(a) and the C2-H(e) bonds are enlarged, on the other hand. Since the C2-H bonds are on the carbon adjacent to the carbonyl func-

tion, they are likely to influence the carbonyl chemistry much more than any other C-H bond elsewhere in the molecule. From the data on 6-31G level, the following two points emerge: (i) the elongation in the C2-H(a) bond on protonation is more pronounced than the elongation in the C2-H(e) bond. This is to suggest further improved interaction of the former with the carbonyl function on cation complexation. The p orbital on the carbonyl carbon is enabled to develop more on the axial face for favorable stereoelectronic effects and, hence, the increased axial attack of nucleophiles. (ii) On protonation, the elongation in C2-H(a) in 4-ax-species is 1.5-6.0 times the elongation in the same in species with 4-eq-substitution and almost 10 times the elongation in the unsubstituted cyclohexanone. These, when coupled with the observation above, may be taken to reveal that the TS for axial attack in a 4-ax-substituted cyclohexanone must be of lower barrier than the TS for axial attack on a 4-eq-substituted cyclohexanone, and further that the 4-ax-substituted cyclohexanones must react faster than cyclohexanone itself. Both the revelations are in accord of experiments<sup>71</sup> (Table 1.9).

Agreed that the (uncomplexed) molecules in question have plane of symmetry, the environment in the immediate neighborhood of the carbonyl and, hence, its two faces can never be the same for the ring arrangement of nuclei. The C2-H(a) and C6-H(a) bonds must interact with the carbonyl  $\pi$ -bond to perturb its charge distribution for their antiperiplanar relationship and, thus, accommodate their known higher acidity and faster exchangeability than those of the equatorial hydrogens. Consequently, the depletion of electron density must be more from the axial face than that from the alternate equatorial direction. This interaction is, in fact, typical of such a spatial arrangement observed in 2-ax-X-cyclohexanones (X = Cl, Br, OH, OAc) where the UV- $\lambda_{\text{max}}$  shift to higher values by 10-30 nm.<sup>114</sup>



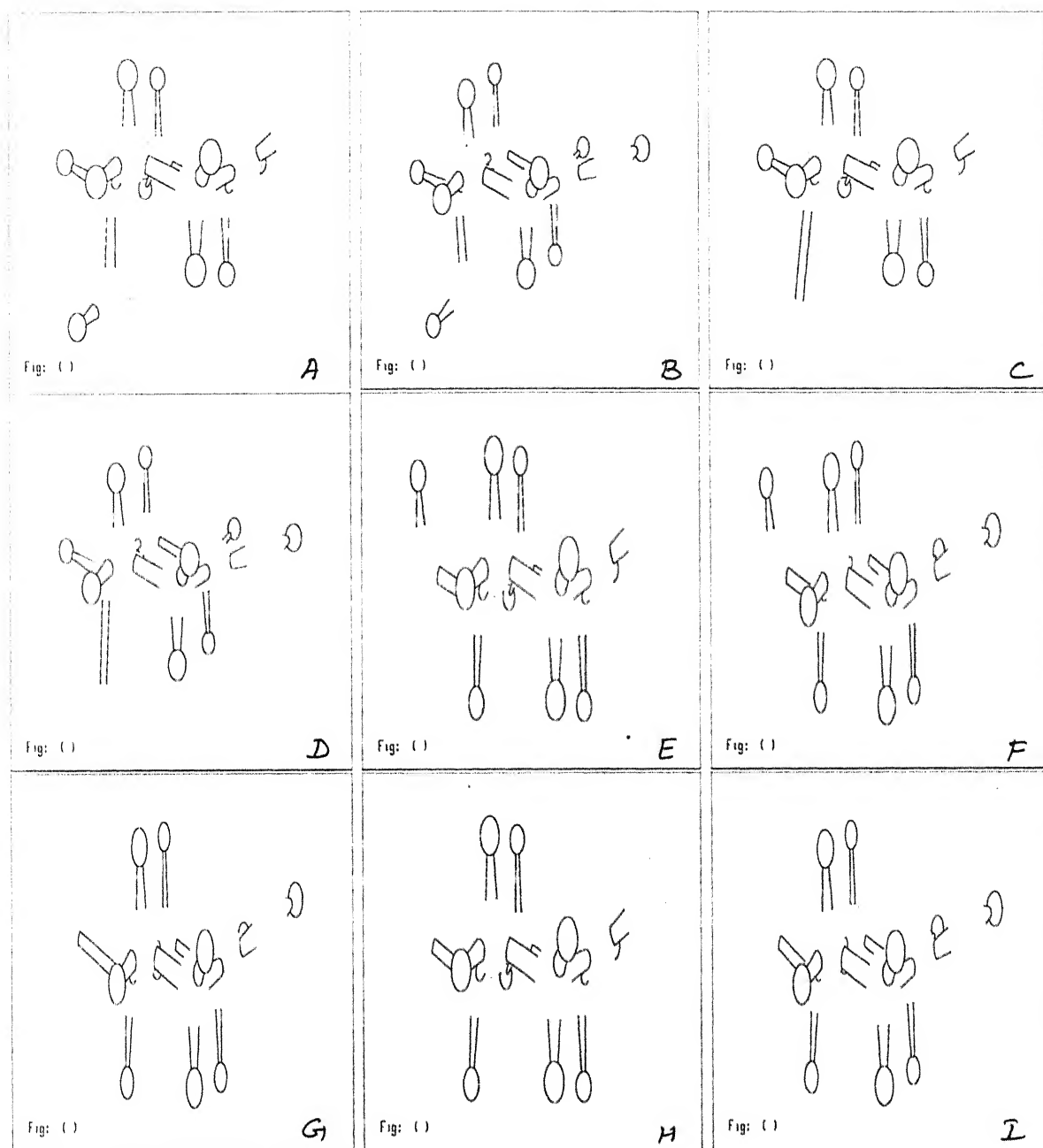


Figure 1.4: 3D structure of both protonated and unprotonated 4-X-cyclohexanones A. X=OH(a) B. A-H<sup>+</sup> C. X=Cl(a) D. C-H<sup>+</sup> E. X=OH(e) F. E-H<sup>+</sup> G. X=Cl(e)-H<sup>+</sup> H. X=F(e) I. H-H<sup>+</sup>

Table 1.21: Bond lengths in **117**.

X	C2-H2(a)	C2-H2(e)	C3-H3(a)	C3-H3(e)
H	1.0887	1.0816	1.0868	1.0843
	1.0895	1.0826	1.0878	1.0854*
H-H <sup>+</sup>	1.0893	1.0831	1.0843	1.0810
	1.0894	1.0844	1.0853	1.0819*
F(a)	1.0859	1.0810	1.0859	1.0825
	1.0869	1.0822	1.0870	1.0843*
F(a)-H <sup>+</sup>	1.0913	1.0833	1.0832	1.0802
	1.0905	1.0813	1.0846	1.0816*
F(a)-Li <sup>+</sup>	1.0884	1.0810	1.0845	1.0810
F(e)	1.0888	1.0806	1.0847	1.0825
	1.0895	1.0819	1.0865	1.0843*
F(e)-H <sup>+</sup>	1.0922	1.0831	1.0831	1.0804
F(e)-Li <sup>+</sup>	1.0893	1.0803	1.0841	1.0810
Cl(a)	1.0860	1.0811	1.0881	1.0813
	1.0869	1.0823	1.0882	1.0830*
Cl(a)-H <sup>+</sup>	1.0919	1.0838	1.0853	1.0797
	1.0911	1.0818	1.0857	1.0808*
Cl(a)-Li <sup>+</sup>	1.0884	1.0811	1.0867	1.0803
Cl(e)	1.0884	1.0810	1.0841	1.0815
	1.0892	1.0821	1.0856	1.0831*
Cl(e)-H <sup>+</sup>	1.0909	1.0832	1.0829	1.0799
	1.0910	1.0814	1.0842	1.0811*
Cl(e)-Li <sup>+</sup>	1.0889	1.0808	1.0837	1.0805
SH(a)	1.0861	1.0814	1.0880	1.0836
	1.0868	1.0825	1.0885	1.0849*
SH(a)-H <sup>+</sup>	1.0919	1.0808	1.0858	1.0809
	1.0908	1.0817	1.0862	1.0819*
SH(e)	1.0884	1.0814	1.0865	1.0819
	1.0893	1.0825	1.0876	1.0832*
SH(e)-H <sup>+</sup>	1.0898	1.0797	1.0847	1.0800
	1.0905	1.0815	1.0856	1.0809*

\* From calculation at 6-31G\* level

Shi and Boyd<sup>23</sup> have implicated, at least in part, the electrostatic repulsion between

the attacking nucleophile and the C2-H(a) bond in the equatorial TS to explain its larger energy barrier compared to that of the axial TS where such a repulsion does not exist. They have computed the C2-H(a) bond to be more electron rich than the C2-C3 bond. As stated above, the C2-H(a) bond is geometrically parallel to the carbonyl  $\pi$ -plane and, hence, its electron density must be hyperconjugatively delocalized into the latter to render it actually electron deficient, more so on cation complexation, as we have observed in the present study. We, therefore, disfavor Boyd's above contention of electrostatic repulsion. The electron-deprived p orbital on the carbonyl carbon that has oriented axial and, hence, the resultant flattening, both on cation complexation, may be reasons enough to accommodate the difference in barriers.<sup>115</sup>

We conclude that the torsion angle changes<sup>116</sup> around the carbonyl carbon of 4-substituted cyclohexanones after cation complexation predict well the facial discrimination in reactions with nucleophiles. The hyperconjugative electron donations from C2-H(a) and C6-H(a) to the electron-depleted p orbital on the carbonyl carbon make them electron-deficient and, hence, any electrostatic repulsion for a nucleophile in an equatorial attack, as proposed by Shi and Boyd,<sup>23</sup> can be ruled out safely. The 4-axial substituents exert their influence on diastereoselectivity primarily through the field effects.

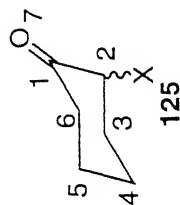
#### 1.2.4 Face Selection of Nucleophilic Reactions to 2-Substituted Cyclohexanones 125

First, we consider 2-ax-halo-cyclohexanones. The results demonstrate that it is indeed prudent to rely on the torsion angle changes around the carbonyl carbon upon cation complexation to predict the facial preference of nucleophilic attacks and that the 2-ax-Cl- and the 2-ax-F-cyclohexanones must exhibit, respectively, axial and equatorial selectivities under conditions of strong cation complexation. The torsion angle changes are in perfect tune with the stereoelectronic stabilization of the electron-poor p orbital. It is important

to note that the rigidity of the 6-ring geometry is very likely to limit the geometrical changes ensued upon complexation and, thus, disallow the full impact from being realized. In the Table 1.22, we have collected data on the relevant torsion angles, bond angles and the total energies (Hartrees). The data on cyclohexanone itself are, once again, to serve quick comparison. We have mimicked the complexation by using  $H^+$ . In a few cases where we have used  $Li^+$ , the calculated trend in parameter changes was found to be the same as that calculated<sup>117</sup> from complexation with  $H^+$ . The quantum of geometrical changes with  $Li^+$  was, however, lower than that with  $H^+$ . From the total energy data, it is clear that a complexation of the oxygen electron pair which is app to C2 is favored over the alternate arrangement in which the other electron pair which is *syn* to C2 is complexed. The enlargements in D1 and D2 in the Cl-derivatives indicate the development of the electron-poor p orbital on the axial face. A preference for axial attack must, therefore, be predicted. This is in full accord with experiments.<sup>70, 84</sup> The same parameters for the F-derivatives have, however, reduced to almost a tetrahedral value to indicate that the said p orbital has developed on the equatorial side and, hence, an equatorial attack must be in order.

Since the ground state structures after cation complexation will lead to the TS structures, the near tetrahedral values of D1 and D2 leave little room for a nucleophile to approach the carbonyl from the axial face. Given that the angle of nucleophilic attack must be greater than  $90^\circ$ , the trajectory of attack on the axial face in protonated 2-ax-F-cyclohexanone will, at best, be some  $20^\circ$  away from C3 and C5. This translates into the reaction trajectory passing very close to the C3- and C5-ax-hydrogens. On the contrary, the increased exposure of the equatorial face is very likely to insure the very minimal torsional effects in the equatorial nucleophilic approach. The genesis of the above differential facial preference is evident in the uncomplexed species as well. D1 and D3 in 2-ax-F-cyclohexanone are  $6-9^\circ$  smaller than those in 2-ax-Cl-cyclohexanone. The diastereoselec-

Table 1.22: Angles and Torsion Angles in 125



X	D1=O7C1C2C3	D2=O7C1C6C5	D3=C6C1O7C2	A1=O7C1C2	A2=O7C1C6	E(Hartrees)
H	131.53	131.53	179.47	122.31	122.31	
H-H <sup>+</sup>	132.72	132.88	179.94	122.51	117.18	
Cl(a)	128.71	126.85	176.96	120.29	123.62	
Cl(a)-H <sup>+</sup> ( <i>anti</i> )	137.57	135.36	179.84	115.71	123.30	-767.125659
Cl(a)-H <sup>+</sup> ( <i>syn</i> )	143.76	141.73	178.30	121.12	117.48	-767.124484
Cl(a)-Li <sup>+</sup> ( <i>anti</i> )	140.30	139.89	178.79	119.50	122.14	-774.1154899
Cl(a)-Li <sup>+</sup> ( <i>syn</i> )	140.24	137.80	178.83	119.49	122.16	-774.1154897
F(a)-H <sup>+</sup> ( <i>anti</i> )	110.27	112.34	171.73	116.67	124.74	-407.0757978
F(a)-H <sup>+</sup> ( <i>syn</i> )	111.80	114.42	172.58	122.31	119.21	-407.0735924
F'(a)	119.33	120.78	175.69	121.32	124.34	
OH(a)	129.78	129.82	179.27	121.26	123.35	
OH(a)-H <sup>+</sup> ( <i>anti</i> )	114.58	115.95	173.85	116.96	124.13	-383.0852836
OH(a)-H <sup>+</sup> ( <i>syn</i> )	112.94	115.26	173.46	122.67	118.53	-383.0823954
SH(a)	137.65	134.93	179.25	120.36	122.61	
SH(a)-H <sup>+</sup> ( <i>anti</i> )	145.25	142.89	178.20	116.03	121.91	-705.7424785
SH(a)-H <sup>+</sup> ( <i>syn</i> )	141.76	139.96	178.78	121.72	116.53	-705.7396457
OH(c)	128.35	129.17	179.85	120.45	123.54	
OH(c)-H <sup>+</sup> ( <i>anti</i> )	127.46	126.92	178.45	111.07	123.04	-383.0852401
OH(c)-H <sup>+</sup> ( <i>syn</i> )	125.87	126.88	177.37	119.29	120.17	-383.0997800
F'(c)	125.79	126.71	179.17	122.34	123.57	
F'(c)-H <sup>+</sup> ( <i>anti</i> )	121.33	125.09	177.40	116.95	124.10	-407.0769543
F'(c)-H <sup>+</sup> ( <i>syn</i> )	123.53	125.30	176.47	119.62	120.43	-407.0859729

The torsion angles D1-D3 represent the angles on the axial face. Their signs have, therefore, been omitted.

All the values in the table are obtained from calculations at HF/6-31G\* level of theory.

tivity of 2-ax-F-cyclohexanone has not been reported. For a greater visual appreciation of the effects of such geometrical changes, the 3D structures of the selected species, before and after protonation, are collected in the Fig.1.5.

Table 1.23 lists the net Mulliken and NBO charges on selected atoms in both protonated and unprotonated species. A close inspection reveals the followings:

(a) Whereas the C2 in all the 2-ax-Cl-derivatives is sufficiently electron rich, the Cl atom itself bears only slight positive charge to indicate electron release from Cl to C2. This is in agreement with a recent report from Alkorta *et al.*<sup>113</sup> This will help the electron-poor orbital on carbonyl carbon orient axial for their app arrangement. An axial nucleophilic attack must, therefore, be in order.

(b) The C2 in all the 2-ax-F-derivatives is moderately positively charged and the attached fluorine bears sufficient negative charge. This leads to electron withdrawal from C2 to F and, hence, stereoelectronic destabilization of any axially oriented electron-poor orbital on the carbonyl carbon. Consequently, the geometrical changes, specifically the torsion angle changes, take a course which is opposite to that in the related Cl-derivatives. This allows the electron-poor orbital develop predominantly on the equatorial face. A preference for equatorial attack must, therefore, be predicted.

(c) Though the positive charges on both the axial and equatorial hydrogens on C6 go up on complexation, this is more prevalent for the axial hydrogen than that for the equatorial one. This is to indicate greater interaction of an axial C-H bond over that of an equatorial one with the carbonyl function. This is not surprising given the fact that the axial C-H bond orbital is parallel to the p orbitals of the carbonyl  $\pi$ -bond. Likewise, an axial C2-X bond will also be expected to moderate<sup>114</sup> the chemistry of the carbonyl function by virtue of being in interaction with it. This interaction becomes more important after complexation because the orbital coefficient on carbonyl carbon is now enlarged to seek greater electron donation to it. It is this additional electron requirement that necessitates

Table 1.23: Net atomic charges in 125

X	O	C1	C2	C6	C6-Ha	C6-He	X
H	-0.5298	0.5364	-0.4099	-0.4099	0.1792	0.2054	.....*
Cl	-0.5063	0.55536	-0.3352	-0.4130	0.2080	0.2113	-0.0898
	-0.6031	0.6700	-0.2732	-0.5305	0.2463	0.2503	-0.0975*
Cl-H <sup>+</sup> ( <i>anti</i> )	-0.5489	0.6059	-0.3615	-0.4574	0.2936	0.2431	0.0489
	-0.6343	0.8511	-0.3088	-0.5702	0.3090	0.2655	0.0155*
Cl-H <sup>+</sup> ( <i>syn</i> )	-0.5505	0.6131	-0.3878	-0.4434	0.2844	0.2791	0.0626
F	-0.5154	0.4947	0.2942	-0.4109	0.2034	0.2075	-0.4265
	-0.6092	0.6476	0.1994	-0.5321	0.2437	0.2469	-0.44404*
F-H <sup>+</sup> ( <i>anti</i> )	-0.5536	0.5543	0.2168	-0.4556	0.2941	0.2446	-0.3776
	-0.66376	0.8344	0.2004	-0.5732	0.3073	0.2649	-0.4030*
F-H <sup>+</sup> ( <i>syn</i> )	-0.5500	0.5585	0.2009	-0.4388	0.2825	0.2762	-0.3688
SH	-0.5262	0.5482	-0.4055	-0.4125	0.2071	0.2078	-0.0571
	-0.6251	0.6779	-0.4480	-0.5302	0.2067	0.2487	-0.0276*
SH-H <sup>+</sup> ( <i>anti</i> )	-0.5716	0.5985	-0.4429	-0.4586	0.2902	0.2397	0.0595
	-0.6540	0.8350	-0.4738	-0.5645	0.3060	0.2643	0.0771*
SH-H <sup>+</sup> ( <i>syn</i> )	-0.5658	0.6121	-0.4735	-0.4408	0.2820	0.2732	0.0825
	-0.6464	0.8433	-0.4971	-0.5501	0.3008	0.2864	0.0904*
OH	-0.5299	0.5093	0.0736	-0.4039	0.1981	0.2028	-0.7501
	-0.6248	0.6598	0.0717	-0.5316	0.2428	0.2444	-0.8039*
OH-H <sup>+</sup> ( <i>anti</i> )	-0.5593	0.6026	0.0748	-0.4485	0.2997	0.2359	-0.7357
	-0.6399	0.8665	0.0712	-0.5721	0.3115	0.2594	-0.7997*
OH-H <sup>+</sup> ( <i>syn</i> )	-0.5586	0.5867	0.0442	-0.4310	0.2809	0.2684	0.7130

The anti and syn in the first column indicate protonation anti and syn to C2, respectively.

\* These numbers are obtained from Natural Bond Orbital (NBO) analyses.

We have also computed 2-ax-SH- 2-ax-OH-cyclohexanones and their protonated derivatives. The relevant geometrical parameters such as D1-D3 and A1-A2 are given in the Table 1.22 and the net atomic charges on selected atoms in the Table 1.23. D1 and D2 are enlarged by some 8° on complexation in favor of axial attack to 2-ax-SH-cyclohexanone. This is fully supported from a recent report<sup>86</sup> on 2-ax-SMe-cyclohexanone which underwent exclusive axial attack on reduction with hydrides. The data on atomic charges indicate the

behavior of S to be similar to that of Cl. In contrast, the torsion angles D1 and D2 in 2-ax-OH-cyclohexanone are reduced by  $15^\circ$  on carbonyl protonation to indicate equatorial orientation of the p orbital and, hence, equatorial attack. This prediction is also in excellent accord with experiments. The reaction of *trans*-4-Bu<sup>t</sup>-2-OMe cyclohexanone with allylindium generated predominantly the axial carbinol.<sup>88</sup> The reaction with ally chromium was also highly selective to the axial carbinol. Thus, our model which so correctly recognizes the 2-ax-Cl- and 2-ax-SH-cyclohexanones for their axial diastereoselectivities and the 2-ax-OH-cyclohexanone for its equatorial selectivity is very likely to correctly interpret the 2-ax-F-cyclohexanone as well for its equatorial attack. The equatorial attack in 2-ax-O-substituted cyclohexanones may be additionally enhanced through chelation-controlled equatorial delivery of the nucleophile.<sup>88</sup>

Since very high equatorial selectivity has been observed for *cis*-4-Bu<sup>t</sup>-2-methoxy cyclohexanone in reaction with allyl nucleophiles derived from various sources,<sup>88</sup> it became highly pertinent to study such a system as well. We have computed 2-eq-OH-cyclohexanone, both before and after protonation. The 2-eq-F-cyclohexanone was also computed for the purposes of comparison yet once again because both had predicted for equatorial selectivity in the axial series. The geometrical parameters of significance are collected in Table 1.22. Here, the protonation *syn* to C2 was energetically more beneficial than the alternate *anti* to C2 protonation. the energy differences were as much as 9.12 and 5.66 kcal/mol OH- and F-substituted derivatives. The geometrical changes on protonation are such that the C2-X bond goes more in the plane of the C=O  $\sigma$  bond. Consequently, the torsion angle X8C2C1O7 is reduced from 5.35 to  $2.65^\circ$  in the HO-derivative and from 4.04 to  $2.04^\circ$  in the F-derivative. During the process, the torsion angles D1 and D2 are reduced to facilitate equatorial attacks. The congestion on the axial face coupled with the possible cation-chelation by these substituents may further promote equatorial attack.

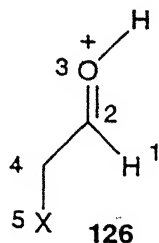
In conclusion, we have developed an approach to the understanding as well as prediction



of the diastereofacial selectivity of substituted 2-ax-cyclohexanones ( $X = \text{Cl}, \text{F}, \text{OH}, \text{SH}$ ). Whereas the Cl- and the S-derivatives are predicted for axial attack and the O-derivatives for equatorial attack in conformity of experiments, the F-derivative must exhibit equatorial preference. The results for the F and oxygen substituents are to be contrasted with the Anh-Felkin model and the TS models of both Houk and Frenking which predict axial preference for enhanced torsional effects in the alternate equatorial transition states.

### 1.2.5 Acyclic system

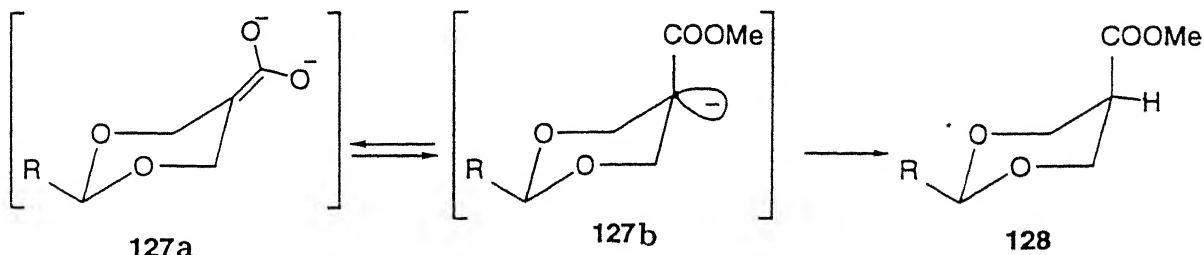
The above heteroatom-based geometrical changes are general. We have computed<sup>117</sup> at 6-31G\* level, the 2-Cl-, 2-F-, and 2-SH-acetaldehydes **126**, both before and after carbonyl protonation. The torsion angle X5C4C2O3 changed from 156.49 to 110.84° for  $X=\text{Cl}$  and from 129.37 to 98.2° for  $X=\text{SH}$  on protonation. Both of these changes are in line with the arguments presented above and indicate the participation of both the C-Cl and C-S bonds in stereoelectronic stabilization of the protonated carbonyl through electron donation. Again, both the Cl and S atoms in the respective species bear positive charge and the carbon to which they are attached is significantly negatively charged. The magnitudes of these charges increased considerably on carbonyl protonation. For  $X=\text{F}$ , the said torsion angle changed little and was near zero in either species. This is to indicate an orthogonal arrangement of the C-F bond with the  $\pi$  orbitals of the carbonyl system. Also, whereas the carbon bearing F is slightly positively charged, F itself bears significant negative charge in both the unprotonated and the protonated species. These charge distributions are clear indications of the strong electron-attracting nature of a C-F bond as opposed to that of a C-Cl bond.



2-X-acetaldehyde - H  
X = Cl, F, SH

### 1.2.6 Evidence

It has been observed by Bank<sup>118</sup> that the enolate **127a** gave, on quenching with  $H^+$ , only the axial isomer **128**. This can be explained very easily by stereoelectronic effects. The reaction should go through the intermediate **127b** wherein the filled electron orbital is oriented antiperiplanar to the less electron-donating C-O bond. This orbital captures  $H^+$  in this equatorial orientation.



Very recently, Fraser and coworkers<sup>69</sup> have reported the effect of  $\alpha$  substituents on the face reactivity of the conformationally rigid bisaryl ketones **129** towards metal hydrides. The observed face selectivities followed neither the theory of Cieplak nor that of Anh. The results are collected in the Table 1.24. Fraser explained the major influence of the substituents by the through-bond interactions and the difference between the ax and eq effects by electrostatic (through-space) interactions with the transition state. According

to the Cieplak theory, nucleophile should come only from the equatorial face for 2-ax-halo-substituted cyclohexanones which is contrary to the experimental observations. Our approach correctly predicts the 2-ax-X-substituted cyclohexanones.

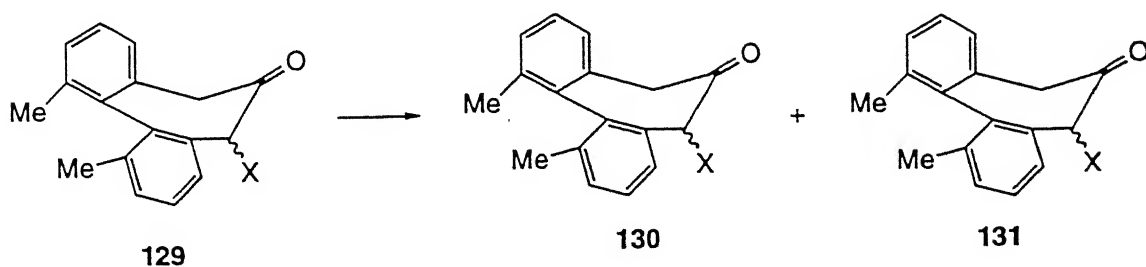
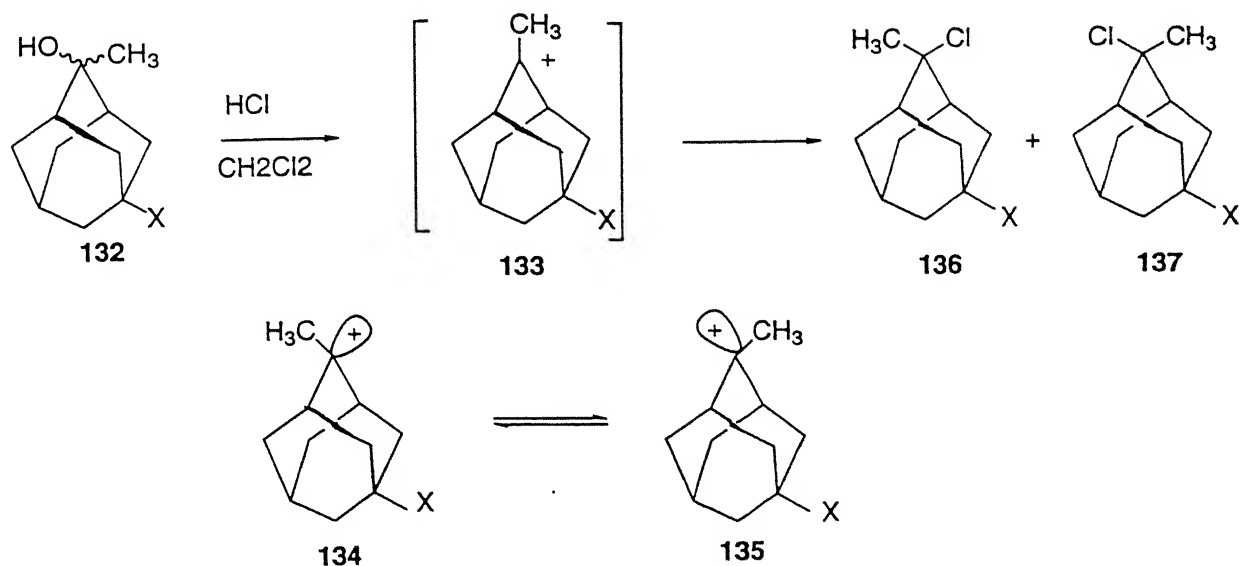


Table 1.24:  $\pi$ -Facial selectivity of **129**

Substituent	LiAlH <sub>4</sub>	NaBH <sub>4</sub>	Et <sub>3</sub> SiH
H	1.0	1.0	1.0
Me(a)	11.9	6.5	11.5
SMe(a)	>19		
OMe(a)	>19	>19	>19
Cl(a)	>19	>19	
Me(e)	4.5	2	2
SMe(e)	>19	>19	>19
OMe(e)	>19	>19	>19
Cl(e)	8.2	5.3	7.0
F(e)	7.6	5.9	7.9

Adcock *et al.*<sup>119, 120</sup> have observed that halogenation (Cl, F) of alcohols **132** (Table 1.25 and Table 1.26) gave the *anti* **137** as major product when the substituent was electron-donating. On the contrary, it gave the *syn* product **136** when the substituent was electron-withdrawing. The additions were found to proceed through a pair of equilibrating carbo-cation intermediates, **134** and **135**, as shown.

Table 1.25: Product Distribution from the hydrochlorination of **132**<sup>a</sup>

X	% <b>137</b>	% <b>136</b>	X	% <b>137</b>	% <b>136</b>
F	27	73	SiMe <sub>3</sub>	61	39
F	25	75	SiMe <sub>3</sub>	60	40
Cl	30	70	C <sub>6</sub> H <sub>5</sub>	42	58
Cl	29	71	<i>p</i> -FC <sub>6</sub> H <sub>4</sub>	39	61
Br	39	61	<i>p</i> -BrC <sub>6</sub> H <sub>4</sub>	38	62
Me	41	59	<i>p</i> -MeC <sub>6</sub> H <sub>4</sub>	43	57

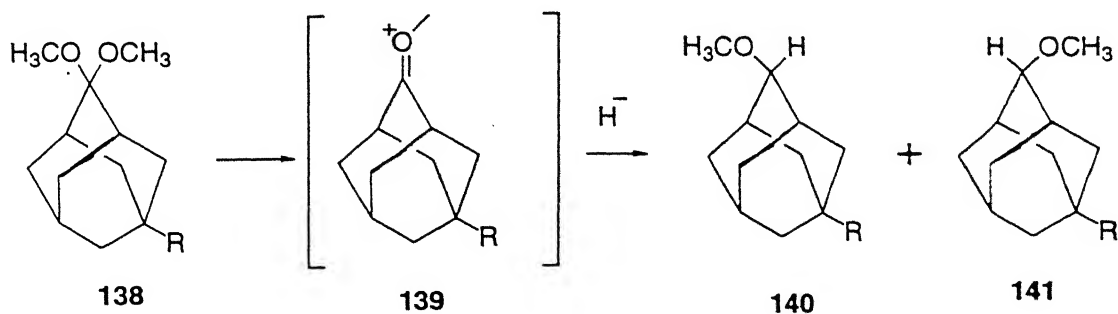
<sup>a</sup> - Product ratios were calculated from <sup>13</sup>C and <sup>19</sup>F or <sup>13</sup>C and <sup>1</sup>H spectra.

Table 1.26: Product Distribution from the hydrofluorination of **132**<sup>a</sup>

X	% <b>137</b>	% <b>136</b>	X	% <b>137</b>	% <b>136</b>
NO <sub>2</sub>	5	95	OCOMe	21	79
NO <sub>2</sub>	7	93	NMe <sub>2</sub>	28	72
CN	11	89	CH <sub>3</sub>	38	62
CO <sub>2</sub> Me	30	70	SiMe <sub>3</sub>	84	16
CO <sub>2</sub> Me	30	70	SnMe <sub>3</sub>	100	0
F	10	70	SnMe <sub>3</sub>	>98	trace
F	6	94	C <sub>6</sub> H <sub>5</sub>	41	59
Cl	15	85	<i>p</i> -NO <sub>2</sub> C <sub>6</sub> H <sub>4</sub>	35	65
Cl	16	84	<i>p</i> -CNC <sub>6</sub> H <sub>4</sub>	35	65
Br	18	82	<i>p</i> -CNC <sub>6</sub> H <sub>4</sub>	35	65
Br	19	81	<i>p</i> -MeO <sub>2</sub> CC <sub>6</sub> H <sub>4</sub>	39	61
I	35	65	<i>p</i> -FC <sub>6</sub> H <sub>4</sub>	41	59
I	38	62	<i>p</i> -BrC <sub>6</sub> H <sub>4</sub>	36	64
OMe	34	66	<i>p</i> -BrC <sub>6</sub> H <sub>4</sub>	38	62
OMe	33	67	<i>p</i> -MeOC <sub>6</sub> H <sub>4</sub>	45	55
OCOMe	20	80	<i>p</i> -Me <sub>2</sub> NC <sub>6</sub> H <sub>4</sub>	39	61

<sup>a</sup> - Multiple results are based upon <sup>13</sup>C, ~~<sup>19</sup>F~~ NMR, GC.

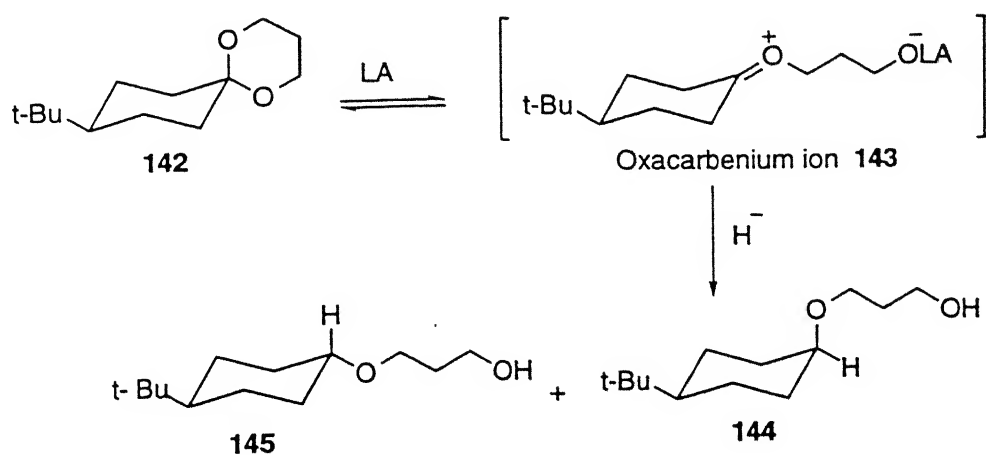
The observed results can be explained very easily by stereoelectronic effects. When, X is electron-donating, the empty p orbital must orient *anti* to X which is stabilized. It is reversed for an electron-withdrawing substituent. In another similar study, Adcock<sup>121</sup> reported reduction of 2,2-dimethoxy 5-substituted adamantanes **138**. The results are given in the Table 1.27. The cation **139** which lies on the reaction pathway obeys, once again, stereoelectronic effects for stabilization. The orientation of the p orbital on C2 is determined by the nature of R.

Table 1.27: Product Distribution from the Reduction of **138**<sup>a</sup>

X	% <b>140</b>	% <b>141</b>
CO <sub>2</sub> Me	62	38
F	75	25
Cl	67	33
Br	63	37
Me	51	49
OMe	72	28
C <sub>6</sub> H <sub>5</sub>	47	53
<i>p</i> -NO <sub>2</sub> C <sub>6</sub> H <sub>4</sub>	45	55
<i>p</i> -BrC <sub>6</sub> H <sub>4</sub>	47	53
SiMe <sub>3</sub>	35	65
SnMe <sub>3</sub>	33	67

<sup>a</sup>-Results are based on <sup>13</sup>C- NMR.

Finally, Steel and coworkers<sup>103</sup> have observed that the Lewis acid catalysed reduction of **142** gave mainly the equatorial alcohol derivative **145**. This reaction must generally go through the oxacarbenium ion intermediate **143**.



### 1.3 Conclusion

The cation complexation activates the carbonyl carbon for reaction with a nucleophile by increasing the coefficient of the electron-poor p orbital on the carbonyl carbon and, thus, lowering the energy of activation. This complexation must precede the actual nucleophilic attack and, further, this must occur in the carbonyl  $\sigma$  plane. The cation complexation causes significant geometrical changes around the carbonyl carbon. Naturally, the nature of these changes must be such that the molecule achieves maximum possible conformational stability. The theory of stereoelectronic effects would dictate that the significantly developed electron-poor p orbital on the carbonyl carbon must be oriented, respectively, antiparallel and orthogonal to an electron-donating and an electron-attracting bond at the adjacent carbon. The resultant axial and equatorial orientations of the p orbital will determine the axial and equatorial preferences, respectively, for nucleophilic attacks. We fully subscribe to the view that a nucleophilic attack is a consequence of electrostatic attraction between two oppositely charged species, the nucleophile and the electron-poor p orbital. An increase in the torsion angles on the axial face predicts preferential axial attack. Likewise, a reduction in the torsion angles indicates the equatorial attack. The torsion angle

changes are dependent on the nature, orientation, and relative position from the carbonyl function of a ring substituent.

## 1.4 Experimental

### 4-Mesyloxycyclohexanone (121):

To a solution of 4-hydroxycyclohexanone (0.104 g, 1.0 mmol) in dry  $\text{CH}_2\text{Cl}_2$  (4 mL) at 0 °C was added  $\text{Et}_3\text{N}$  (1.3 mmol, 0.18 mL) and  $\text{MsCl}$  (1.2 mmol, 0.1 mL). The reaction mixture was stirred for 30 min for the reaction to complete (TLC). This was diluted with  $\text{CH}_2\text{Cl}_2$  (10 mL) and washed with water (2 x 5 mL) and brine (1 x 5 mL). Drying and solvent removal furnished the crude mesylate in quantitative yield.

### 4-*eq*-SPh-cyclohexanone (122):

To a solution of the above crude mesylate in THF (5 mL) was added  $\text{PhSNa}$  (0.198 g, 1.5 mmol) and the resultant mixture stirred at rt for 4 h. The solvent was evaporated under reduced pressure and the residue extracted with  $\text{EtOAc}$  (2 x 5 mL). The  $\text{EtOAc}$  was removed and the residue chromatographed to isolate pure **122** in >75% yield.

### Reduction of 122 with LAH:

LAH (8 mg, 0.2 mmol) was added to a solution of **122** (21 mg, 0.1 mmol) in  $\text{Et}_2\text{O}$  (3 mL) at 0 °C and the contents stirred until the reaction was complete (2 h). Water (2-3 drops) was added and the contents stirred for 5 min. This was dried with  $\text{Na}_2\text{SO}_4$  and filtered. Evaporation of the solvent and filtration of the residue through a short silica gel column furnished a mixture of the equatorial and axial alcohols in 55:45 proportion in quantitative yield.

### Reduction of 122 with $\text{NaBH}_4$ :

To a solution of **122** (21 mg, 0.1 mmol) in MeOH (3 mL) was added  $\text{NaBH}_4$  (8 mg, 0.2 mmol). The contents were stirred for 30 min when the solvent was removed under reduced pressure on a rotovap. Saturated aqueous  $\text{NH}_4\text{Cl}$  (2 mL) was added, the contents stirred,



and extracted with EtOAc (3 x 3 mL). The combined EtOAc extract was dried and the solvent removed. The residue was filtered through a short bed of silica gel to isolate a 61:39 mixture of the equatorial and axial alcohols, respectively.

**Reduction of 122 with Na(CN)BH<sub>3</sub>:**

To a solution of **122** (21 mg, 0.1 mmol) in MeOH (3 mL) were added few drops of 2N aqueous HCl to achieve a pH of 1.0. Na(CN)BH<sub>3</sub> (13 mg, 0.2 mmol) was added and the contents stirred at rt for 30 min. The methanol was removed and the residue extracted with Et<sub>2</sub>O (3 x 5 mL). The combined Et<sub>2</sub>O extract was washed with saturated aqueous NaHCO<sub>3</sub> and dried. The Et<sub>2</sub>O was removed and the residue filtered through a short bed of silica gel to obtain a 64:36 mixture of the equatorial and axial alcohols, respectively.

# References

- [1] Barton, D.H.R. *J. Chem. Soc.* **1953**, 1027.
- [2] Cram, D.J.; Elhafez, F.A.A. *J. Am. Chem. Soc.* **1952**, *74*, 5828.
- [3] Dauben, W.G.; Fonken, G.J.; Noyce, D.S. *J. Am. Chem. Soc.* **1956**, *78*, 2579.
- [4] Karabatsos, G.J. *J. Am. Chem. Soc.* **1967**, *89*, 1367.
- [5] Cherest, M.; Felkin, H.; Prudent, N. *Tetrahedron Lett.* **1968**, 2199.
- [6] Anh, N.T.; Eisenstein, O.; Lefour, J.M.; Dau, M-E.T.H. *J. Am. Chem. Soc.* **1973**, *95*, 6146.
- [7] Richer, J.C. *J. Org. Chem.* **1965**, *30*, 324.
- [8] Klein, J. *Tetrahedron Lett.* **1973**, *29*, 4307.
- [9] Klein, J. *Tetrahedron*. **1974**, *30*, 3349.
- [10] Liotta, C.L. *Tetrahedron Lett.* **1975**, 519, 523.
- [11] Liotta, C.L.; Burgess, L.M.; Eberhardt, W.H. *J. Am. Chem. Soc.* **1984**, *106*, 4849.
- [12] Wipke, W.T.; Gund, P. *J. Am. Chem. Soc.* **1976**, *98*, 5107.
- [13] Perlberger, J.-C; Muller, P. *J. Am. Chem. Soc.* **1977**, *99*, 6316.
- [14] Wigfield, D.C. *Tetrahedron*. **1979**, *35*, 449.
- [15] Royer, J. *Tetrahedron Lett.* **1978**, 1343.
- [16] Giddings, M.R.; Hudec, J. *Can J Chem.* **1981**, *59*, 459.
- [17] Cieplak, A.S. *J. Am. Chem. Soc.* **1981**, *103*, 4540.
- [18] Wu, Y.-D.; Houk, K.N. *J. Am Chem. Soc.* **1987**, *109*, 906.
- [19] Kurita, Y.; Takayama, C. *Tetrahedron*. **1990**, *46*, 3789.
- [20] Frenking, G.; Kohler, K.F.; Reetz, M.T. *Angew. Chem. Int. Ed. Engl.* **1991**, *30*, 1146.
- [21] Huang, X.; Dannenberg, J.J. *J. Am. Chem. Soc.* **1993**, *115*, 6017.

- [22] Coxon, J.M.; Luibrand, R.T. *Tetrahedron Lett.* **1993**, *34*, 7097.
- [23] Shi, Z.; Boyd, R.J. *J. Am. Chem. Soc.* **1993**, *115*, 9614.
- [24] Li, H.; le Noble W.J. *Recl. Trav. Chim. Pays-Bas.* **1992**, *111*, 119, We are thankful to Prof. W.J. le Noble for his reprints.
- [25] Cornforth, J.W.; Cornforth, R.H.; Mathew, K.K. *J. Chem. Soc.* **1959**, 112.
- [26] Anh, N.T.; Eisenstein, O. *Tetrahedron Lett.* **1976**, 155.
- [27] Anh, N.T.; Eisensin, O. *Nouv. J. Chim.* **1977**, *1*, 61.
- [28] Burgi, H.B.; Dunitz, J.D.; Lehn, J.M.; Wipff, G. *Tetrahedron.* **1974**, *30*, 1563.
- [29] Paddon-Row, M.N.; Rondan, N.G.; Houk, K.N. *J. Am. Chem. Soc.* **1982**, *104*, 7162.
- [30] Wong, S.S; Paddon-Row, M.N. *J. Chem. Soc., Chem. Commun.* **1991**, 327.
- [31] Eliel, E.L.; Senda, Y. *Tetrahedron.* **1970**, *26*, 2411.
- [32] Ashby, E.C.; Boone, J.R. *J. Org. Chem.* **1976**, *41*, 2890.
- [33] le Noble W.J. *Croatica Chemica Acta.* **1992**, *65*, 489.
- [34] Gung, B.W. *Tetrahedron.* **1996**, *52*, 5263.
- [35] Bellucci, G.; Chiappe, C.; Moro, G.L.; Ingrosso, G. *J. Org. Chem.* **1995**, *60*, 6214.
- [36] Halterman, R.L.; McEvoy, M.A. *Tetrahedron Lett.* **1992**, *33*, 753.
- [37] le Noble W.J.; Chiou, D.-M.; Maluszynska, H.; Okaya, Y. *Tetrahedron Lett.* **1977**, 3865.
- [38] le Noble W.J.; Chiou, D.-M.; Okaya, Y. *J. Am. Chem. Soc.* **1979**, *101*, 3244.
- [39] Bodepudi. V.R.; le Noble W.J. *J. Org. Chem.* **1994**, *59*, 3265.
- [40] le Noble W.J.; Srivastava, S.; Cheung, C.K. *J. Org. Chem.* **1983**, *48*, 1099.
- [41] Srivastava. S.; le Noble W.J. *J. Am. Chem. Soc.* **1987**, *109*, 5874.
- [42] Li, M.-H.; Silver, J.E.; le Noble W.J. *J. Org. Chem.* **1988**, *53*, 5155.
- [43] Cheung, C.-K.; Tseng, L.-T.; Lin, M.-h.; Srivastava, S.; le Noble W.J. *J. Am. Chem. Soc.* **1986**, *108*, 1598.
- [44] Li, H.; le Noble W.J. *Tetrahedron Lett.* **1990**, *31*, 4391.
- [45] Chung, W.-S.; Turro, N.J.; Srivastava, S.; Li, H.; le Noble W.J. *J. Am. Chem. Soc.* **1988**, *110*, 7882.
- [46] Lin, M.-h.; le Noble W.J. *J. Org. Chem.* **1989**, *54*, 997.
- [47] Xie, M.; le Noble W.J. *J. Org. Chem.* **1989**, *54*, 3836.

- [48] Bodepudi, V.R.; le Noble W.J. *J. Org. Chem.* **1991**, *56*, 2001.
- [49] Li, H.; le Noble W.J. *Tetrahedron Lett.* **1990**, *31*, 2001.
- [50] Hahn, J.M.; le Noble W.J. *J. Am. Chem. Soc.* **1992**, *114*, 1916.
- [51] Song, I.H.; le Noble W.J. *J. Org. Chem.* **1994**, *59*, 58.
- [52] Bodepudi, V.R.; le Noble W.J. *J. Org. Chem.* **1994**, *59*, 3270.
- [53] Chung, W.-S.; Turro, N.J.; Srivastava, S.; le Noble W.J. *J. Org. Chem.* **1991**, *56*, 5020.
- [54] Li, H.; Silver, J.E.; Watson, W.H.; Kashyap, R.P.; le Noble W.J. *J. Org. Chem.* **1991**, *56*, 5932.
- [55] Chung, W.S.; Turro, N.J.; Srivastava, S.; Li, H.; le Noble W.J. *J. Am. Chem. Soc.* **1988**, *110*, 7882.
- [56] Chung, W.S.; Tsai, T.L.; Ho, C.C.; Chiang, M.Y.N.; le Noble W.J. *J. Org. Chem.* **1997**, *62*, 4672.
- [57] Lin, M.; Watson, W.H.; Kashyap, R.P.; le Noble W.J. *J. Org. Chem.* **1990**, *55*, 3597.
- [58] Mukherjee, A.; Wu, Q.; le Noble W.J. *J. Org. Chem.* **1994**, *59*, 3270.
- [59] Srivastava, S.; le Noble W.J. *Synth. Commun.* **1984**, *14*, 65.
- [60] Halterman, R.L.; McEvoy, M.A. *J. Am. Chem. Soc.* **1990**, *112*, 6690.
- [61] Mehta, G.; Subramanian, U.R.; Pramanik, A.; Chandrasekar, J.; Nethaji, M. *J. Chem. Soc., Chem. Commun.* **1995**, 677.
- [62] Ganguly, B.; Chandrasekher, J.; Khan, F.A.; Mehta, G. *J. Org. Chem.* **1993**, *58*, 1734.
- [63] Mehta, G.; Khan, F.A.; Ganguly, B.; Chandrasekher, J. *J. Chem. Soc., Chem. Commun.* **1992**, 1711.
- [64] Kumar, V.A.; Venkatesan, K.; Ganguly, B.; Chandrasekher, J.; Khan, F.A.; Mehta, G. *Tetrahedron Lett.* **1992**, *33*, 3069.
- [65] Mehta, G.; Khan, F.A. *Tetrahedron Lett.* **1992**, *33*, 3065.
- [66] Mehta, G.; Khan, F.A. *J. Chem. Soc., Chem. Commun.* **1991**, 18.
- [67] Li, H.; Mehta, G.; Padma, S.; le Noble W.J. *J. Org. Chem.* **1991**, *56*, 2011.
- [68] Meyers, A.I.; Wallace, R.H. *J. Org. Chem.* **1989**, *54*, 2509.
- [69] Fraser, R.R.; Faibish, N.C.; Kong, F.; Bednarski, K.J. *J. Org. Chem.* **1997**, *62*, 6164.
- [70] Bartlett, P.D.; Rosenwald, R.H. *J. Am. Chem. Soc.* **1934**, *56*, 1990.
- [71] Wu, Y.-D.; Tucker, J.A.; Houk, K.N. *J. Am. Chem. Soc.* **1991**, *113*, 5018.

- [72] Wu, Y.-D.; Houk, K.N.; Paddon-Row, M.N. *Angew. Chem. Int. Ed. Engl.* **1992**, *31*, 1019.
- [73] Kobayashi, Y.M.; Lambrecht, J.; Jochims, J.C.; Burkert, U. *Chem. Ber.* **1978**, *111*, 3442.
- [74] Jochims, J.C.; Kobayashi, Y.M.; Skrzewski, E. *Tetrahedron Lett.* **1974**, *571*, 575.
- [75] Terasama, T.; Okada, T. *J. Chem. Soc., Perkin Trans.1.* **1978**, 1252.
- [76] Harada, T.; Nakajima, H.; Ohnishi, T.; Takeuchi, M.; Oku, A. *J. Org. Chem.* **1992**, *57*, 720.
- [77] House, H.O.; Babad, H.; Toothill, R.B.; Nolts, A.W. *J. Org. Chem.* **1962**, *27*, 4141.
- [78] Rothberg, I.; Sundoro, B.; Balanikas, G.; Kirsch, S. *J. Org. Chem.* **1983**, *48*, 4345.
- [79] Cieplak, A.S.; Tait, B.D.; Johnson, C.R. *J. Am. Chem. Soc.* **1989**, *111*, 8447.
- [80] Kaselj, M.; le Noble W.J. *J. Org. Chem.* **1996**, *61*, 4157.
- [81] Nagao, Y.; Goto, M.; Ochiai M.and Shiro, M. *Chem. Lett.* **1990**, 1503.
- [82] Nagao, Y.; Goto, M.; Ochiai. M. *Chem. Lett.* **1990**, 1507.
- [83] Monson, R.S.; Przybycien, D.; Baraze, A. *J. Org. Chem.* **1970**, *35*, 1700.
- [84] Bartlett, P.D.; Rosenwald, R.H. *J. Am. Chem. Soc.* **1934**, *56*, 1990.
- [85] Corey, E.J.; Burke. *J. Am. Chem. Soc.* **1955**, *77*, 5418.
- [86] Carreno, M.C.; E. Dominguez. E.; Ruano, J.L.G.; Rubio, A. *J. Org. Chem.* **1987**, *52*, 3619.
- [87] Maruoka, K.; Itoh, T.; Sakurai. M.; Nonoshita, K.; Yamamoto. H. *J. Am. Chem. Soc.* **1988**, *110*, 3588.
- [88] Paquette, L.A.; Lobben, P.C. *J. Am. Chem. Soc.* **1996**, *118*, 1917.
- [89] Power, M.B.; Bott, S.G.; Atwood, J.L.; Barron, A.R. *J. Am. Chem. Soc.* **1990**, *112*, 3446.
- [90] Ashby, E.C. *Quart. Rev. Chem. Soc.* **1967**, *21*, 259.
- [91] Morrison J., D.; Ridgway R.. W. *Tetrahedron Lett.* **1969**, 569.
- [92] Brown, H.C.; Hess, H.M. *J. Org. Chem.* **1969**, *34*, 2206.
- [93] Nasipuri, D.; Ghosh, C.K.; Mukherjee, P.R.; Venkataraman. S. *Tetrahedron Lett.* **1971**, 1587.
- [94] Pierre, J.-L.; Handel, H. *Tetrahedron Lett.* **1974**, 2317.
- [95] Laemmle, J.; Ashby E., C.; Neumann H., M. *J. Am. Chem. Soc.* **1971**, 5120.
- [96] Boone, J.R.; Ashby, E.C. *Top. Stereochem.*; 1979, V-11, p-53.

- [97] Lozach, D.; Molle, G.; Bauer, P.; Dubois J., E. *Tetrahedron Lett.* **1983**, *24*, 4213.
- [98] Al-Aseer M., A.; Smith S., G. *J. Org. Chem.* **1984**, *49*, 2608.
- [99] Al-Aseer M., A.; Allison B., D.; Smith S., G. *J. Org. Chem.* **1985**, *50*, 2715.
- [100] Kaufmann, E.; Schleyer, P.R.; Houk, E.N.; Wu, Y.D. *J. Am. Chem. Soc.* **1985**, *107*, 5560.
- [101] Evans, D.A. *Science*. **1988**, *240*, 420.
- [102] Narasaka, K. *Synthesis*. **1991**, *1*.
- [103] Newitt L., A.; Steel P., G. *J. Chem. Soc., Perkin Trans. 1*. **1997**, 2033.
- [104] Doyle, M.P.; West, C.T. *J. Org. Chem.* **1975**, *40*, 3821.
- [105] Ashby, E.C.; Boone, J.R.; Oliver, J.P. *J. Am. Chem. Soc.* **1973**, *95*, 5427.
- [106] Laemmle, J.T.; Ashby, E.C.; Roling, P.V. *J. Org. Chem.* **1973**, *38*, 2526.
- [107] Poirier, R.A.; Peterson, M.R.; Yadav, A. *MUNGAUSS1989*; Department of Chemistry, Memorial University of Newfoundland, Canada, and Department of Chemistry, Indian Institute of Technology, Kanpur, India,.
- [108] Jeyaraj, D.A.; Yadav, A.; Yadav, V.K. *Tetrahedron Lett.* **1997**, *38*, 4483.
- [109] Brown, H.C.; Krishnamurthy, S. *J. Am. Chem. Soc.* **1972**, *93*, 94.
- [110] Jeyaraj, D.A.; Yadav, V.K. *Tetrahedron Lett.* **1997**, *38*, 6095.
- [111] Haslanger, M.; Lawton, R.G. *Synth. Commun.* **1974**, *4*, 155.
- [112] Cohen, T.; Yu, L.-C.; Daniewski, J. *J. Org. Chem.* **1985**, *50*, 4596.
- [113] Alkorta, I.; Rozas, I.; Elguero, J. *J. Org. Chem.* **1997**, *62*, 4687.
- [114] R.M., Silverstein; G.C., Bassler; T.C., Morrill. *Spectroscopic Identification of Organic Compounds*; John-Wiley and Sons: 1981.
- [115] Senju, T.; Tomada, S. *Chemistry Lett.* **1997**, 433.
- [116] Yadav, V.K.; Jeyaraj, D.A. *J. Org. Chem.* **1998**, *63*, 000.
- [117] Frish, M.; Trucks, G.W.; Schlegel, H.B.; Gill, P.M.; Johnson, B.G.; Robb, M.A.; Cheeseman, J.R.; Keith, T.; Petersson, G.A.; Montgomery, J.A.; Raghavachari, K.; Al-Laham, M.A.; Zakrzewski, V.G.; Ortiz, J.V.; Foresman, J.B.; Cioslowski, J.; Stefanov, B.B.; Nanayakkara, A.; Challacombe, M.; Peng, C.Y.; Ayala, P.Y.; Chen, W.; Wong, M.W.; Andres, J.L.; Replogle, E.S.; Gomperts, R.; Martin, R.L.; Fox, D.J.; Binkley, J.S.; Defrees, D.J.; Baker, J.; Stewart, J.P.; Head-Gordon, M.; Gonzalez, C.; Pople, J.A. *Gaussian, Inc.* Pittsburgh PA, 1995.
- [118] Banks, H.D. *J. Org. Chem.* **1981**, *46*, 1743.
- [119] Adcock, W.; Cotton, J.; Trout, N.A. *J. Org. Chem.* **1994**, *59*, 1867.
- [120] Adcock, W.; Clark, C.I.; Trout, N.A. *Tetrahedron Lett.* **1994**, *35*, 297.
- [121] Adcock, W.; Head, N.J.; Lokan, N.R.; Trout, N.A. *J. Org. Chem.* **1997**, *62*, 6177.

## Chapter 2

# Allylic Substituted Hemithio Acetal in Face Selection: An Experimental Study

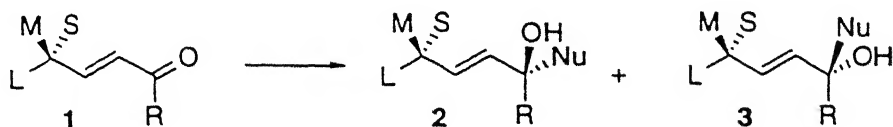
### 2.1 Introduction

#### 2.1.1 1,2-Diastereoselectivity

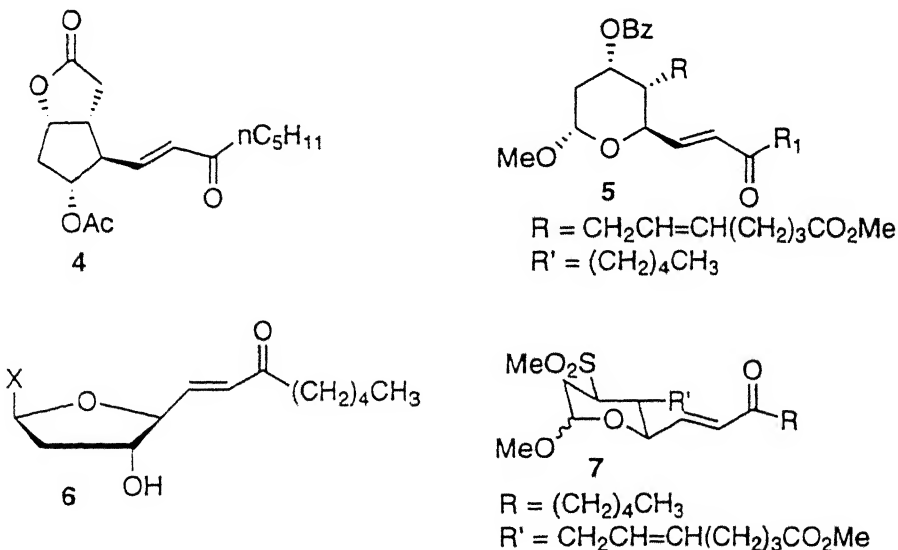
The study of diastereoface selection due to a strategically located heteroatom is of much current interest.<sup>1</sup> It has been shown<sup>2-7</sup> that the nucleophile attacks *syn* to an oxygen and *anti* to a sulfur, the heteroatom being placed on a carbon adjacent to the center of nucleophilic attack.

#### 2.1.2 1,4-Diastereofacial Selectivity

A heteroatom/chiral center which is vinylogously adjacent to a center of nucleophilic attack such as in **1** may also be expected to relay its directing influence through the  $\pi$ -bond to produce either **2** or **3** predominantly. There has not been much study to understand the influence of such a chiral center or hetero atom on the observed diastereoselection. A brief account of the scattered literature is collected below.

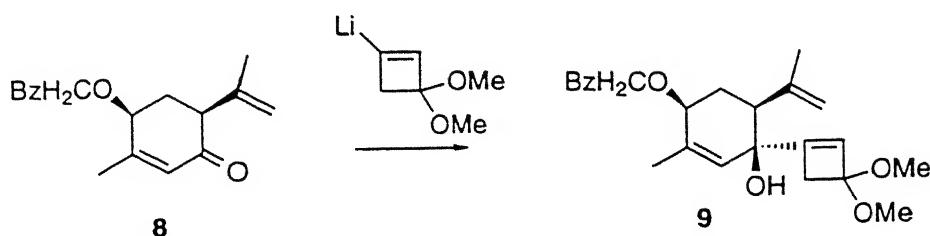


During the synthesis of prostagladins, Corey and coworkers<sup>8</sup> observed that the reduction of the enone **4** gave a 1:1 mixture of the two possible alcohols. During the synthesis of thromboxane  $B_2$ , Hannessian and Lavalley<sup>9</sup> have observed no selectivity in the reduction of **5** even though it had more than one chiral center. Just and Oh<sup>10</sup> have observed almost 1:1 selectivity on reduction of **6** during the synthesis of 8R,11R,15(R&S)-trihydroxy-9S,12S-oxyeicosa-5Z,13E-dienoic acid which is an oxidation product of arachidonic acid. Kale and Clive<sup>11</sup> did not observe any selectivity on reduction of **7** during a planned synthesis of optically active 9 $\alpha$ ,H $\alpha$ -thiathromboxane  $A_2$ , even when the chiral center is part of a sugar residue.

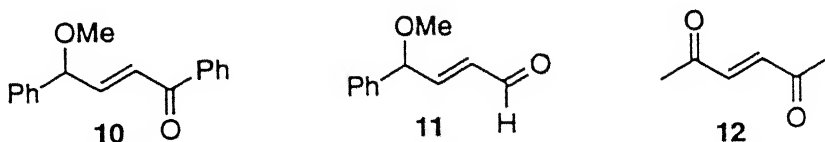


Still and coworkers<sup>12</sup> obtained good selectivity (6:1) in reaction of **8** with a nucleophile. The predominant attack was from the  $\alpha$  face and **9** constituted the major product. The reaction is apparently controlled by the stereochemistry of the bulky isopropenyl substituent.



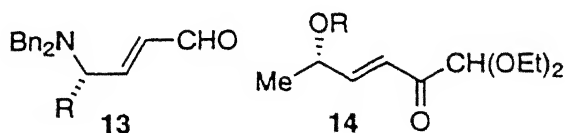


Fleming and coworkers<sup>13</sup> have carried out a systematic study to understand the electronic influence of heteroatoms on the reaction site. The chiral center was held spatially away from the center undergoing reaction. In this situation, the electronic information might reasonably be relayed to the prochiral center but steric information can not.

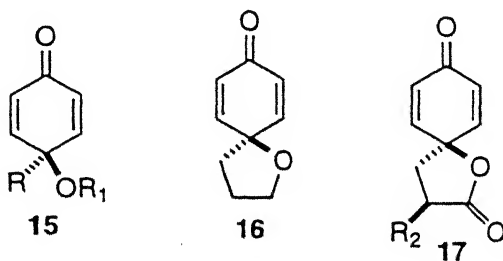


The methyl ether **10** yielded, on reduction with LAH, only a 1:1 mixture of two alcohols. The aldehyde **11**, which can reasonably be expected to exist largely in the *s-trans* conformation, reacted with PhMgBr to furnish a 1:1 mixture of two alcohols. The reduction of ketone **12** with DIBAL-H furnished, once again, a 1:1 mixture of two 1,4-diols. After taking into account all these informations, these authors concluded that the chiral information was very inefficiently transmitted by conjugation to the reaction site.

Reetz and coworkers<sup>14</sup> did not observe any selectivity in reaction of the enals **13** with various alkyllithium and Grignard reagents. The possible electronic and steric effects, therefore, appeared not to have transmitted through or across the alkene  $\pi$ -system. Floch and coworkers<sup>15</sup> observed no selectivity on reduction of **14**. The use of non-chiral, and even bulky reagents gave very little or no asymmetric reduction.



Wipf and Kim<sup>16</sup> have reported very good diastereoselection ranging from 4.8:1 to 32:1 in favour of *anti* to the oxygen substituents at C-4 in 4-alkoxy-4-alkylcyclohexadienones 15-17 (Table 2.1).

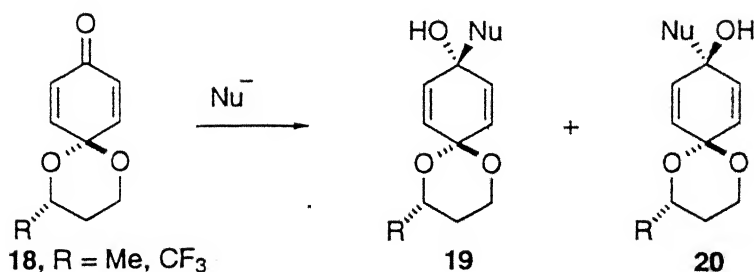


In all the cases, the predominant attack is from *anti* to the C4-oxygen substituent. The changes in reaction parameters led to only reduction in the above *anti* to oxygen facial selectivity. Ahn-Eisenstein,<sup>17</sup> vinylogous Cieplak<sup>18</sup> (Vinylogous Cieplak effect would be equivalent to an allylic inversion of the normal Cieplak effect), and principle of frontier orbital distortion failed to explain these observations. Wipf explained the observed selectivity by an electrostatic control mechanism. The excellent linear correlation of calculated dipole moments with the  $\ln$  of the facial selectivity supported the notion that the kinetic selectivity of irreversible C-C bond formation was strongly influenced by dipole-dipole interaction between the reagent and the substrate. As the dipole moment increased, the selectivity also increased in the direction of the dipole.

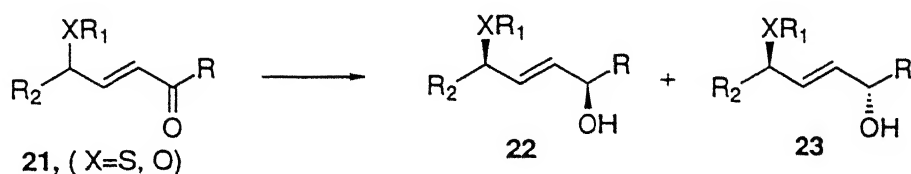
Table 2.1: Nucleophilic additions to 15-17

Entry	Dienone	Nucleophile	% Yield	<i>anti/syn</i> selectivity
1	15, R=R1=Me	MeMgBr	86	4.8:1
2	15, R=TMS, R1=Me	NaBH <sub>4</sub> or LiBH <sub>4</sub>	100	1:1
3	15, R=R1=Me	HC≡CMgBr	70	1:1
4	15, R=R1=Me	C <sub>4</sub> H <sub>9</sub> C≡CLi	26	1.1:1
5	15, R=R1=Me	PhMgBr	83	3.6:1
6	15, R=R1=Me	MeLi/THF	87	2.1:1
7	15, R=R1=Me	MeLi/Et <sub>2</sub> O	77	3.3:1
8	15, R=R1=Me	BnOCH <sub>2</sub> Li	84	3:1
9	15, R=Me, R1=Bz	MeMgBr	> 61	10.1:1
10	15, R=Bz, R1=H	MeMgBr	81	7.9:1
11	15, R=Me, R1=TMS	MeMgBr	93	17.7:1
12	16	MeMgBr	75	8.6:1
13	17, R <sub>2</sub> =H	MeMgBr	79	32:1
14	17, R <sub>2</sub> =N(Cbz) <sub>2</sub>	BnOCH <sub>2</sub> Li	>50	5:1
15	17, R <sub>2</sub> =NBoc <sub>2</sub>	MeMgBr	84	6:1

Wipf and Jung<sup>19</sup> have also studied the molecules **18** (R=Me, CF<sub>3</sub>) in reaction with nucleophiles. While **18** (R=Me) furnished a mixture of **19** and **20** in a ratio of 1:1, **18** (R=CF<sub>3</sub>) was more diastereoselective as a 1:1.5 mixture of **19** and **20** was obtained. These were also to follow the direction of the dipole. The observations with naphthoquinones were similar to those with quinones studied earlier.<sup>16</sup>



Sato *et al.*<sup>20</sup> have studied acyclic 4-sulfenyl- and 4-alkoxy-2-enones **21**. While the sulfenyl and silyloxy derivatives generated preferably the *syn* products **22**, the benzyloxy derivatives furnished the *anti* products **23** in reduction with hydride reagents. Obviously, the hydride delivery was from *anti* to the sulfenyl and silyloxy substituents and *syn* to the benzyloxy variant. The results from the sulfenyl species are collected in the Table 2.2.

Table 2.2: Reduction of **21**

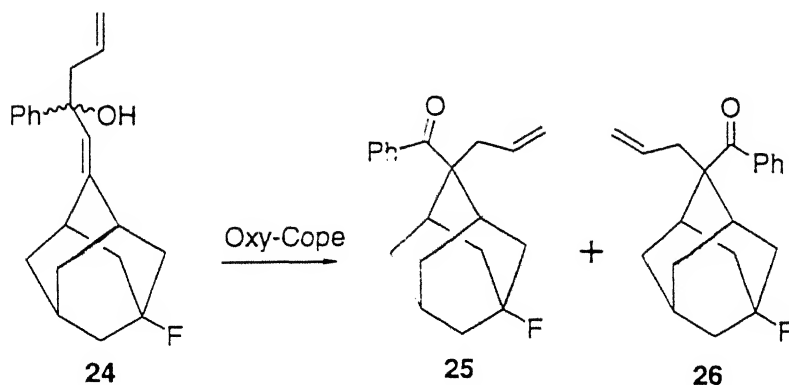
Entry	X	R	R1	R2	22 : 23
1	X=S	Bu <sup>t</sup>	Ph	Bu <sup>t</sup>	97:3
2	X=S	Bu <sup>t</sup>	Ph	Pr <sup>i</sup>	96:4
3	X=S	Bu <sup>t</sup>	Ph	Me	95:5
4	X=S	Pr <sup>i</sup>	Ph	Bu <sup>t</sup>	94:6
5	X=S	Me	Ph	Bu <sup>t</sup>	91:9
6	X=S	n-C <sub>7</sub> H <sub>11</sub>	Ph	n-C <sub>7</sub> H <sub>15</sub>	93:7
7	X=S	Bu <sup>t</sup>	Ph	n-C <sub>6</sub> H <sub>13</sub>	93:7
8	X=S	Bu <sup>t</sup>	Me	n-C <sub>6</sub> H <sub>13</sub>	93:7
9	X=O	Bu <sup>t</sup>	CH <sub>2</sub> Ph	cylo-C <sub>6</sub> H <sub>11</sub>	30:70
10	X=O	Bu <sup>t</sup>	CH <sub>2</sub> Ph	Bu <sup>t</sup>	25:75
11	X=O	Bu <sup>t</sup>	TBDMS	cylo-C <sub>6</sub> H <sub>11</sub>	71:29
12	X=O	Bu <sup>t</sup>	TBDMS	Bu <sup>t</sup>	72:28

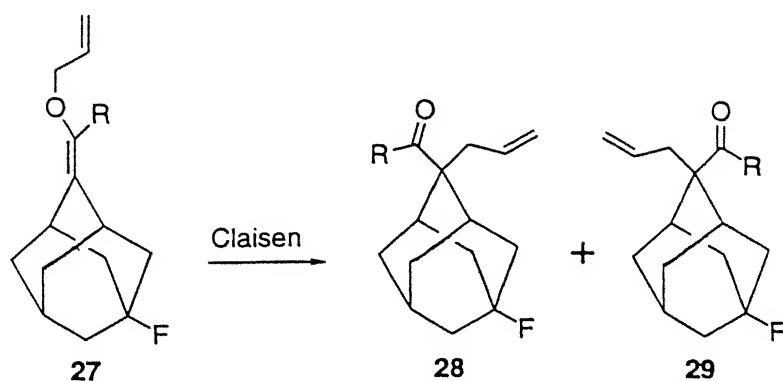
The variation in selectivity of the  $\gamma$ -oxygenated species was attributed to the differences in the preferred ground state conformations. While the  $\gamma$ -benzyloxy compounds prefer the C-H eclipse the olefin, the corresponding silyl ethers favor the C-O to eclipse. The superior selectivity of the sulfenyl material was attributed to the effective  $\sigma$ - $\pi^*$  interaction which fixes the C-S bond orthogonal to one side of the enone. Obviously, the "vinyllogous effect"<sup>16</sup>

did not apply: the stereochemical outcome would otherwise have reversed for the sulfenyl example. The lower diastereoselectivity observed with the  $\gamma$ -alkoxy enones was attributed to the rotation around the  $C_\beta$ - $C_\gamma$  bond which can not be completely suppressed by the weak hyperconjugative effects of the C-O, C-C, or C-H bonds and leads, therefore, to stereochemical fluctuation.

### 2.1.3 Sigmatropic rearrangements

[3.3]Sigmatropic rearrangements of the type Claisen and its variations are very important in organic synthesis. The new C-C bond is formed next to an existing chiral center from the sterically less hindered face.<sup>21-23</sup> To know the electronic influence of hetero atoms in sigmatropic shifts, le Noble and coworkers<sup>24, 25</sup> have studied both oxy-Cope and Claisen rearrangements. The results were reported to favor Cieplak model. When the system was substituted by an electron-withdrawing group, the selectivity was in favor of *syn* to it. For instance, the fluoro-derivative **24** furnished a mixture of **25** and **26**, predominated by **25** to the extent of 81%, from the oxy-Cope rearrangement. Likewise, from a Claisen rearrangement process, **27** (R=H and Ph) furnished a 60:40 mixture of **28** and **29**.





## 2.2 Facial Selectivity in Diels-Alder reactions

Diels-Alder reaction<sup>26</sup> is one of the most important reactions in organic synthesis through which one can generate four new stereogenic centers at a time. In recent years, there has been much interest<sup>27-49</sup> in the diastereofacial selectivity of Diels-Alder reaction.  $\pi$ -Facial diastereoselectivity arises when either of the diene or dienophile possesses two different reactive faces. The requirements to achieve enhanced face discrimination involve proper mechanistic understanding and identification of the control elements. The presence of at least one chiral center is sufficient to influence the diastereofacial selectivity. The facial selectivity can also be influenced by either covalently bonded chiral auxiliary or chiral Lewis acid catalysts. In both the cases, propagation of chirality is achieved by blocking one prochiral face of the substrate so that the addend will come from the least hindered face to avoid the steric congestion. The facial selectivity can also be influenced by a single stereogenic center in an allylic position of either a diene or a dienophile, particularly when a hetero atom is present.

Overman and coworkers<sup>50</sup> have studied Diels-Alder reaction of semicyclic dienes such as 30. The data are collected in the Table 2.3. Only *endo* cycloaddition was observed. Reaction with N-phenylmaleimide (NPM) gave only the *anti* product when the allylic sub-

stituent was a methyl ether or a silicon ether. The addition was favored *syn* by 1.8:1 when the allylic position was substituted by a hydroxy function. Reaction with tetracyanoethylene also favored the *syn* addition somewhat.

Oveman did not find any evidence for a *syn*-directing effect of an allylic oxygen substituent which contrasts the observation of Fallis<sup>51</sup> from 5-heterosubstituted cyclopentadienes. The *anti* selectivity was explained by steric influence. In reaction with NPM *syn* to R, there is steric interaction between them. Additionally, there is repulsive electrostatic interaction between an allylic oxygen and the proximal carbonyl oxygen of the imide. These raise the energy of the TS from reaction *syn* to R and thus, lead to addition *anti* to the substituent.

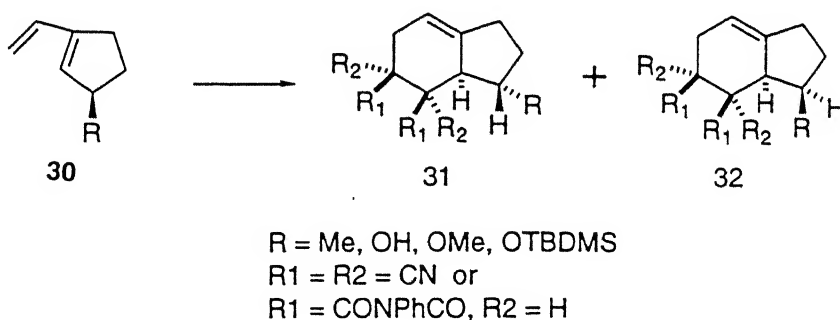


Table 2.3: Diels-Alder additions to 30

Entry	Diene 30	Dienophile	<i>Syn:Anti</i>
1	R=OH	NPM	64:36
2	R=OMe	NPM	0:100
3	R=OTBDMS	NPM	0:100
4	R=OH	TCNE	25:75
5	R=OTBDMS	TCNE	31:69
6	R=Me	NPM	17:83
7	R=Me	TCNE	18:82

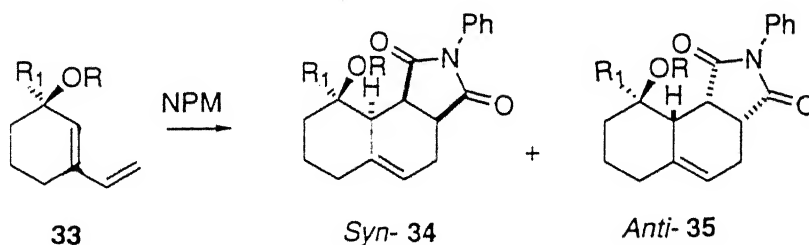
All the reaction were conducted in toluene

The considerably stronger *anti* directing ability of OMe and Me in cycloadditions with NPM is not consistent with conventional measures of the steric size of these groups. The

A-values of OMe and Me is 0.6 and 1.7, respectively. It could be rationalized only by the importance of electrostatic repulsion in destabilizing the endo-*syn* TS. In contrast, the electrostatic interaction is less important in cycloaddition with TCNE, otherwise OMe and Me substituents would have had comparable effects on the facial selectivity. These authors have, therefore, concluded that one can not extrapolate the Diels-Alder results of 5-heterosubstituted cyclopentadienes to other dienes.

The cycloaddition of the hydroxy substituted diene was highly solvent dependent. Reaction with NPM favored *syn* selectivity in nonpolar solvents. This was due to the favorable interaction between the *syn*-OH substituent and the proximal carbonyl oxygen of the imide dienophile. When the solvent was methanol, the selectivity was reversed. It is obvious that the -OH is solvated in methanol so that the *syn* attack becomes difficult.

Franck and coworkers<sup>52</sup> have studied Diels-Alder reaction of semicyclic dienes **33** with an allylic chiral center in the ring. Cycloaddition occurred only endo. The results were in accord with Overman's study. Reaction with N-phenylmaleimide gave only the *anti* product when the allylic substituent was a methyl ether or a silicon ether. The results are collected in the Table 2.4.

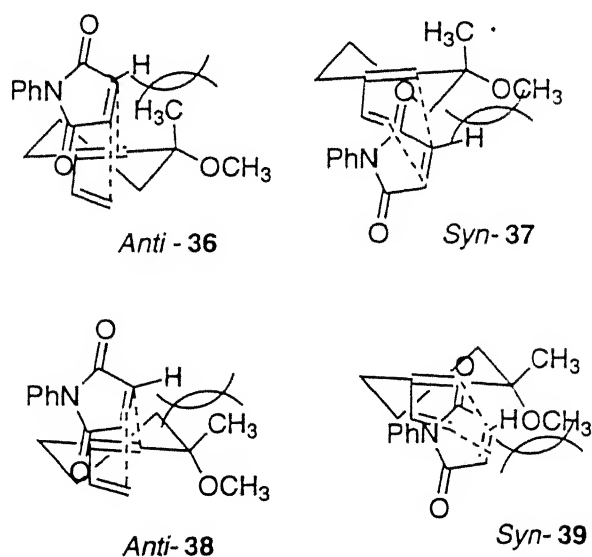


The possible transition states are given in the Fig 2.1. The transition states **38** and **39** will have higher energies of activation compared to **36** and **37** because of the unfavorable interaction of the C-O bond function parallel to the developing bonds in the transition states. The TS **36** is more favored than **37** since the Vogtle-Forster n-value,<sup>53</sup> which is



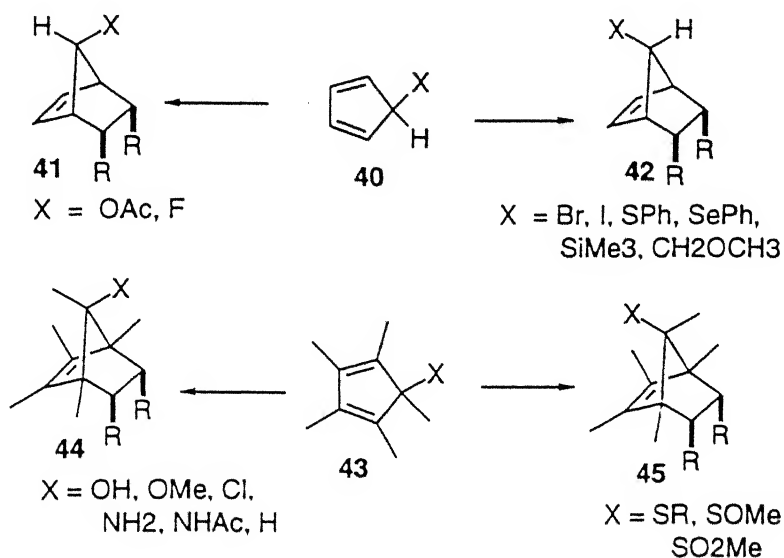
Table 2.4: Diels-Alder additions to **33**

Diene	Dienophile	solvent	Temp.(°C)	<i>Syn</i> : <i>Anti</i>
R1=H.R=H	NPM	C <sub>6</sub> H <sub>6</sub>	25	63:37
R1=H.R=H	NPM	MeOH	25	36:64
R1=H.R=H	NPM	DMF	25	17:83
R1=H.R=Me	NPM	C <sub>6</sub> H <sub>6</sub>	25	11:89
R1=H.R=Me	NPM	DMF	25	10:90
R1=H.R=TMS	NPM	C <sub>6</sub> H <sub>6</sub>	25	9:91
R1=H.R=H	DMAD	C <sub>6</sub> H <sub>6</sub>	Reflux	20:80
R1=H.R=H	DMAD	C <sub>2</sub> Cl <sub>2</sub>	25	19:81
R1=H.R=TMS	DMAD	C <sub>6</sub> H <sub>6</sub>	Reflux	8:92
R1=H.R=TMS	DMAD	CH <sub>2</sub> Cl <sub>2</sub>	25	9:91
R1=H.R=TMS	PTAD	CH <sub>2</sub> Cl <sub>2</sub> : THF	-78 to rt	100:0
R1=Me.R=H	NPM	C <sub>6</sub> H <sub>6</sub>	25	92:8
R1=Me.R=H	NPM	DMF	25	45:55
R1=Me.R=Me	NPM	CH <sub>2</sub> Cl <sub>2</sub>	25	26:74
R1=Me.R=Me	NPM	C <sub>6</sub> H <sub>6</sub>	50	25:75
R1=Me.R=TMS	NPM	C <sub>6</sub> H <sub>6</sub>	25	23:77
R1=Me.R=TMS	NPM	DMF	25	17:83

Figure 2.1: TS for the Diels-Alder reaction of semicyclic dienes **33** with NPM

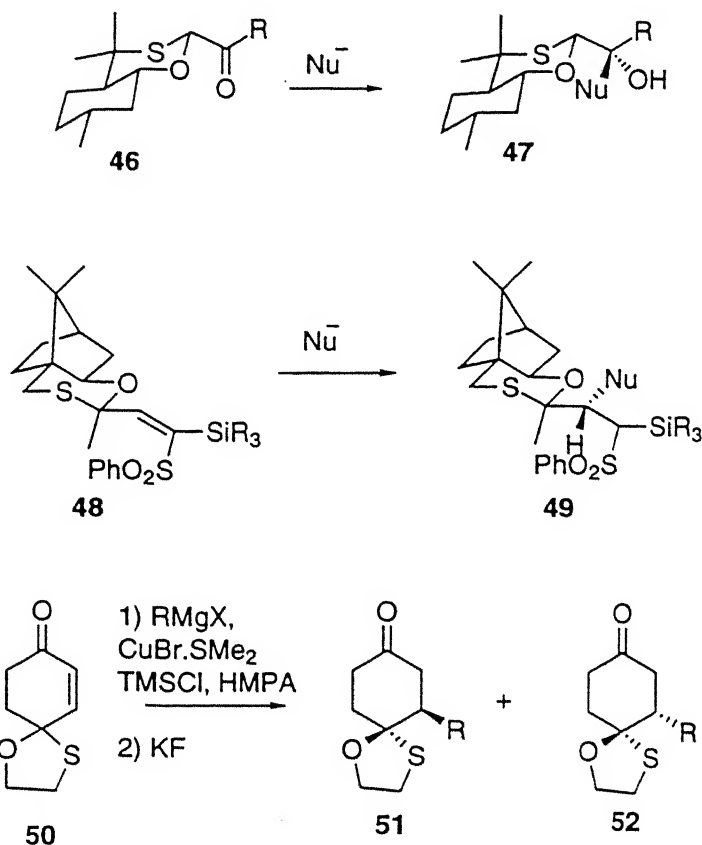
a better quantitative descriptor of the volume of a group in electroneutral intermolecular reactions, is higher for OMe than that of Me (the A-value of OMe is less than that of Me).

Woodward<sup>54</sup> was the first to observe exclusively *syn* to oxygen addition of ethylene to 5-acetoxy cyclopentadiene **40**. Fallis and Macaulay<sup>51, 55</sup> have studied the intermolecular Diels-Alder reactions of 5-sulfur substituted pentamethyl cyclopentadienes **43** and reported the preponderance of *anti* to sulfur diastereoface selection. The selectivity observed for the substituted cyclopentadienes with different heteroatoms at allylic position are collected below.<sup>56-66</sup>



When coupled together the above *syn* to oxygen and *anti* to sulfur additions, one is led to anticipate enhanced *anti* to sulfur face selection in reactions with species having both these heteroatoms at the same carbon. The literature on this subject is as follows.

Nucleophilic reaction of substrate **46**<sup>67</sup> gave only **47** in which the nucleophilic attack is *syn* to oxygen. Also, it has been observed that addition of a nucleophile to **48**<sup>68</sup> yielded only **49**. Recently Takei and coworkers<sup>3</sup> have observed the conjugate additions to **50** proceed predominantly *syn* to oxygen *i.e.* *anti* to sulfur to furnish **51**. The results are collected in the Table 2.5.

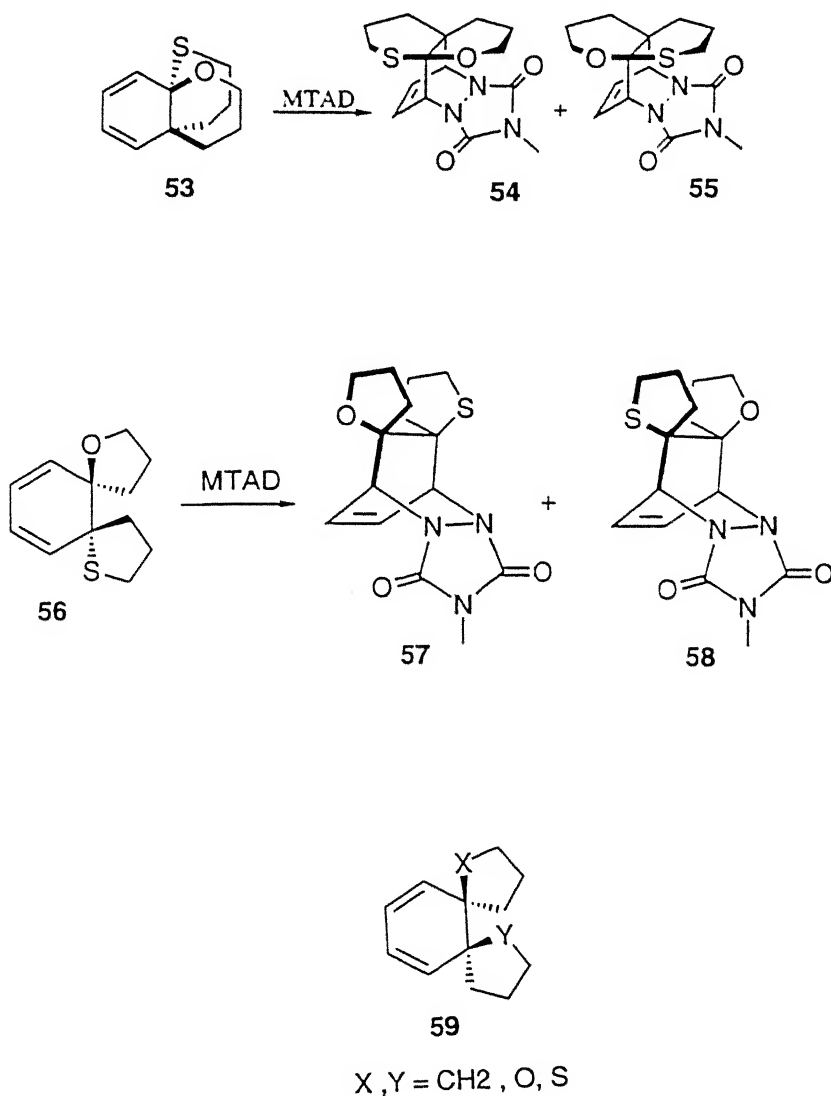
Table 2.5: Copper(I) catalyzed conjugate addition of  $RMgX$  to 50

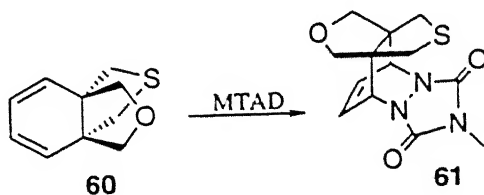
Entry	$RMgX$	Ratio of 51:52
1	$MeMgBr$	93:7 <sup>a</sup>
2	$Bu^nMgBr$	93:7 <sup>a</sup>
3	$BnMgCl$	92:8 <sup>a</sup>
4	$PhMgBr$	96:4 <sup>a</sup>
5	$Pr^iMgBr$	87:13 <sup>a</sup>
6	$Bu^tMgCl$	76:24 <sup>b</sup>

<sup>a</sup> Ratio by  $^{13}C$ -NMR <sup>b</sup> Ratio by capillary GC

Paquette *et al.*<sup>69, 70</sup> have observed from the intermolecular Diels-Alder reaction of a cyclohexadiene consisting of an allylically placed hemithioacetal 53 with reactive dienophiles such as N-methyl- (MTAD) and N-phenyltriazolinedione (PTAD) as high a diastereoface

selection as 20:1 in favor of *syn* to oxygen. However, dienophiles as strong as triazoline-diones are reported<sup>70</sup> to exhibit reverse face selection in the selected examples studied. Consequently, one would have expected predominantly *syn* to sulfur selection from the above studies of Paquette *et al.* To know the real effect of hetero atoms, Paquette *et al.*<sup>71</sup> have further studied the cycloaddition of dienes **56** and **59** with different dienophiles. The results are collected in the Table 2.6.



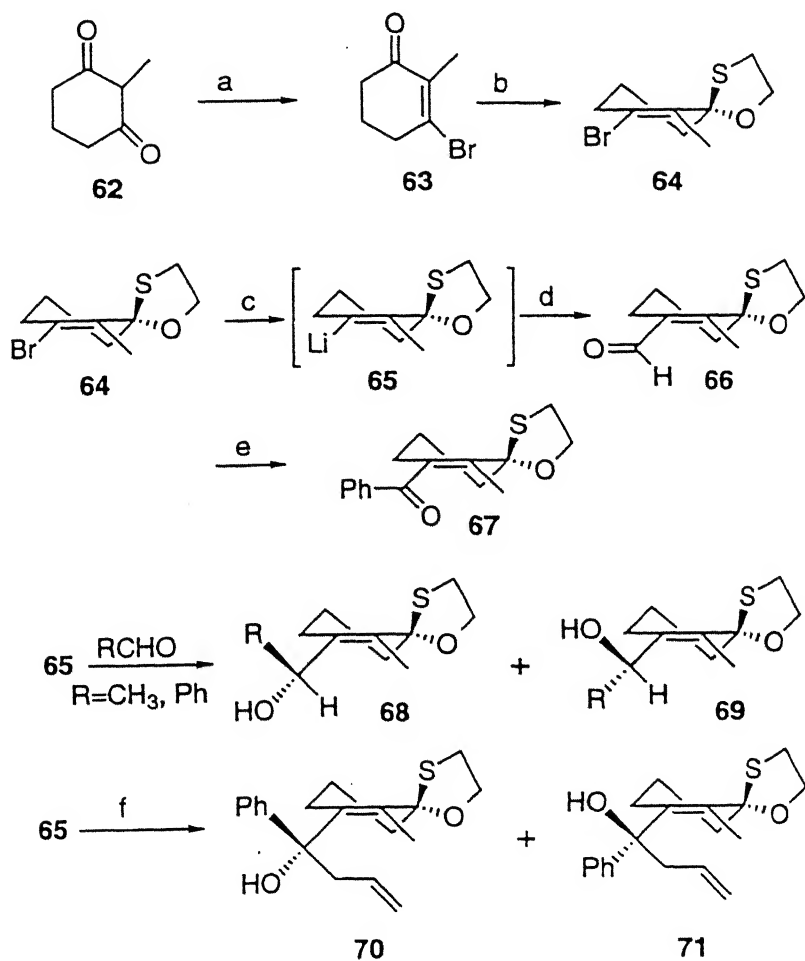


## 2.3 Present Study

### 2.3.1 Diastereofacial Selectivity of Nucleophilic Additions to 6-Methyl-1-oxa-4-thiaspiro[4.5]dec-6-en-7-carbaldehyde

In this section we discuss our studies focused on substrates **66** and **67** (Scheme 2.1) wherein both the oxygen and sulfur atoms are placed at the  $\gamma$ -carbon with fixed stereodispositions. The C-S bond is pseudoaxial and the C-O pseudoequatorial. These orientations were deduced from the X-ray structures<sup>74</sup> of the alcohols **68** (R=Me: *p*-OMe-benzoate **76**) (Fig. 2.2) and **69** (R=Ph) (Fig. 2.3) which were synthesized as shown.

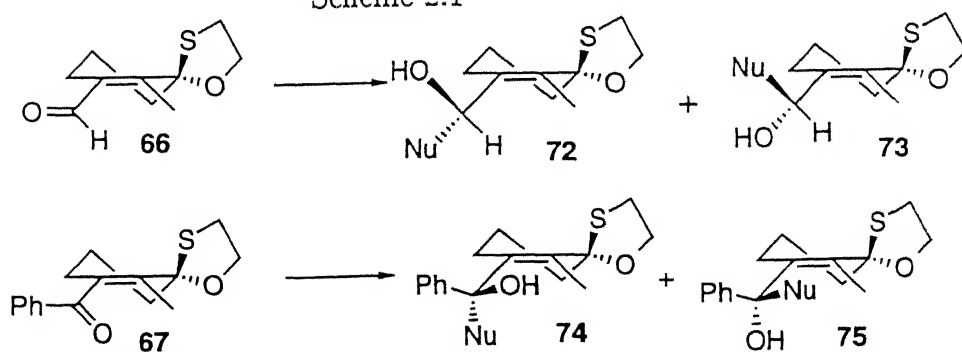
Whereas the more polar **68** of the pair **68/69** (R=Me) had the carbinol oxygen *syn* to the oxygen of the acetal across the cyclohexene mean plane, the less polar **69** of the pair **68/69** (R=Ph) had them *anti*. Since the oxygen atom binds better with silica gel than sulfur, both the oxygens placed *syn* are, therefore, likely to raise the polarity of the material in question. This notion finds further support from the X-ray structure of the more polar **70** (Fig. 2.4) of the pair **70/71**. This diastereomeric pair of alcohols was prepared from reaction of either **65** with allyl phenyl ketone or reaction of **67** with allyl Grignard, as shown in the Scheme 2.1 and 2.2. This polarity-based stereochemical characterization can, therefore, be safely extended to other derivatives as well.



Reagents:

- (a)  $\text{Et}_3\text{N}$ ,  $\text{MsCl}$ ,  $\text{CH}_2\text{Cl}_2$ ,  $0^\circ\text{C}$ ;  $\text{BzEt}_3\text{NBr}$ ,  $\text{BF}_3\cdot\text{OEt}_2$ ,  $\text{CH}_2\text{Cl}_2$   
 (b)  $\text{HOCH}_2\text{CH}_2\text{SH}$ ,  $\text{PTSA}$ ,  $\text{C}_6\text{H}_6$ , reflux (c)  $n\text{-BuLi}$ ,  $\text{THF}$ ,  $-80^\circ\text{C}$   
 (d)  $\text{DMF}$  (e)  $\text{PhCONMe}_2$  (f) allylphenyl ketone

Scheme 2.1



Scheme 2.2

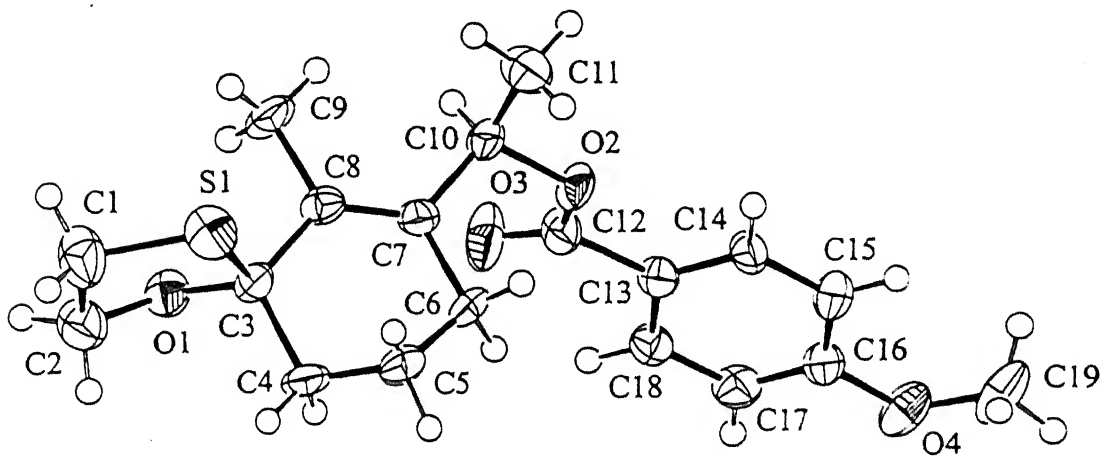
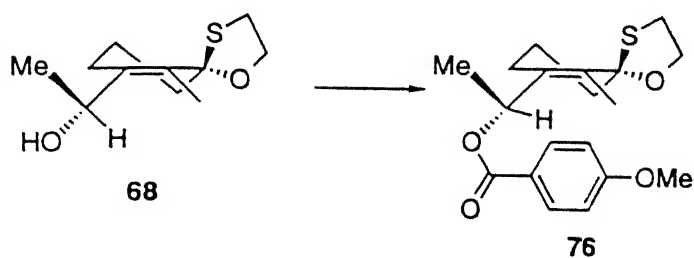


Figure 2.2: ORTEP drawing of 76

Selected bond lengths ( $\text{\AA}$ ) in 76:

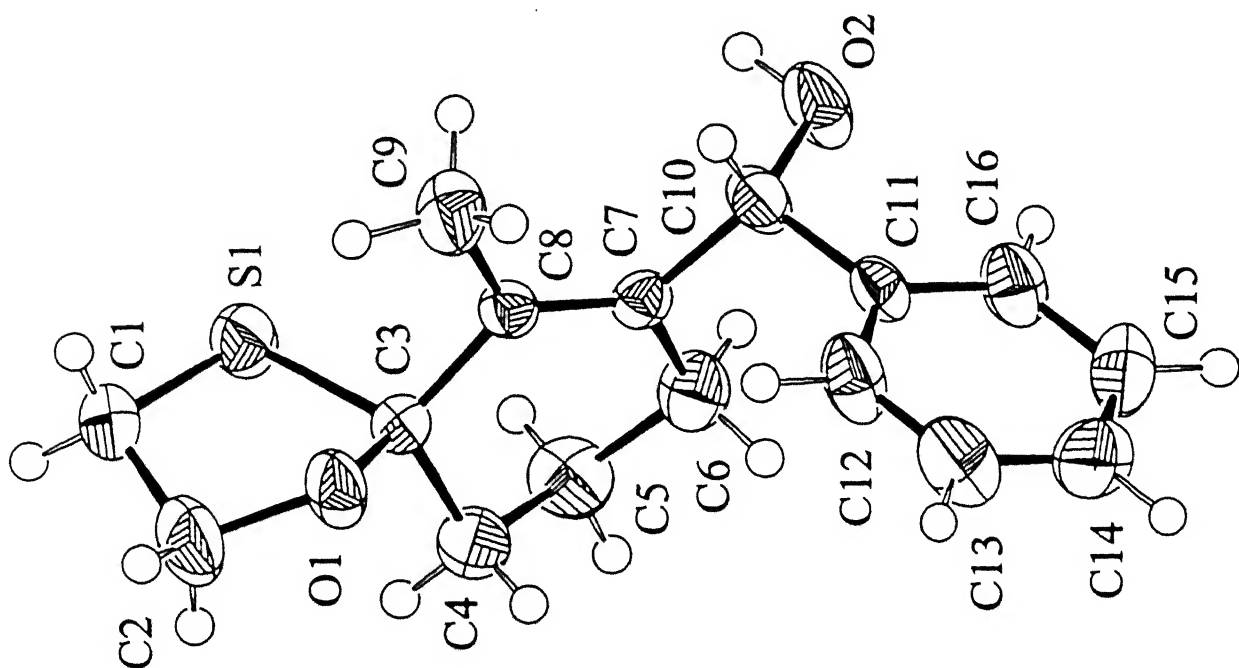
S1-C3 1.89(1)	S1-C1 1.78(1)	O1-C3 1.39(1)	O1-C2 1.43(1)
C8-C7 1.33(1)	C7-C10 1.51(1)	C10-O2 1.49(1)	C12-O2 1.35(1)
C12-O3 1.18(1)			

Selected bond angles ( $^\circ$ ):

C1-S1-C3 91.7(4)	S1-C3-O1 105.0(6)	C2-O1-C3 112.3(7)	C3-C8-C7 122.9(8)
C3-C8-C9 112.9(8)	C9-C8-C7 124.2(8)	C8-C7-C10 121.1(8)	C10-O2-C12 114.6(7)
O2-C12-O3 125.2(8)	O2-C12-C13 110.0(8)		

Selected torsion angles ( $^\circ$ ):

O1C3C8C7 -142.3(9)	S1C3C8C7 102.7(9)	C8C7C10C11 95.0(1)
C10O2C12O3 -2(1)	C8C7C10O2 -148.7(9)	

Figure 2.3: ORTEP drawing of **69** (R=Ph)

Selected bond lengths ( Å) in **69** (R=Ph):

S1-C3 1.867(4)	S1-C1 1.800(4)	O1-C3 1.416(4)	O1-C2 1.426(1)
C3-C8 1.518(4)	C8-C9 1.514(5)	C8-C7 1.333(4)	C7-C10 1.519(5)
C10-O2 1.416(4)			

Selected bond angles (°):

C1-S1-C3 92.3(2)	S1-C3-O1 105.0(2)	C2-O1-C3 111.2(3)	C3-C8-C7 121.3(4)
C3-C8-C9 114.1(3)	C9-C8-C7 124.6(3)	C8-C7-C10 122.5(4)	

Selected torsion angles (°):

O1C3C8C7 134.2(3)	S1C3C8C7 -111.5(3)	C9C8C7C10 6.5(6)
C8C7C10C11 113.7(4)	C16C11C10O2 -7.3(5)	O2C10C7C6 56.4(5)
C8C7C10O2 -125.7(4)		



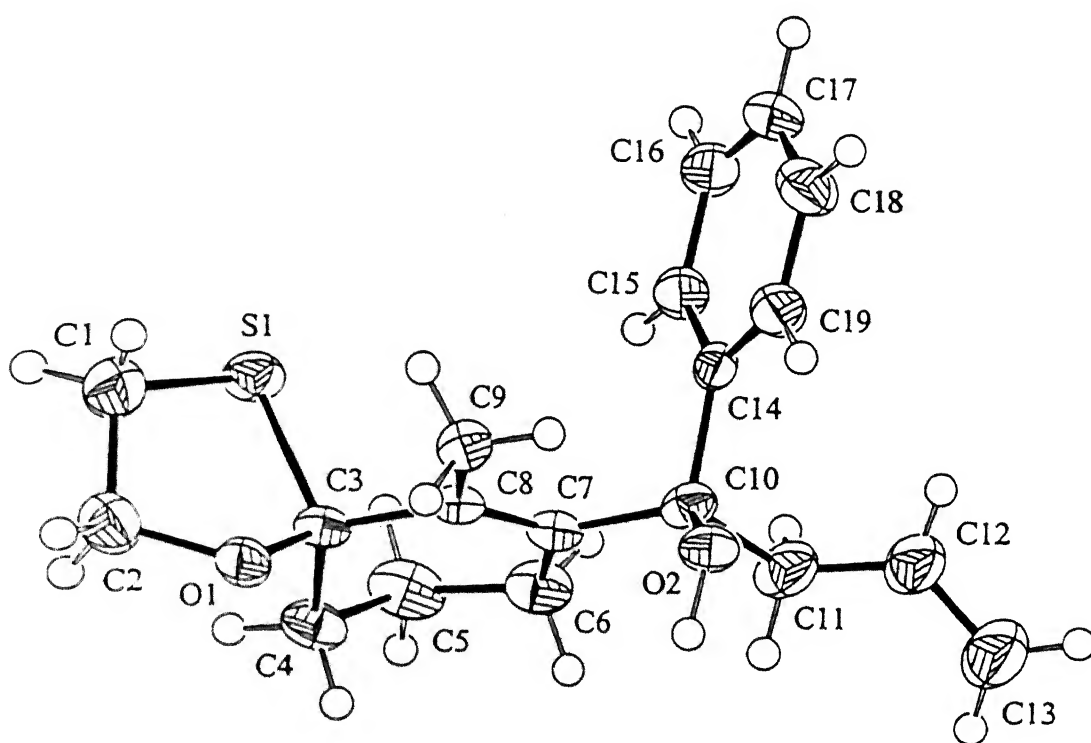


Figure 2.4: ORTEP drawing of 70

Selected bond lengths ( Å) in 70:

S1-C3 1.870(2)	S1-C1 1.810(3)	O1-C3 1.434(2)	O1-C2 1.426(4)
C3-C8 1.510(3)	C8-C7 1.338(3)	C7-C10 1.544(3)	C10-O2 1.433(3)
C12-C13 1.313(4)			

Selected bond angles (°):

C1-S1-C3 92.8(1)	S1-C3-O1 104.6(1)	C2-O1-C3 111.2(2)	C3-C8-C7 121.4(2)
C3-C8-C9 113.5(2)	C9-C8-C7 125.1(2)	C8-C7-C10 122.1(2)	O2C10C14 106.6(2)

Selected torsion angles (°):

S1C3O1C2 32.6(2)	O1C3C8C7 147.2(2)	S1C3C8C7 -99.2(2)
C9C8C7C10 1.2(3)	C8C7C10C11 167.1(2)	C12C11C10O2 -48.3(3)
C8C7C10O2 46.6(3)	C10C11C12C13 141.0(3)	

Table 2.7: Crystal data

	76	69	70
Formula	C <sub>19</sub> H <sub>24</sub> O <sub>4</sub> S	C <sub>16</sub> H <sub>20</sub> O <sub>2</sub> S	C <sub>19</sub> H <sub>24</sub> O <sub>2</sub> S
FW	348.46	276.39	316.46
Crystal Dimensions, mm	0.50 X 0.33 X 0.31	0.52 X 0.40 X 0.30	0.45 X 0.30 X 0.27
Crystal colour, Habit	colourless, prism	colourless, prism	colourless, prism
Crystal System	monoclinic	triclinic	triclinic
a, Å	6.620(3)	10.955(2)	10.150(2)
b, Å	11.322(3)	11.186(2)	11.800(1)
c, Å	12.297(3)	6.221(2)	7.502(1)
$\beta$ , °	103.52(3)	100.69(2)	104.06(1)
V, Å <sup>3</sup>	896.1(5)	733.4(3)	852.8(2)
Z	2	2	2
D <sub>calc</sub> , g/cm <sup>3</sup>	1.291	1.252	1.232
F <sub>000</sub>	372.00	296.00	340.00
$\mu$ (MoK $\alpha$ ), cm <sup>-1</sup>	1.90	2.06	1.85
Space Group	P2 <sub>1</sub> (# 4)	P $\bar{1}$ (# 2)	P $\bar{1}$ (# 2)
Temp. (°C)	-73.0	-103.0	-103.0
R	0.052	0.048	0.041
Rw	0.051	0.036	0.033

The C-S bond orbital will be expected to interact with the  $\pi_{C=C}$  by virtue of being axial. While the alkyl group at the  $\gamma$ -carbon is forced by the ring-geometry to eclipse with the olefin, the oxygen atom is in a configuration which resembles the configuration of the  $\gamma$ -benzyloxy- $\alpha$ -enones studied by Sato *et al.*<sup>70</sup> The designated *s-trans* conformation of the enal **66** is in accord with the literature.<sup>75, 76</sup> A 300 MHz <sup>1</sup>H spectrum in CDCl<sub>3</sub> showed only single singlet for the -CH=O ( $\delta$  10.14) and the Me ( $\delta$  2.20) (Fig. 2.7). The lower than the normal <sup>1</sup>H chemical shift of -CH=O will be attributed to the deshielding effect of the proximate  $\pi$  bond which could be experienced only in the *s-trans* arrangement.<sup>76</sup> The *s-cis* conformation will be disfavored for steric interactions between the carbonyl oxygen and the methyl substituent.<sup>77, 78</sup> Following the observations of Sato *et al.*, the nucleophile

is predicted to attack *anti* to the more electron-donating sulfur<sup>20</sup> group and, hence, a preponderance of **72** over that of **73** (Scheme 2.2) will be predicted. Likewise, the ketone **67** must exist in the designated *s-cis* conformation to avoid the severe steric interactions between the Ph and the Me groups in the alternate *s-trans* conformer and the product **74** will be predicted to predominate over **75**.

The results of our experiments with several representative nucleophiles are collected in the Table 2.8. The diastereoselectivity with all the  $sp^3$  nucleophiles (entries 1-6 and 16) was, at best, in only marginal favor of the less polar **72** when compared to the high selectivity reported by Sato *et al.*. This result is, indeed, very surprising. Further, there was a clean reversal in diastereoselectivity in reactions with  $sp^2$  nucleophiles (entries 7-15). The highest selectivity (**73**:**72** = 3.5:1.0) was observed with PhMgBr in Et<sub>2</sub>O at -80 °C (entry 7). The selectivity dropped to 2.5:1.0 in reaction with 1-naphthyl-MgBr (entry 12). The selectivity with vinyl-MgBr (entry 14) under identical conditions was 1.8:1.0. It is interesting to note that the nucleophiles which may be considered intermediate to  $sp^3$  and  $sp^2$  (entries 17-21) showed no noticeable selectivity. The  $sp$  nucleophiles also exhibited reverse diastereoselection (entries 22-24). The diastereoselectivity was zero in reaction of allylmagnesium bromide with the single ketone example that we have examined (entry 18). All the diastereoselectivities were determined from the weights of the individual alcoholic products with the results being consistent over at least two independent experiments. Two significant points emerged:

(i) the level of diastereoselection achieved from  $sp^3$  nucleophiles was unexpectedly very low, and

(ii) the facial selectivity was reversed in reactions with  $sp^2$  and  $sp$  nucleophiles.

It is important to note that all the products were found stable to silica gel chromatography. The conversion of one diastereomer into the other was not observed. The products of reaction with PhMgBr, in particular, may be expected to be vulnerable to silica gel for

experiments in which both the diastereomers were separately stirred with column-grade silica gel in benzene for 12h; in no instance was the other isomer detected by TLC.

The change in selectivity pattern led us also to consider whether there was interconversion of the products formed under the conditions of the reaction. This interconversion could take place at the stage of either the metal-alcoholate or the alcohol itself which was formed after quenching the reaction with MeOH at  $-80^{\circ}\text{C}$  and then allowed to warm to rt. Two experiments were performed on **72** (Nu=Ph). In the first, the lithium salt was generated on reaction with  $\text{Bu}^n\text{Li}$  at  $-80^{\circ}\text{C}$ . After 30 min, a TLC immediately on quench with MeOH at  $-80^{\circ}\text{C}$  and then again at rt did not show any of the isomer **73** (Nu=Ph). In the second, the Mg-salt was prepared by reaction with  $\text{Bu}^t\text{MgCl}$  at  $-80^{\circ}\text{C}$  and quenched with MeOH 30 min later. Again, **73** was not detected by TLC at either of the above two stages. Similar experiments on **72** (Nu=PhCC; Li salt) and **73** (Nu=Me; Mg salt) did not show any interconversion either. It is, therefore, reasonable to expect a similar behaviour of the other alcohols too. The ratios of the isomers reported are, therefore, the true ratios of the isomers actually produced.

The change in diastereoselectivity with the change in the hybridization character of the attacking nucleophile from  $\text{sp}^3$  to  $\text{sp}^2$  and  $\text{sp}$  is not totally unprecedented. From the studies on *cis*-[9.3.1]bicyclic ketones, Paquette *et al.*<sup>79</sup> have observed the selectivity change from 21:79 in favor of attack *syn* to the larger ring in reaction with  $\text{BuMgBr}$  to 56:44 in reaction with  $\text{PhMgBr}$ . Wipf and coworkers<sup>16, 19</sup> have observed only reduction in the level of selectivity from 4.8:1 to 3.6:1 in favor of attack from *anti* to the OMe substituent when the nucleophile was changed from  $\text{MeMgBr}$  to  $\text{PhMgBr}$  in reactions of 4-methoxy-4-methyl-2,5-cyclohexadienone (**15**, R=R1=Me). These authors have recognized the sensitivity of stereoselection to the electronic structure and, hence, the state of aggregation of the nucleophile. Other variations in reaction parameters such as the solvent and the counter cation were attempted but in no case were these authors able to observe the selectivity change in

favor of *syn* to OMe. Clark and Warkentin<sup>80</sup> have studied 2-norbornen-7-one and reported the selectivity change from 77:23 in favor of *syn* to the  $\pi$  bond with MeLi to 30:70 and 28:72 in reactions with vinyl lithium and PhLi, respectively.

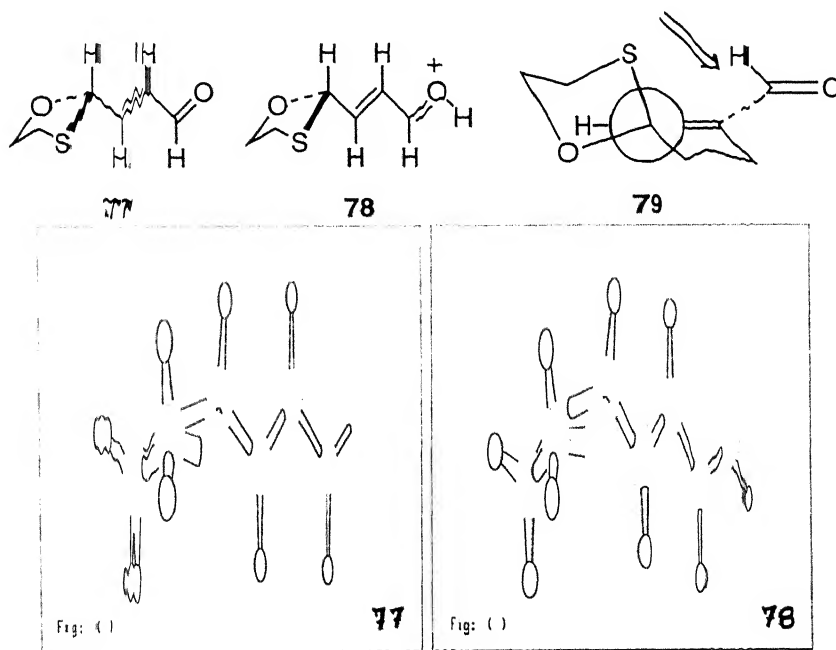
Paquette has attributed the above change in selectivity to the larger steric requirement of PhMgBr than that of BuMgBr. However, since the *syn* face in 2-norbornen-7-one is somewhat less hindered than the *anti* face, the reversal in selectivity in reactions with vinyl lithium and PhLi appears surprising. The strong preference for *anti* attack by these lithium reagents was attributed to the fact that these compounds are more polar than their saturated analogs and that the negative charge approaching the carbonyl from the *syn* face encounters a repulsive interaction with the double bond. However, this contrasted the observation that both Bu<sup>n</sup>Li and PhLi gave the exact same stereochemistry in both polar (Et<sub>2</sub>O) and nonpolar (n-hexane) solvents because the ionic character of the C-Li bond would otherwise be expected to be significantly different in the two solvents. The present reversal in diastereoselectivity is definitely not steric in origin because, had it been so, a selectivity better than that achieved from PhMgBr must have been observed from 1-naphthyl-MgBr. Further, contrary to the observed results, a similar reversal in face-selection must have also taken place when the nucleophile was changed from MeMgI to Bu<sup>t</sup>MgCl. Both, however, exhibited identical results. That the observed change in selectivity was indeed not steric in origin was further supported from the reported reactions of 4-*tert*-butylcyclohexanone in Et<sub>2</sub>O with Grignard reagents such as Bu<sup>t</sup>MgBr, PhCH<sub>2</sub>MgCl, EtMgBr, and PhMgBr which are, respectively, 100, 76, 71, and 49% equatorial-selective. Obviously, had it been the steric of the nucleophile involved, the selectivity with PhMgBr must have been better than those with EtMgBr and PhCH<sub>2</sub>MgCl, and, almost certainly, comparable to that with Bu<sup>t</sup>MgBr.

Although the observed  $\pi$ -facial reversal can be easily explained by invoking an opportune conformational change in the enal subunit from *s-trans* to *s-cis*, such a prospect is

hardly tenable. Everything else but the actual nucleophile being the same, it is highly unlikely that such a conformational change will occur only in those cases where  $sp^2$  and  $sp$  nucleophiles are involved. Wipf and coworkers<sup>16, 19</sup> have recently correlated the diastereoselectivity of 4,4-disubstituted cyclohexadienones and naphthoquinones with the direction of molecule's dipole along the Z axis. The nucleophile approached the carbonyl on the face which constituted its positive end. Given the fact that a S-C bond is electron-releasing from S to C and that a C-O bond is electron-attracting from C to O, a simple vector analysis of the dipoles in **66** would indicate a substantial component of this dipole along the axis that is orthogonal to the molecular plane and points from the face containing S to the face possessing the acetal's O. This was confirmed from AM1 calculation<sup>81</sup> of dipoles; the component along the Z direction was 1.03 D. Nucleophiles will, therefore, be predicted to approach the carbonyl predominantly on the face that is *syn* to S. In sharp contrast to this, the  $sp^3$  nucleophiles exhibited attack *anti* to the sulfur. The level of the observed diastereoselectivity was, however, only marginal. The  $sp^2$  and  $sp$  nucleophiles may appear to follow the dipole model since they exhibited preference for attack *syn* to S but then, again, it is not so for the dipole reasons. A reaction that was carried out with PhMgBr in a 9:1 mixture of Et<sub>2</sub>O and HMPA (entry 10) exhibited a drop in selectivity to 1.6:1 from 3.5:1 in Et<sub>2</sub>O. Must the system obey the dipoles model, a raise in the dielectric constant of the reaction medium will be expected to raise the selectivity further due to a raise in the induced dipole moment of the substrate. On the contrary and even more interestingly, a reaction conducted in a 1:1 mixture of Et<sub>2</sub>O and n-hexane had the selectivity enhanced considerably to 7.2:1 (entry 11). The predominant attack *anti* to S in the acyclic examples **21** studied by Sato *et al.* also contradicts the dipole model.

Sato *et al.*<sup>20</sup> have claimed the diastereoselectivity of their acyclic systems a consequence of the electronic effects originating from the S. The fact that the C-S bond in **66** is (pseudo)axial in spite of the large bulk of S in comparison to that of the acetal's O

is, in itself, indicative of some electronic effects. The enone unit, being electron-deficient, must prefer the C-S bond parallel to its  $\pi$ -orbitals. This is achieved by having the C-S bond (pseudo)axial. This parallelism must be strengthened on allowing the enone become even more electron-attracting by, say, cation complexation of the carbonyl oxygen.<sup>82-88</sup> That this is indeed so is demonstrated by *ab initio* MO calculations at 6-31G\* level on the molecule **77** and its protonated derivative **78**. The torsion angle 5 1 2 3 (arbitrary numbering) changed from 70.32° in **77** to 82.79° in **78**. This conformational change is supported additionally by forcing the acetal's electron-attracting C-O bond more in the  $\sigma$  plane of the enone system. The torsion angle 6 1 2 4 changed from 137.97° in **77** to 149.78° in **78**. Since a similar conformational change must be expected of **66** in its reactions with nucleophiles, the utterly poor diastereoselectivity with all the  $sp^3$  nucleophiles remains unexplained by the above electronic effects. The preferred *syn* to S attack in reactions with  $sp^2$  and  $sp$  nucleophiles can not be explained by these electronic effects either.



The above analysis led us to examine the materials (21) studied by Sato *et al.*<sup>20</sup> more closely. In all but one S-containing substrates, the substituent on S is phenyl which is likely to orient over the enone function in an exercise to lower the energy through  $\pi$ -complexation.<sup>89</sup> This will restrict the rotation around the C $_{\gamma}$ -S bond and, thus, block this face effectively to allow nucleophiles enter predominantly from the *anti* face, as observed indeed. Since a substrate with Me as a substituent on S does not benefit from such a prospect and, also, since a Me group is smaller in size than a phenyl group, the diastereoselectivity observed is likely to be reduced. However, since a large alkyl substituent such as Bu<sup>t</sup>, Pr<sup>t</sup>, n-C<sub>6</sub>H<sub>13</sub> and n-C<sub>7</sub>H<sub>15</sub> (actually used in Sato's studies) on C $_{\gamma}$  will also be expected to restrict the rotation around C $_{\gamma}$ -S bond to a large extent, the diastereoselectivity may still not reduce as much as expected above. This is also in good accord of the reported experimental results (cf. entries 7 and 8 in the Table 2.2). The selectivity was reduced from 93:7 to 87:13 when the substituent on S was changed from Ph to Me. The diastereoselectivities observed by Sato *et al.* are, therefore, in perfect tune with the Cram's steric approach model.<sup>90</sup> The electronic effects arising from S influence primarily the stable conformer determination. If there is any influence of these electronic effects on the observed diastereoselectivity, it is substantially small. A similar reasoning for the enone substrates bearing an oxygen on C $_{\gamma}$  holds good as well.

For the study of true electronic effects on diastereoselection, the substituents and the attacking reagent must be as small as possible. Moreover, the substituents must have no ability to complex with either the other reagent or a function within the same molecule. The substrate 66 which meets these criteria appears well suited to such a study. Whereas the very poor selectivity with the sp<sup>3</sup> nucleophiles is a consequence of only subtle electronic effects arising from the acetal function, the preferred attack *syn* to S by sp<sup>2</sup>/sp nucleophiles remains yet to be accounted for. In the transition structure 79, the nucleophile is likely to suffer from some steric interaction with the axially substituted large S atom and, hence,



more attack from the *anti* face will be predicted. The observed *syn* attack may, therefore, be a consequence of some significant electrostatic attraction of S for  $sp^2$  and  $sp$  nucleophiles which ensures the observed *syn* to S delivery of these nucleophile to the carbonyl carbon. Why this electrostatic attraction of S only for the  $sp^2$  and  $sp$  nucleophiles and not for the  $sp^3$  counterparts? It is not clear to us for the absence of significant physical data on such species. However, the known larger polar character of the  $sp^2$  and  $sp$  nucleophiles<sup>91</sup> and, hence, larger concentration of the negative charge on the carbon in these species than those in the  $sp^3$  nucleophiles may be held responsible for their special recognition by S.

In view of the literature (*vide supra*) and our own results, Sato's report constitutes the only report that has invoked the participation of a  $\gamma_{C-S}$  bond to have caused enough perturbation in the extended  $\pi$ -system of an acyclic enone that the *anti* to S face reacted in preference to the other. To the best of our knowledge, there is no other report on face selection of an enone system bearing a sulfur on the  $\gamma$ -carbon. It is, therefore, not surprising to seek an explanation for the high diastereoselection observed by Sato in Cram's steric approach model.

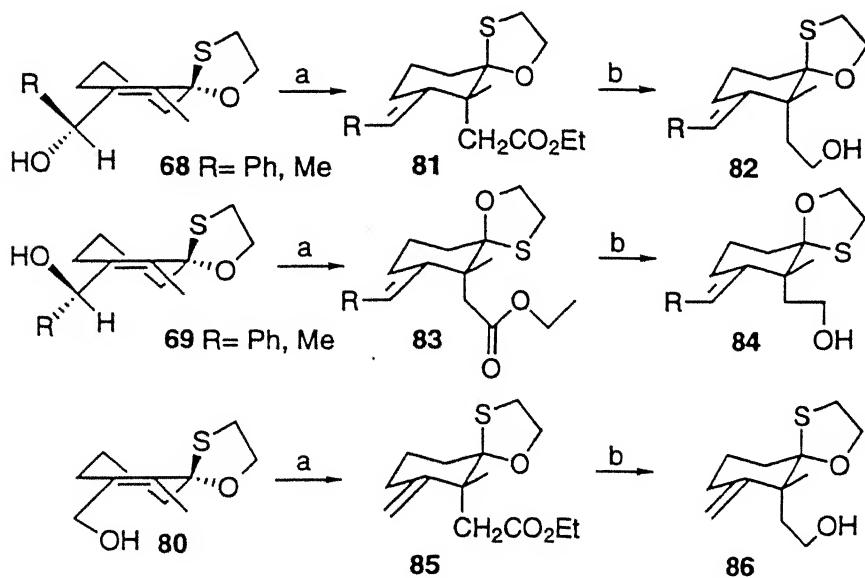
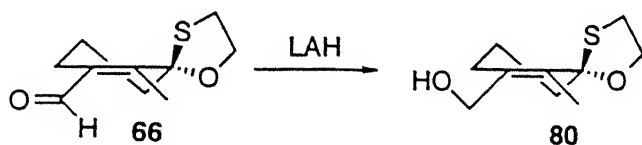
Recently, the indium-promoted allylation reaction has been shown to exhibit higher selectivity in the reactions of  $\alpha$ -alkoxycyclohexanones than the related reactions involving other organometallic species.<sup>92-94</sup> The reaction is reported to be even more selective when conducted in water than when performed under strictly anhydrous conditions.<sup>95</sup> We, however, observed no selectivity in anhydrous THF (entry 21). The pH of the solution is reported to be lowered to 2.9 when the reaction is conducted in water.<sup>96</sup> For the fear of destroying the acetal function at such a low pH, we did not use water as the reaction medium. Instead, we used phosphate buffer (pH 6.8) and witnessed no reaction. A combination of buffer and THF was also unyielding.

In conclusion, a change in hybridization from  $sp^3$  to  $sp^2$  and  $sp$  of the nucleophile changed the diastereosense of the reaction of 6-methyl-1-oxa-4-thiaspiro[4.5]dec-6-en-7-

carbaldehyde. Whereas the selectivity with  $sp^3$  nucleophiles was surprisingly only in marginal favor of attack *anti* to S, the  $sp^2$  and  $sp$  nucleophiles exhibited relatively much improved but reversed  $\pi$ -selection. The reason for this reversal is believed to be a meaningful electrostatic attraction of the electron-deficient S for the  $sp^2$  and  $sp$  nucleophiles which, unlike the  $sp^3$  counterparts, have the negative charge concentrated largely on the carbon for their significant polar characters. The observed diastereoselectivity is neither steric in nature nor does it obey the dipole model proposed by Wipf. The observation that the electronic effects are not manifest in the observed diastereoselection is in support of the observations of other researchers.

### 2.3.2 Orthoester Claisen rearrangements of substituted 6-methyl-1-oxa-4-thiaspiro[4.5]dec-6-en-7-carbinol

The choice of a [3.3] sigmatropic shift reaction was based largely upon the fact that the bond formation between the termini of the diene unit will be in the immediate vicinity of the acetal function and thus the maximum diastereofacial impact of the latter must be in force. The Me substituent on the 6-ring was expected to act as a marker and help the determination of diastereoface selection. The carbinols **68** and **69** were prepared as shown in the Scheme 2.1. Lithiation of the vinyl bromide **64** with  $Bu^{\text{n}}Li$  in THF at  $-80\text{ }^{\circ}C$  and reaction of the so derived vinyl lithium with  $RCHO$  ( $R=Me, Ph$ ) furnished an almost 1:1 mixture of the carbinols **68** and **69** in  $>60\%$  yields. Likewise, reaction of the above vinyl lithium with DMF furnished the aldehyde **66** in 70% yields. This was reduced with LAH in  $Et_2O$  at  $0\text{ }^{\circ}C$  to furnish the carbinol **80** in quantitative yield. The stereostructures of **68** ( $R=Me$ ; *p*-methoxybenzoate, **76**) and **69** ( $R=Ph$ ) were discerned from their single crystal X-ray crystallographic studies. The vinyl bromide **64** was synthesised from the diketone **62** as outlined in the Scheme 2.1 by known procedures.<sup>97-100</sup>



Reagents :

(a)  $\text{MeC(OEt)}_3$ , Toluene, reflux (b) LAH,  $\text{Et}_2\text{O}$ , 0 to 20 °C

All the rearrangements were performed in boiling toluene without any acid catalyst. We have also attempted these reactions in boiling benzene. However, the reactions took longer time. The use of an acid catalyst, e.g. *p*-toluenesulfonic acid, caused decomposition involving cleavage of the acetal function. In the event, a toluene solution of one of the above carbinols and triethyl orthoacetate was refluxed under nitrogen until a complete disappearance of the carbinol. The solvent was removed in vacuo and the residue chromatographed over silica gel to isolate the product(s). In each case, the yield of the rearrangement product was >90%. The more polar carbinols **68** (R=Me, Ph) furnished a single ester product **81**. This was reduced with LAH in  $\text{Et}_2\text{O}$  at 0 °C to receive a single alcohol **82** (R=Me, Ph). The reaction had proceeded exclusively *syn* to the oxygen. The stereochemical char-

acterization of **82** was made possible from a combination of ROESY (Fig. 2.43 and Fig. 2.47) and 1D nOe spectra. Both demonstrated the quaternary Me *syn* to the S for the good interaction with  $\text{CH}_2\text{S}$ . Likewise, the stereochemistry of the rearranged ester product **81** was confirmed from a combination of ROESY (Fig. 2.36), NOESY (Fig. 2.38), and 1D nOe. Whereas both ROESY and NOESY exhibited interaction between the quaternary Me and  $\text{CH}_2\text{S}$ , 1D nOe established interaction between  $\text{CH}_2\text{CO}_2\text{Et}$  and the  $\text{CH}_2\text{O}$  of the acetal.

The less polar carbinols **69** ( $\text{R}=\text{Me}$ ,  $\text{Ph}$ ) also furnished a single ester product **83** which was, once again, reduced by LAH to isolate the only alcohol **84**. Whereas the stereochemical identification of **84** ( $\text{R}=\text{Me}$ ) was secured from a single crystal X-ray structure determination, that of **84** ( $\text{R}=\text{Ph}$ ) was based on exclusive 1D nOe results. An interaction between the quaternary Me and the  $\text{CH}_2\text{O}$  of the acetal supported the assignment. The rearrangement of **69** had, therefore, proceeded exclusively *syn* to the sulfur. The crystal structure of **84**( $\text{R}=\text{Me}$ ) was composed of two independent molecules per asymmetric unit. An ORTEP drawing is given in the Fig. 2.5.

Finally, the carbinol **80** reacted under the above typical conditions of orthoester Claisen rearrangement to furnish a single ester **85**. This was reduced to the alcohol **86**. The stereochemical determination of **86** was made from ROESY (Fig. 2.57) and 1D nOe spectra. Both of these exhibited good interaction between the quaternary Me and  $\text{CH}_2\text{S}$ . The reaction had, therefore, proceeded exclusively *syn* to the acetal's oxygen.

The stereostructures of the carbinol products **82**, **84**, and **86** were also supported from a definite pattern of  $^1\text{H}$  absorptions for the quaternary Me and  $\text{CH}_2\text{OH}$  (Fig. 2.40, 2.44, 2.48, 2.50 and 2.54). An equatorial quaternary Me *syn* to the S, as in **82** and **86**, appeared almost 0.03 ppm downfield compared to the same when it was as in **84**. Further, both the  $\text{CH}_2\text{OH}$  appeared as a single multiplet when the corresponding carbinol chain was *syn* to S, as in **84**, as two multiplets, back to back, when the said *syn* to the acetal's oxygen.

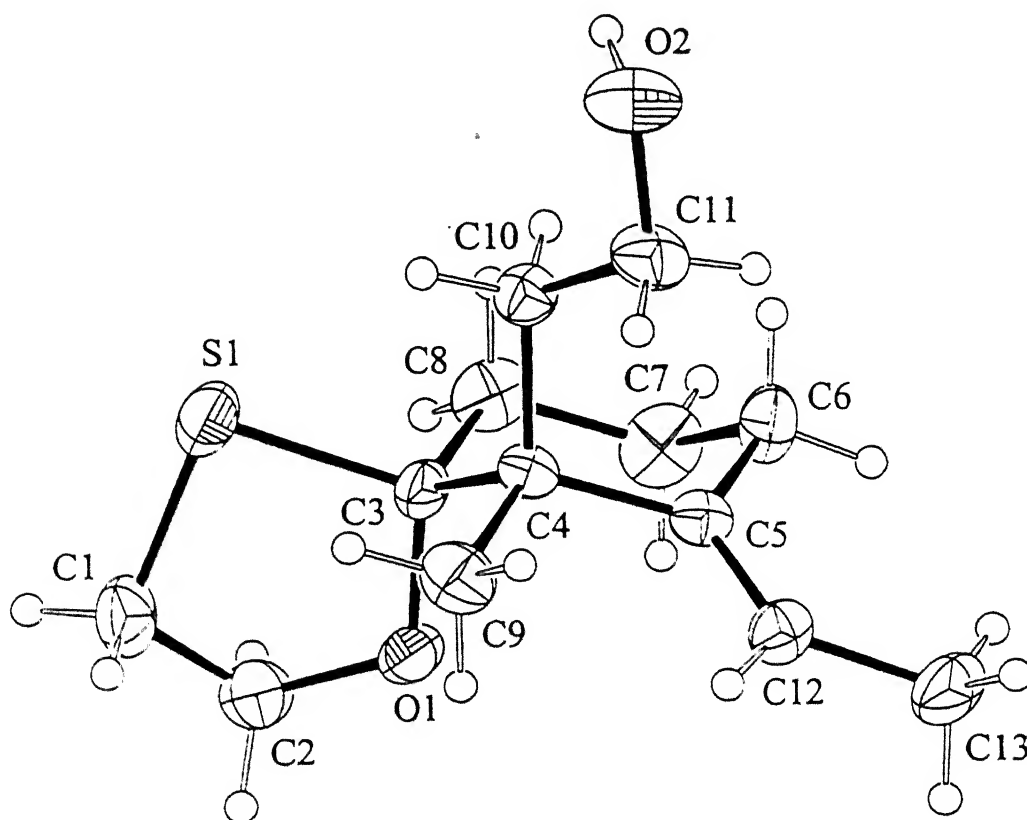


Figure 2.5: ORTEP drawing of 84(R=Me)

**Crystal Data:** MF=C<sub>13</sub>H<sub>22</sub>O<sub>2</sub>S, FW=242.38, colourless prism, monoclinic. Crystal Dimensions 0.50 X 0.29 X 0.21 mm.  $a=12.435(3)$  Å,  $b=7.517(3)$  Å,  $c=28.790(4)$  Å,  $\beta=93.34(2)^\circ$ ,  $V=2687(1)$  Å<sup>3</sup>, Space Group  $P2_1/c$  (14),  $Z=8$ ,  $D_{\text{calc}}=1.198$  g/cm<sup>3</sup>,  $F_{000}=1056.00$ ,  $\mu(\text{MoK}\alpha)$  2.16 cm<sup>-1</sup>, Temp.=23.0°C,  $R=0.057$ ,  $R_w=0.049$ .

Selected bond lengths ( Å):

S1-C3 1.563(7)	S1-C1 1.805(7)	O1-C3 1.418(7)	O1-C2 1.426(7)
C5-C12 1.317(8)	C12-C13 1.509(9)	C11-O2 1.419(7)	

Selected bond angles (°):

C1-S1-C3 92.0(3)	S1-C3-O1 106.2(4)	C2-O1-C3 111.3(5)
C4-C5-C12 123.8(6)	C12-C5-C6 122.6(7)	C5-C12-C13 127.8(7)

Selected torsion angles ( $^{\circ}$ ):

S1C3O1C2 27.0(7)	C1C2O1C3 -46.3(8)	S1C3C4C9 62.4(6)
O1C3C4C9 -53.8(7)	S1C3C4C10 -55.9(6)	C9C4C5C12 -3.4(9)
C4C5C12C13 179.7(6)		

chain is *syn* to O, as in **82** and **86**. The  $^{13}\text{C}$  spectral features were also of much consequence. An equatorial quaternary Me which was *syn* to the S, as in **82** and **86**, appeared 0.8 to 0.9 ppm downfield (Figs. 2.41, 2.45 and 2.55) compared to the Me which was *syn* to O, as in **84** (Figs. 2.49 and 2.51). A definitive  $^{13}\text{C}$  assignment for the quaternary Me was made from a HMQC spectrum (Fig. 2.37) of **81** (R=Me). The characteristic  $^1\text{H}$  and  $^{13}\text{C}$  absorptions are collected in the Table 2.9. These differential  $^1\text{H}$  and  $^{13}\text{C}$  absorptions must prove valuable in stereochemical assignments in future endeavors such as this.

The Claisen rearrangement prefers a chair-TS over the related boat. The rearrangement of **68** *syn* to the oxygen is favored over the alternate rearrangement *syn* to S for :

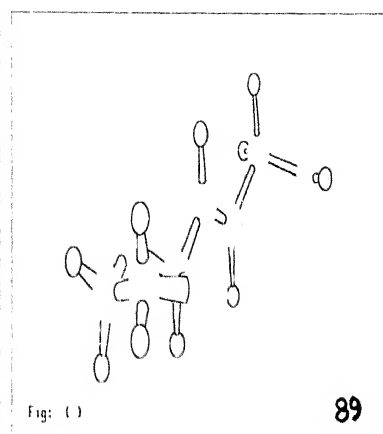
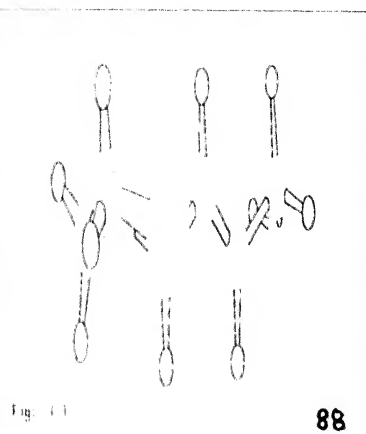
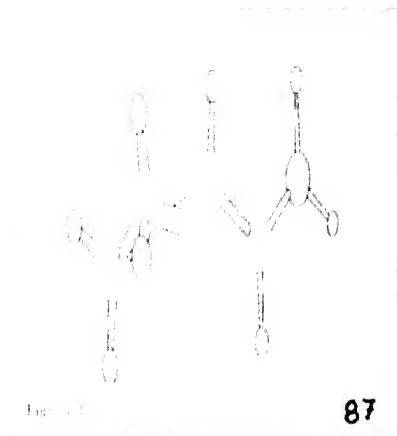
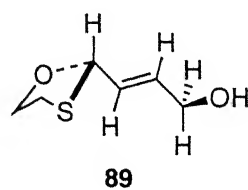
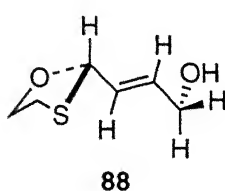
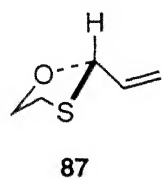
- (a) the new C-C bond will be formed axial on the pre-existing cyclohexene ring,<sup>101, 102</sup>
- (b) R will be directed equatorial on the 6-ring chair-TS to avoid the otherwise intense steric interactions of the axial R with the ring-Me,<sup>103, 104</sup> and
- (c) the least reorganisational movement in constituting the TS for the already *syn* to the oxygen disposition of the carbinol oxygen.<sup>21, 105, 106</sup>

Here, it is realistic to consider the solid state carbinol conformation being retained in solution. The orientation of the carbinol oxygen *syn* to the S will require a rotation around the bond between the carbinol carbon and the adjacent ring carbon. This rotation is highly restricted because either of the substituents R and OH must go past the ring Me, both are high energy processes. On a similar note, the rearrangement of **69** is favored to proceed *syn* to the S. Is the C-C bond in **69** formed equatorial? We provide evidence below that this bond is formed axial and that a ring flip is in order to allow that happen.

Table 2.9: Selected  $^1\text{H}$  and  $^{13}\text{C}$  chemical shifts in the products **82**, **84** and **86**

Compound	$^1\text{H}$			$^{13}\text{C}$
	ring-Me	$\text{CH}_2\text{OH}$	$\text{CH}_2\text{S}$	ring-Me
<b>82</b> , R=Me	1.226	3.65-3.59 (m) 3.55-3.49 (m)	2.89-2.84 (m)	18.30
<b>84</b> , R=Me	1.200	3.65-3.63 (m)	2.99-2.93 (m) 2.91-2.83 (m)	17.40
<b>82</b> , R=Ph	1.381	3.78-3.72 (m) 3.65-3.60 (m)	2.97-2.93 (m)	18.43
<b>84</b> , R=Ph	1.350	3.70-3.60 (m)	3.03-2.98 (m) 2.96-2.90 (m)	17.67
<b>86</b>	1.276	3.72-3.64 (m) 3.62-3.53 (m)	2.89-2.84 (m)	18.34

We have computed the ground state geometry of **87** and the energy of a rotamer in which the torsion angles of the acetal's O and S with the terminal  $\text{sp}^2$  carbon were mutually exchanged to mimic and estimate the energy requirement for the above conformational mobility. The said rotamer was 0.71 kcal/mol higher than the conformational minimum **87**. A similar rotamer of the carbinol **88** was also 0.71 kcal/mol higher. The additional carbinol function has, therefore, little effect on the conformational profile of **87**. The approximate total energy requirement for the above ring flip must, therefore, be the energy required for the flip of one half chair to the other plus 0.71 kcal/mol. This energy is rather small for the boiling temperature of toluene and, hence, the flip could occur with ease. Since the ring flip is permissible and there is no R *vs* Me interaction in **80**, it may be expected to rearrange *syn* to both the O and S. However, the *syn* to the O rearrangement may still predominate, as it indeed does, because it is an energy saving process in not requiring the ring flip. Furthermore, the conformer **88**, which has the carbinol function *syn* to the O, computed 0.06 kcal/mol lower than the conformer **89** wherein the same are *anti*.



Cieplak model<sup>18</sup> favors a nucleophilic attack from *anti* to the more electron-donating C $\alpha$ -substituent. As pointed out earlier also, on invoking the independent contributions of both the S and O atoms to the face selection, an enormously enhanced *syn* to the O selectivity will be predicted. On the contrary, Anh-Felkin model<sup>17, 107</sup> supports the attack of a nucleophile *anti* to the more electron-attracting C $\alpha$ -substituent. The reactions will, therefore, be predicted to proceed *syn* to the S. Wipf's<sup>16, 19</sup> dipole model supports attack of a nucleophile on the face that constitutes the positive end of the dipole along the Z-axis. A simple vector analysis of the dipoles arising from the acetal function will readily establish the face *syn* to S as the face constituting the positive end of such dipoles. The molecule **80** may, therefore, be considered to be ingeniously designed to provide a composite test of these models. Very obviously, the last two models do not apply to **80**. The observed *anti* to the S addition may appear to follow the Cieplak model but, as presented above,

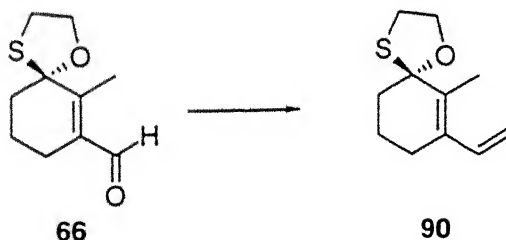


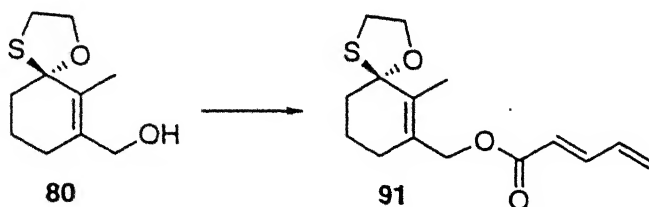
it is actually a consequence of primarily the carbinol conformational preference and the favored axial attack following stereoelectronic effects. All these observations are confirmed further from the Diels-Alder additions where we have observed no selectivity (*vide infra*). The predominant *anti* to S addition observed in the studies of Takei *et al.*<sup>3</sup> is, therefore, a consequence of stereoelectronically favored axial attack. It is incidental that the same diastereoselectivity is predicted by the Cieplak model as well.

In conclusion, **80** and its derivatives underwent orthoester Claisen rearrangement with exceptionally high diastereoface selection. The observed diastereoselections support neither of the Cieplak model, Anh-Felkin model, and Wipf's dipole model but the stereoelectronically supported prospect for axial bond formation. The initial ground state geometry of the carbinol also contributes to the observed facial selection.

### 2.3.3 Diels-Alder Reaction of 1-Oxa-4-thia-7-vinylspiro[4.5]dec-6-ene

We have attempted the Diels-Alder reaction of substrates **90** and **91**. These materials were prepared as shown below. Wittig reaction of the aldehyde **66** with  $\text{Ph}_3\text{P}=\text{CH}_2$  gave the diene **90**. The substrate **91** was prepared from the alcohol **80** and pentanedienoic acid by DCC coupling.<sup>108</sup>



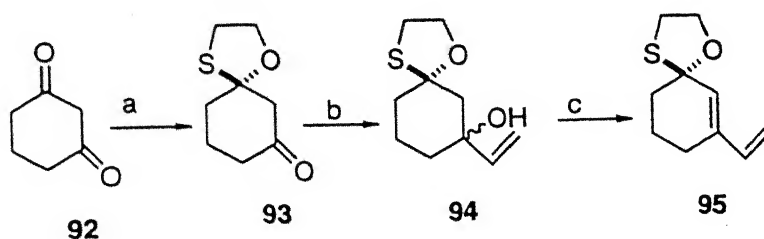


The diene **90** did not react with dienophiles such as NPM, MA, MTAD, and TCNE even when the reactions were carried out in sealed tubes at high temperatures (210 °C). This may be due to the highly preferred *s-trans* conformation of such dienes.<sup>76</sup> The substrate **91** which was designed for intramolecular Diels-Alder addition underwent extensive decomposition under all the conditions that we attempted. We next designed **95** to carry on with this study.

The diene **95** was prepared from 1,3-cyclohexadione **92** (Scheme 2.3). This was selectively protected by a known<sup>109</sup> procedure. The monoprotected ketone **93** furnished, on reaction with vinyl magnesium bromide, a mixture of alcohols **94** which on further reaction with Et<sub>3</sub>N and MsCl gave the desired diene **95**.

The diene **95** was reacted with selected dienophiles such as NPM, MTAD, and TCNE. With NPM at reflux in toluene, a 1:1 mixture of the two diastereomers **96** and **97** (Scheme 2.4) was obtained. Likewise, MTAD also yielded a 1:1 mixture of the Diels-Alder adducts. Only reaction with TCNE was somewhat selective; the observed ratio was 1:1.6. The individual isomers were not identified.

Had the explanation of Paquette for his observed facial selections was valid, we also must have observed primarily *anti* to the S addition. Cieplak model also does not follow. We, therefore, conclude that the acetal function has little effect on selectivity, particularly the facial selectivity of the diene **95** in Diels-Alder additions.

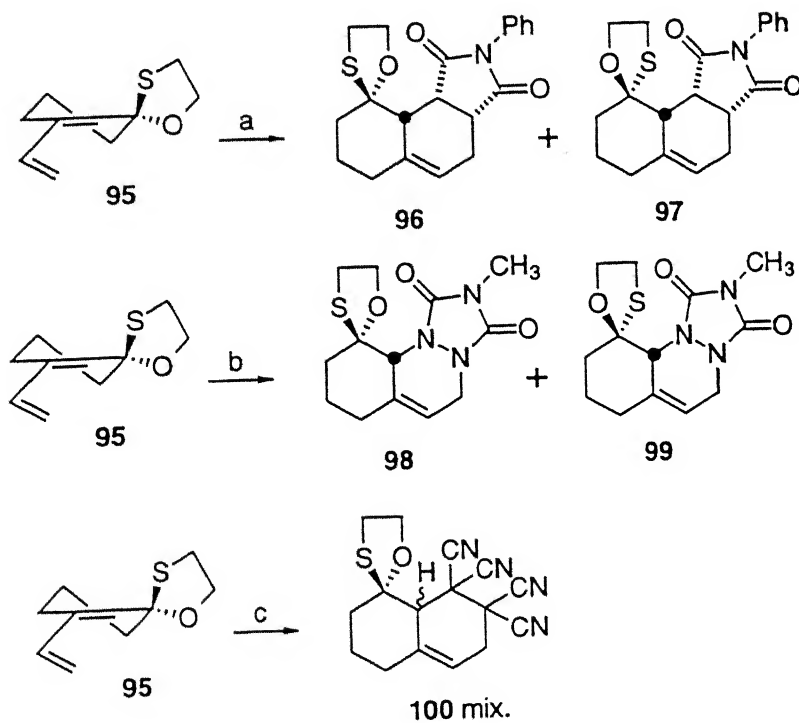


Reagents:

a.  $\text{HOCH}_2\text{CH}_2\text{SH}$ ,  $\text{C}_6\text{H}_6$ , Reflux b.  $\text{vinylMgBr}$ , THF,  $0^\circ\text{C}$

c.  $\text{MsCl}$ ,  $\text{Et}_3\text{N}$ ,  $\text{CH}_2\text{Cl}_2$

Scheme 2.3



Reagents:

a. NPM, toluene, sealed tube,  $140^\circ\text{C}$

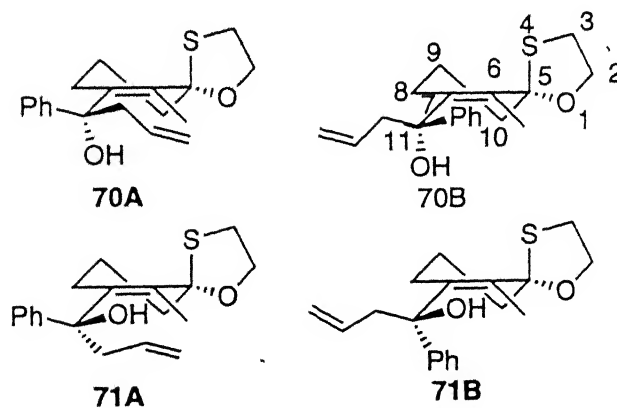
b. MTAD,  $\text{THF-CH}_2\text{Cl}_2$  (1:1),  $-78^\circ\text{C}$  to rt

c. TCNE, THF,  $0^\circ\text{C}$  to rt

Scheme 2.4

### 2.3.4 Oxy-Cope Rearrangement

Finally, we have studied oxy-Cope rearrangement to understand the electronic influence of the ketal function. The requisite substrates **70** and **71** were prepared as a 1:1 mixture of two isomers as shown in the Scheme 2.1. These were readily separated by radial chromatography. The stereoidentity of the more polar **70** was secured from single crystal X-ray analysis (Fig. 2.4.). Since the rotation around C7-C11 bond is restricted, the alcohol **70** can, in fact, be a mixture of two rotamers **70A** and **70B** even though both are more polar. It is possible that during the recrystallization, **70B** recrystallized in preference to **70A**. Likewise, the alcohol **71** can also have two orientations, **71A** and **71B**. The existence of **70A/B** and **71A/B** can be examined by making derivatives such as Mosher esters. We, However, have not confirmed the same. Of the two isomers **70A** and **70B**, **70A** can give the desired oxy-Cope product but **70B** can not since the allyl group in it is far away from the other reaction site. This can be extended to **71** also. Once again, **71A** can undergo smooth rearrangement but **71B** can not. It is probably for this reason that we have observed decomposition during rearrangement and, hence, low yields of the products from the reactions of both **70** and **71**. The components that are conformationally unsuitable for rearrangement may undergo decomposition rather than rearrangement.

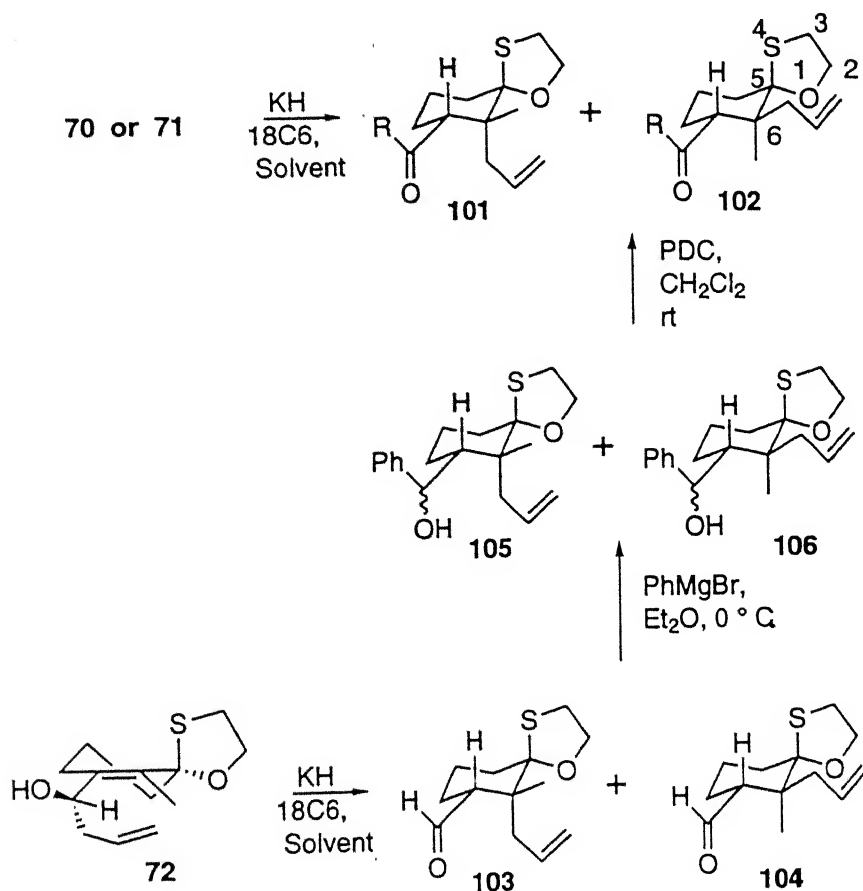


The alcohols **70** and **71** were treated separately with KH and 18-Crown-6 in three different solvents at 0 °C to rt followed by reflux for 30 min. There was no reaction at 0 ° to rt. A mixture of the same two products **101** and **102** was obtained from each (Scheme 2.5). The results are collected in the Table 2.10. Although there were two Me signals observed in the  $^1\text{H}$  spectrum yet the ratio calculation from their integrals was tedious for the fact that other signals also appeared in their neighbourhood. The ratios were determined rather more accurately from the  $^1\text{H}$  integrals of the internal vinylic hydrogens.

The products were separated by repeated radial chromatography for individual spectroscopic characterization. While COSY helped secure various characteristic hydrogen assignments and ROESY established the relative stereorelationships of the three stereogenic centers. Accordingly, we have assigned structures **101** (Fig. 2.67) and **102** (Fig. 2.69), respectively, to the products emanating from reactions *anti* and *syn* to the sulfur. The internal vinylic hydrogen absorbs in the region 6.00-5.87 and 5.85-5.71 in **101** and **102**, respectively. The C3-H appears as a doublet of doublet in **101** ( $\delta$  3.70-3.65,  $J=12.6$  and 3.3 Hz) and **102** ( $\delta$  3.93-3.89,  $J=10$  and 3 Hz); the larger  $J$  value clearly indicating this hydrogen to be axial in both. The compound **101** showed good nOe (Fig. 2.68) between the Me and the  $\text{SCH}_2$  which is possible only if the configuration is as shown in **101**. Also, the nOe of Me with C3-H showed these two *cis*. The ortho protons of phenyl showed nOe with C3-H which indicated that the phenyl was above the plane of the cyclohexane ring and the carbonyl below the plane.

The compound **102** did not show any direct nOe between any of the two  $\text{CH}_2$ 's of the acetal unit and the substituents at C6 (Fig. 2.71). The reversal of stereochemistry at C6 was, however, discerned from nOe between the C3-H and the allylic  $\text{CH}_2$  which is possible only if the allyl substituent is equatorial and the Me, therefore, axial. This axial disposition of the methyl was confirmed further from nOe between this Me and a hydrogen on C10. The above stereochemical assignments were further supported from the chemical shift of

the quaternary Me which resonates at  $\delta$  0.94 and 1.43 in **101** and **102**, respectively. The downfield absorption of Me in **102** as compared to that in **101** is expected because the Me in **102** is likely to experience the anisotropic effect of the acetal's oxygen and the carbonyl function.  $^{13}\text{C}$  NMR showed two different Me signals. The Me which is *syn* to sulfur, as in **101**, appeared at  $\delta$  20.83 and the Me which is *anti* to sulfur, as in **102**, appeared at 19.69 (Fig. 2.65).



Scheme 2.5

The unsubstituted species **72** (Nu=allyl) was also treated with  $\text{KH}$  and 18-Crown-6 in two different solvents. The results are collected in the Table 2.10. The ratios were calculated by converting the mixture of aldehydes **103** and **104** to the phenyl ketones **101**

and 102, respectively, as shown in the Scheme 2.5.

Table 2.10: Oxy-Cope rearrangement of alcohls 70-72

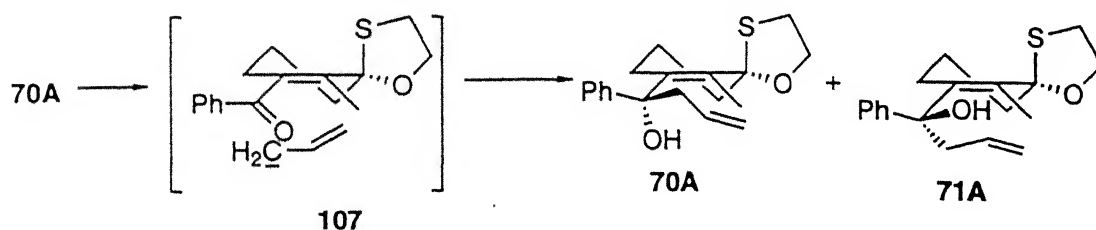
Alcohol	Solvent	Syn:Anti to Oxygen
70	THF	1:1
71	THF	4:1
70	C <sub>6</sub> H <sub>6</sub>	1:2.7
71	C <sub>6</sub> H <sub>6</sub>	1:1
70	DME	1:5.4
71	DME	1:2
72	THF	2:1
72	DME	1.1:1

The change in facial selectivity with change in solvent is indeed remarkable. The reaction of the more polar alcohol 70 turns from almost non-selective (101:102 = 1:1) in THF to *syn* to sulfur selective in DME (101:102 = 1: 5.4). This selectivity in benzene was 1:2.7 which is intermediate to the values in THF and DME. Interestingly, while the reaction of the less polar alcohol 71 was selective *anti* to sulfur in THF (101:102 = 4:1), the reaction turned moderately *syn* to sulfur (101:102 = 1:2) when the solvent was changed, once again, from THF to DME. The rearrangement of the alcohol 72 gave a mixture of 103 and 104 in a ratio of 2:1 and 1.1:1 in THF and DME, respectively. The isomer 73 was not studied.

The three distinct diastereoface control elements in the substrates under examination are the hemithioacetal function, the substituents on the carbinol carbon, and the oxy-anion.<sup>110</sup> Since the effect of the acetal function has already been determined to be substantially small,<sup>82</sup> the oxy-anion and the substituent would appear to be the only two control elements that one may like to explore further. In studies designed to understand the effect of oxy-anion orientation on diastereoface selection, Paquette and Maynard<sup>92</sup> have observed

only subtle changes in the level of facial control but not reversal of the sort reported herein on change of solvent from THF to DME.

Alcohol **70A** will be expected to give only *syn* to the sulfur attack since the allyl group is oriented *syn* to sulfur. However, this may not be favored since the oxy-anion is oriented axial. In contrast, we observed both *syn* to the oxygen and *syn* to the sulfur rearranged products. This is possible only if the intramolecular reaction can proceed, atleast partly, by a two step process consisting of scission of the bisallylic C-C bond to form a phenyl vinyl ketone and an allyl anion. Recombination of these will afford both **70A** and **71A**. The latter would then rearrange *syn* to the oxygen as shown in the Scheme 2.6. Similar but radicalar decomposition under thermal conditions has been invoked earlier.<sup>111-113</sup>



Scheme 2.6

Likewise, the alcohol **71** will be expected to rearrange only *syn* to the oxygen. However, it also gave a mixture of both **101** and **102**. Once again the oxy-anion will be oriented axial in the TS for rearrangement. Finally, the alcohol **72** will be expected to rearrange only *syn* to the oxygen. But, again, a mixture of products arising from rearrangement from *syn* to both the O and S was obtained. It appears, once again, that similar to the orthoester Claisen rearrangement, the stereochemical outcome in oxy-Cope process is controlled largely by the conformation and also the orientation of the oxy-anion.



## 2.4 Conclusion

From the studies above on 1,4-diastereoselection, ortho ester Claisen rearrangement, Diels-Alder reaction; it is concluded that the hemithio acetal function has little effect on the facial selectivity of the molecules studied. This is surprisingly in contradiction to the Diels-Alder results of Paquette *et al.*<sup>70</sup>

## 2.5 Experimental

<sup>1</sup>H NMR spectra were recorded on either Bruker WM400 or Bruker DRX-300 or Bruker DPX-200 or Bruker WP-80 in CDCl<sub>3</sub> and on Varian EM-360L spectrometer in CCl<sub>4</sub>. <sup>13</sup>C NMR spectra were measured on Bruker DRX-300 at 75 MHz. Signal positions are reported  $\delta$  scale relative to TMS used as an internal standard. IR spectra were recorded on Perkin Elmer 1320 spectrometer. Melting points were determined in a Fischer-John melting point apparatus and are uncorrected. Solvents were dried as per established procedures.<sup>114</sup> All separations were performed by Chromatotron using silica gel 60 GF254 (Fluka) coated plates. All the reactions were performed in an atmosphere of dry nitrogen. Bu<sup>t</sup>MgCl and Bu<sup>s</sup>MgCl (both in Et<sub>2</sub>O), and vinylmagnesium bromide (THF solution) were purchased from Aldrich. The other Grignard reagents were prepared using standard methods in the requisite solvent. PhLi was prepared from PhBr on reaction with Bu<sup>n</sup>Li at -80 °C for 5 min. The column grade silica gel (100-200 mesh) used for chromatography was purchased from Acme Synthetic Chemicals, India. Ether, whenever used, stands for diethyl ether. All organic extracts were dried with anhydrous Na<sub>2</sub>SO<sub>4</sub>.

### 3-Bromo-2-methyl-2-cyclohexenone (63)

3-Bromo-2-methyl-2-cyclohexenone was prepared from 2-methyl-1,3-cyclohexanedione (62) via its mesylate in an overall yield of 80% following modification of a literature procedure.<sup>97</sup> We have discovered that a simple replacement of K<sub>2</sub>CO<sub>3</sub> by Et<sub>3</sub>N was more

convenient. The yield, however, remained unaltered. The  $^1\text{H}$  spectral characteristics corresponded well to those reported in the literature.<sup>97</sup>

### 7-Bromo-6-methyl-1-oxa-4-thiaspiro[4.5]dec-6-ene (64)

The procedure followed was that of Shih and Swenton<sup>99</sup> but under more dilute conditions. When 60 mLs of  $\text{C}_6\text{H}_6$  for every mmol of the bromoketone **63** was used, not only did the yield improve from 45% to 88% but also the formation of the bis-acetal of 2-methyl-1,3-cyclohexanedione was reduced from substantial to none. This acetal is highly unstable. When kept neat in a refrigerator at  $-10\text{ }^\circ\text{C}$ , it decomposed within 3 days. This material, however, can be stored as solution in hexane for months without significant decomposition.

$^1\text{H}$  NMR (60 MHz); (Fig. 2.6):

$\delta$  4.6-3.8 (2H, m), 3.2-2.9 (2H, m), 2.7-2.3 (2H, m), 2.2-1.5 (4H, m), 1.9 (3H, t,  $J=2$  Hz).

Anal. Calcd for  $\text{C}_9\text{H}_{13}\text{BrOS}$ : C, 43.55; H, 5.28. Found: C, 43.36; H, 5.40

### 6-Methyl-1-oxa-4-thiaspiro[4.5]dec-6-en-7-carbaldehyde (66):

A solution of **64** (249 mg, 1.0 mmol) in dry THF (5 mL) was cooled to  $-80\text{ }^\circ\text{C}$  and mixed with  $\text{Bu}^n\text{Li}$  (625  $\mu\text{L}$  of a 1.6 M solution in hexane). After stirring for 10 min, DMF (310  $\mu\text{L}$ , 4.0 mmol) was added. The reaction mixture was stirred further for 30 min at  $-80\text{ }^\circ\text{C}$ , quenched with MeOH (82  $\mu\text{L}$ , 2.0 mmol), and allowed to warm to  $20\text{ }^\circ\text{C}$ . The reaction mixture was diluted with  $\text{Et}_2\text{O}$  (15 mL), mixed with saturated aqueous  $\text{NH}_4\text{Cl}$  (5 mL), and stirred for 10 min. The layers were separated and the aqueous layer extracted with ether (2 x 5 mL). The combined extracts were dried and concentrated to furnish a light yellow solid, 0.156 g. Purification yielded the pure aldehyde, 0.140 g, 70%, mp  $48\text{ }^\circ\text{C}$ .

$^1\text{H}$  NMR (300 MHz); (Fig. 2.7):

$\delta$  10.14 (1H, s), 4.52-4.46 (1H, m), 4.18-4.10 (1H, m), 3.23-3.10 (2H, m), 2.21 (3H, t,  $J=1.8$  Hz), 2.30-1.50 (6H, m).

IR ( $\text{CCl}_4$ ): 1655, 1615, 750  $\text{cm}^{-1}$ .

Anal. Calcd for  $C_{10}H_{14}O_2S$ : C, 60.58; H, 7.12. Found: C, 60.35; H, 7.16.

#### Preparation of 67:

Reaction of vinyl lithium 65 with dimethyl benzamide using the procedure used for the conversion of 65 to 66 gave 66% of the ketone 67.

$^1H$  NMR (80 MHz):

$\delta$  8.0-7.8 (2H, m), 7.6-7.3 (3H, m), 4.0-4.6 (2H, m), 3.0-3.2 (2H, m), 2.5-1.9 (6H, m), 1.7 (3H, s).

#### General Procedure for reaction of 66 with Grignard reagents:

All the reactions were carried out on 0.5 mmol of 66. The solution/suspension of the Grignard reagent (0.6 mmol) in  $Et_2O$ /THF (3 mL) was cooled to  $-80^\circ C$  and mixed with a solution of 66 in the same solvent (2 mL). The reaction mixture was stirred for 1 h and then quenched by adding 4 equivalent of MeOH at  $-80^\circ C$ . The reaction contents were diluted with  $Et_2O$  (5 mL) and saturated  $NH_4Cl$  (5 mL). The layers were separated and the aqueous layer extracted with  $Et_2O$  (2 x 5 mL). The combined extracts were dried and concentrated to furnish a residue which was chromatographed to isolate the two expected alcohols.

#### Reformatsky reaction of $BrCH_2CO_2Et$ with 66:

The procedure followed was that of Furstner.<sup>115</sup> Ethyl bromoacetate and granular Zn were taken in a 3:1 benzene-THF solution and stirred at  $20^\circ C$  until complete disappearance of Zn. The contents were cooled to  $-80^\circ C$  and mixed with a solution of the aldehyde in the same solvent mixture. The reaction was quenched at  $-80^\circ C$  and then brought to  $20^\circ C$  before the aqueous workup.

#### The reaction of allylzinc bromide with 66:

A literature protocol<sup>116</sup> was used. The aldehyde and the allyl bromide were mixed in DMF and stirred with granular Zn at  $30^\circ C$  until complete disappearance of the aldehyde.

Only for the subtle differences in the multiplicity of the methylene protons, the  $^1H$

spectra of the two isomeric alcohols were almost identical in each instance and, hence, the characteristic data on only one isomer are given below.

**73 (Nu=Me)**

$^1\text{H}$  NMR (300 MHz); (Fig. 2.9):

$\delta$  4.80-4.73 (1H, q,  $J=6.5$  Hz), 4.41-4.35 (1H, m), 4.09-4.00 (1H, m), 3.16-3.03 (2H, m), 1.74 (3H, t,  $J=1.5$  Hz), 2.05-1.55 (7H, m), 1.20 (3H, d,  $J=6.5$  Hz).

IR ( $\text{CHCl}_3$ ): 3420, 1625, 1435, 1040  $\text{cm}^{-1}$ .

Anal. Calcd for  $\text{C}_{11}\text{H}_{18}\text{O}_2\text{S}$ : C, 61.65; H, 8.47. Found: C, 61.50; H, 8.62.5

**72 (Nu=Ph)**

$^1\text{H}$  NMR (300 MHz); (Fig. 2.10):

$\delta$  7.37-7.24 (5H, m), 5.7 (1H, d,  $J=2.4$  Hz), 4.46-4.40 (1H, m), 4.12-4.04 (1H, m), 3.18-3.10 (2H, m), 2.18-2.08 (2H, m), 1.93 (3H, s), 1.90-1.57 (5H, m).

$^{13}\text{C}$  NMR (75.5 MHz): (Fig. 2.11):

$\delta$  142.0, 137.5, 132.0, 128.3, 127.0, 125.6, 95.8, 72.0, 71.1, 38.7, 34.9, 23.0, 20.4, 13.0.

IR ( $\text{CHCl}_3$ ): 3440, 1650, 1220, 750  $\text{cm}^{-1}$ .

Anal. Calcd for  $\text{C}_{15}\text{H}_{20}\text{O}_2\text{S}$ : C, 69.54; H, 7.30. Found: C, 69.46; H, 7.43.

**73 (Nu=Ph)**

$^{13}\text{C}$  NMR (75.5 MHz): (Fig. 2.13):

$\delta$  142.1, 137.5, 132.0, 128.3, 127.1, 125.5, 96.4, 72.1, 71.2, 38.8, 34.9, 23.3, 20.7, 12.9.

**73 (Nu=Et)**

$^1\text{H}$  NMR (60 MHz):

$\delta$  4.7-4.2 (2H, m), 4.2-3.8 (1H, m), 3.2-2.9 (2H, m), 1.7 (3H, bs), 0.9 (3H, t,  $J=5$  Hz), 2.5-1.2 (9H, m).

Anal. Calcd for  $\text{C}_{12}\text{H}_{20}\text{O}_2\text{S}$ : C, 63.13; H, 8.84. Found: C, 62.97; H, 8.94.

**73 (Nu=2-phenylethyl)**

$^1\text{H}$  NMR (60 MHz):

$\delta$  7.2 (5H, s), 4.7-3.7 (3H, m), 3.2-2.8 (2H, m), 2.8-2.4 (2H, m), 2.4-1.5 (9H, m), 1.6 (3H, bs).

IR ( $\text{CHCl}_3$ ): 3440, 1630, 1210, 750  $\text{cm}^{-1}$ .

Anal. Calcd for  $\text{C}_{13}\text{H}_{24}\text{O}_2\text{S}$ : C, 71.02; H, 7.95. Found: C, 69.90; H, 8.10.

**73 (Nu=Bu<sup>s</sup>)**

$^1\text{H}$  NMR (60 MHz):

$\delta$  4.5-3.8 (3H, m), 3.2-2.9 (2H, m), 2.3-1.4 (10H, m), 1.7 (3H, bs), 1.0-0.6 (6H, m).

Anal. Calcd for  $\text{C}_{14}\text{H}_{24}\text{O}_2\text{S}$ : C, 65.59; H, 9.44. Found: C, 65.45; H, 9.60.

**73 (Nu=Bu<sup>t</sup>)**

$^1\text{H}$  NMR (60 MHz):

$\delta$  4.5-3.8 (2H, m), 4.3 (1H, s), 3.2-2.9 (2H, m), 1.7 (3H, t,  $J=1.2$  Hz), 2.3-1.2 (7H, m), 0.9 (9H, s).

Anal. Calcd for  $\text{C}_{14}\text{H}_{24}\text{O}_2\text{S}$ : C, 65.59; H, 9.44. Found: C, 65.42; H, 9.57.

**73(Nu=Pr<sup>i</sup>)**

$^1\text{H}$  NMR (60 MHz):

$\delta$  4.6-3.8 (3H, m), 3.2-2.9 (2H, m), 1.8 (3H, t,  $J=1.8$  Hz), 1.1 (3H, d,  $J=7$  Hz), 0.8 (3H, d,  $J=7$  Hz).

IR ( $\text{CHCl}_3$ ): 3440, 1640, 1455, 1445, 1430, 1205, 1050, 1005, 750  $\text{cm}^{-1}$ .

Anal. Calcd for  $\text{C}_{13}\text{H}_{22}\text{O}_2\text{S}$ : C, 64.43; H, 9.16. Found: C, 64.34; H, 9.30.

**73(Nu=vinyl)**

$^1\text{H}$  NMR (300 MHz): (Fig. 2.26):

$\delta$  5.90-5.79 (1H, m), 5.29-5.28 (1H, td,  $J=17$  and 1.5 Hz), 5.18-5.13 (1H, td,  $J=10.5$ , 1.5 Hz), 5.10 (1H, br s), 4.40-4.38 (1H, m), 4.12-4.04 (1H, m), 3.18-3.04 (2H, m), 2.24-2.05 (2H, m), 1.78 (3H, t,  $J=1.8$  Hz), 2.03-1.50 (5H, m).

$^{13}\text{C}$  NMR (75.5 MHz); (Fig. 2.27):

$\delta$  137.7, 136.5, 130.8, 114.6, 96.4, 71.7, 71.1, 38.8, 34.7, 23.2, 20.7, 12.3.

IR ( $\text{CHCl}_3$ ): 3430, 1620, 1425, 1205  $\text{cm}^{-1}$ .

Anal. Calcd for  $\text{C}_{12}\text{H}_{18}\text{O}_2\text{S}$ : C, 63.69; H, 8.02. Found: C, 63.74; H, 8.16.

### 72 (Nu=vinyl)

$^{13}\text{C}$  NMR (75.5 MHz); (Fig. 2.25):

$\delta$  138.0, 136.6, 131.2, 114.7, 96.5, 71.9, 71.1, 38.9, 35.0, 23.1, 20.6, 12.7.

### 73 (Nu=1-Naphthyl)

$^1\text{H}$  NMR (300 MHz); (Fig. 2.30):

$\delta$  7.87-7.84 (2H, m), 7.77 (1H, d,  $J=8.1$  Hz), 7.66 (1H, d,  $J=7.2$  Hz), 7.51-7.44 (3H, m), 6.25 (1H, s), 4.43-4.38 (1H, m), 4.07-3.99 (1H, m), 3.18-3.05 (2H, m), 2.01 (3H, s), 2.19-1.40 (7H, m).

IR (film): 3410, 1670, 1585, 1495, 1050, 775  $\text{cm}^{-1}$ .

Anal. Calcd for  $\text{C}_{20}\text{H}_{22}\text{O}_2\text{S}$ : C, 73.59; H, 6.80. Found: C, 73.50; H, 6.90.

### 73 (Nu= $\text{Bu}^n$ )

$^1\text{H}$  NMR (80 MHz):

$\delta$  4.72-3.93 (3H, m), 3.25-3.00 (2H, m), 2.50-1.10 (13H, m), 1.78 (3H, bs), 0.90 (3H, t,  $J=5$  Hz).

IR (film): 3400, 1640, 1450, 1440, 1430, 1260, 1165, 1040, 875, 750  $\text{cm}^{-1}$ .

Anal. Calcd for  $\text{C}_{14}\text{H}_{24}\text{O}_2\text{S}$ : C, 65.59; H, 9.44. Found: C, 65.44; H, 9.60.

### 73 (Nu=allyl)

$^1\text{H}$  NMR (200 MHz); (Fig. 2.18):

$\delta$  5.90-5.70 (1H, m), 5.18-5.09 (2H, m), 4.65-4.58 (1H, m), 4.42-4.35 (1H, m), 4.12-4.04 (1H, m), 3.14-3.05 (2H, m), 1.75 (3H, t,  $J=1.8$  Hz), 2.40-1.58 (9H, m).

$^{13}\text{C}$  NMR (75.5 MHz); (Fig. 2.19):

$\delta$  137.6, 134.6, 130.3, 117.7, 96.3, 71.0, 70.3, 39.4, 38.8, 34.8, 23.1, 20.5, 12.4.

IR (film): 3400, 1630, 1430, 1165, 905, 750  $\text{cm}^{-1}$ .

Anal. Calcd for  $\text{C}_{13}\text{H}_{20}\text{O}_2\text{S}$ : C, 64.97; H, 8.39. Found: C, 64.82; H, 8.45.

**72 (Nu=allyl)**

$^{13}\text{C}$  NMR (75.5 MHz); (Fig. 2.17):

$\delta$  137.3, 134.7, 133.6, 130.6, 117.7, 96.6, 71.0, 70.1, 39.4, 38.8, 34.8, 22.8, 20.5, 12.5.

**73 (Nu= $\text{CH}_2\text{CO}_2\text{Et}$ )**

$^1\text{H}$  NMR (60 MHz):

$\delta$  5.0-4.7 (1H, dd,  $J=8.5$  and 5 Hz), 4.4-4.1 (2H, m), 4.1 (2H, q,  $J=7$  Hz), 3.2-2.9 (2H, m), 1.7 (3H, t,  $J=1.8$  Hz), 1.2 (3H, t,  $J=7$  Hz).

Anal. Calcd for  $\text{C}_{14}\text{H}_{22}\text{O}_4\text{S}$ : C, 58.72; H, 7.75. Found: C, 58.88; H, 7.92.

**73 (Nu=PhCC)**

$^1\text{H}$  NMR (200 MHz); (Fig. 2.22):

$\delta$  7.47-7.42 (2H, m), 7.34-7.26 (3H, m), 5.51 (1H, d,  $J=1.8$  Hz), 4.46-4.36 (1H, m), 4.13-4.01 (1H, m), 3.20-3.04 (2H, m), 2.40-2.30 (2H, m), 1.87 (3H, t,  $J=1.8$  Hz), 2.20-1.62 (5H, m).

$^{13}\text{C}$  NMR (75.5 MHz); (Fig. 2.23):

$\delta$  135.1, 132.4, 131.8, 128.4, 128.3, 122.6, 96.2, 88.3, 85.3, 71.1, 62.7, 38.7, 34.8, 24.1, 20.6, 12.6.

IR (film): 3410, 1590, 1500, 1430, 1050, 775  $\text{cm}^{-1}$ .

Anal. Calcd for  $\text{C}_{18}\text{H}_{20}\text{O}_2\text{S}$ : C, 71.97; H, 6.72. Found: C, 72.15; H, 6.85.

**72(Nu=PhCC)**

$^{13}\text{C}$  NMR (75.5 MHz); (Fig. 2.21):

$\delta$  134.9, 132.6, 131.8, 128.4, 128.3, 122.6, 96.2, 88.3, 85.1, 71.2, 62.4, 38.5, 34.8, 23.8, 20.5, 12.6.

**73 (Nu=TBDMSOCH<sub>2</sub>CC)**

<sup>1</sup>H NMR (300 MHz); (Fig. 2.29):

δ 5.32 (1H, s), 4.42-4.37 (1H, m), 4.35 (2H, d, *J*=1.8 Hz), 4.11-4.03 (1H, m), 3.13-3.07 (2H, m), 2.28-2.24 (2H, m), 2.15-2.06 (1H, m), 2.02-1.93 (1H, dt, *J*=11, 3 Hz), 1.89-1.80 (1H, m), 1.79 (3H, t, *J*=1.8 Hz), 1.74-1.64 (1H, m), 0.91 (9H, s), 0.12 (6H, s).

Anal. Calcd for C<sub>19</sub>H<sub>32</sub>O<sub>3</sub>SSi:

C, 61.93; H, 8.76. Found: C, 61.75; H, 8.90.

**75 (Nu=allyl)**

<sup>1</sup>H NMR (300 MHz); (Fig. 2.15):

δ 7.41-7.23 (5H, m), 5.87-5.73 (1H, m), 5.22-5.17 (2H, m), 4.40-4.33 (1H, m), 4.10-4.02 (1H, m), 3.08-3.03 (2H, m), 2.96-2.89 (1H, dd, *J*=13.8, 7.2 Hz), 2.79-2.72 (1H, dd, *J*=13.8, 7.5 Hz), 1.56 (3H, s), 2.40-1.57 (7H, m).

IR (CHCl<sub>3</sub>): 3440, 1650, 1210, 755 cm<sup>-1</sup>.

Anal. Calcd for C<sub>19</sub>H<sub>24</sub>O<sub>2</sub>S: C, 72.12; H, 7.65. Found: C, 71.94; H, 7.78.

**General procedure for orthoester Claisen rearrangement:**

A solution of the carbinol (1.0 mmol) and triethyl orthoacetate (0.5 mL) in dry toluene was refluxed under dry nitrogen until the complete disappearance of the carbinol (6-10 h). The solvent and excess triethyl orthoacetate were removed under reduced pressure on a rotovap and the residue filtered through a short column of silica gel to furnish the product ester in near quantitative yields.

**General procedure for the reduction of esters obtained from orthoester Claisen rearrangement with LAH:**

A solution of the above ester (1.0 mmol) in dry Et<sub>2</sub>O (5 mL) was cooled to 0 °C (ice-water mixture) and treated with LiAlH<sub>4</sub> (2.0 mmol). The cooling bath was removed and the reaction mixture stirred until completion (1-2 h). Water (3-4 drops) was added to



decompose the excess  $\text{LiAlH}_4$ , diluted with more  $\text{Et}_2\text{O}$  (5 mL) and dried with anhydrous  $\text{Na}_2\text{SO}_4$ . Filtration furnished the product in near quantitative yields.

80

$^1\text{H}$  NMR (300 MHz); (Fig. 2.32):

$\delta$  4.43-4.36 (1H, m), 4.19-4.08 (2H, 2d,  $J=12$  Hz), 4.11-4.03 (1H, m), 3.18-3.04 (2H, m), 2.19-2.14 (2H, m), 2.12-2.08 (1H, m), 2.01-1.92 (1H, m), 1.91-1.80 (1H, m), 1.80 (3H, t,  $J=1.2$  Hz), 1.80-1.60 (1H, m).

81,  $\text{R}=\text{Me}$

$^1\text{H}$  NMR (300 MHz); (Fig. 2.33):

$\delta$  5.37-5.34 (1H, dq,  $J=5.6, 1.0$  Hz), 4.39-4.35 (1H, m), 4.08-4.00 (3H, m), 2.92-2.87 (3H, m), 2.51 (1H, d,  $J=13$  Hz), 2.53-2.47 (1H, m), 1.63-1.61 (3H, dd,  $J=6.7, 1.0$  Hz), 2.25-2.05 (2H, m), 2.05-1.92 (1H, m), 1.90-1.75 (2H, m), 1.50-1.35 (1H, m), 1.21-1.16 (3H, t,  $J=7$  Hz).

$^{13}\text{C}$  NMR (75.5 MHz); (Fig. 2.34):

$\delta$  172.18, 140.67, 118.71, 104.22, 71.84, 59.84, 49.67, 39.90, 35.77, 33.40, 23.87, 23.19, 18.99, 14.25, 13.36.

82 ( $\text{R}=\text{Me}$ )

$^1\text{H}$  NMR (300 MHz); (Fig. 2.40):

$\delta$  5.40-5.30, 4.42-4.36 (1H, m), 4.08-4.01 (1H, m), 3.65-3.59 (1H, m), 3.55-3.49 (1H, m), 2.89-2.83 (2H, m), 2.53-2.248 (1H, bd), 2.35-2.27 (1H, dt), 2.12-2.04 (1H, m), 2.01-1.84 (4H, m), 1.46-1.38 (1H, m), 1.23 (3H, s).

$^{13}\text{C}$  NMR (75.5 MHz); (Fig. 2.41):

$\delta$  142.72, 117.92, 104.89, 71.73, 60.31, 48.81, 37.41, 35.32, 33.13, 23.90, 23.05, 18.26, 13.30.

**82 (R=Ph)**

$^1\text{H}$  NMR (300 MHz); (Fig. 2.44):

$\delta$  7.34-7.15 (5H, m), 6.42 (1H, s), 4.45-4.00 (1H, m), 4.12-4.08 (1H, m), 3.78-3.72 (1H, m), 3.65-3.60 (1H, m), 2.96-2.93 (2H, m), 2.75-2.67 H. bd), 2.42-2.34 (1H, dt), 2.24-1.84 (5H, m), 1.55-1.42 (1H, m), 1.38 (3H, s).

$^{13}\text{C}$  NMR (75.5 MHz); (Fig. 2.45):

$\delta$  145.10, 137.00, 128.97, 128.05, 126.20, 124.58, 104.76, 71.82, 60.19, 49.20, 37.75, 35.20, 33.29, 24.42, 24.12, 18.43.

**84 (R=Me)**

$^1\text{H}$  NMR (300 MHz); (Fig. 2.48):

$\delta$  5.40-5.33 (1H, q,  $J=6.6$  Hz), 4.40-4.34 (1H, m), 3.95-3.87 (1H, m), 3.63-3.47 (2H, m), 2.99-2.83 (2H, 2 adjacent m), 2.59-2.53 (1H, td,  $J=14.1, 3.6$  Hz), 2.27-2.06 (3H, m), 2.02-1.93 (1H, dt,  $J=13, 5.1$  Hz), 5.40-5.33 (1H, q,  $J=6.9, 1.72$ -1.41 (3H, m), 1.64 (3H, d,  $J=6.9$  Hz), 1.20 (3H, s).

$^{13}\text{C}$  NMR (75.5 MHz); (Fig. 2.49):

$\delta$  142.0, 118.1, 103.6, 71.0, 59.9, 52.3, 48.6, 39.4, 36.0, 33.0, 29.7, 23.6, 23.5, 17.4, 13.4.

**84 (R=Ph)**

$^1\text{H}$  NMR (300 MHz): (Fig. 2.50):

$\delta$  7.32-7.15 (5H, m), 6.38 (1H, s), 4.42-4.38 (1H, m), 3.97-3.93 (1H, m), 3.74-3.62 (2H, m), 3.02-2.90 (2H, 2 adjacent m), 2.79-2.74 (1H, bd), 2.38-2.32 (1H, m), 2.28-2.05 (3H, m), 1.85-1.78 (1H, m), 1.72-1.57 (3H, m), 1.35 (3H, s).

$^{13}\text{C}$  NMR (75.5 MHz); (Fig. 2.51):

$\delta$  144.89, 138.54, 129.07, 127.99, 126.08, 124.75, 103.72, 71.02, 59.76, 48.97, 39.69, 35.90, 33.14, 24.99, 23.97, 17.67.

86

$^1\text{H}$  NMR (300 MHz); (Fig. 2.54):

$\delta$  4.86 (1H, s), 4.80 (1H, s), 4.43-4.38 (1H, m), 4.06-4.02 (1H, m), 3.72-3.64 (1H, m), 3.62-3.54 (1H, m), 2.89-2.86 (2H, m), 2.39-2.28 (2H, m), 2.20-2.14 (1H, bd), 2.10-1.87 (4H, m), 1.60-1.48 (1H, m), 1.28 (3H, s).

$^{13}\text{C}$  NMR (75.5 MHz); (Fig. 2.55):

$\delta$  152.63, 110.13, 104.35, 71.76, 60.18, 48.61, 37.33, 35.18, 33.25, 31.54, 24.40, 18.34.

### Preparation of diene 90

A solution of  $\text{Ph}_3\text{PCH}_3\text{I}$  (242.5 mg, 0.5 mmol) in dry THF (5 mL) was cooled to 0 °C and mixed with  $\text{Bu}^n\text{Li}$  (0.375 mL of 1.5 M solution in hexane) After stirring for 20 min. **66** (99 mg, 0.5 mmol) was added. The reaction mixture was stirred further for 30 min at 0 °C. The reaction mixture was diluted with  $\text{Et}_2\text{O}$  (15 mL), mixed with saturated aqueous  $\text{NH}_4\text{Cl}$  (5 mL), and stirred for 10 min. The layers were separated and the aqueous layer extracted with ether (2 x 5 mL). The combined extracts were dried and the solvents removed. Purification yielded the pure diene **90**, 68 mg, 70%.

$^1\text{H}$  NMR (60 MHz):

$\delta$  7.0-6.4 (1H, m), 5.1-5.3 (1H, d), 4.9 (1H, bd), 4.4-3.8 (2H, m), 3.1-2.9 (2H, m), 2.3-1.5 (6H, m), 1.9 (3H, s).

### Preparation of diene 91

To a solution of pentadienoic acid (29 mg, 0.6 mmol) in dry  $\text{CH}_2\text{Cl}_2$  (2 mL) was added 4 mg of DMAP and 0.5 mmol (100 mg) of alcohol **80**. DCC (124 mg, 0.6 mmol) was added to the reaction mixture at 0 ° and the content stirred for 5 min at 0 °C and for 1 h at rt. Diluted the mixture with  $\text{CH}_2\text{Cl}_2$  (10 mL) and washed with saturated  $\text{NH}_4\text{Cl}$  (2 x 5 mL). The solvent was dried with anhydrous  $\text{Na}_2\text{SO}_4$ . The solvent was removed and the residue purified by silica gel chromatography to isolate the product **91**, 128 mg, 90%.

$^1\text{H}$  NMR (200 MHz); (Fig. 2.58):

$\delta$  6.58-6.37 (1H, m), 5.96-5.88 (1H, d, 15.4 Hz), 5.66-5.47 (2H, dd, ), 4.67 (2H, s), 4.45-4.36 (1H, m), 4.10-4.02 (1H, m), 3.21-3.04 (2H, m), 2.11-1.97 (7H, m), 1.81 (3H, s).

### 93

$^1\text{H}$  NMR (60 MHz):

$\delta$  4.0-4.3 (2H, t), 3.0-3.2 (2H, t), 2.7 (2H, s), 2.4-1.8 (6H, m).

IR ( $\text{CCl}_4$ ):  $1710\text{ cm}^{-1}$ .

### Preparation of 94:

The solution of **93** (172 mg, 1 mmol) in THF (3 mL) was cooled to  $0^\circ\text{C}$  and mixed with a solution vinyl magnesium bromide (1.1 mL, 1.1 mmol, 1M solution in THF). The reaction mixture was stirred for 30 min and then quenched by adding saturated  $\text{NH}_4\text{Cl}$  (5 mL). The contents were diluted with  $\text{Et}_2\text{O}$  (5 mL) and the layers separated. The aqueous layer was extracted further with  $\text{Et}_2\text{O}$  (2 x 5 mL). The combined extracts were dried and concentrated to furnish a residue which was chromatographed to isolate a mixture of alcohols **94**, 180 mg (90%). NMR of the mixture of alcohols is given below.

$^1\text{H}$  NMR (60 MHz):

$\delta$  6.0-5.3 (2H, m), 5.2-4.8 (1H, m), 4.3-4.1 (2H, t), 3.6 (1H, s), 3.2-2.9 (2H, t), 2.2-1.4 (8H, m).

### Preparation of 95

The solution of **94** (200 mg, 1 mmol) in  $\text{CH}_2\text{Cl}_2$  (5 mL) was cooled to  $0^\circ\text{C}$  and mixed with  $\text{Et}_3\text{N}$  (0.28 mL, 2 mmol) and  $\text{MsCl}$  (0.086 mL, 1 mmol). The reaction mixture was stirred for 4 h. The reaction contents were diluted with  $\text{CH}_2\text{Cl}_2$  (5 mL) and mixed with saturated  $\text{NH}_4\text{Cl}$  (5 mL). The layers were separated and the aqueous layer extracted with  $\text{CH}_2\text{Cl}_2$  (2 x 5 mL). The combined extracts were dried and concentrated to furnish a residue which was purified through silica gel chromatography to isolate **95**, 127 mg, 70%.

$^1\text{H}$  NMR (60 MHz):

$\delta$  6.7-5.6 (2H, m), 5.2-5.1 (1H, d), 4.9 (1H, d), 4.3-4.0 (2H, t), 3.2-2.9 (2H, t), 2.7-1.8 (6H, m).

### Diels-Alder reaction of diene 95 with NPM

A solution of the diene 95 (13 mg, 0.07 mmol) and NPM (17 mg, 0.1 mmol) in dry toluene (2 mL) was heated to reflux under  $\text{N}_2$  for 4 h. The solvent was removed on rotovap under reduced pressure and the residue filtered through a short silica gel column to obtain the products mixture in 60% yield (15 mg). The isomers were separated using radial chromatography.

#### Less polar isomer:

$^1\text{H}$  NMR (300 MHz); (Fig. 2.59):

$\delta$  7.493-7.265 (5H, m), 5.66 (1H, s), 4.21-4.09 (2H, m), 3.39-3.34 (1H, t,  $J=8.5\text{Hz}$ ), 3.25-3.19 (1H, t,  $J=8.3\text{Hz}$ ), 3.1-3.01 (2H, m), 2.846-2.79 (1H, bd,  $J=18\text{Hz}$ ), 2.69-2.36 (4H, m), 2.23-2.18 (1H, bd,  $J=13.8\text{Hz}$ ), 2.11-2.06 (1H, dt,  $J=3.6\text{Hz}$ ) 1.97-1.88 (1H, dt,  $J=12.6\text{Hz}$ ), 1.538-1.26 (2H, m).

#### More polar isomer:

$^1\text{H}$  NMR (300 MHz); (Fig. 2.60):

$\delta$  7.48-7.24 (5H, m), 5.59 (H, s), 4.16-4.04 (2H, septet,  $J=5.8\text{Hz}$ ), 3.38-3.33 (1H, t,  $J=8.5\text{Hz}$ ), 3.24-3.19 (1H, t,  $J=8.5\text{Hz}$ ), 3.09-3.05 (1H, t), 2.86-2.69 (2H, m), 2.578-2.24 (4H, m), 2.02-1.68 (3H, m), 1.635-1.5 (1H, m).

### Diels-Alder addition of diene 95 with MTAD:

A solution of the diene 95 (15 mg, 0.08 mmol) and MTAD (10 mg, 0.09 mmol) in an 1:1 mixture of THF and  $\text{CH}_2\text{Cl}_2$  (2 mL) was allowed to stand at  $-78$  to  $20^\circ\text{C}$  for 4 h. The solvents were removed and the residue filtered through a short silica gel column to obtain the products mixture 22 mg, 77%.

The NMR of the mixture of isomers 98, 99 is given in Fig. 2.61.

**Diels-Alder addition of diene 95 with TCNE:**

A solution of the diene **95** (15 mg, 0.08 mmol) and TCNE (12 mg, 0.09 mmol) in THF (2 mL) was allowed to stand at -78 to 20 °C for 4 h. The solvents were removed and the residue filtered through a short silica gel column to obtain the products mixture 18 mg, 70%.

**Minor isomer of 100:**

$^1\text{H}$  NMR (300 MHz): (fig. 2.63):

$\delta$  5.57-5.55 (1H, m), 4.18-4.08 (2H, m), 3.21-2.95 (4H, m), 2.84-2.78 (1H, dd,  $J=2.7$ , 15.3), 2.62-2.57 (1H, bd,  $J=15\text{Hz}$ ), 2.43-2.36 (1H, bdt,  $J=3.3$ , 13.8Hz), 2.256-2.23 (2H, ), 2.18-2.09 (1H,  $J=12.3$ , 3.3 Hz), 2.04-1.94 (1H, td,  $J=4.8$ , 13.8Hz).

**Major isomer of 100:**

$^1\text{H}$  NMR (300 MHz): (Fig. 2.64):

$\delta$  5.66-5.63 (1H, m), 4.25-4.21 (2H, m), 3.24-3.15 (1H, dq), 3.18-3.03 (3H, m), 2.99-2.96 (1H, bd,  $J=7.8\text{Hz}$ ), 2.76-2.71 (1H, dd,  $J=2.4$ , 13.8Hz), 2.66-2.61 (1H, bd,  $J=14.1\text{Hz}$ ), 2.49-2.42 (1H, m), 2.27-2.22 (1H, m), 2.07-1.92 (2H, m).

**The oxy-Cope precursors 70 and 71**

A solution of **64** (498 mg, 2.0 mmol) in dry THF (10 mL) was cooled to -80 °C and mixed with  $\text{Bu}^n\text{Li}$  1.38 mL of a 1.6 M solution in hexane. 2.2 mmol). After stirring for 10 min, allylphenyl ketone (292 mg, 2.0 mmol) was added in THF (2 mL). The reaction mixture was stirred further for 30 min at -80 °C, quenched with MeOH (164  $\mu\text{L}$ , 4.0 mmol), and allowed to warm to 20 °C. The reaction mixture was diluted with  $\text{Et}_2\text{O}$  (20 mL), mixed with saturated aqueous  $\text{NH}_4\text{Cl}$  (10 mL), and stirred for 10 min. The layers were separated and the aqueous layer extracted with ether (2 x 10 mL). The combined extracts were washed with water (10 mL) and brine (10 mL), dried and concentrated. The two alcohols **70** and **71**, which were formed in almost equal amounts and in a combined yield of 0.348 g, 55%, were separated by radial chromatography. Purification yielded the pure aldehyde, 0.140 g, 70%, mp 48 °C.

**Oxy-Cope rearrangement of alcohols 70 and 71:**

A solution (2 mL) of the alcohol **70** (95 mg, 0.3 mmol) was slowly added to a suspension of KH (24 mg, 0.6 mmol) in the same solvent (2 mL) at 0 °C. Now, a solution (1 mL) of 18-crown-6 (80 mg, 0.3 mmol) was added and the resultant allowed to come to rt. The contents were allowed to reflux for 30 min when a TLC indicated complete disappearance of the reactant alcohol. After cooling the contents to rt, the reaction was quenched with MeOH (2 equiv) and stirred with saturated aq  $\text{NH}_4\text{Cl}$  (5 mL) for 5 min. The products were extracted into ether (3 x 6 mL). The combined extracts were washed with brine, dried with anhyd.  $\text{Na}_2\text{SO}_4$ , and filtered. Evaporation of the solvents under reduced pressure furnished the crude material which was purified for the mixture of the two desired products **101** and **102** by column chromatography. The combined yield was 42 mg; 45%. The product **101** was separated from the product **102** by radial chromatography.

**Oxy-Cope rearrangement of alcohol 72**

The procedure mentioned above was followed. The mixture of products **102** and **103** was isolated in >70% yield. The NMR of the mixture of isomers is given in Fig. 2.66.

**Reaction of phenyl magnesium bromide with aldehydes 103 and 104:**

The solution of the Grignard reagent (1 mmol) in  $\text{Et}_2\text{O}$  (3 mL) was cooled to 0 °C and mixed with a solution of a mixture of **103** and **104** (120 mg, 0.5 mmol) in the same solvent (2 mL). The reaction mixture was stirred for 1 h and then quenched by adding saturated  $\text{NH}_4\text{Cl}$  (5 mL). The contents were diluted with  $\text{Et}_2\text{O}$  (5 mL) and the layers were separated. The aqueous layer was extracted with  $\text{Et}_2\text{O}$  (2 x 5 mL). The combined extracts were dried and concentrated to furnish a residue which was purified to isolate a mixture of alcohols **105** and **106**. 151 mg, 95%.

**Oxidation of 105 and 106:**

Chromium trioxide (140 mg, 1.4 mmol) was added to a solution of dry pyridine (0.23 mL, 2.9 mmol) in 2.5 mL of  $\text{CH}_2\text{Cl}_2$ . After stirring at rt for 15 min, a solution of a mixture of

**105** and **106** (77 mg, 0.24 mmol) in  $\text{CH}_2\text{Cl}_2$  (1 mL) was added in one portion and stirred further for 10 min. The solution was decanted from the residue and the solvent evaporated to leave a black residue. This was dissolved in ether (10 mL) and filtered through silica gel. The solvent was removed and the residue chromatographed to isolate a mixture of ketones **101** and **102**, 53 mg, 70%.

### **101**

$^1\text{H}$  NMR (300 MHz) (Fig. 2.67):

$\delta$  8.00-7.97 (2H, m), 7.56-7.53 (1H, m), 7.49-7.44 (2H, m), 6.00-5.86 (1H, m), 4.96-4.85 (2H, m), 4.45-4.40 (1H, m), 4.04-3.96 (1H, m), 3.70-3.65 (1H, dd,  $J=12.6$  and 3.3 Hz), 2.94-2.85 (2H, m), 2.70-2.62 (2H, m), 2.21-2.17 (1H, m), 2.15-1.90 (3H, m), 1.84-1.40 (2H, m), 0.94 (3H, s).

### **102**

$^1\text{H}$  NMR (300 MHz): (Fig. 2.69):

$\delta$  7.94-7.91 (2H, d,  $J=7.2$  Hz), 7.55-7.50 (1H, t,  $J=7.2$  Hz), 7.45-7.40 (2H, t,  $J=7.2$  Hz), 5.85-5.71 (1H, m), 4.62-4.57 (2H, m), 4.64-4.42 (1H, bt,  $J=6.9$  Hz), 4.04-3.96 (1H, dt,  $J=9.6, 5.1$  Hz), 3.93-3.89 (1H, bd,  $J=9.9$  Hz), 3.00-2.95 (1H, illresolved m), 2.93-2.84 (1H, dt,  $J=9.9, 6.0$  Hz), 2.48-2.45 (2H, d,  $J=7.5$  Hz), 2.10-2.08 (2H, bd,  $J=5.4$  Hz), 1.80-1.60 (4H, m), 1.43 (3H, s).



- [21] Uskokovic, M.R.; Lewis, R.L.; Partridge, J.J.; Despreaux, C.W.; Pruess, D.L. *J. Am. Chem. Soc.* **1979**, *101*, 6742.
- [22] Ireland, R.E.; Marshall, J.A. *J. Org. Chem.* **1962**, *27*, 1620.
- [23] Church, R.T.; Ireland, R.E. *J. Org. Chem.* **1963**, *28*, 17.
- [24] Lin, M.; Watson, W.H.; Kashyap, R.P.; le Noble W.J. *J. Org. Chem.* **1990**, *55*, 3597.
- [25] Mukherjee, A.; Wu, Q.; le Noble W.J. *J. Org. Chem.* **1994**, *59*, 3270.
- [26] Paquette, L.A. *Asymmetric Synthesis*; J.D. Morrison Ed.; Academic: New York: 1984, Chapter 7.
- [27] Letourneau, J.E.; Wellman, M.A.; Burnell, J.D. *J. Org. Chem.* **1997**, *62*, 7272.
- [28] Chung, W.S.; Turro, N.J.; Srivastava, S.; Li, H.; le Noble W.J. *J. Am. Chem. Soc.* **1988**, *110*, 7882.
- [29] Fleming, I.; Sarkar, A.K.; Doyle, M.J.; Raithby, P.R. *J. Chem. Soc., Perkin Trans I* **1989**, 2023.
- [30] Wellmann, M.A.; Burry, L.C.; Letourneau, J.E.; Bridson, J.N.; Miller, D.O.; Burnell, D.J. *J. Org. Chem.* **1997**, *62*, 939.
- [31] Sbail, A.; Branchadeil, V.; Oliva, A. *J. Org. Chem.* **1996**, *61*, 621.
- [32] Poirier, R.A.; Pye, C.C.; Xidos, J.D.; Burnell, J.D. *J. Org. Chem.* **1995**, *60*, 2328.
- [33] Adam, w.; Jacob, U.; Prein, M. *J. Chem. Soc., Chem. Commun.* **1995**, 839.
- [34] Poirier, R.A.; Pye, C.C.; Xidos, J.D.; Burnell, D.J. *J. Org. Chem.* **1995**, *60*, 2328.
- [35] Kaila, N.; Franck, R.W.; Dannenberg, J.J. *J. Org. Chem.* **1989**, *54*, 4206.
- [36] Haller, J.; Niwawama, S.; Duh, H.Y.; Houk, K.N. *J. Org. Chem.* **1997**, *62*, 5728.
- [37] Crisp, G.T.; Gebauer, M.G. *J. Org. Chem.* **1996**, *61*, 8425.
- [38] Jones, P.G.; Weinmann, H.; Winterfeldt, E. *Angew. Chem. Int. Ed. Engl.* **1995**, *34*, 448.
- [39] Chung, W.S.; Tsai, T.L.; Ho, C.C.; Chiang, M.Y.N.; le Noble W.J. *J. Org. Chem.* **1997**, *62*, 4672.
- [40] Carreno, M.C.; Ruano, J.L.G.; Toledo, M.A.; Urbano, A.; Remor, C.Z.; Stefani, V.; Fischer, J. *J. Org. Chem.* **1996**, *61*, 503.
- [41] Gandolfi, R.; Amade, M.S.; Rastelli, A.; Bagatti, M.; Montanari, D. *Tetrahedron Lett.* **1996**, *37*, 517.
- [42] Mataka, S.; Ma, J.; Thiemann, T.; Rudzinski, J.M.; Sawada, T.; Tashiro, M. *Tetrahedron Lett.* **1995**, *36*, 6105.
- [43] Mehta, G.; Uma, R. *Tetrahedron Lett.* **1995**, *37*, 4873.

- [44] Mehta, G.; Subramanian, U.R.; Pramanik, A.; Chandrasekar, J.; Nethaji, M. *J. Chem. Soc., Chem. Commun.* **1995**, 677.
- [45] Tsuji, T.; Ohkita, m.; Nishida, S. *J. Org. Chem.* **1991**, 56, 997.
- [46] Gleiter, R.; Paquette, L.A. *Acc. Chem. Res.* **1983**, 16, 328.
- [47] Casas, R.; Parella, T.; Branchadell, V.; Oliva, A.; Ortuno, M.; Guingant, A. *Tetrahedron*. **1992**, 48, 2659.
- [48] Franck, R.W.; Argade, S.; Subramaniam, C.S.; Frechet, D.M. *Tetrahedron Lett.* **1985**, 26, 3187.
- [49] Tripathy, R.; Carroll, P.J.; Thornton, E.R. *J. Am. Chem. Soc.* **1991**, 113, 7630.
- [50] Fisher, M.J.; Hehre, W.J.; Kahn, S.D.; Overman, L.E. *J. Am. Chem. Soc.* **1988**, 110, 4625.
- [51] Macaulay, J.B.; Fallis, A.G. *J. Am. Chem. Soc.* **1990**, 112, 1336.
- [52] Datta, S.C.; Franck, R.W.; Tripathy, R.; Quigley, G.J.; Huang, L.; Chen, S.; Sihaed, A. *J. Am. Chem. Soc.* **1990**, 112, 8472.
- [53] H. Forster; Vogtle, F. *Angew. Chem. Int. Ed. Engl.* **1977**, 16, 429.
- [54] Winstein, S.; Shatavsky, M.; Norton, C.; Woodward, R.B. *J. Am. Chem. Soc.* **1955**, 77, 4183.
- [55] Macaulay, J.B.; Fallis, A.G. *J. Am. Chem. Soc.* **1988**, 110, 4074.
- [56] Breslow, R.; Jr., Hoffmann J.M. *J. Am. Chem. Soc.* **1972**, 94, 2110.
- [57] Breslow, R.; Jr. Perchonok C., Hoffmann J.M. *Tetrahedron Lett.* **1973**, 3723.
- [58] Franck-Neumann, M.; Sedrati, M. *Tetrahedron Lett.* **1983**, 24, 1391.
- [59] Ishida, M.; Aoyama, T.; Kato, S. *Chem. Lett.* **1989**, 663.
- [60] Ishida, M.; Beniya, Y.; Inagaki, S.; Kato, S. *J. Am. Chem. Soc.* **1990**, 112, 8980.
- [61] Ishida, M.; Aoyama, T.; Beniya, Y.; Yamabe, S.; Kato, S. *Bull. Chem. Soc. Jpn.* **1993**, 66, 3430.
- [62] Fleming, I.; Michael, J.P. *J. Chem. Soc., Chem. Commun.* **1978**, 245.
- [63] Fleming, I.; Williams, R.V. *J. Chem. Soc., Perkin. Trans. I.* **1981**, 645.
- [64] Fleming, I.; Sarker, A.k.; Doyle, M.J.; Raithby, P.R. *J. Chem. Soc., Perkin Trans. I.* **1989**, 2023.
- [65] Corey, E.J.; Weinshenker, N.M.; Schaaf, T.K.; Huber, W. *J. Am. Chem. Soc.* **1969**, 91, 5675.
- [66] Wright, M.E.; Hoover, J.F.; Nelson, G.O.; Scottt, C.P.; Glass, R.S. *J. Org. Chem.* **1984**, 49, 3059.

- [67] Frye, S.V.; Eliel, E.L. *Tetrahedron Lett.* **1986**, *27*, 3223.
- [68] Isobe, M.; Obeyama, J.; Funabashi, Y.; Goto, T. *Tetrahedron Lett.* **1988**, *29*, 4773.
- [69] Branan, B.M.; Paquette, L.A. *J. Am. Chem. Soc.* **1994**, *116*, 7658.
- [70] Paquette, L.A.; Branan, B.M.; Rogers, R.D.; Bond, A.H.; Lange, H.; Gleiter, R. *J. Am. Chem. Soc.* **1995**, *117*, 5992.
- [71] Paquette, L.A.; Lobben, P.C. *J. Am. Chem. Soc.* **1996**, *118*, 1917.
- [72] Gleiter, R.; Ginsburg, D. *Pure Appl. Chem.* **1979**, *51*, 1301.
- [73] Ginsburg, D. *Tetrahedron.* **1983**, *39*, 2095.
- [74] Parvez, M.; Jeyaraj, D.A.; Yadav, V.K. *Acta. Cryst.* **1997**, *C53*, 1961.
- [75] Liljefors, T.; Allinger, N.L. *J. Am. Chem. Soc.* **1976**, *98*, 2745.
- [76] Yeo, S.-K.; Shiro, M.; Kanematsu, K. *J. Org. Chem.* **1994**, *59*, 1621.
- [77] Jaime, C.; Osawa, E. *J. Mol. Struct.* **1985**, *126*, 363.
- [78] Devaquet, A.J.P.; Hehre, W.J. *J. Am. Chem. Soc.* **1976**, *98*, 4068.
- [79] Paquette L., A.; Undermer, T.L.; Gallucci, J. *J. Org. Chem.* **1992**, *57*, 86.
- [80] Clark, F.R.S.; Warkentin, J. *Can. J. Chem.* **1971**, *49*, 2221.
- [81] Frish, M.; Trucks, G.W.; Schlegel, H.B.; Gill, P.M.; Johnson, B.G.; Robb, M.A.; Cheeseman, J.R.; Keith, T.; Petersson, G.A.; Montgomery, J.A.; Raghavachari, K.; Al-Laham, M.A.; Zakrzewski, V.G.; Ortiz, J.V.; Foresman, J.B.; Cioslowski, J.; Stefanov, B.B.; Nanayakkara, A.; Challacombe, M.; Peng, C.Y.; Ayala, P.Y.; Chen, W.; Wong, M.W.; Andres, J.L.; Replogle, E.S.; Gomperts, R.; Martin, R.L.; Fox, D.J.; Binkley, J.S.; Defrees, D.J.; Baker, J.; Stewart, J.P.; Head-Gordon, M.; Gonzalez, C.; Pople, J.A. *Gaussian, Inc.* Pittsburgh PA, 1995.
- [82] Yadav, V.K.; Jeyaraj, D.A. *J. Org. Chem.* **1998**, *63*, 000.
- [83] Jeyaraj, D.A.; Yadav, A.; Yadav, V.K. *Tetrahedron Lett.* **1997**, *38*, 4483.
- [84] Jeyaraj, D.A.; Yadav, V.K. *Tetrahedron Lett.* **1997**, *38*, 6095.
- [85] Fraser, R.R.; Faibish, N.C.; Kong, F.; Bednarski, K.J. *J. Org. Chem.* **1997**, *62*, 6164.
- [86] Power, M.B.; Bott, S.G.; Atwood, J.L.; Barron, A.R. *J. Am. Chem. Soc.* **1990**, *112*, 3446.
- [87] Maruoka, K.; Itoh, T.; Sakurai, M.; Nonoshita, K.; Yamamoto, H. *J. Am. Chem. Soc.* **1988**, *110*, 3588.
- [88] Evans, D.A. *Science*. **1988**, *240*, 420.
- [89] Jones, G.P.; Chapman, B.J. *Synthesis*. **1995**, 475.
- [90] Cram, D.J.; Elhafez, F.A.A. *J. Am. Chem. Soc.* **1952**, *74*, 5828.

- [91] Ashby, E.C.; Laemmle, J.T. *Chem. Rev.* **1975**, *75*, 521.
- [92] Paquette, L.A.; Maynard, G.D. *J. Am. Chem. Soc.* **1992**, *114*, 5018.
- [93] Araki, S.; Shimizu, T.; Johar, P.S.; Jin, S.-J.; Butsugan, Y. *J. Org. Chem.* **1991**, *56*, 2538.
- [94] Yamamoto, Y.; Asao, N. *Chem. Rev.* **1993**, *93*, 2207.
- [95] Lubineau, A.; Auge, J.; Queneau, Y. *Synthesis*. **1994**, 741.
- [96] Paquette, L.A.; Mitzel, T.M. *J. Org. Chem.* **1996**, *61*, 8799.
- [97] Kowalski, C.J.; Fields, K.W. *J. Org. Chem.* **1981**, *46*, 197.
- [98] Piers, E.; Nagakura, I. *Syn. Commun.* **1975**, *5*, 193.
- [99] Shih, C.; Swenton, J.S. *J. Org. Chem.* **1982**, *47*, 2825.
- [100] Kress, M.H.; Kishi, Y. *Tetrahedron Lett.* **1995**, *36*, 4583.
- [101] Deslongchamps, P. *Stereoelectronic Effects in Organic Synthesis*; Pergamon Press: 1983.
- [102] Ireland, R.E.; Varney, M.D. *J. Org. Chem.* **1983**, *48*, 1829.
- [103] Ireland, R.E.; Muller, R.H.; Willard, A.K. *J. Am. Chem. Soc.* **1976**, 2868.
- [104] Johnson, W.H.; Werthemann, L.; Bartlett, W.R.; Brocksom, T.J.; Li, T.; Faulkner, D.J.; Petersen, M.R. *J. Am. Chem. Soc.* **1970**, *92*, 741.
- [105] Yadav, V.K.; Yadav, A.; Pande, P.; Kapoor, K.K. *Ind. J. Chem.* **1994**, *33B*, 1129.
- [106] Lounasmaa, M.; Hanhinen, P.; Jokela, R. *Tetrahedron*. **1995**, *51*, 8623.
- [107] Cherest, M.; Felkin, H.; Prudent, N. *Tetrahedron Lett.* **1968**, 2199.
- [108] Neises, B.; Steglich, W. *Angew. Chem. Int. Ed. Engl.* **1978**, *17*, 522.
- [109] Mertes, M.P. *J. Am. Chem. Soc.* **1961**, *26*, 5236.
- [110] Paquette, L.A. *Angew. Chem. Int. Ed. Engl.* **1990**, *29*, 609.
- [111] Hammond, G.S.; DeBoer, C.D. *J. Am. Chem. Soc.* **1964**, *86*, 899.
- [112] Viola, A.; Iorio, E.J.; Chen, K.K.; Glover, G.M.; Nayak, U.; Kocienski, P.J. *J. Am. Chem. Soc.* **1967**, *89*, 3462.
- [113] Viola, A.; Iorio, E.J. *J. Org. Chem.* **1970**, *35*, 856.
- [114] Furniss, B.S.; Hannaford, A.J.; Smith, P.W.G.; Tatchell, A.R. *Vogel's Textbook of Practical Organic Chemistry*; Longman Group U.K. Ltd: 1989.
- [115] Furstner, A. *Synthesis*. **1989**, 571.
- [116] Shono, T.; Ishifune, M.; Kashimura, S. *Chem. Lett.* **1990**, 449.

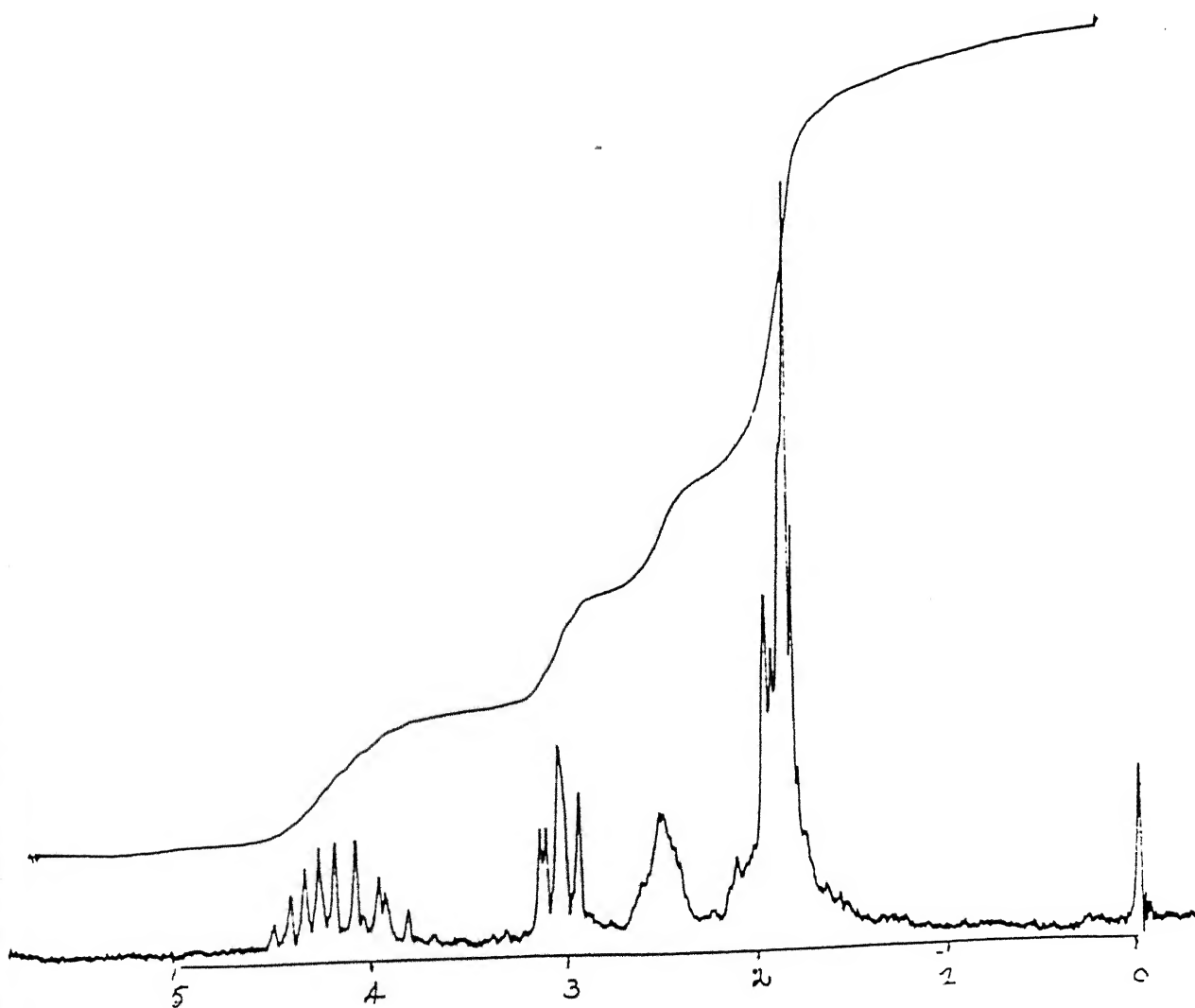
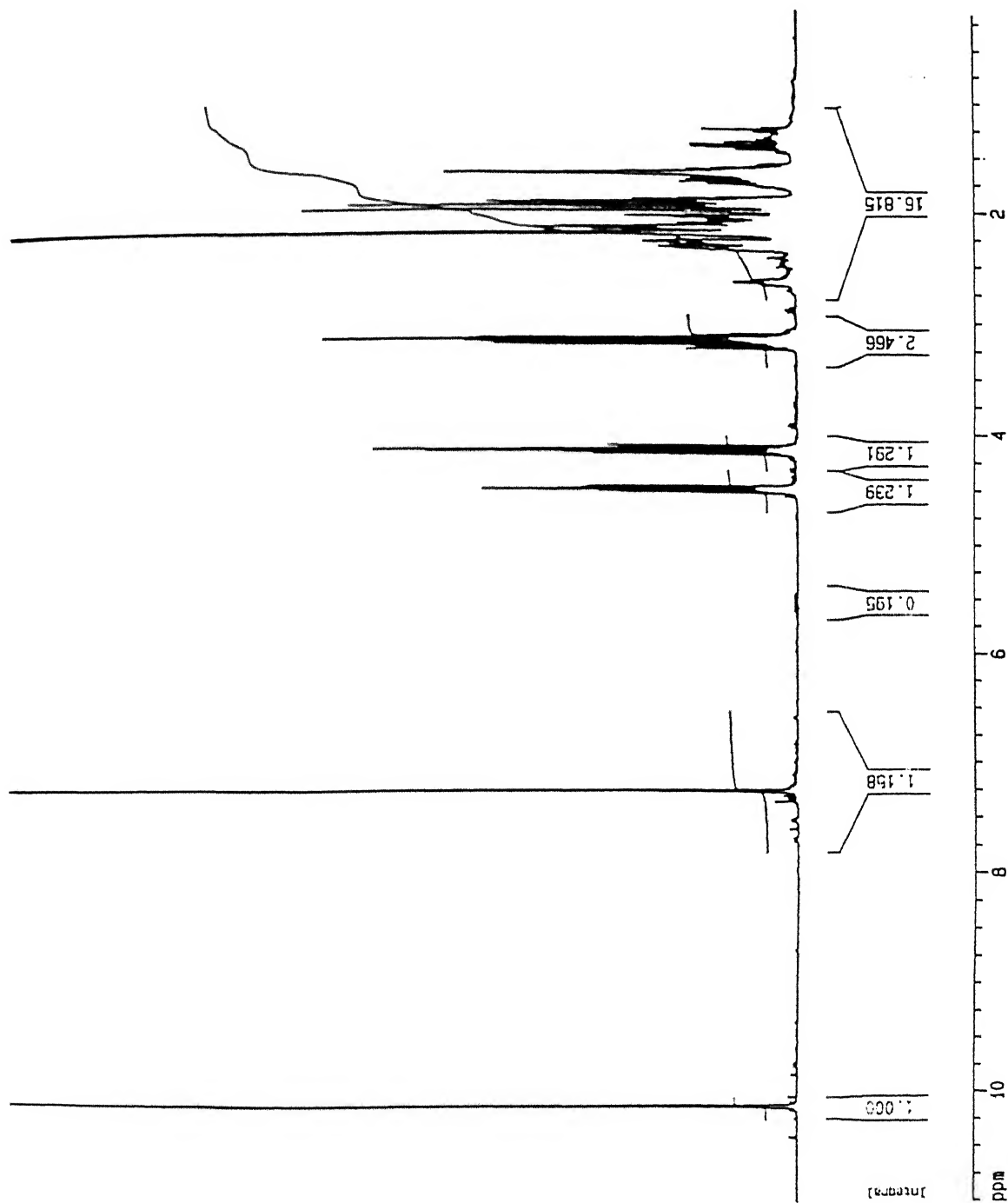


Figure 2.6: 60 MHz  $^1\text{H}$  NMR spectra of 64

Figure 2.7: 300 MHz  $^1\text{H}$  NMR spectra of 66

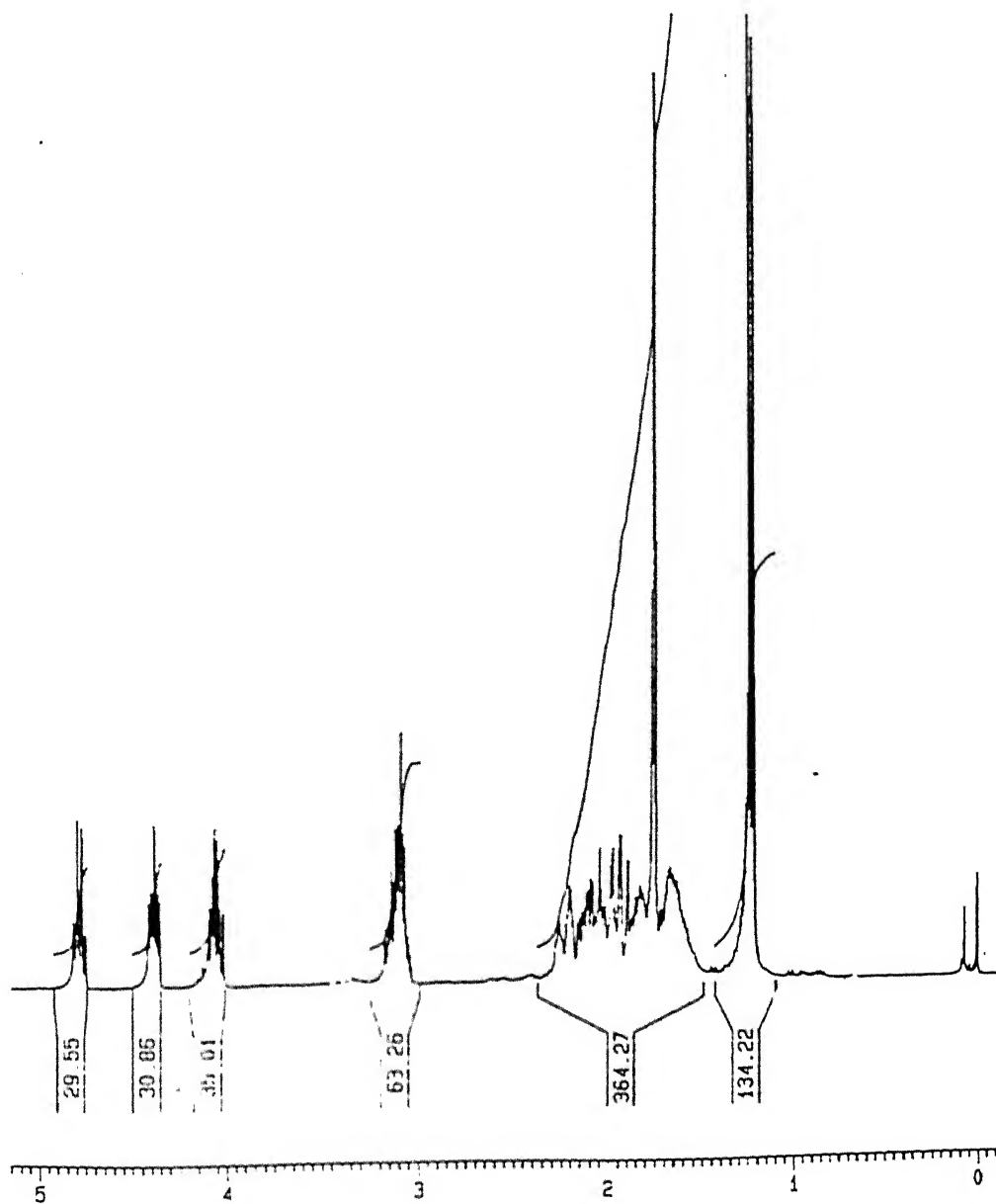
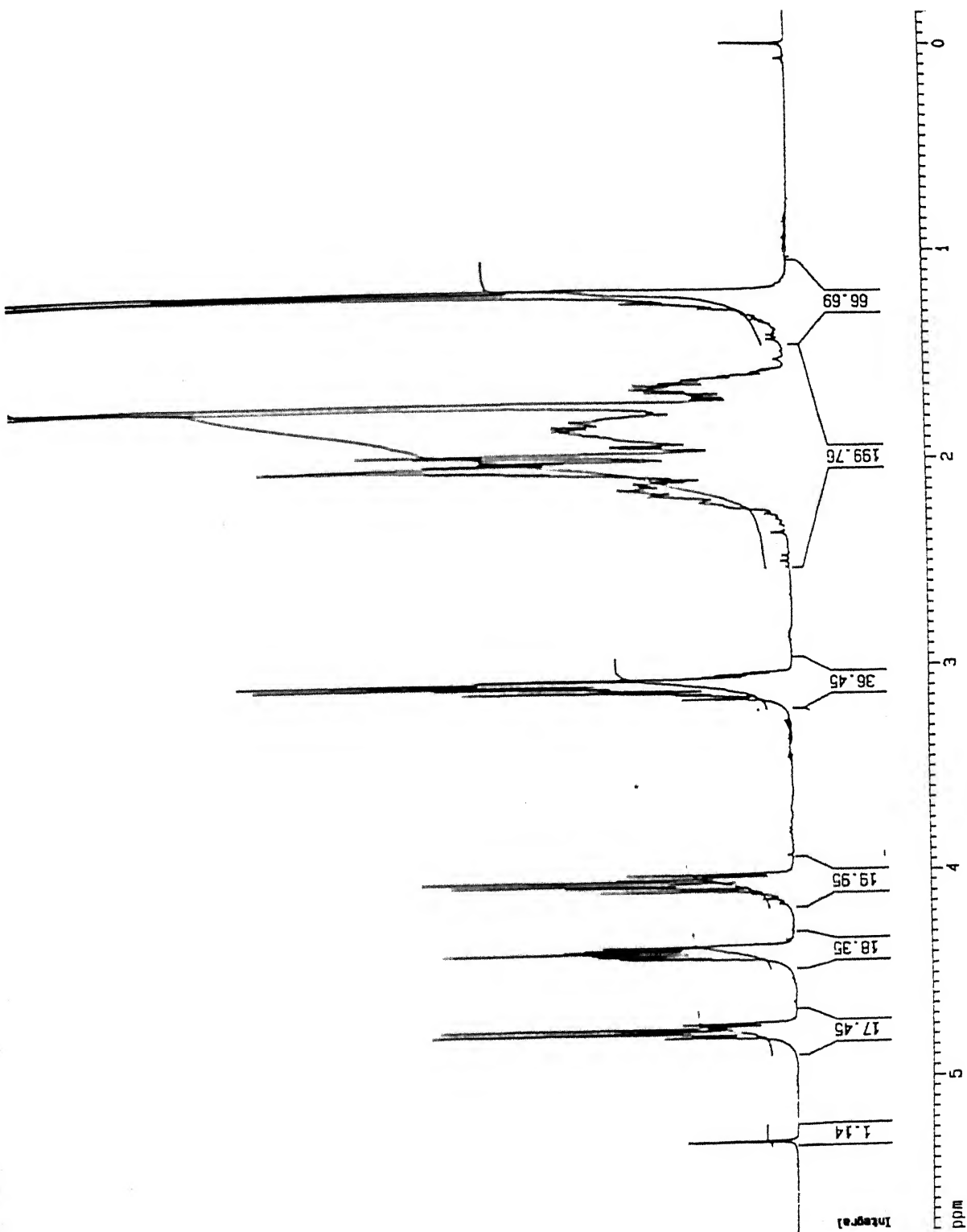
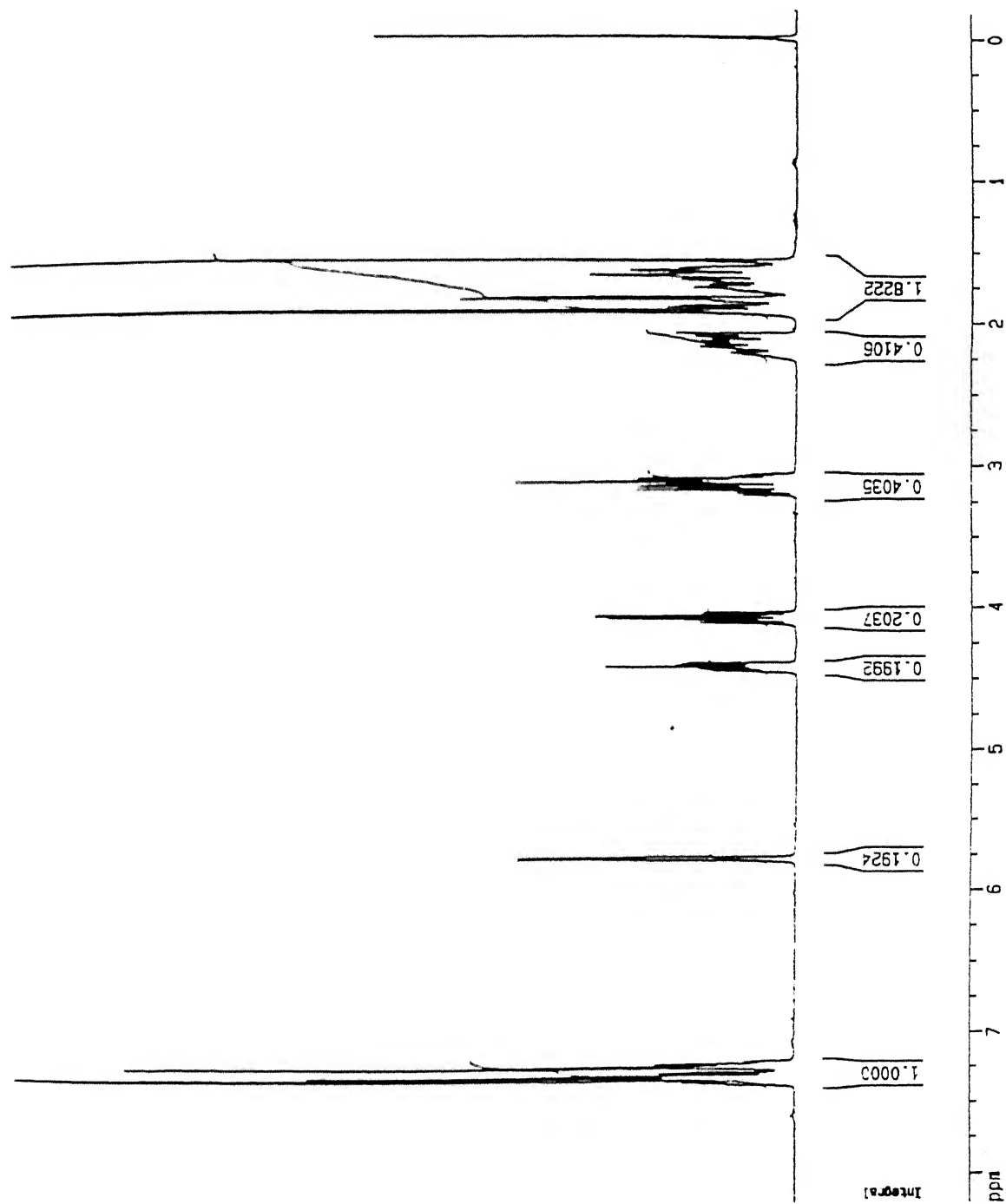


Figure 2.S: 300 MHz  $^1\text{H}$  NMR spectra of 72, Nu=Me

Figure 2.9: 300 MHz  $^1\text{H}$  NMR spectra of 73, Nu=Me



Figure 2.10: 300 MHz  $^1\text{H}$  NMR spectra of 72, Nu=Ph

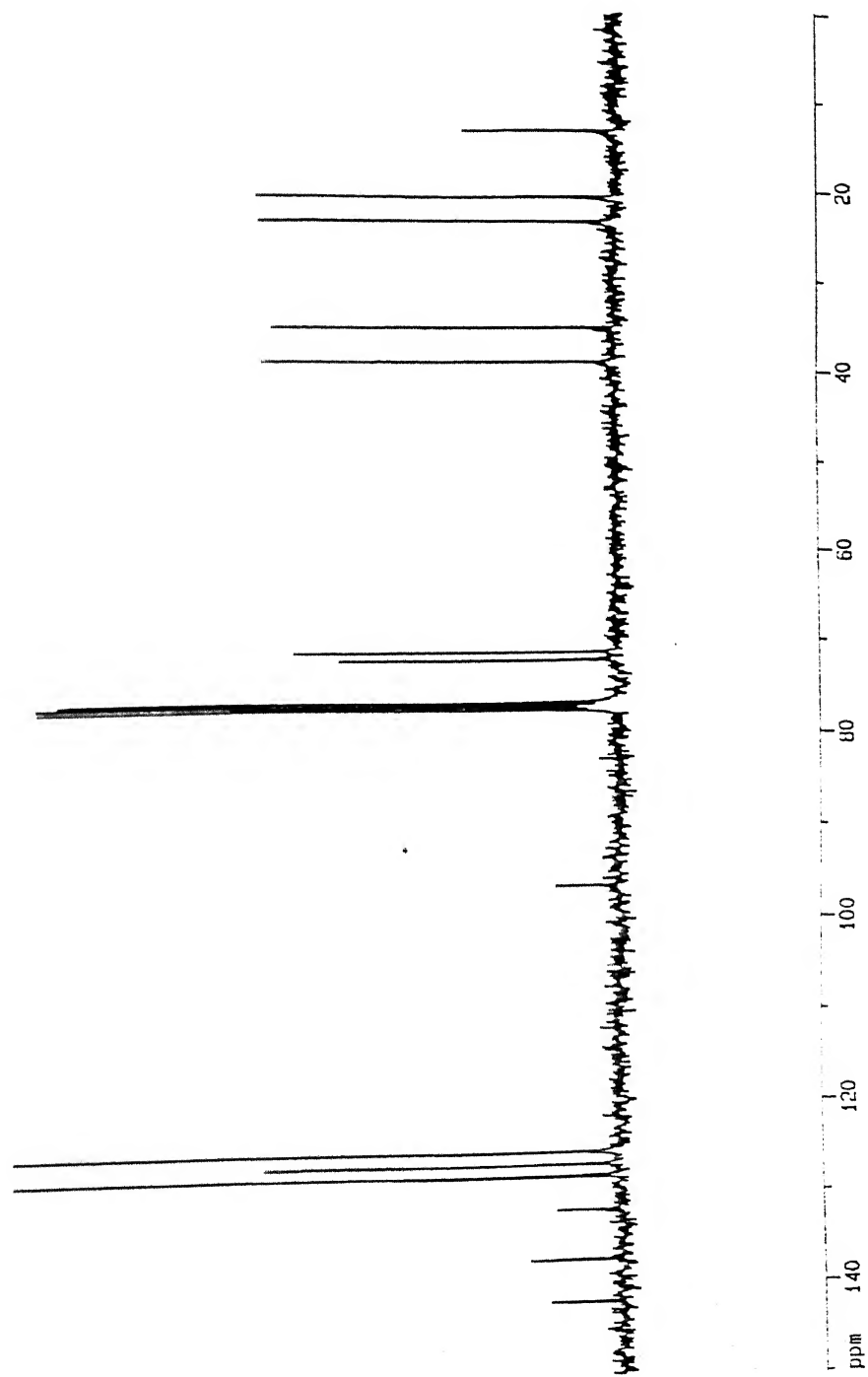


Figure 2.11: 75.5 MHz  $^{13}\text{C}$  NMR spectra of 72, Nu=Ph

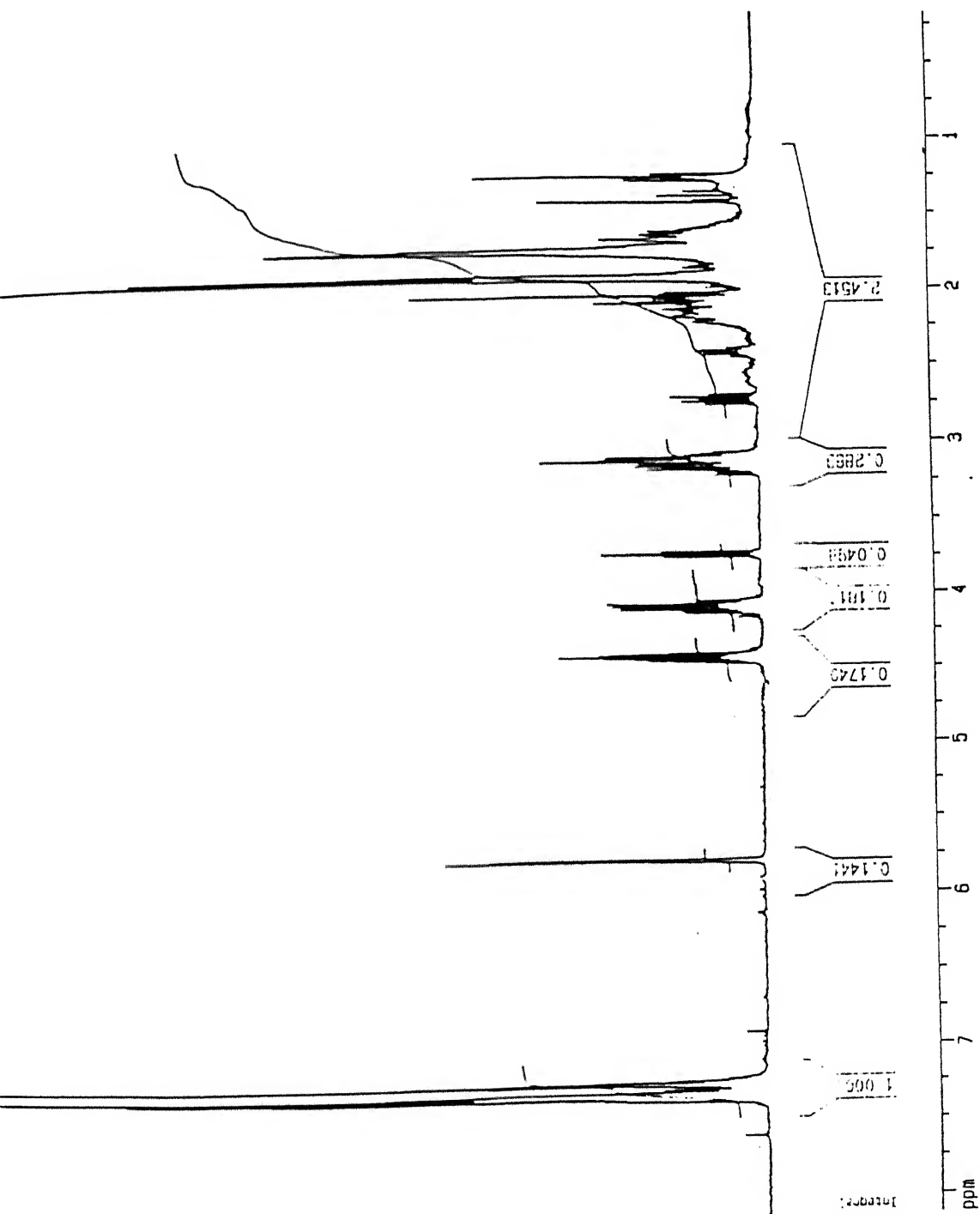
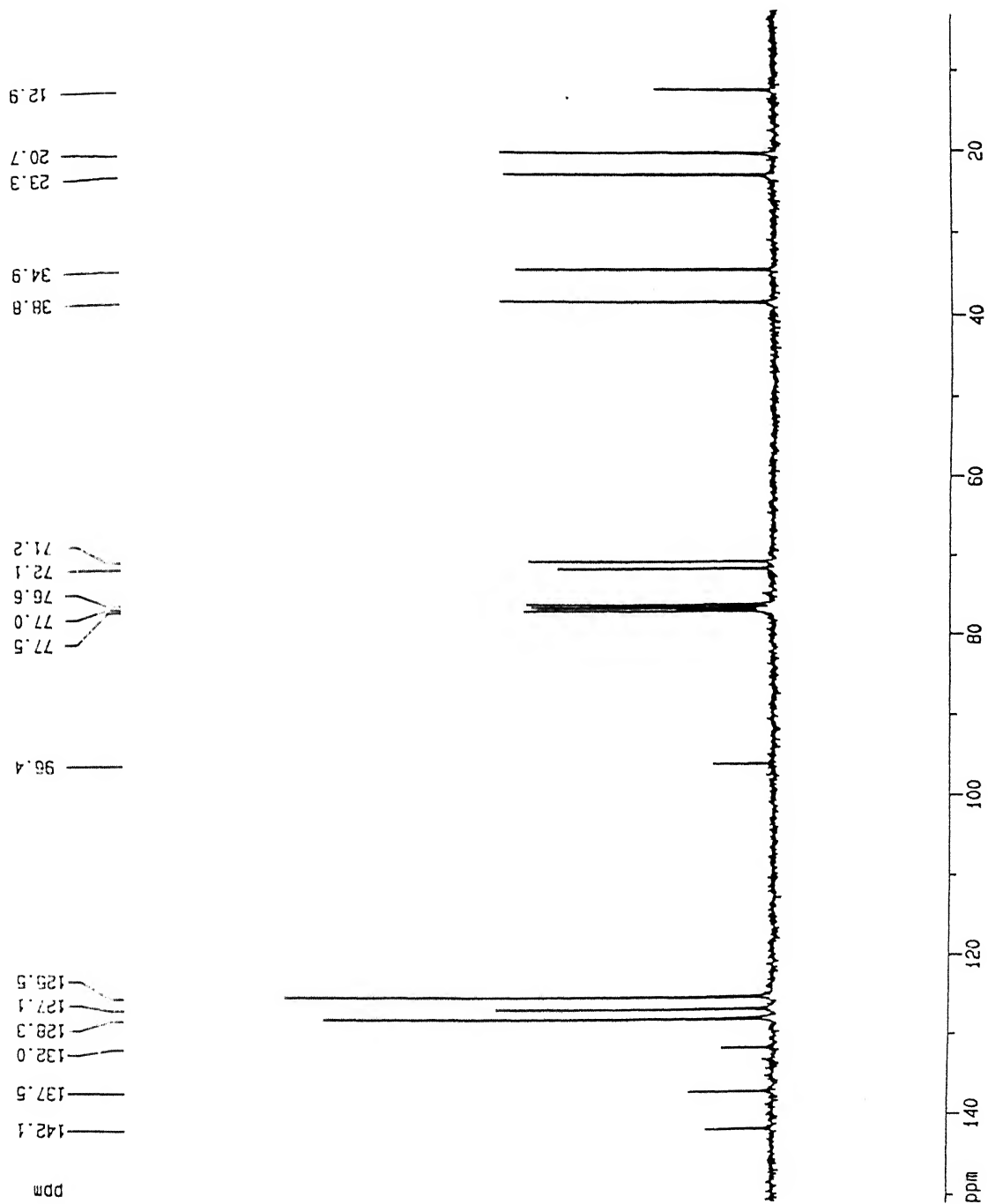
Figure 2.12: 300 MHz  $^1\text{H}$  NMR spectra of 73, Nu=Ph

Figure 2.13: 75.5 MHz  $^{13}\text{C}$  NMR spectra of 73, Nu=Ph

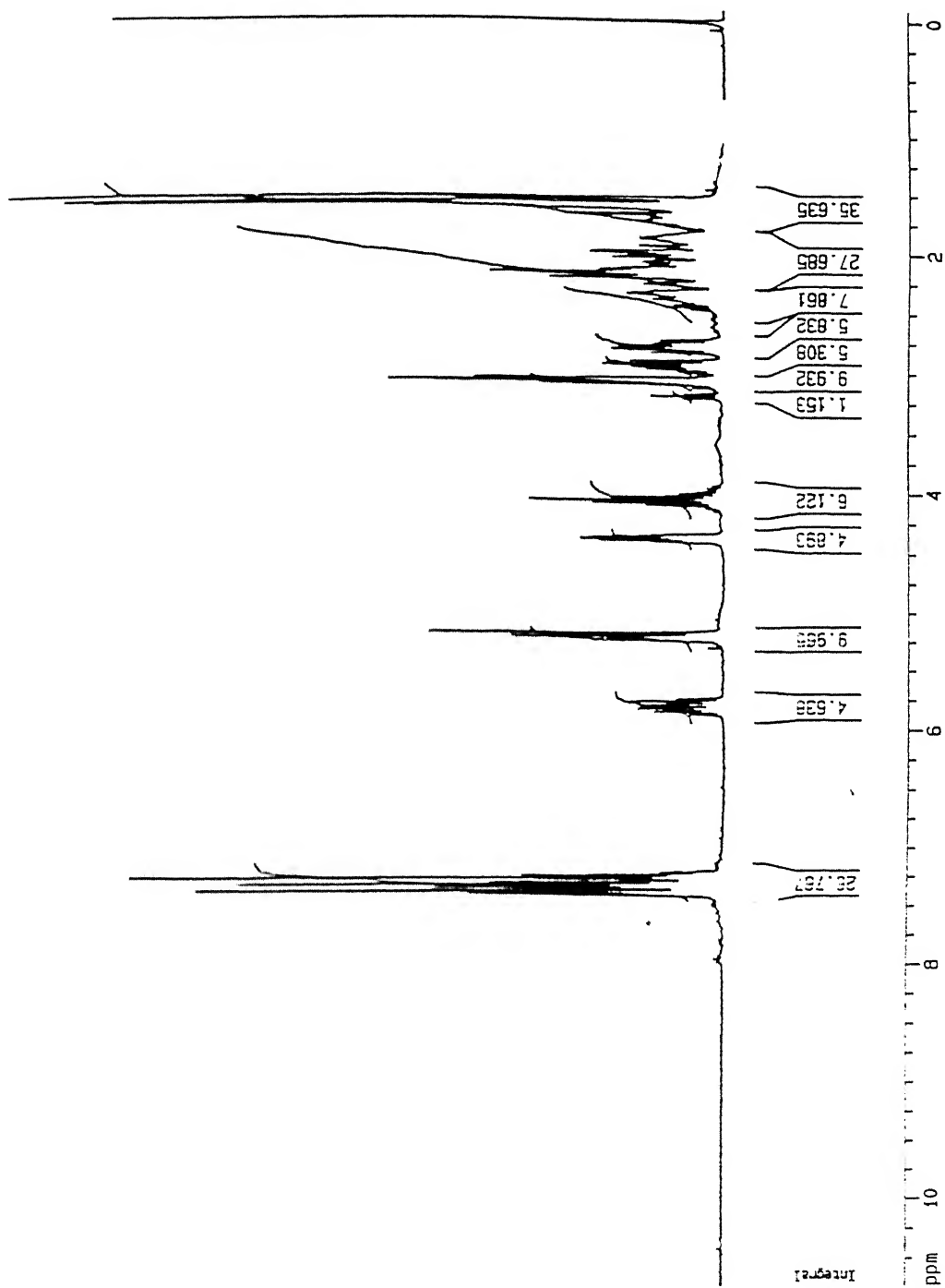
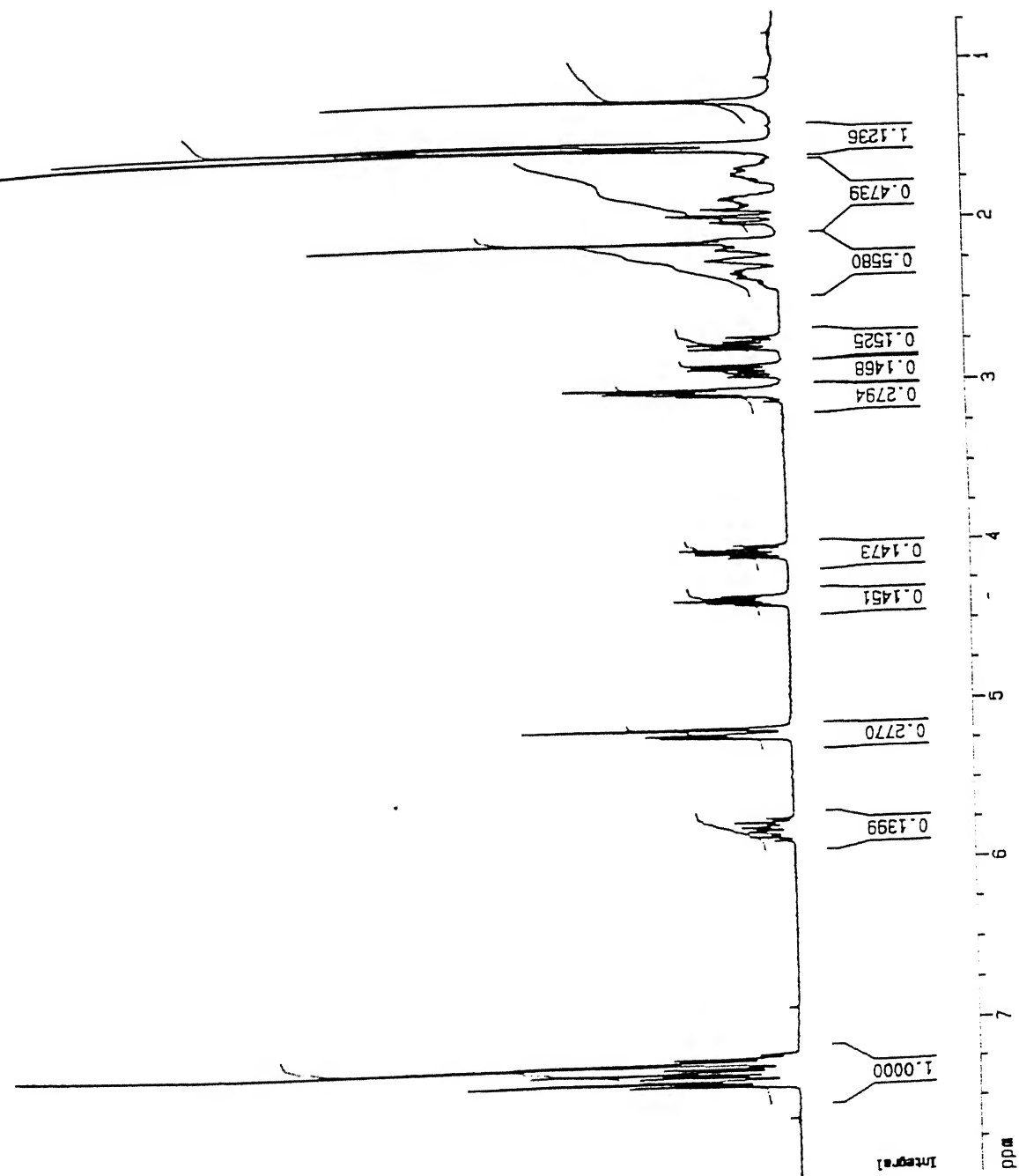
Figure 2.14: 300 MHz  $^1\text{H}$  NMR spectra of 74, Nu=allyl

Figure 2.15: 300 MHz  $^1\text{H}$  NMR spectra of 75, Nu=allyl

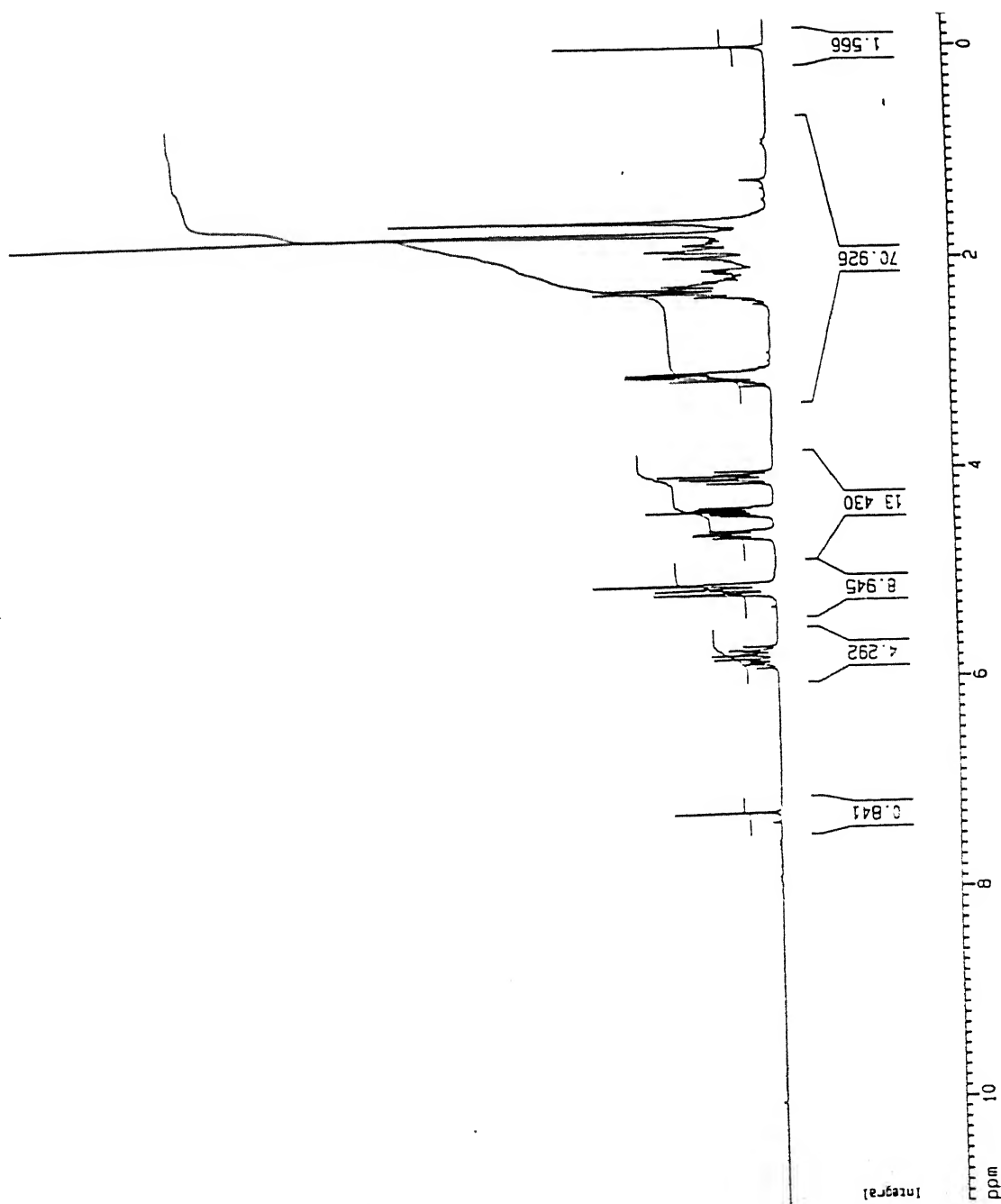


Figure 2.16: 200 MHz  ${}^1\text{H}$  NMR spectra of 72, Nu=allyl

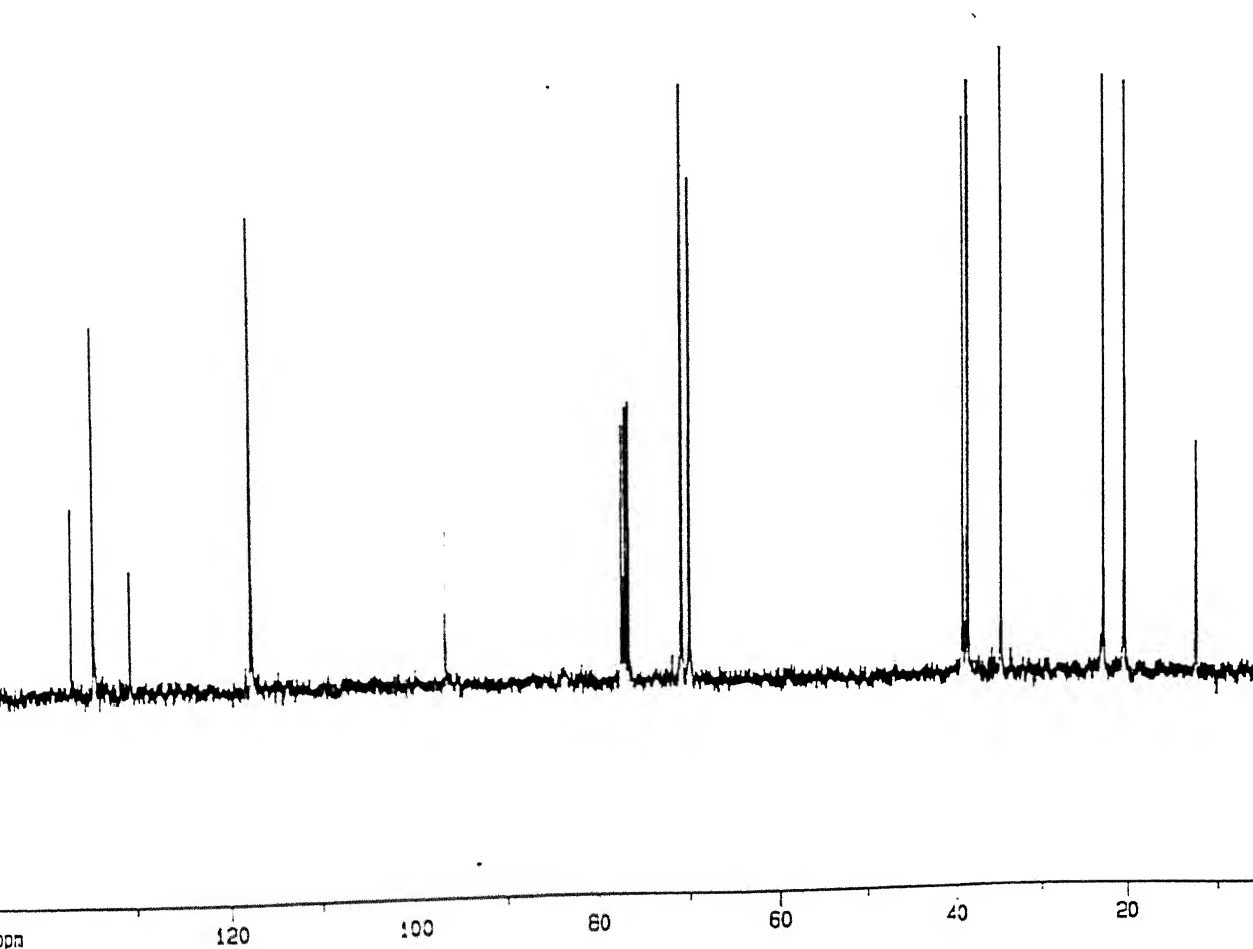


Figure 2.17: 75.5 MHz  $^{13}\text{C}$  NMR spectra of 72, Nu=allyl



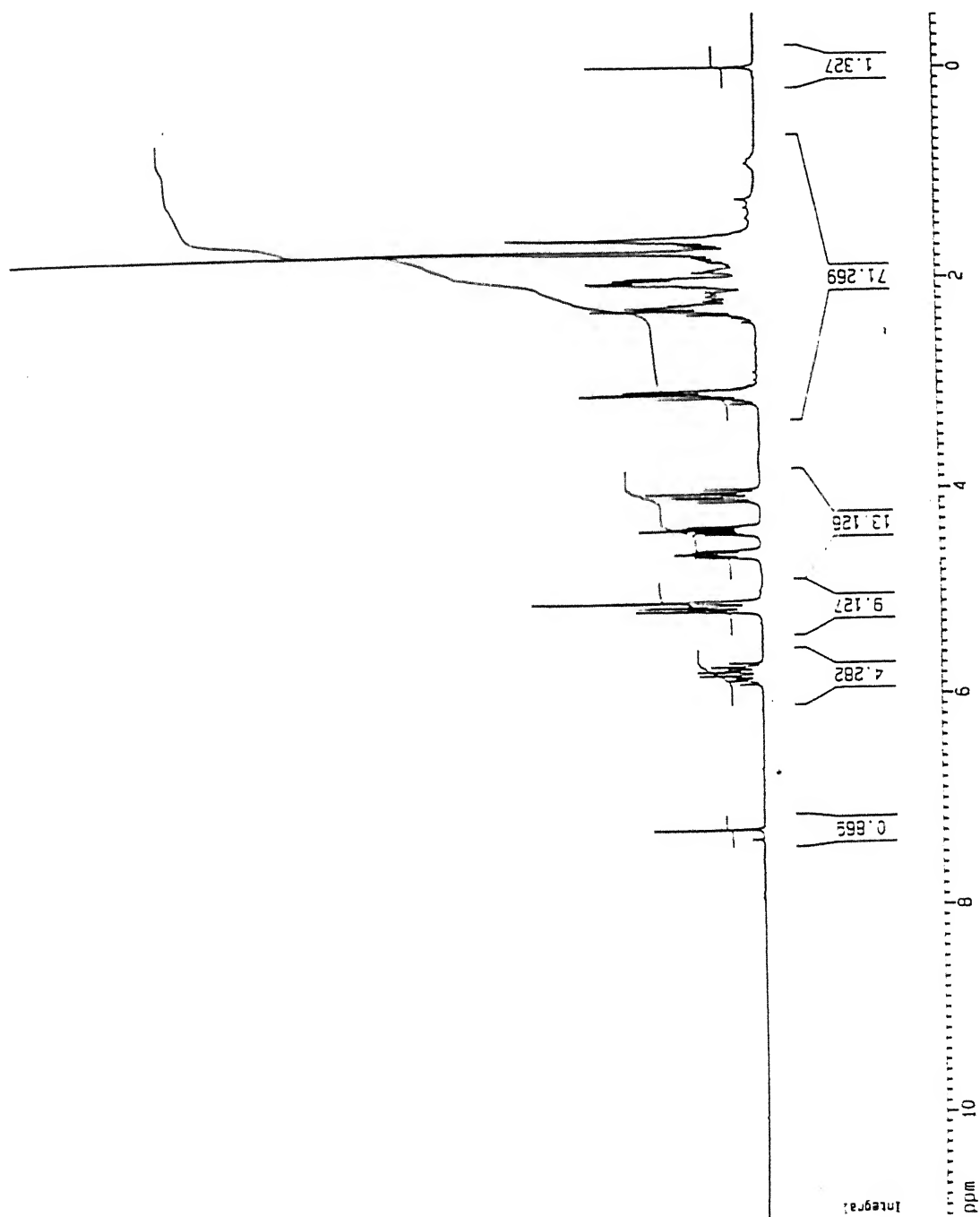


Figure 2.18: 200 MHz  $^1\text{H}$  NMR spectra of 73, Nu=allyl

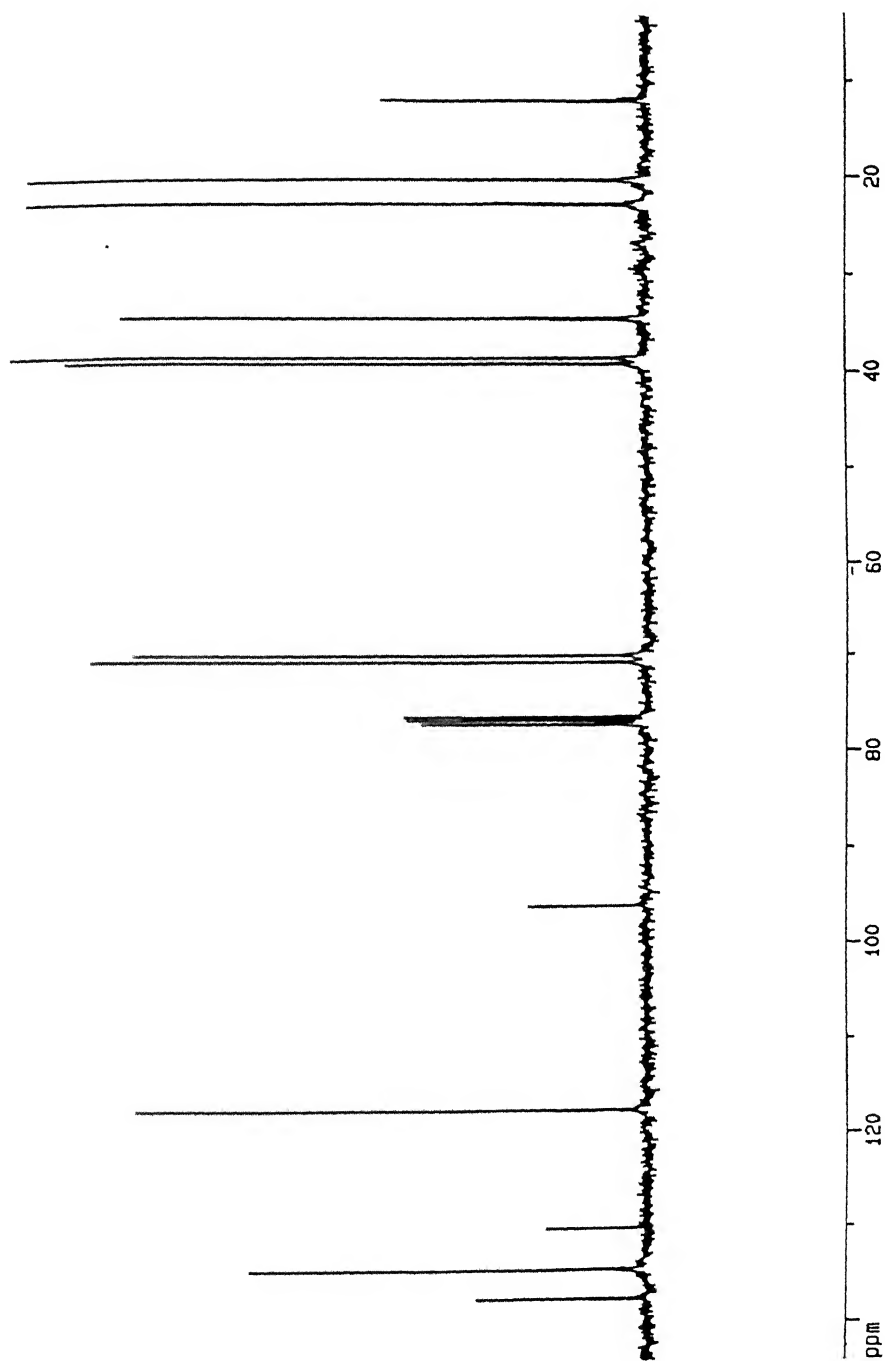


Figure 2.19: 75.5 MHz  $^{13}\text{C}$  NMR spectra of 73, Nu=allyl

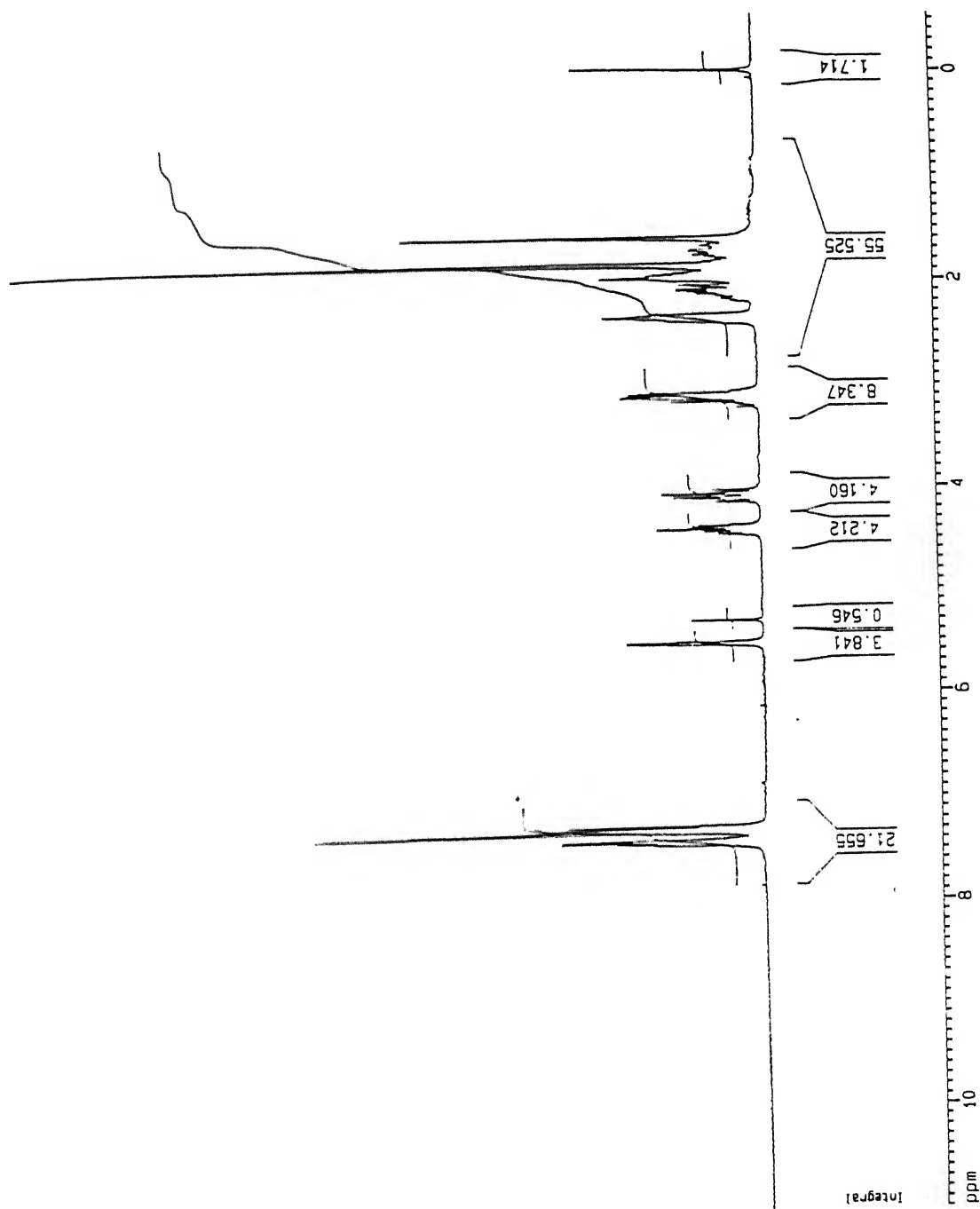


Figure 2.20: 200 MHz  $^1\text{H}$  NMR spectra of 72, Nu=CCPh

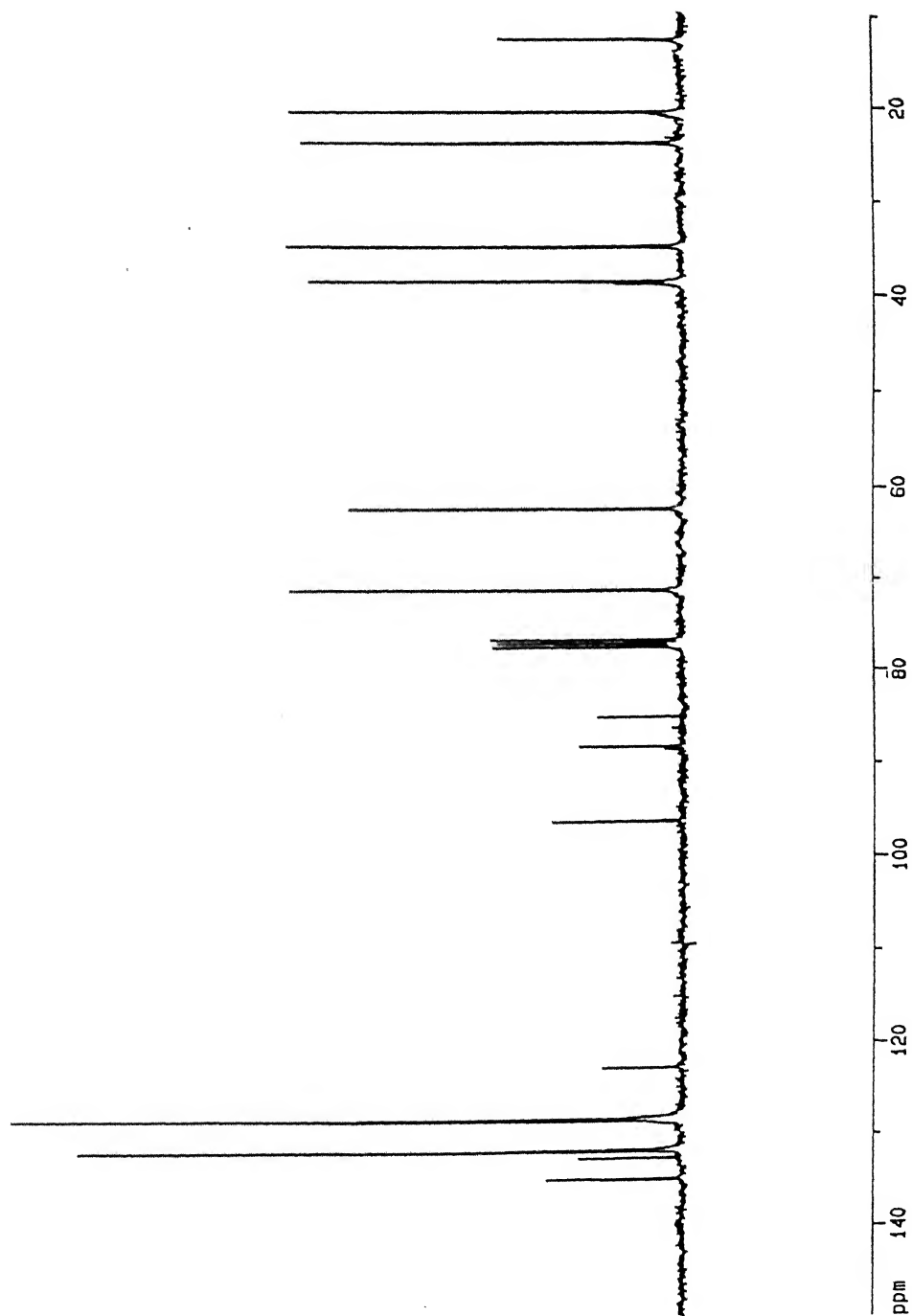


Figure 2.21: 75.5 MHz  $^{13}\text{C}$  NMR spectra of 72, Nu=CCPh

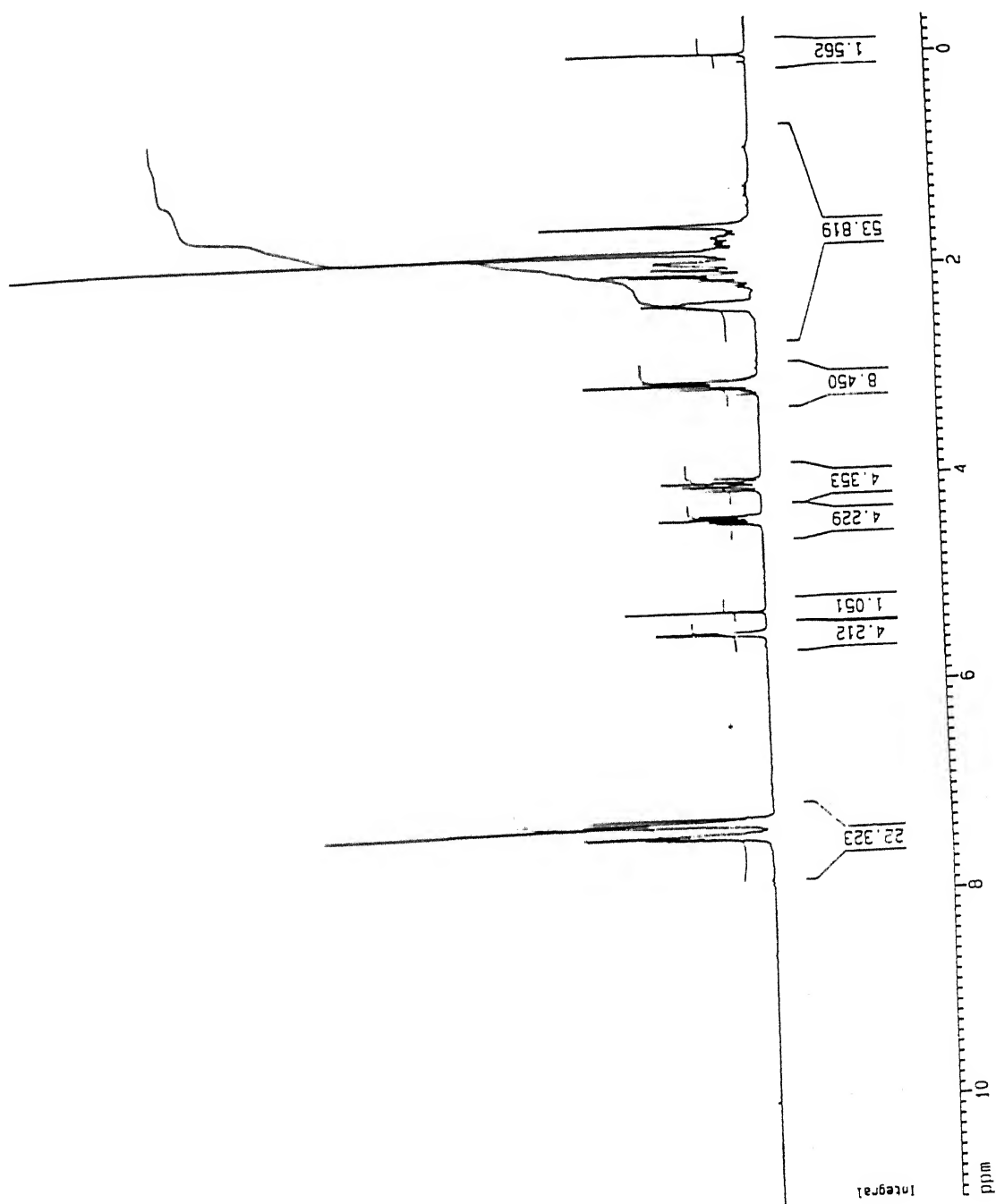


Figure 2.22: 200 MHz  $^1\text{H}$  NMR spectra of 73, Nu=CCPh

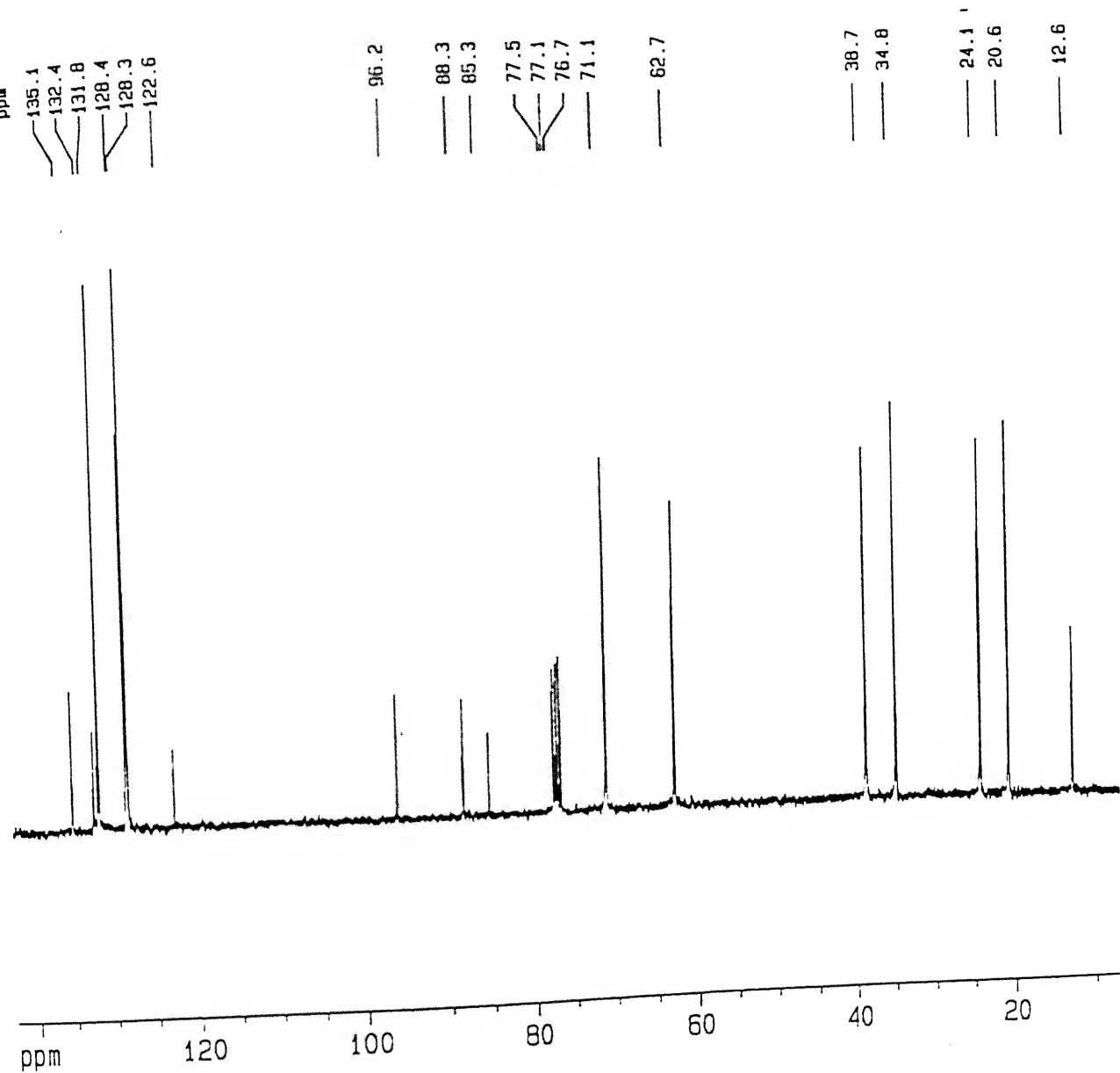
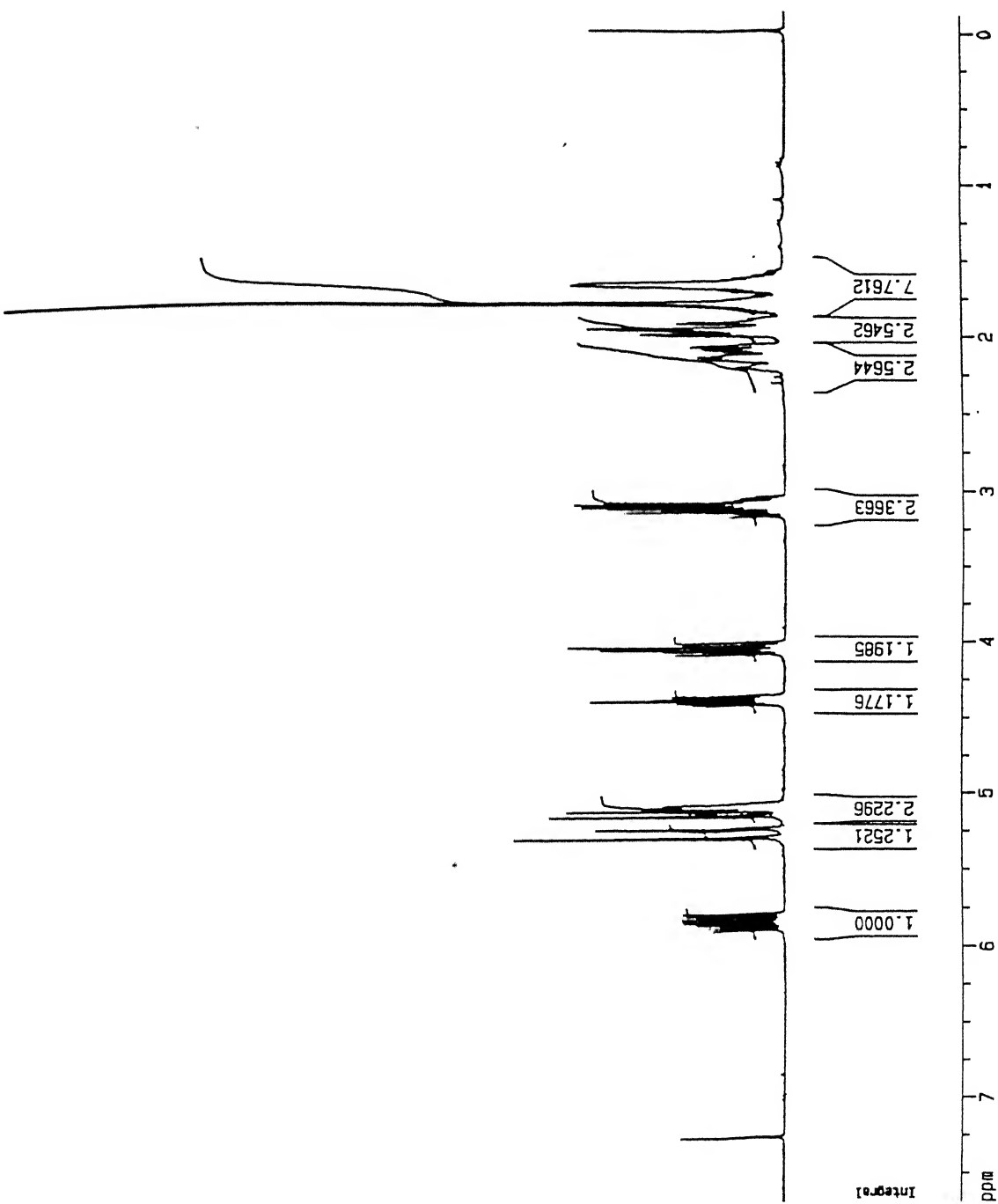


Figure 2.23: 75.5 MHz  $^{13}\text{C}$  NMR spectra of **73**, Nu=CCPh

Figure 2.2-4: 300 MHz  $^1\text{H}$  NMR spectra of **72**, Nu=vinyl

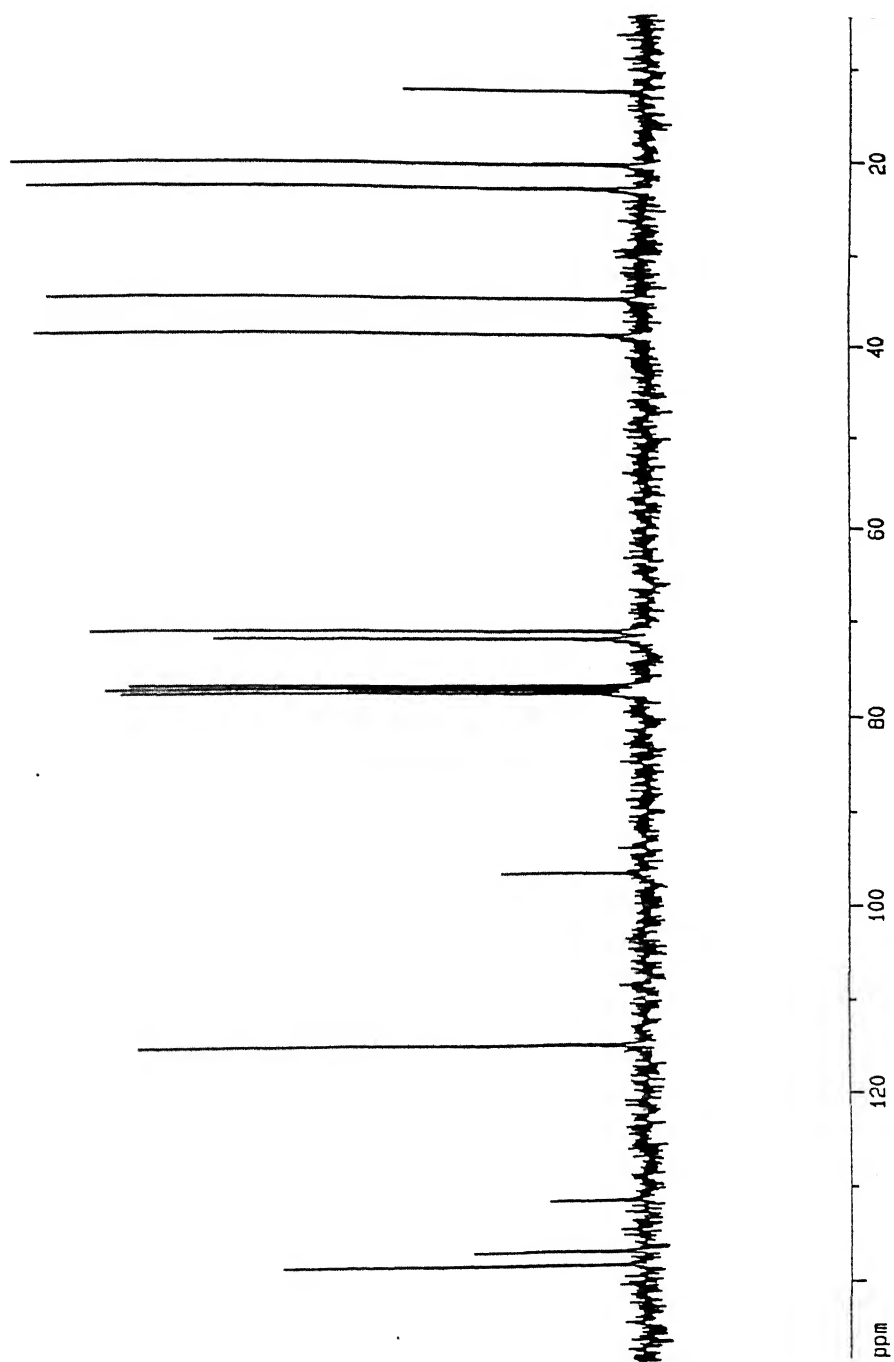
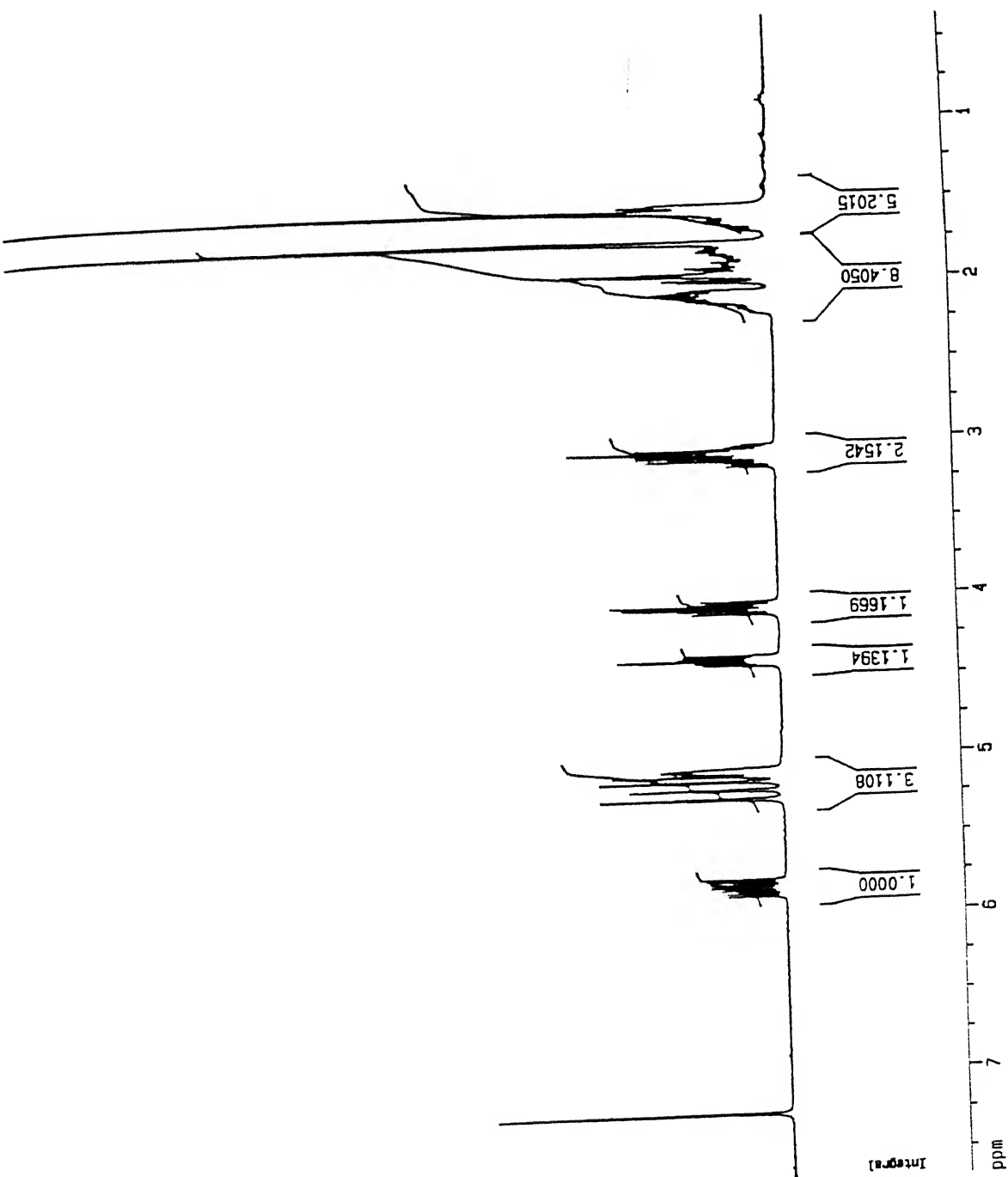


Figure 2.25: 75.5 MHz  $^{13}\text{C}$  NMR spectra of 72, Nu=vinyl



Figure 2.26: 300 MHz  $^1\text{H}$  NMR spectra of 73, Nu=vinyl

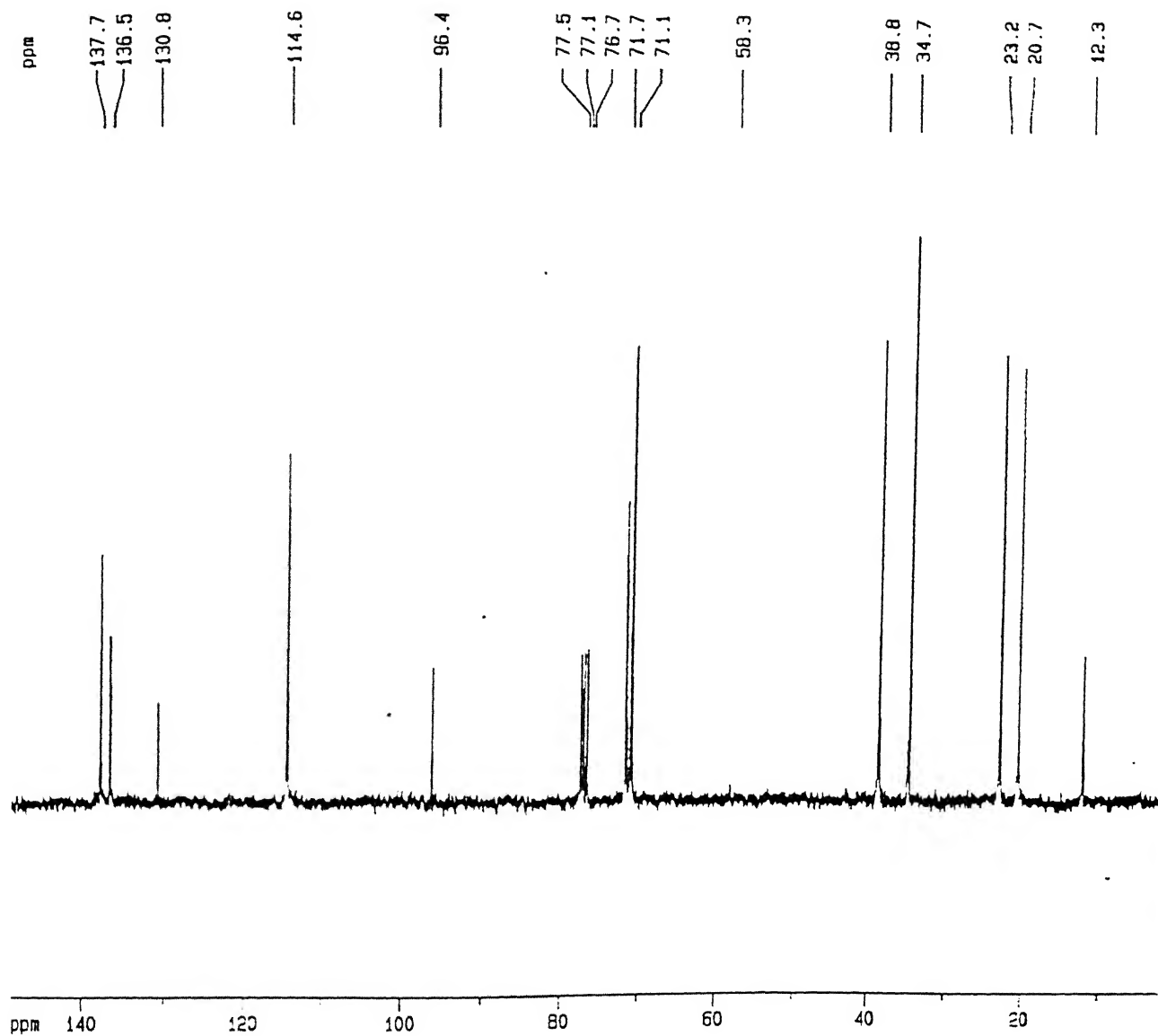


Figure 2.27: 75.5 MHz  $^{13}\text{C}$  NMR spectra of 73. Nu=vinyl

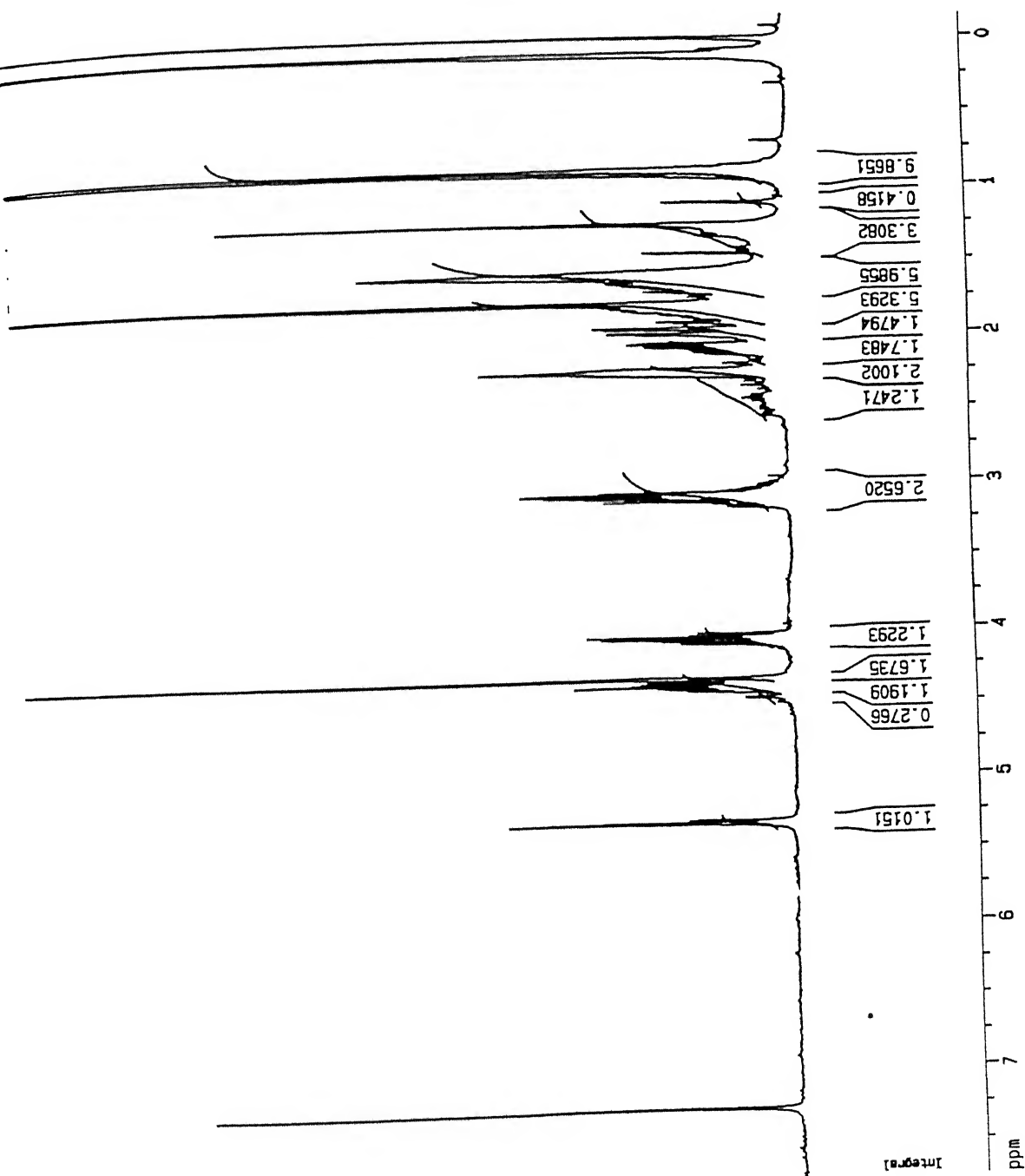
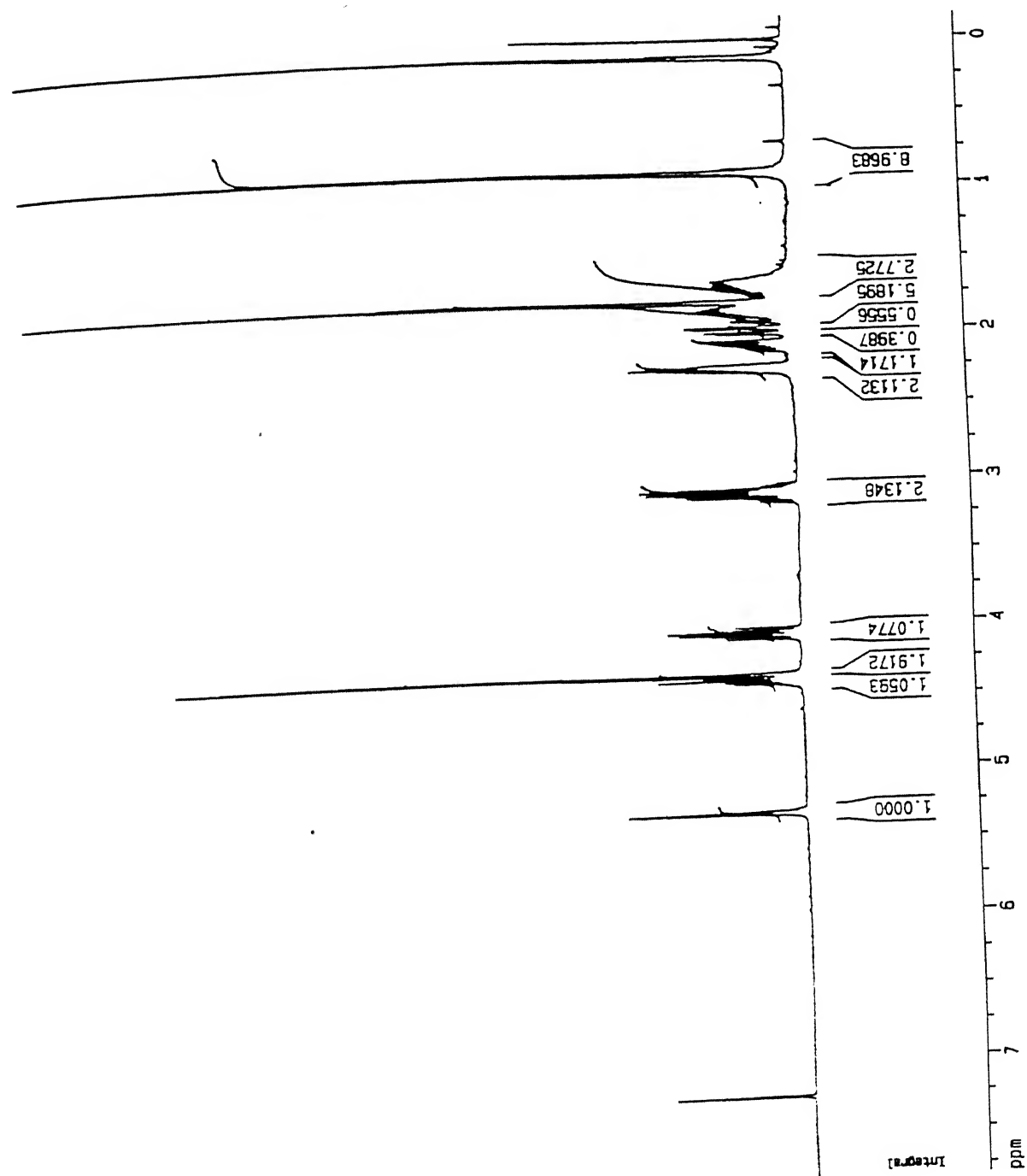
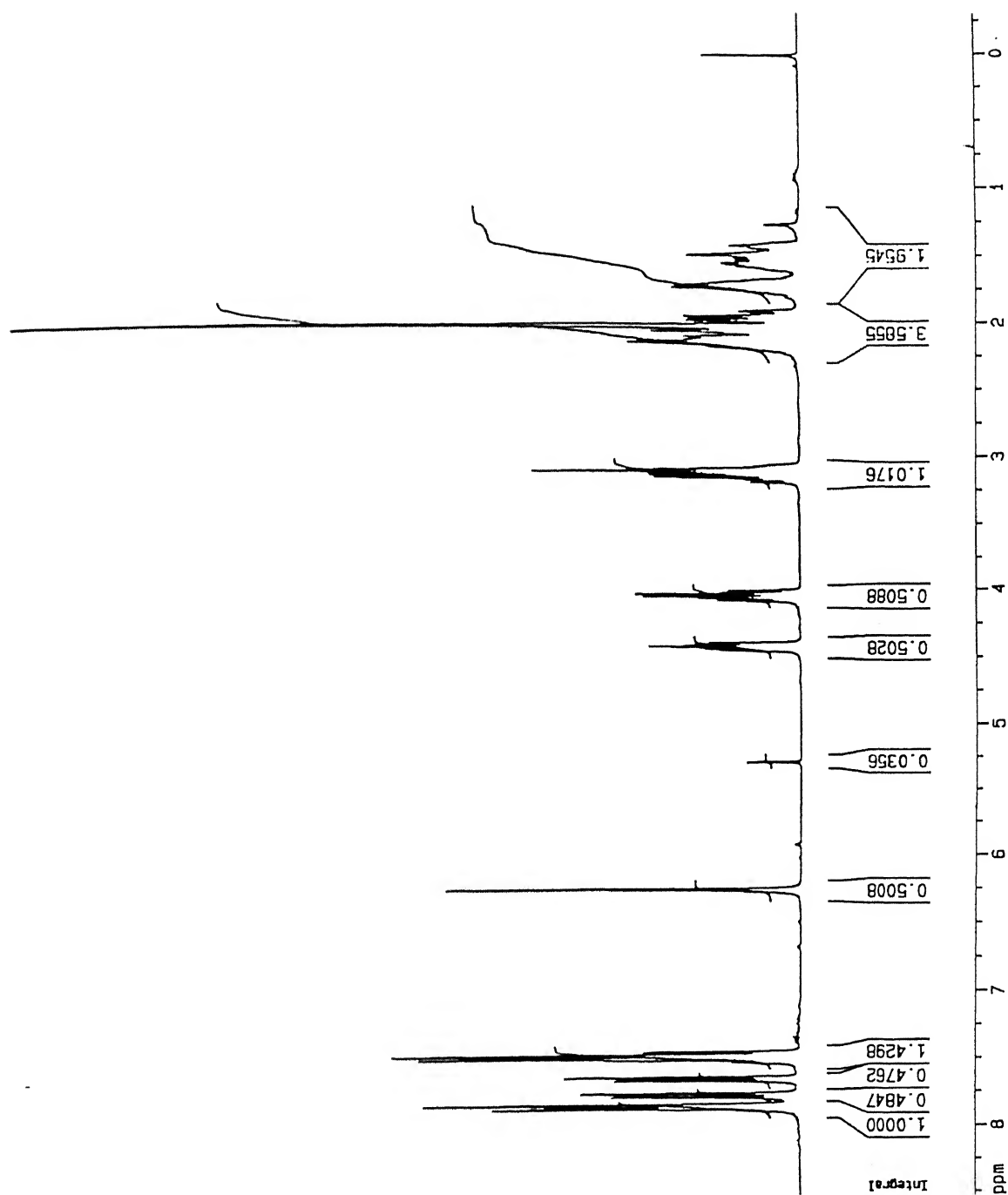
Figure 2.28: 300 MHz  $^1\text{H}$  NMR spectra of 72,  $\text{Nu}=\text{CCCH}_2\text{OTBDMS}$ 

Figure 2.29: 300 MHz  $^1\text{H}$  NMR spectra of 73,  $\text{Nu}=\text{CCCH}_2\text{OTBDMS}$ 

Figure 2.30: 300 MHz  $^1\text{H}$  NMR spectra of 73, Nu=naphthyl

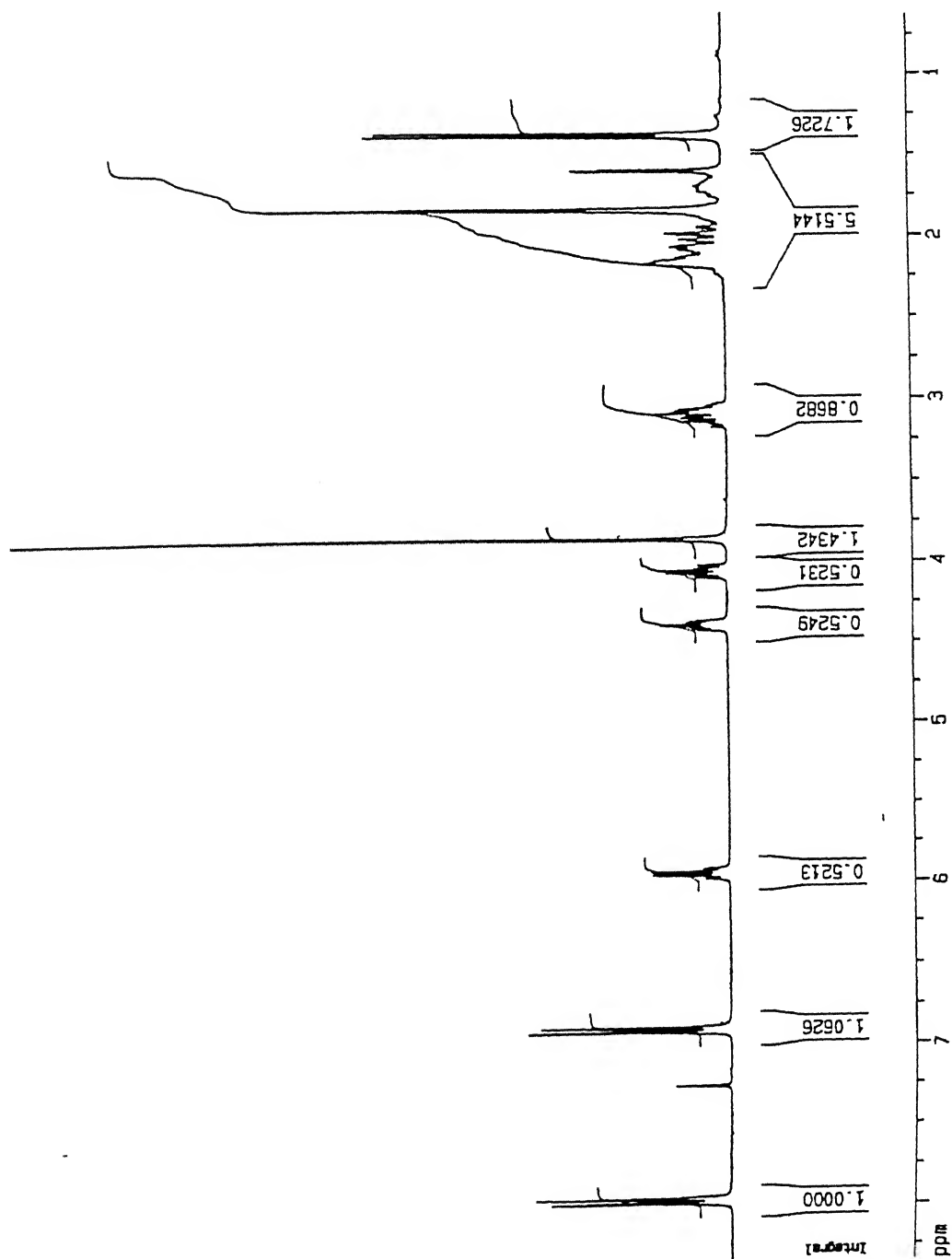
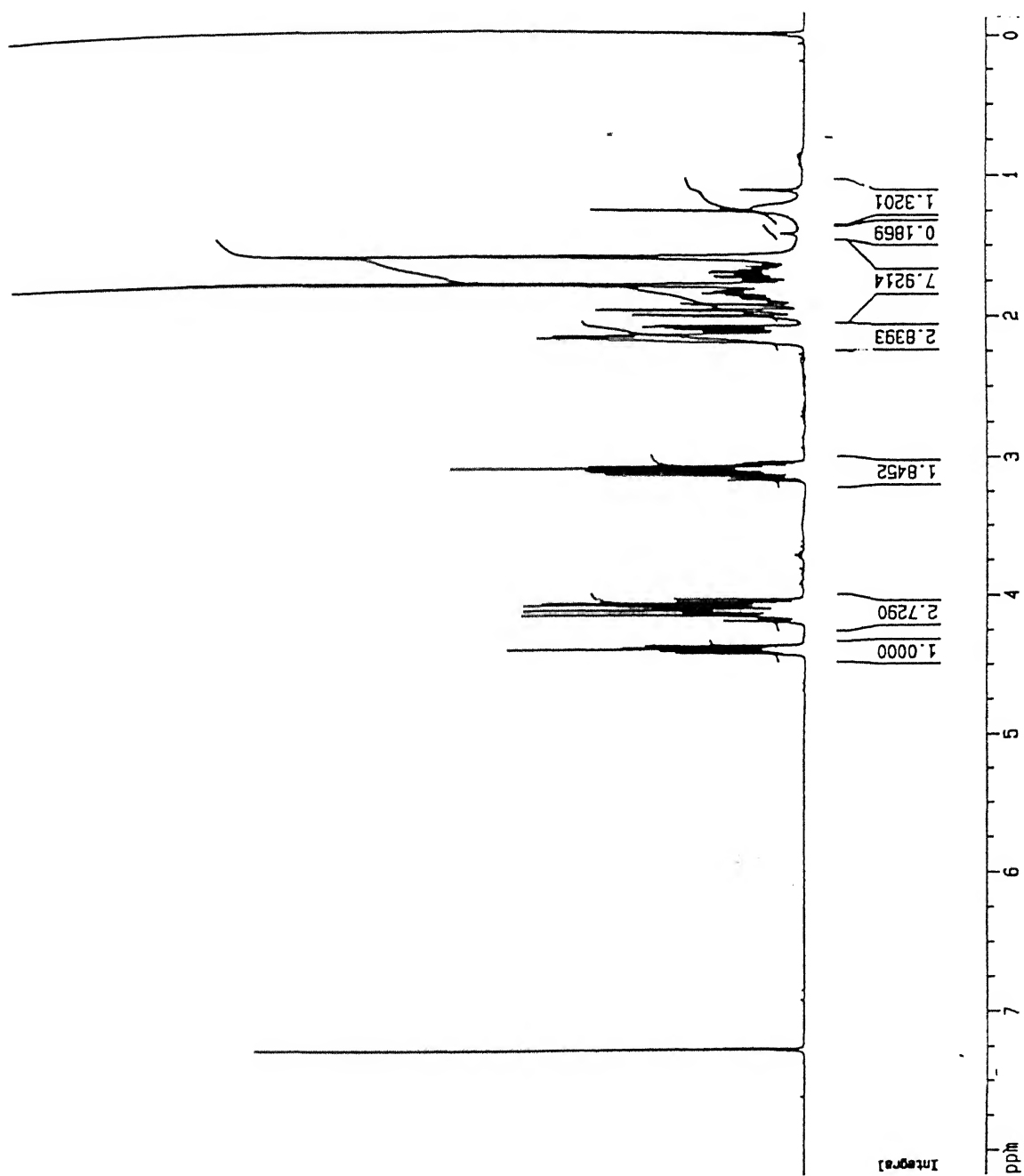
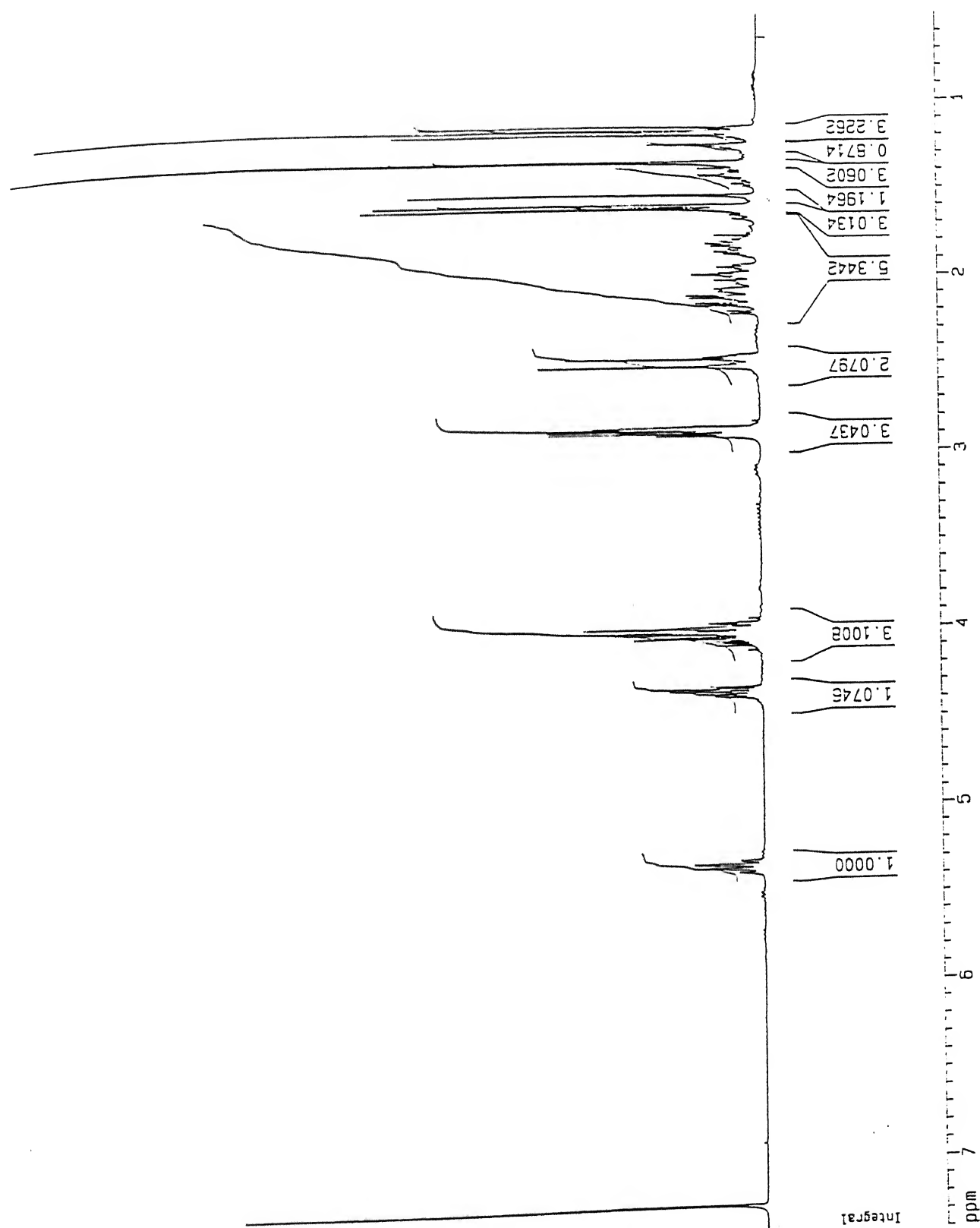
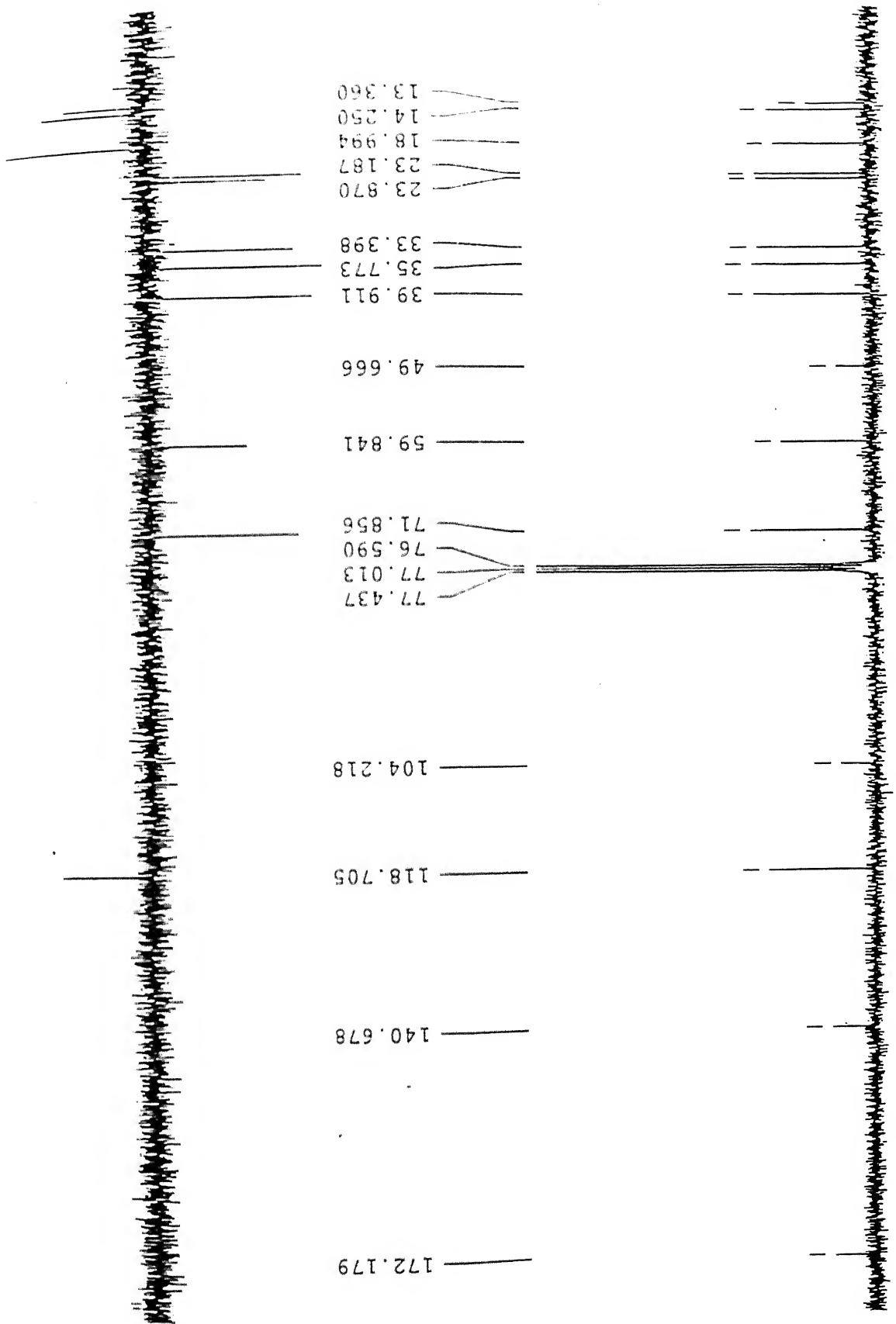
Figure 2.31: 300 MHz  $^1\text{H}$  NMR spectra of 76

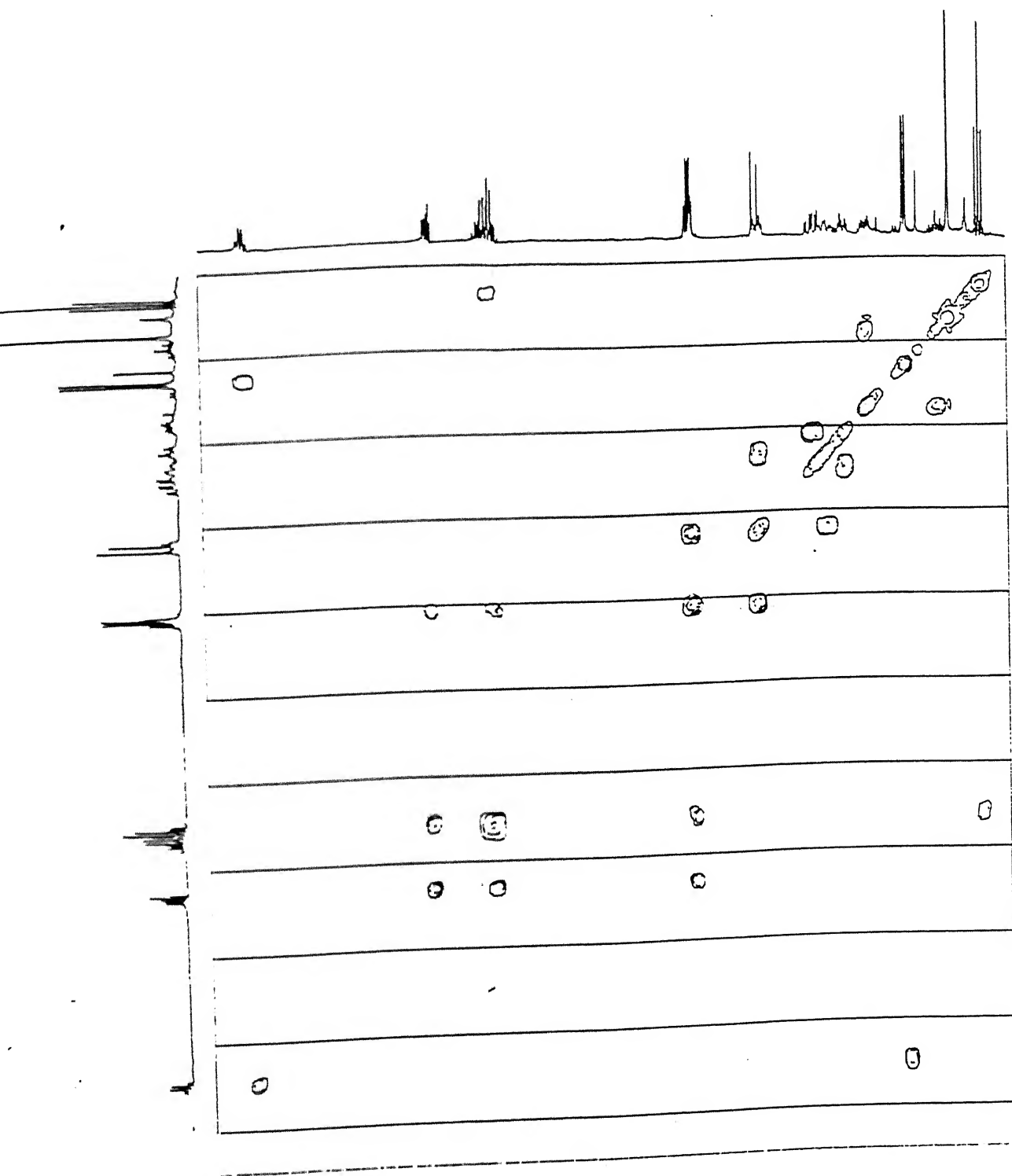
Figure 2.32: 300 MHz  $^1\text{H}$  NMR spectra of 80

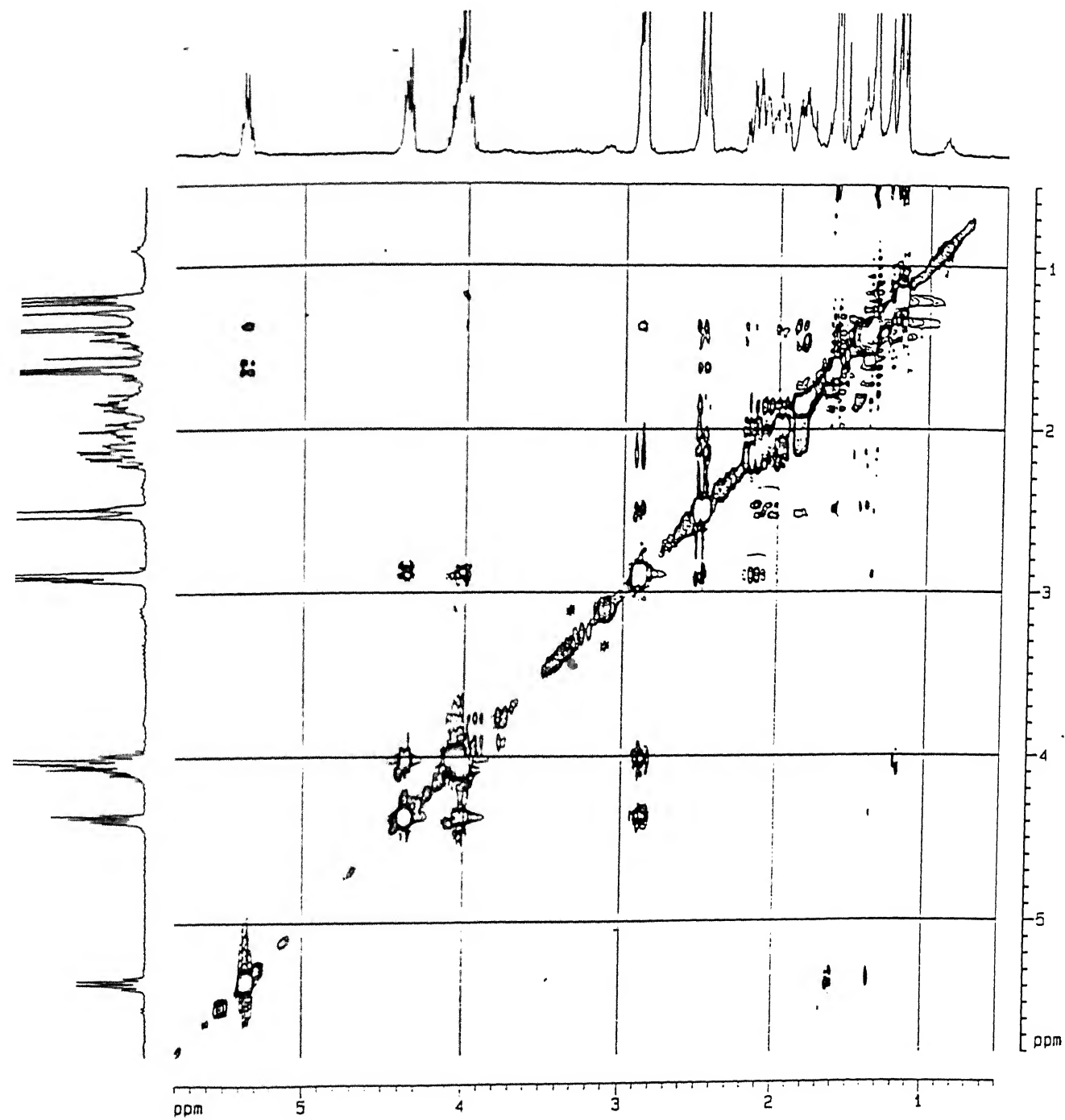
Figure 2.33: 300 MHz  $^1\text{H}$  NMR spectra of 81, R=Me



191 wdd 10 20 30 40 50 60 70 80 90 100 110 120 130 140 150 160 170







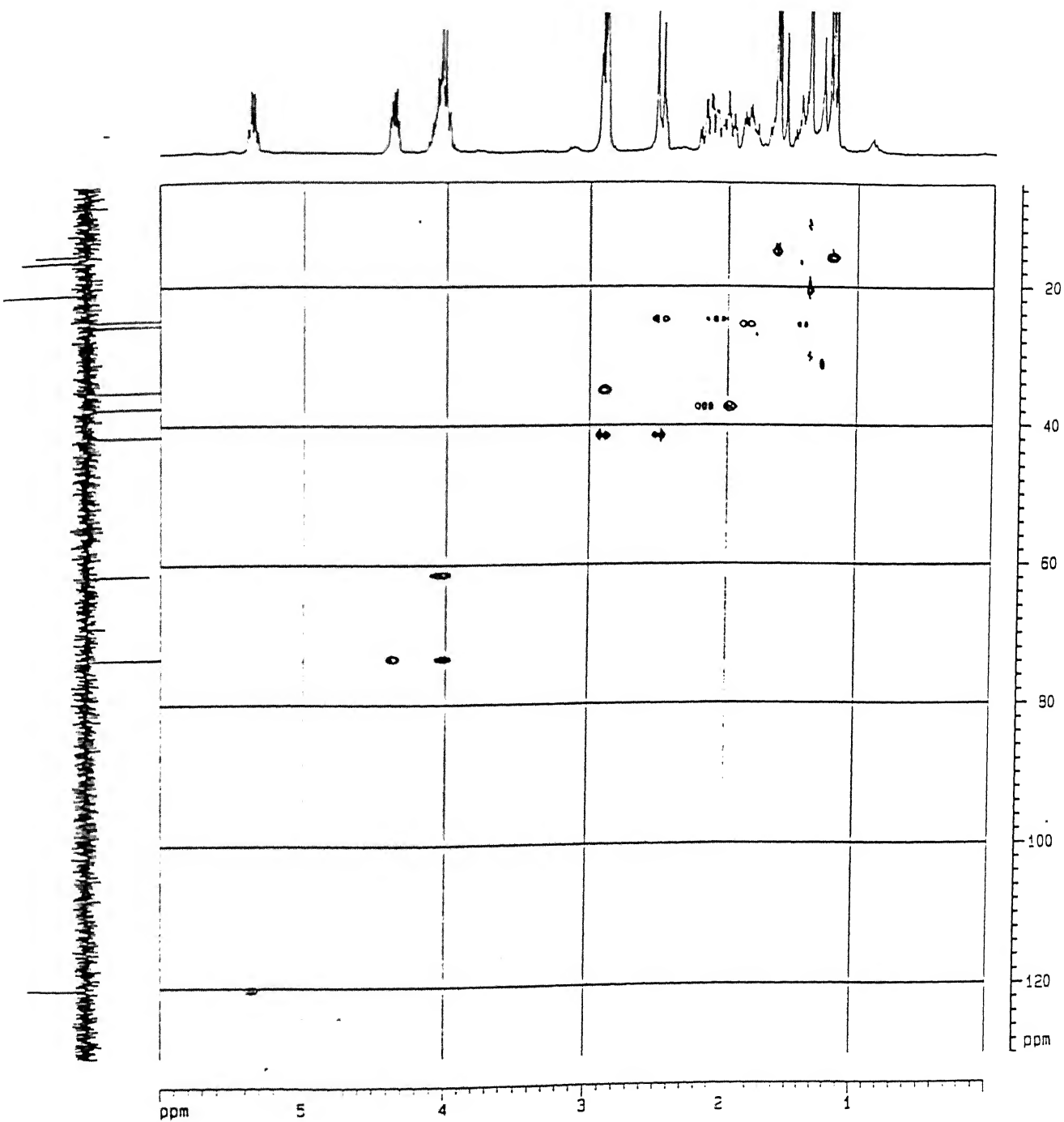


Figure 2.37: 300 MHz HMQC spectra of 81, R=Me

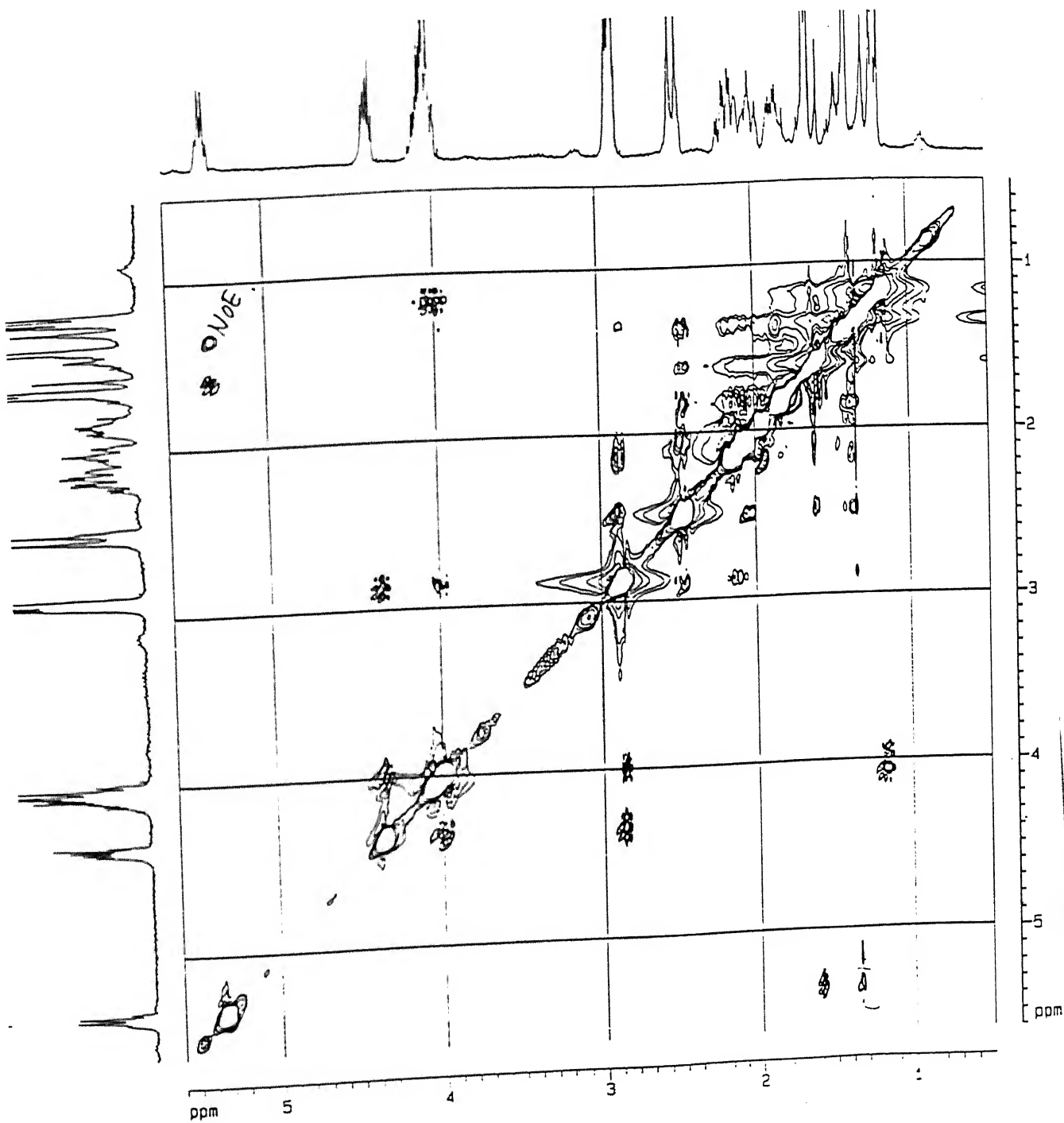
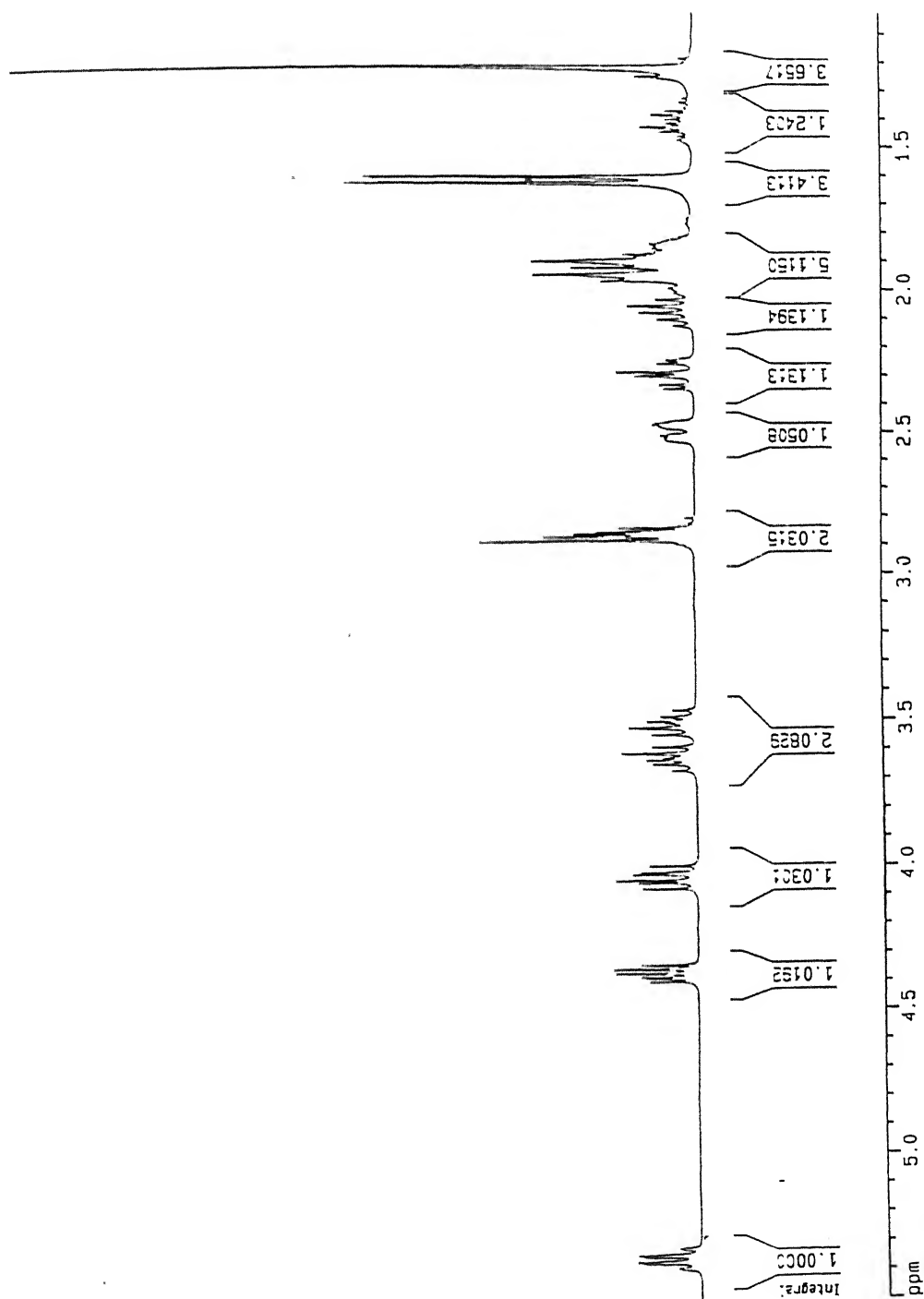
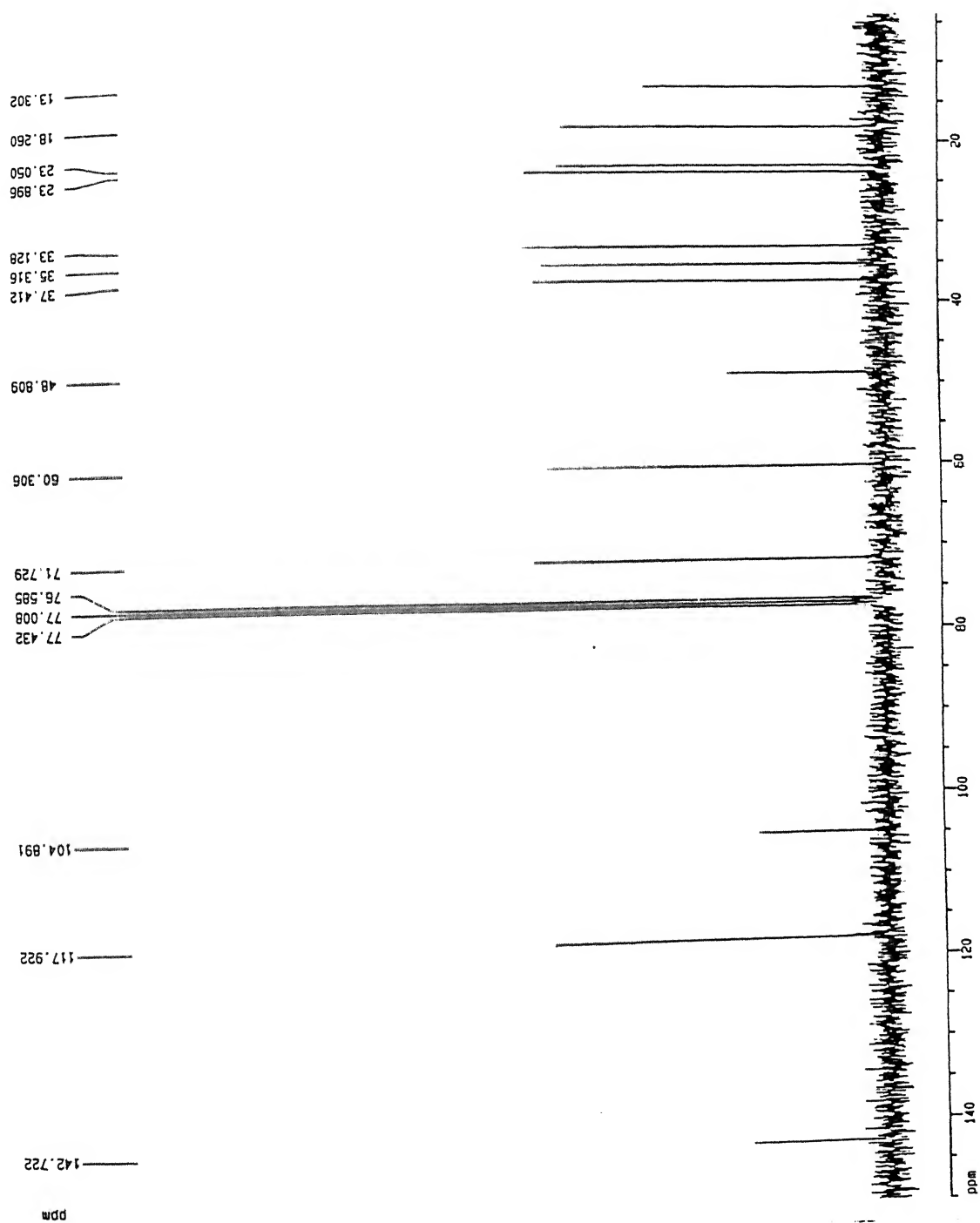


Figure 2.38: 300 MHz NOESY spectra of 81, R=Me

Figure 2.40: 300 MHz  $^1\text{H}$  NMR spectra of 82, R=Me

Figure 2,41: 75.5 MHz  $^{13}\text{C}$  NMR spectra of 82, R=Me

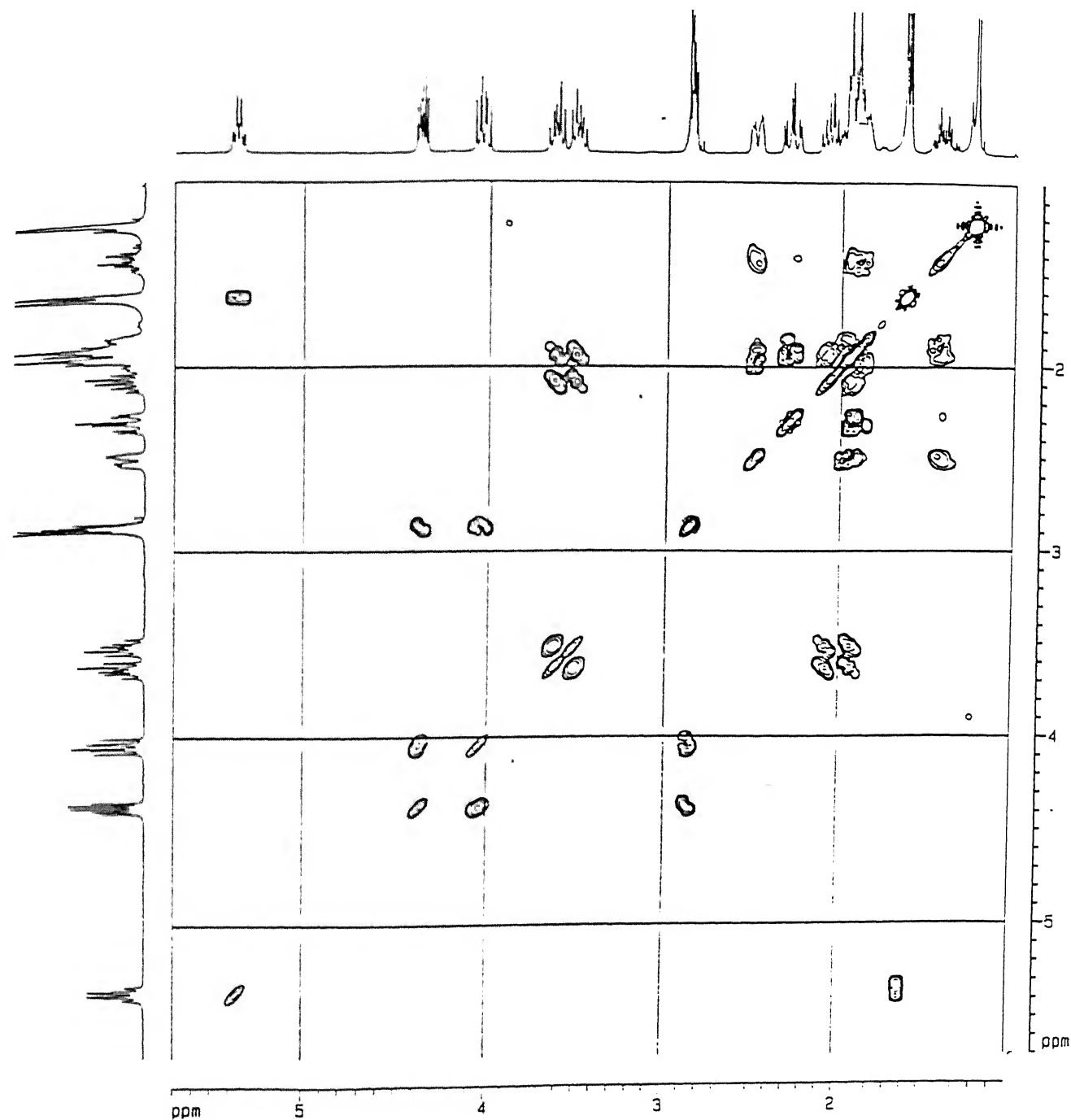


Figure 2.42: 300 MHz COSY spectra of 82, R=Me



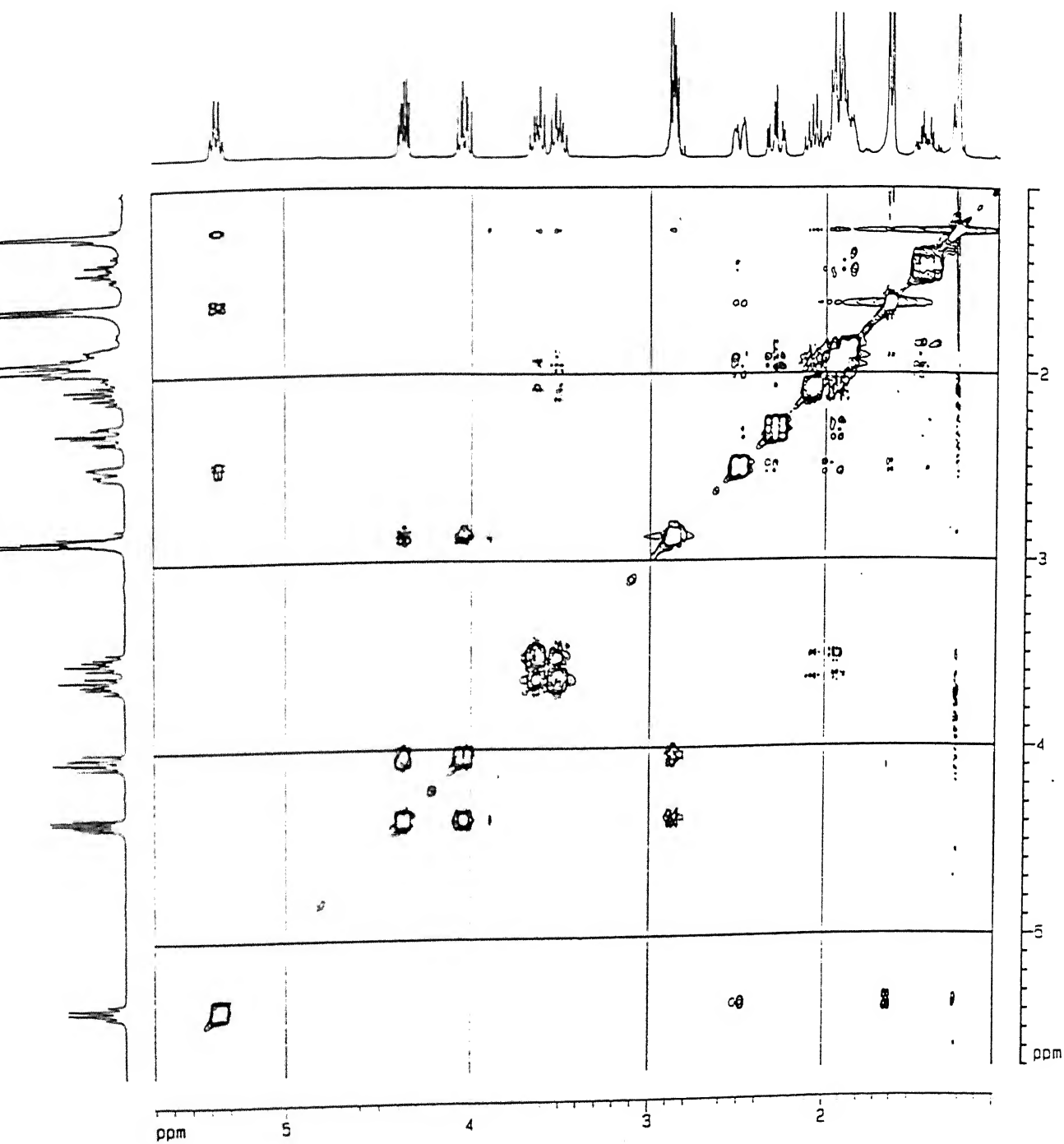


Figure 2.43: 300 MHz ROESY spectra of 82, R=Me

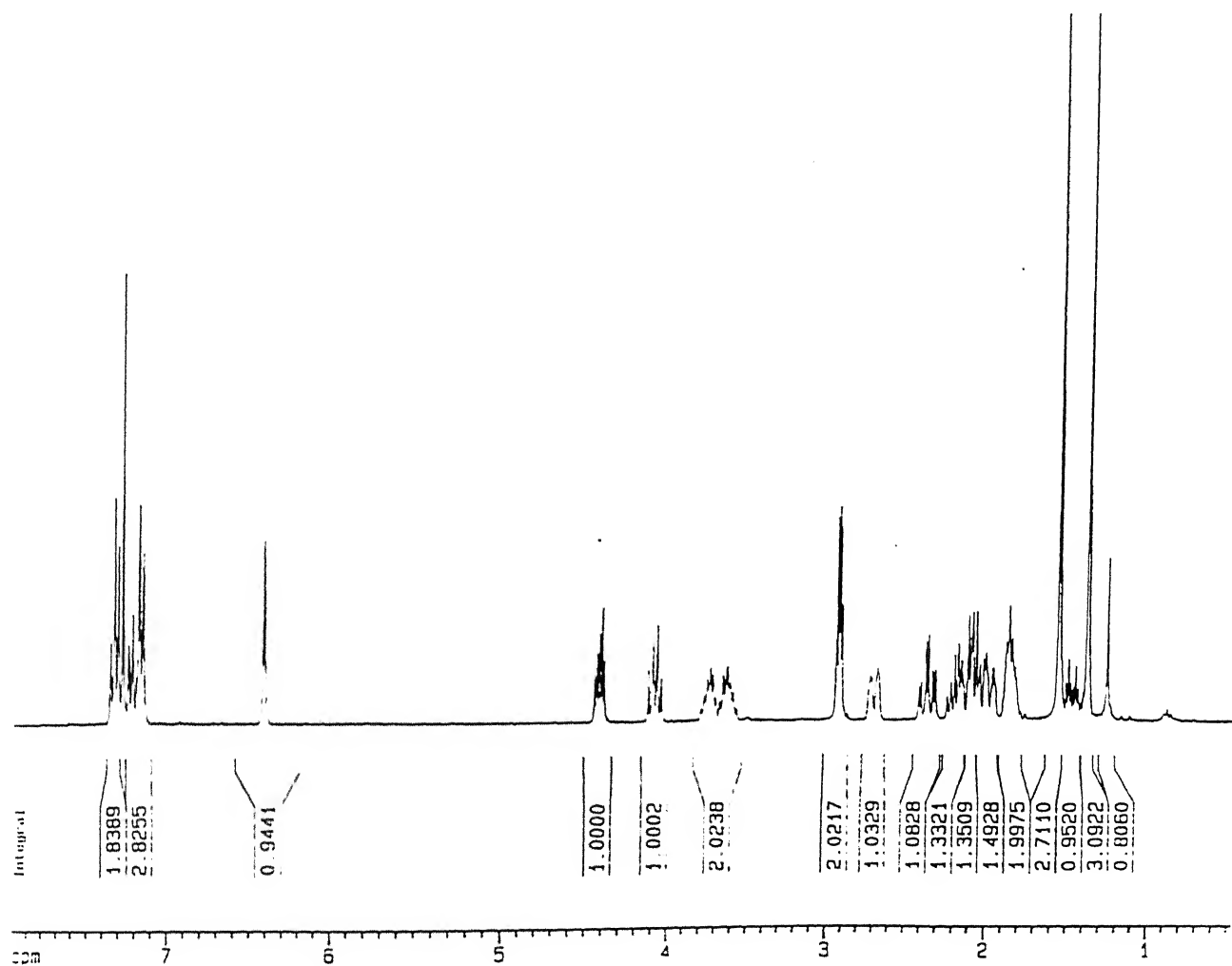


Figure 2.44: 300 MHz  $^1\text{H}$  NMR spectra of **82**,  $\text{R}=\text{Ph}$

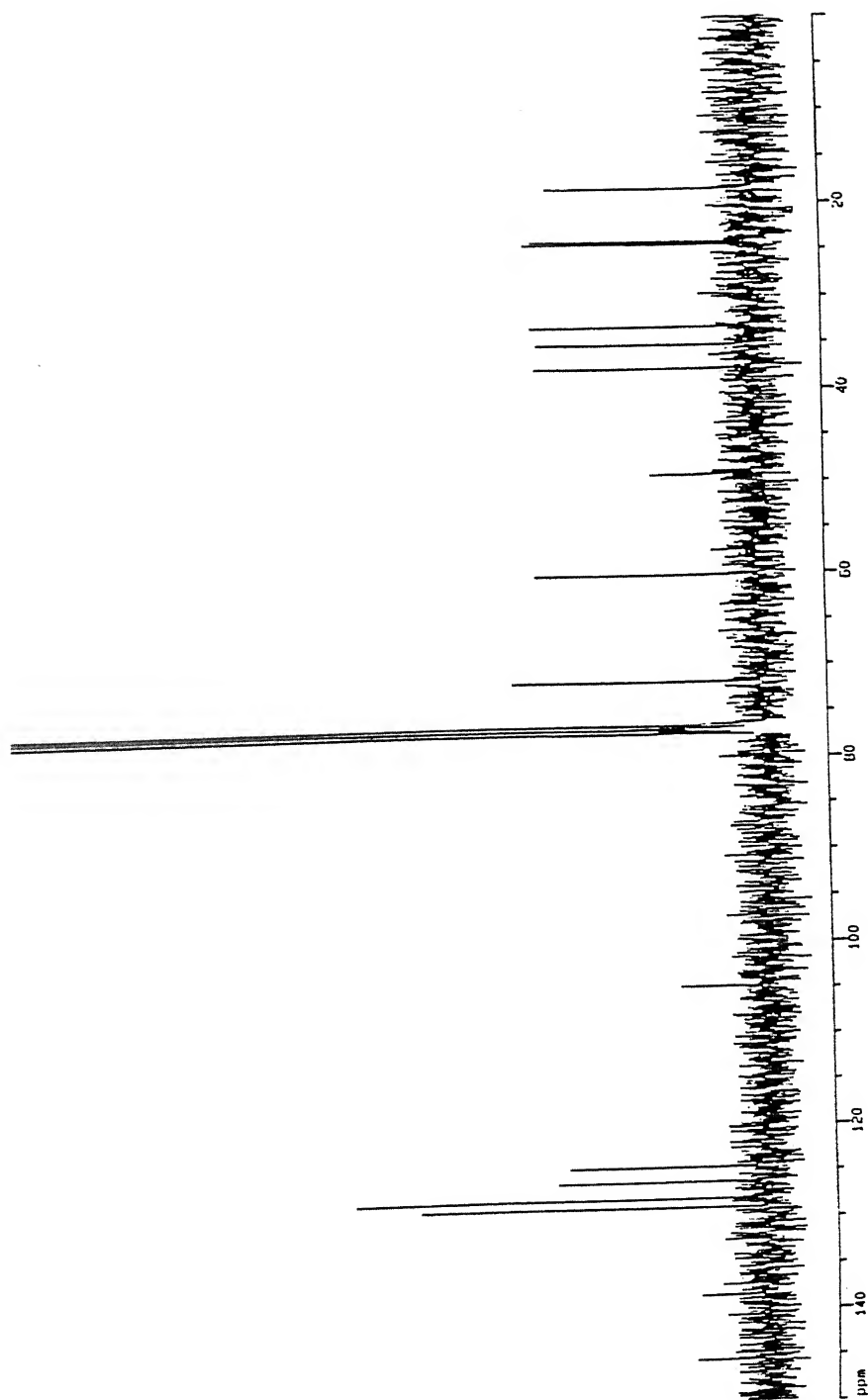


Figure 2.15: 75.5 MHz  $^{13}\text{C}$  NMR spectra of 82,  $\text{R}=\text{Ph}$

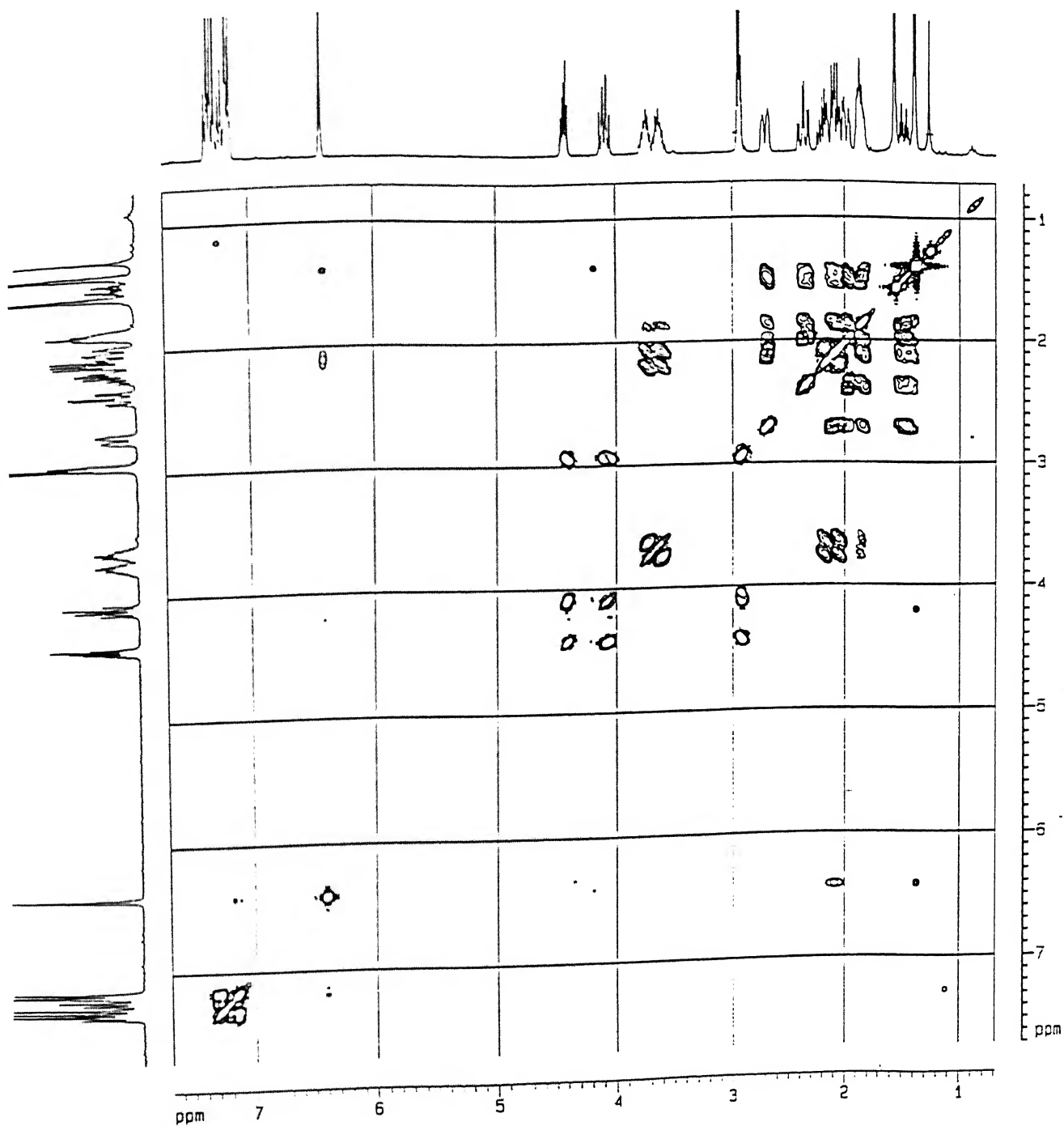


Figure 2.46: 300 MHz COSY spectra of 82, R=Ph

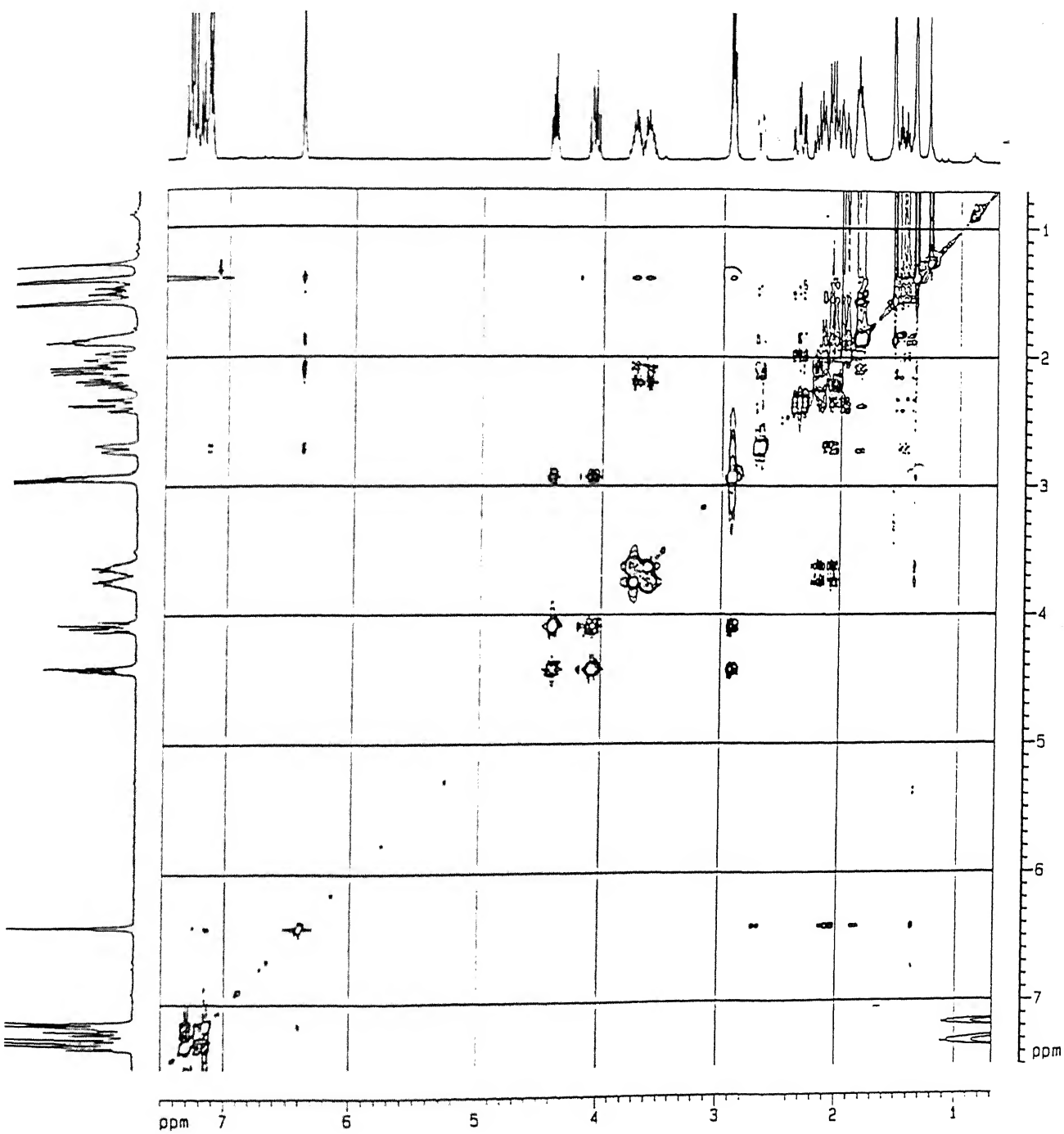
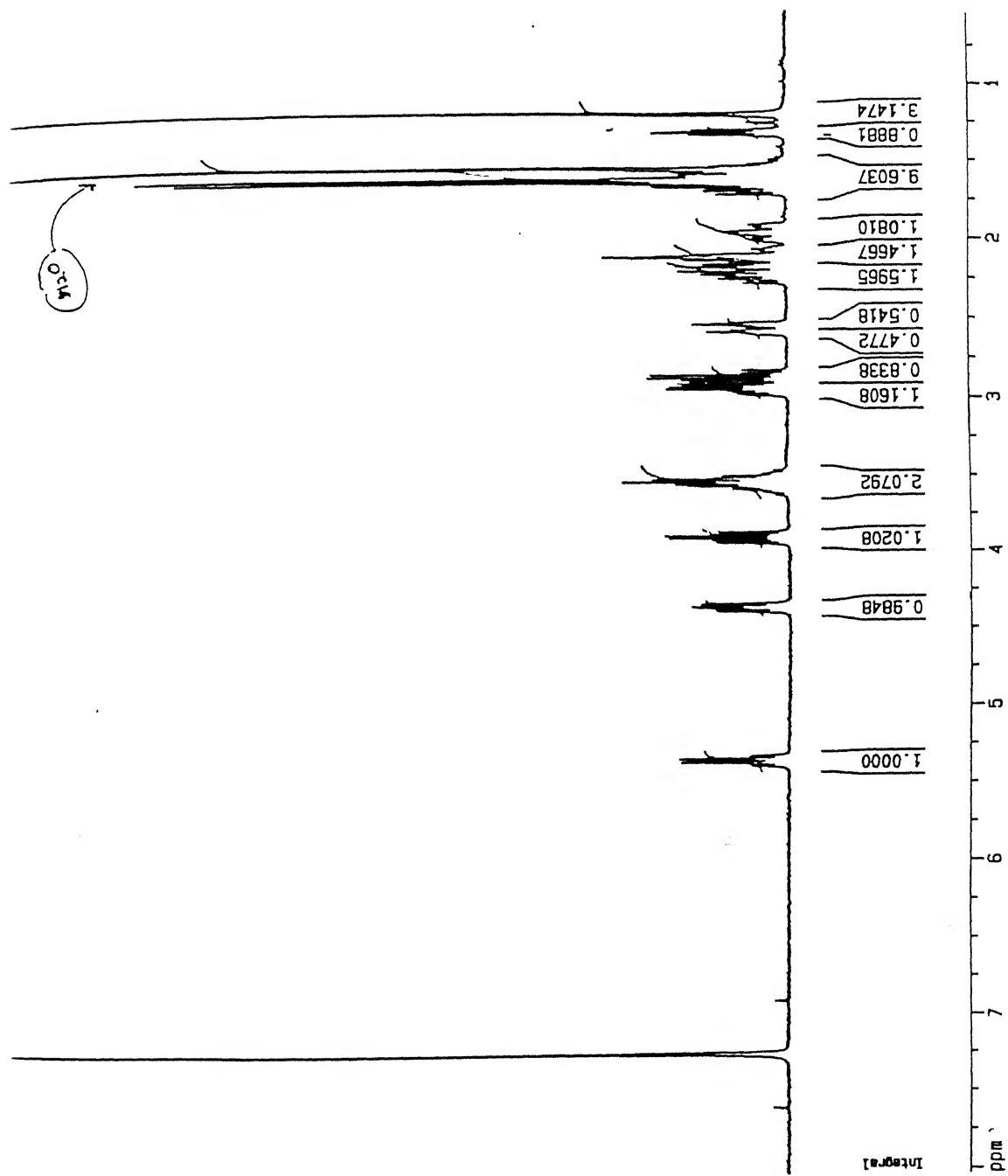
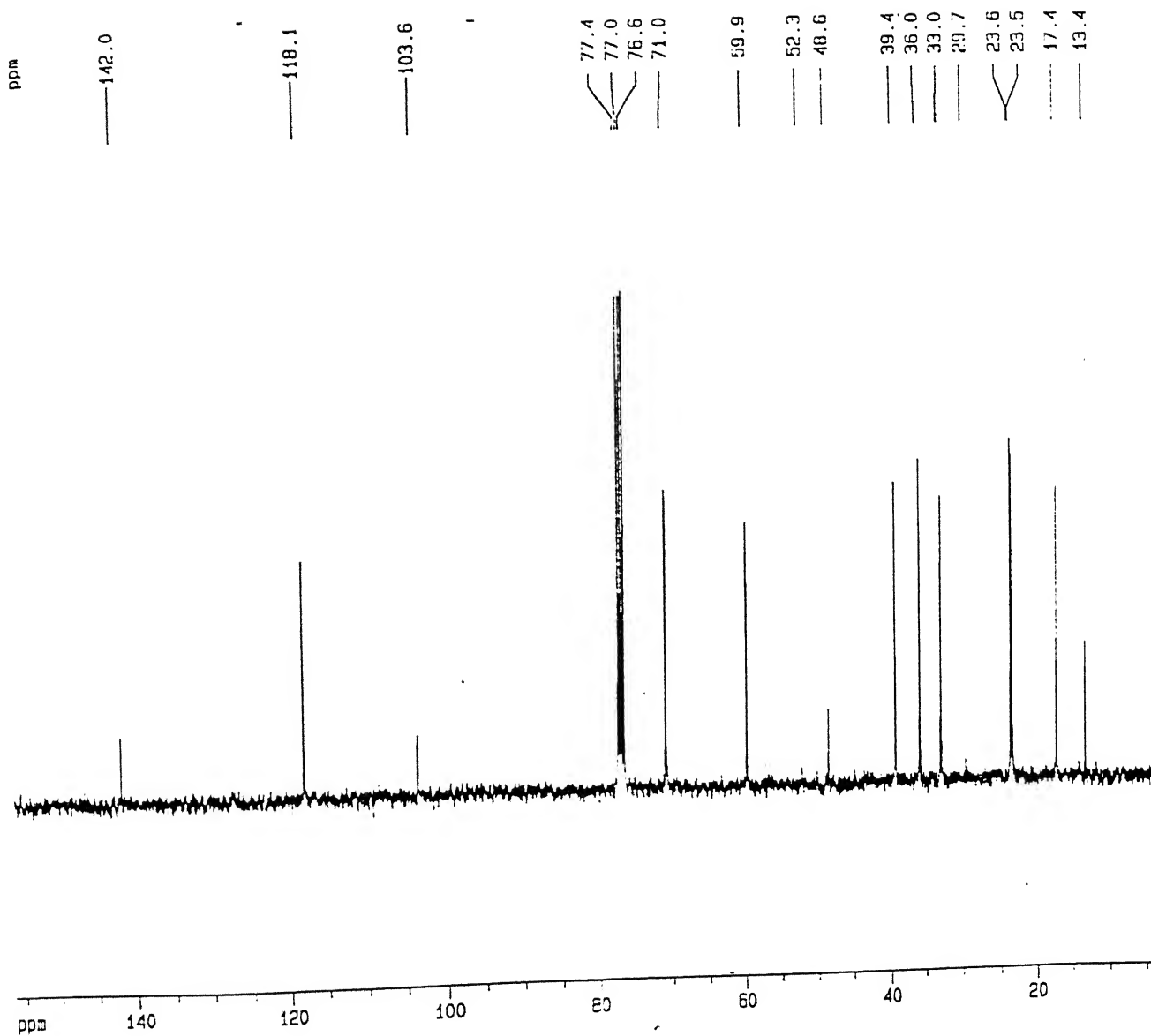


Figure 2.47: 300 MHz ROESY spectra of 82, R=Ph

Figure 2.48: 300 MHz  $^1\text{H}$  NMR spectra of 84,  $\text{R}=\text{Me}$

Figure 2.49: 75.5 MHz  $^{13}\text{C}$  NMR spectra of 84, R=Me

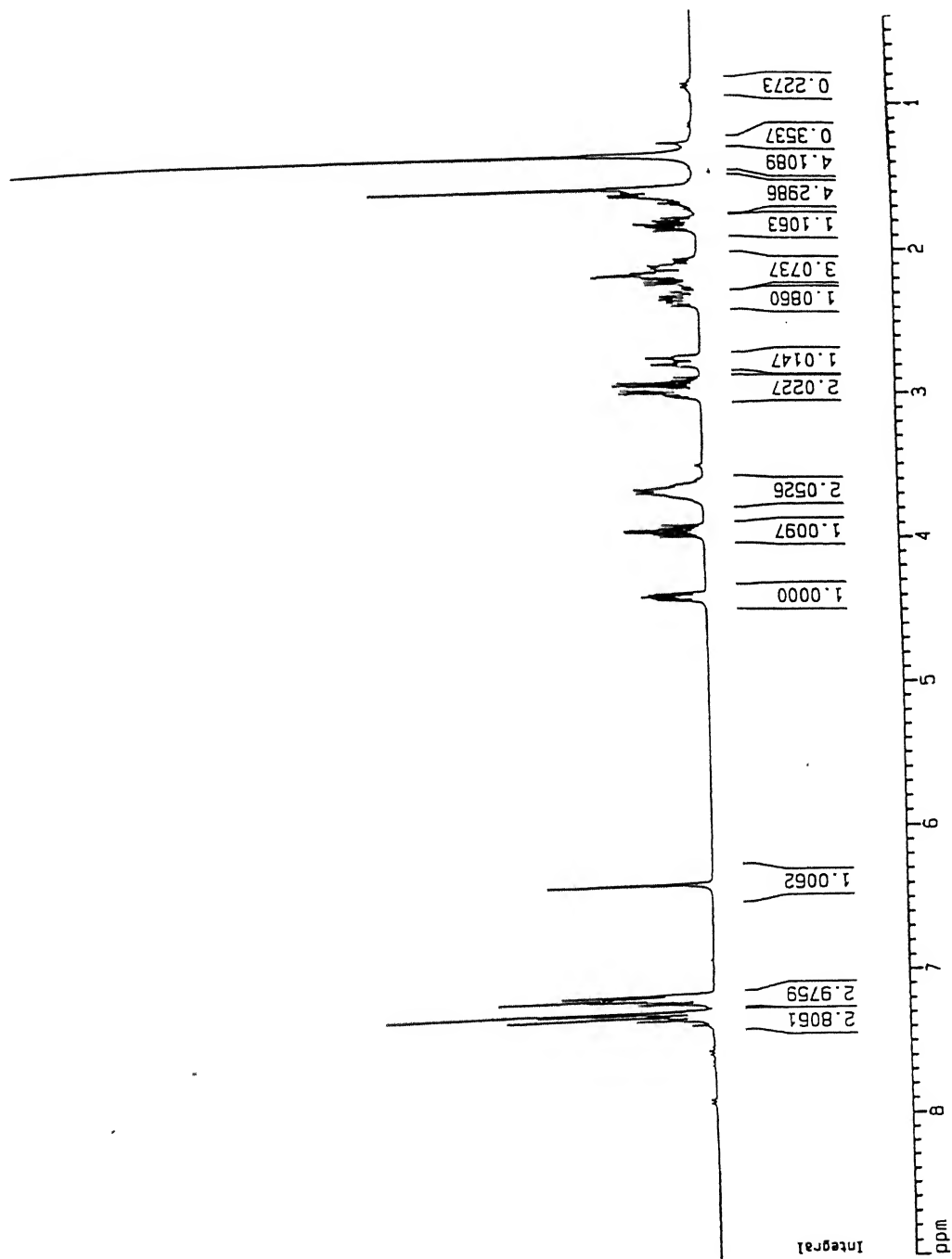
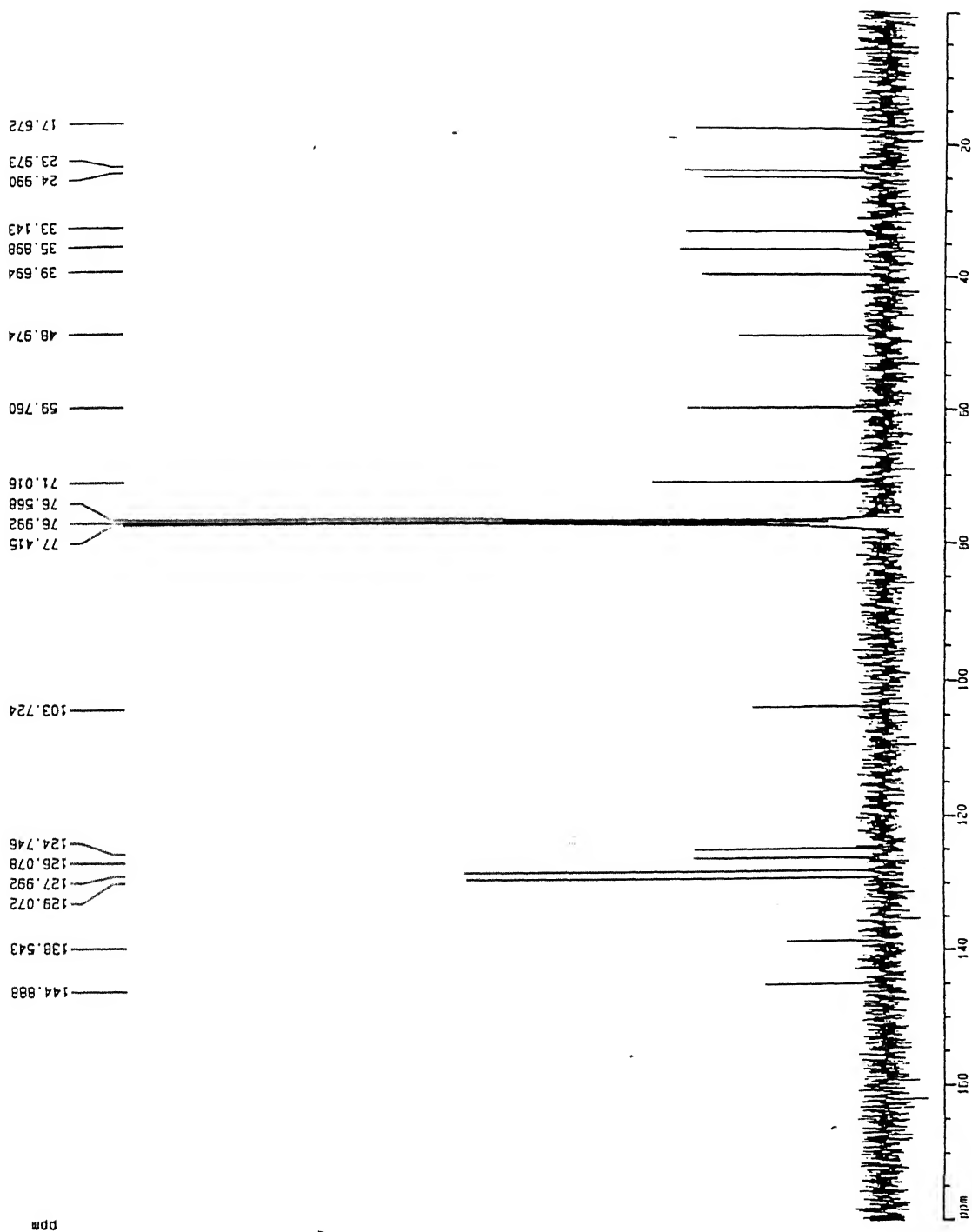
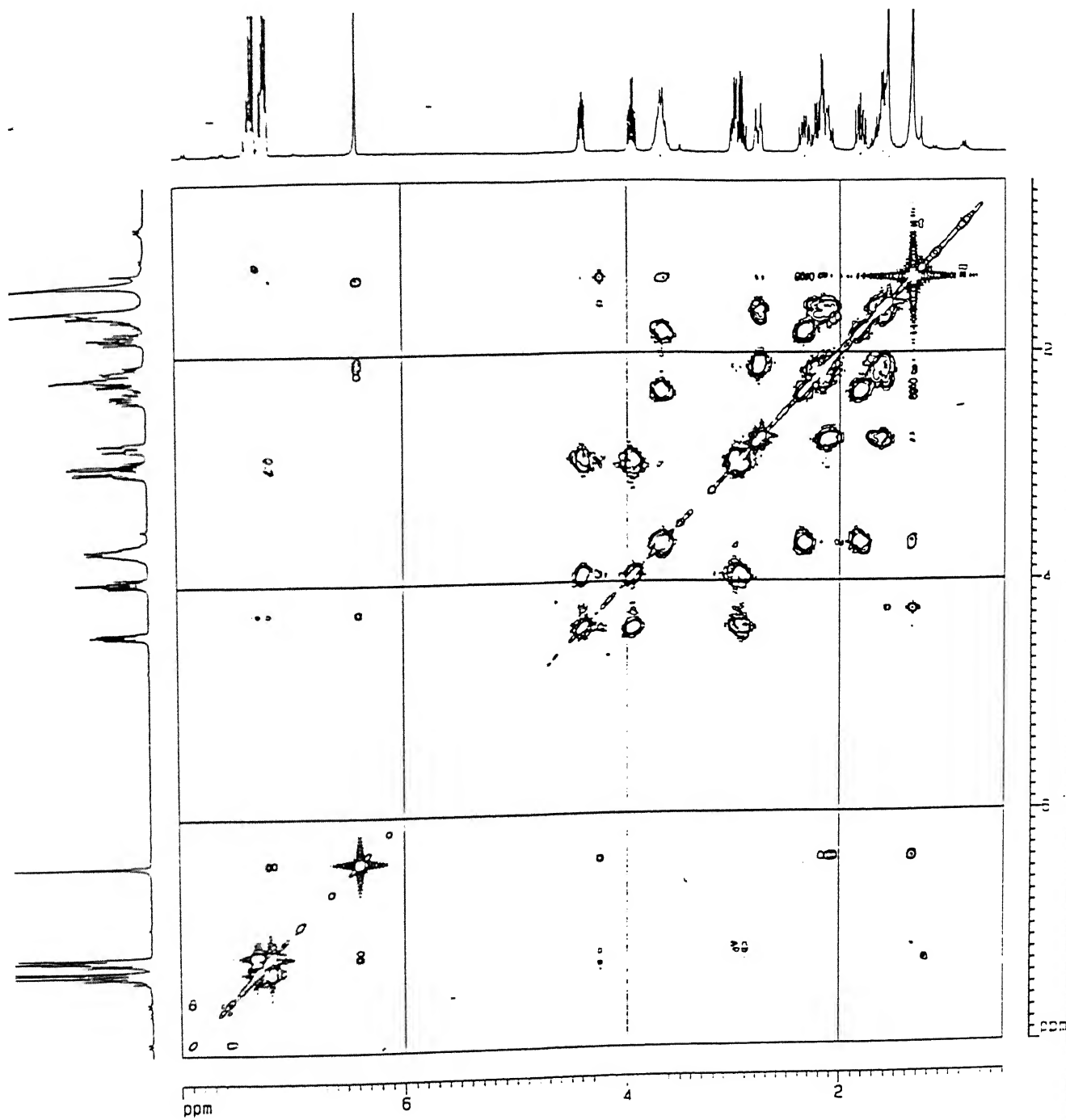
Figure 2.50: 300 MHz  $^1\text{H}$  NMR spectra of 84, R=Ph



Figure 2.51: 75.5 MHz  $^{13}\text{C}$  NMR spectra of 84, R=Ph



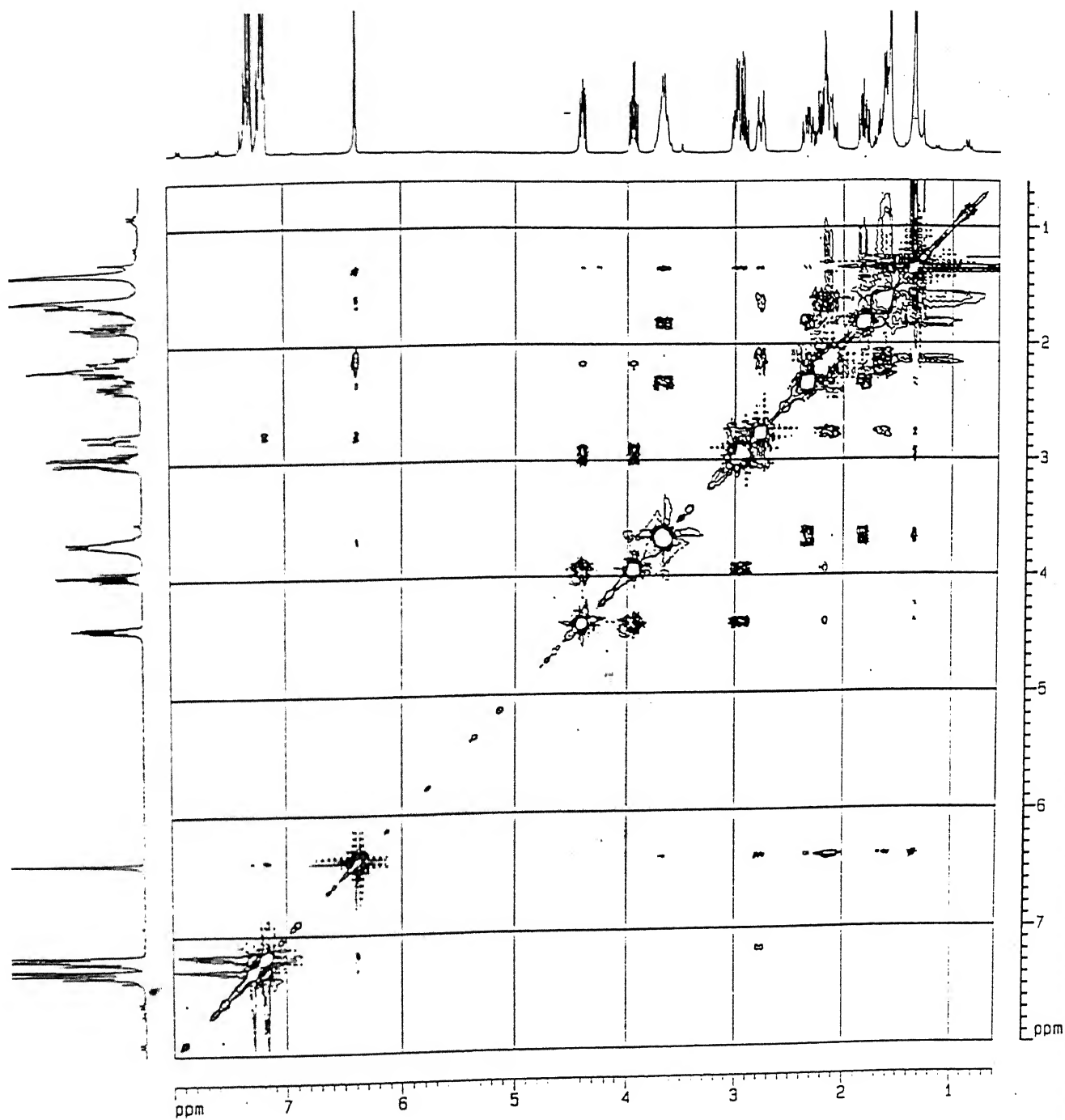


Figure 2.53: 300 MHz ROESY spectra of 84, R=Ph

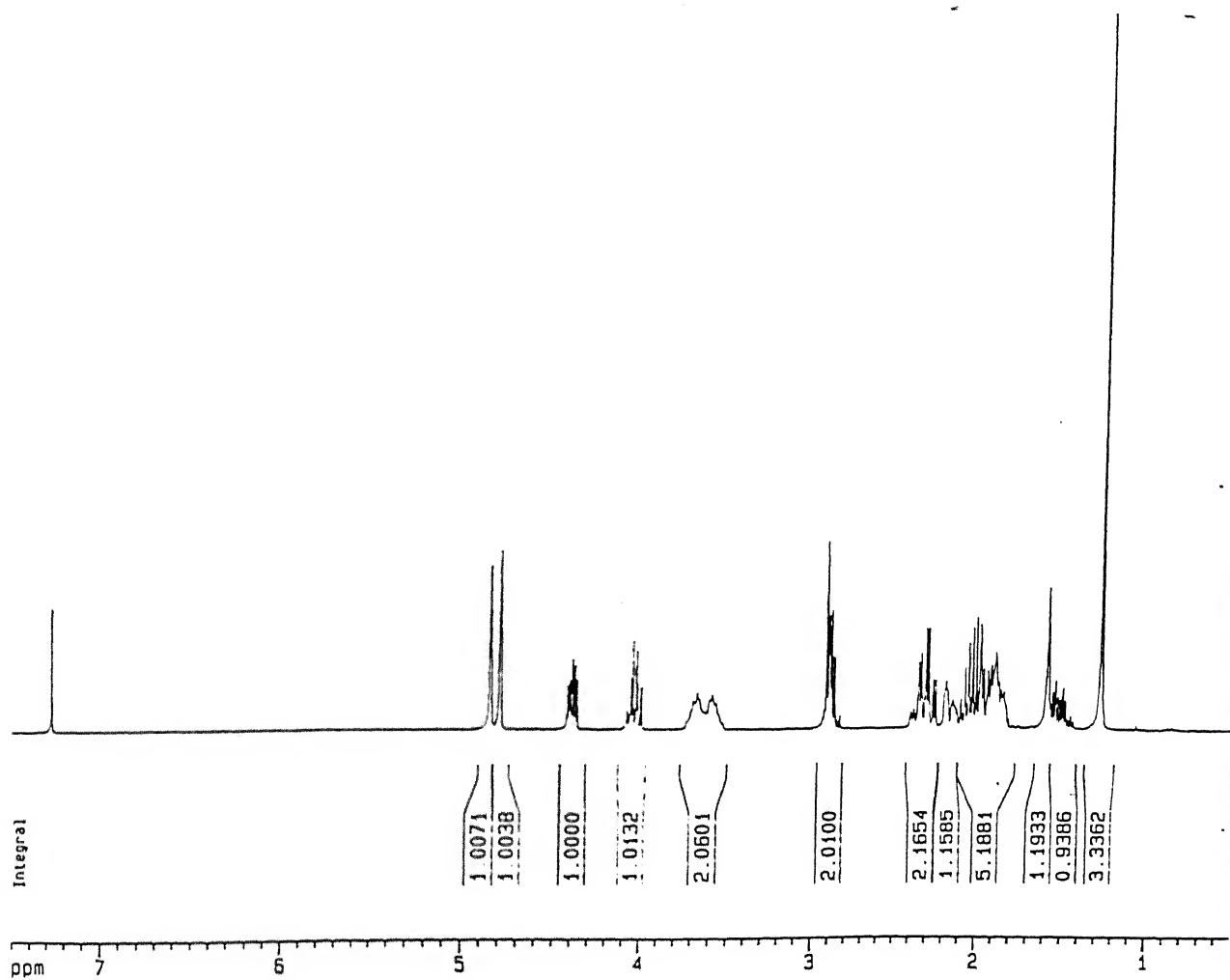


Figure 2.54: 300 MHz  $^1\text{H}$  NMR spectra of 86

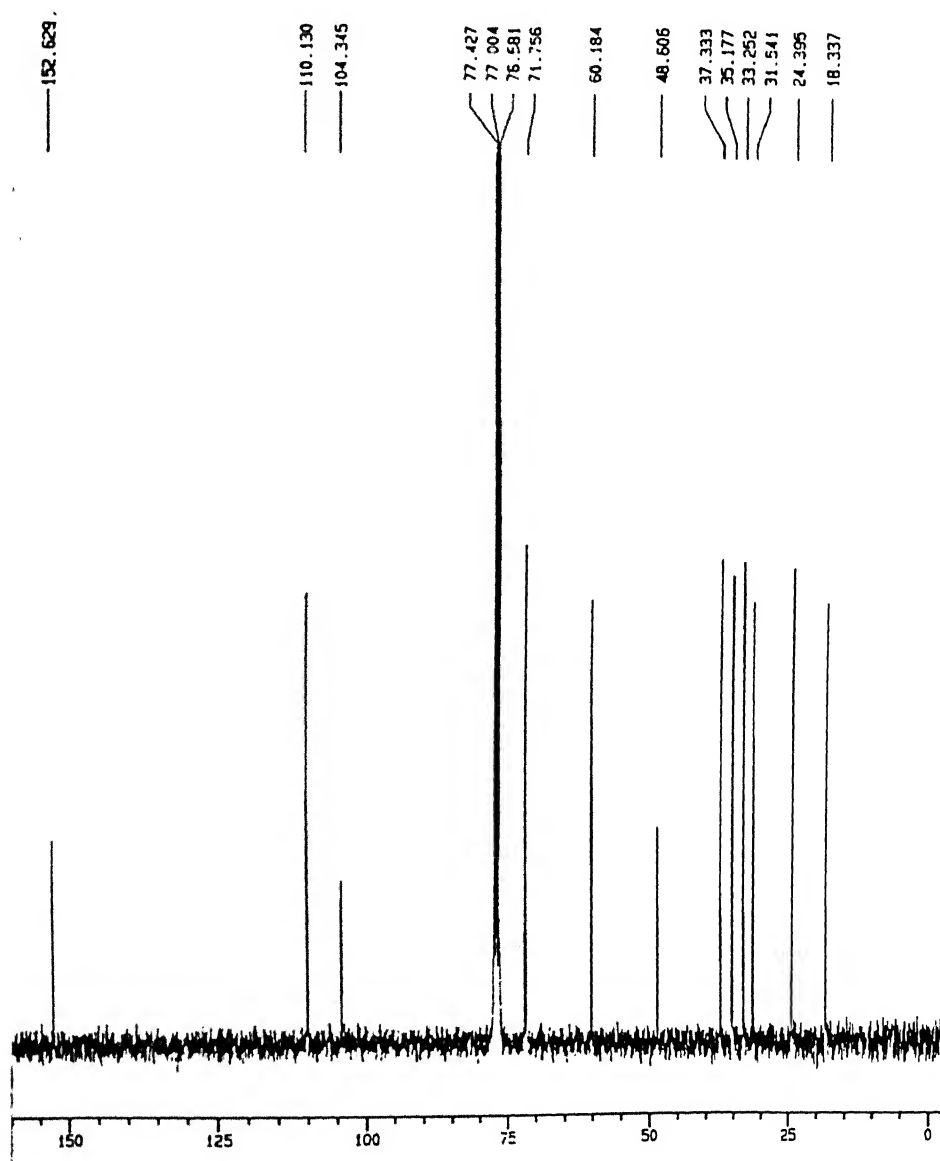


Figure 2.55: 75.5 MHz  $^{13}\text{C}$  NMR spectra of 86

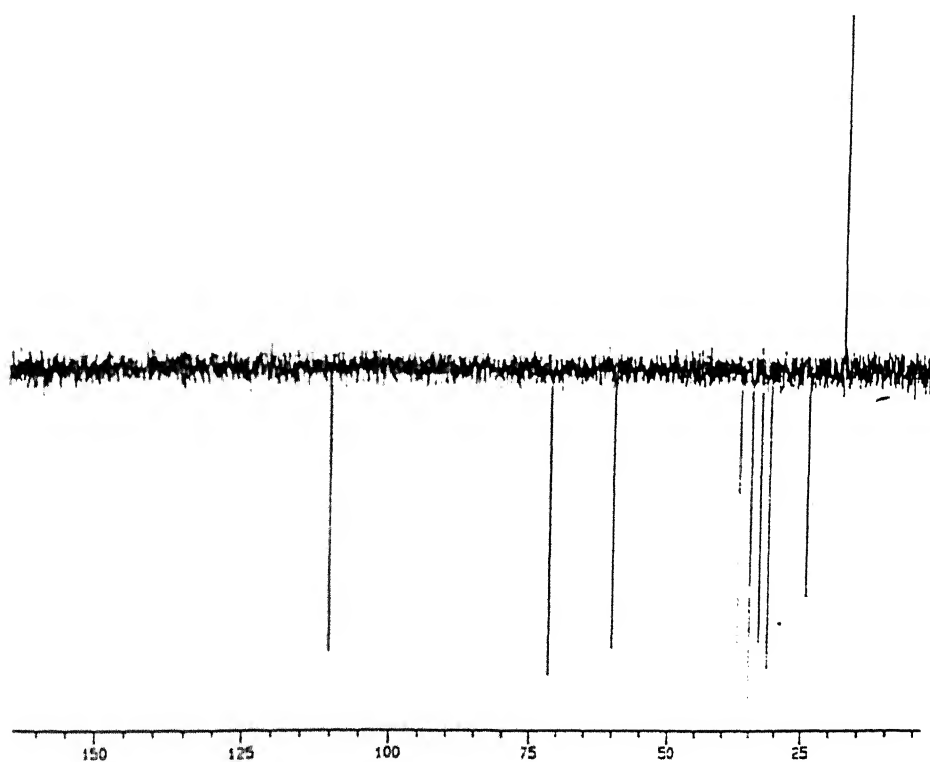


Figure 2.5a: 75.5 MHz  $^{13}\text{C}$  NMR spectra of **86**

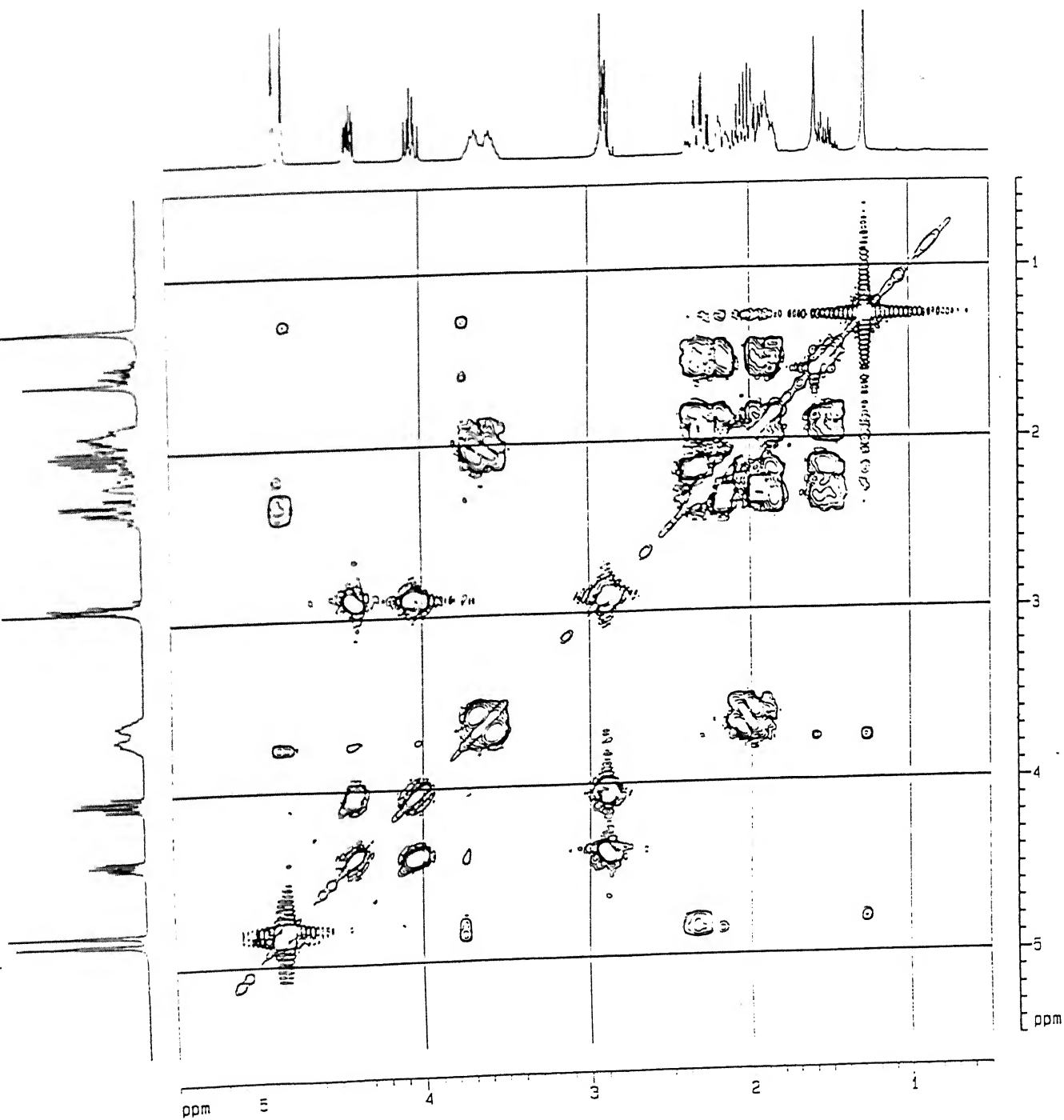


Figure 2.56: 300 MHz COSY spectra of 86

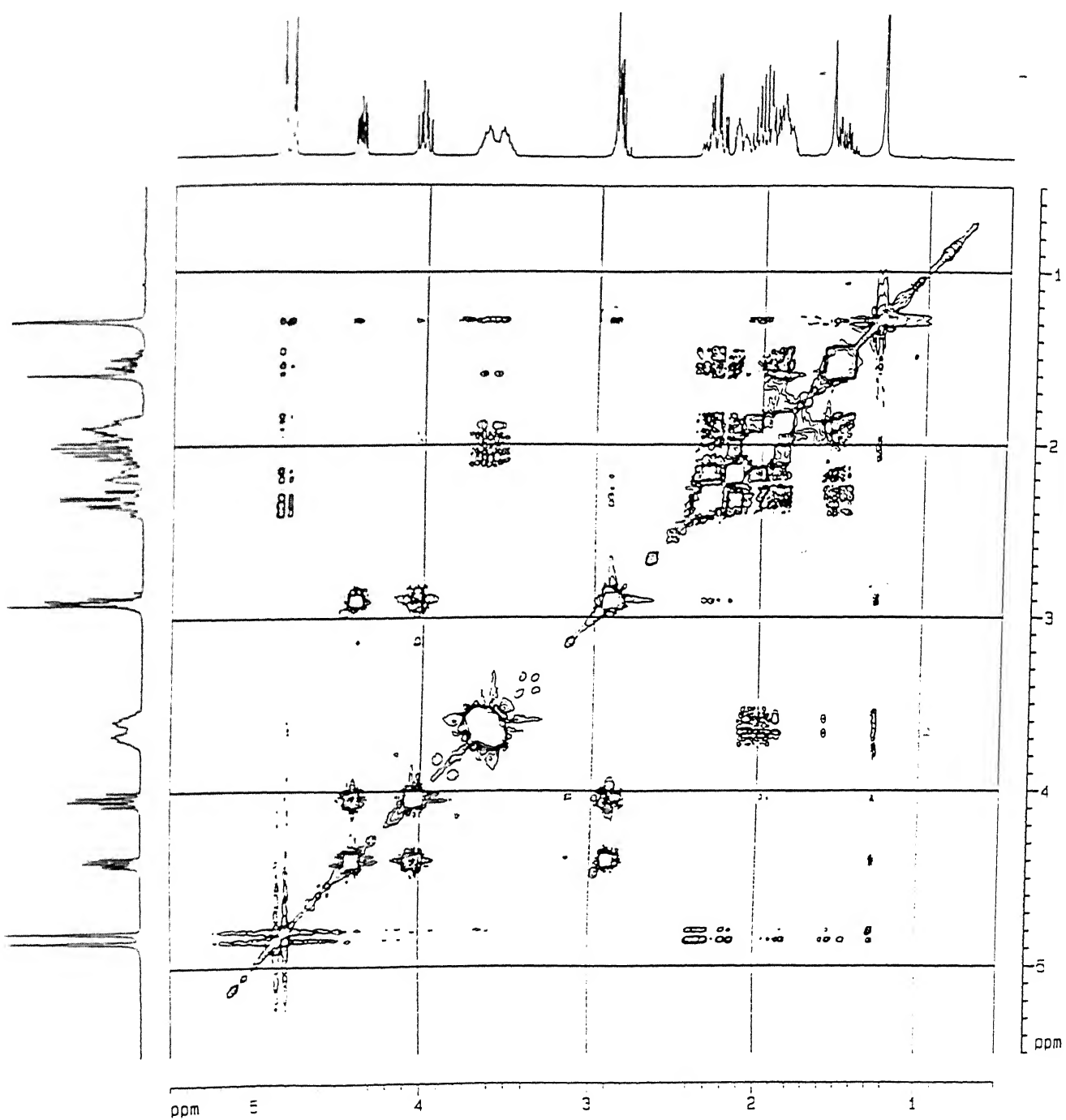
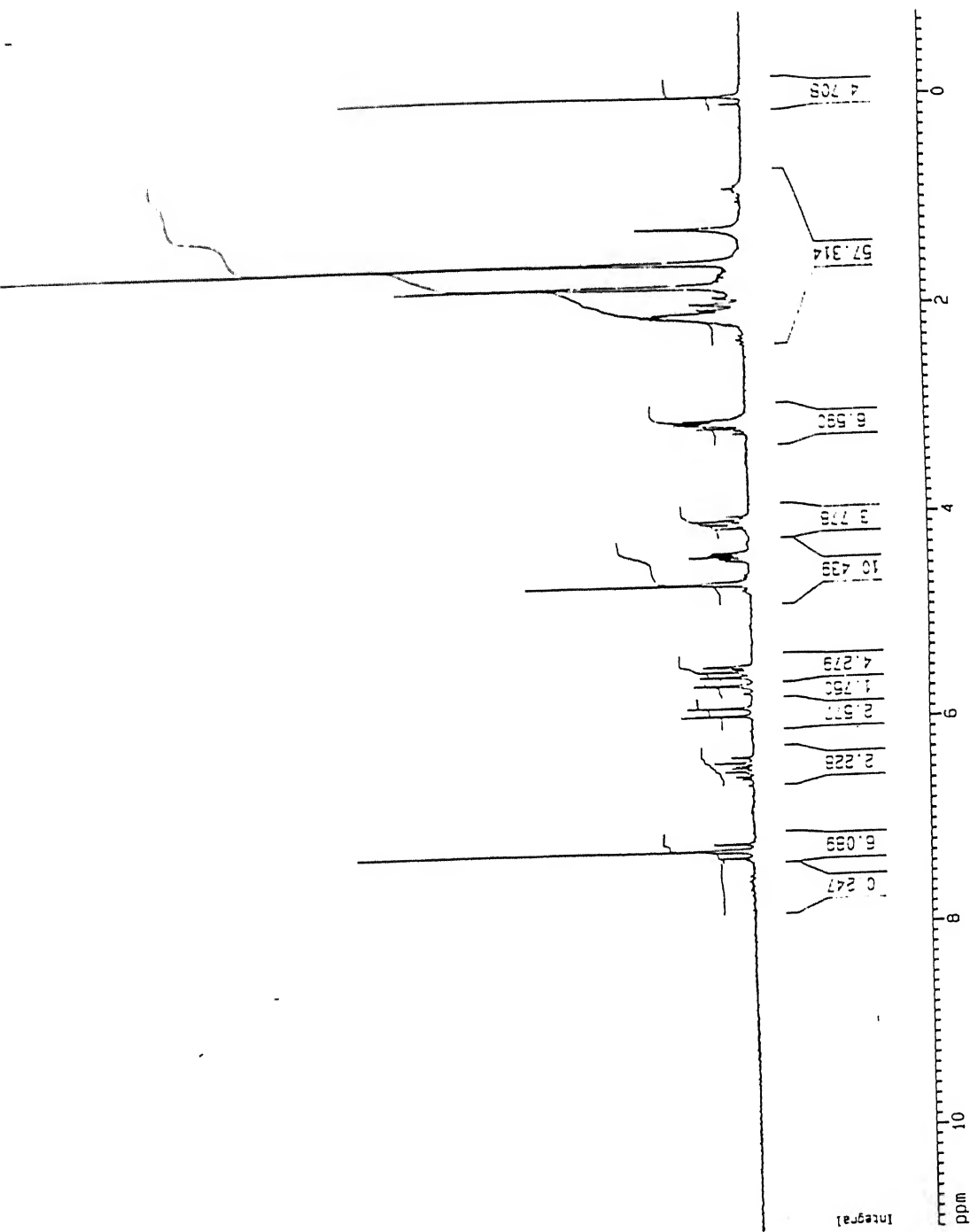


Figure 2.57: 300 MHz ROESY spectra of 86



Figure 2.58:200 MHz  $^1\text{H}$  NMR spectra of 91

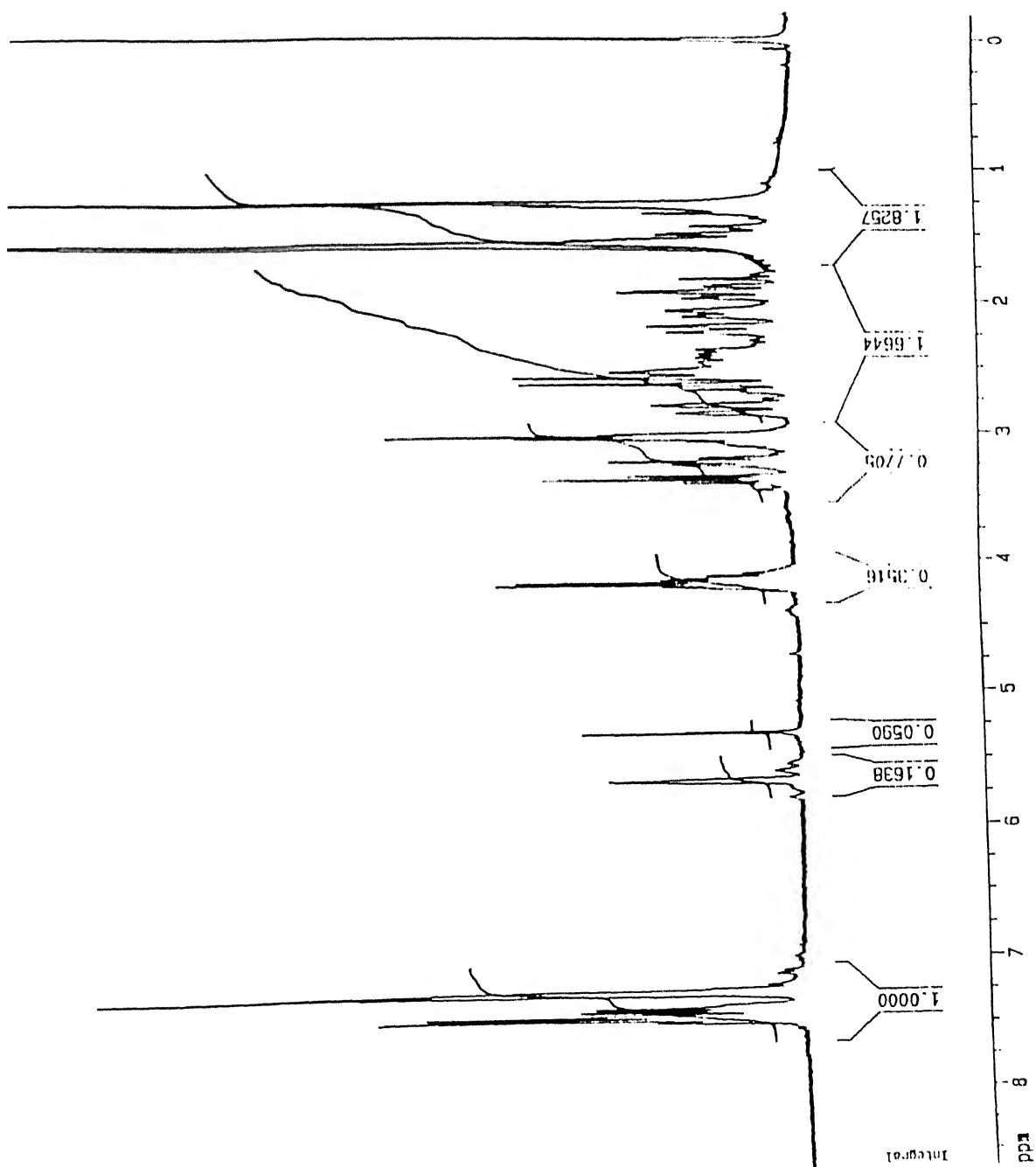


Figure 2.59: 300 MHz  $^1\text{H}$  NMR spectra of less polar isomer isolated from the Diels-Alder reaction of diene **10** with NPM

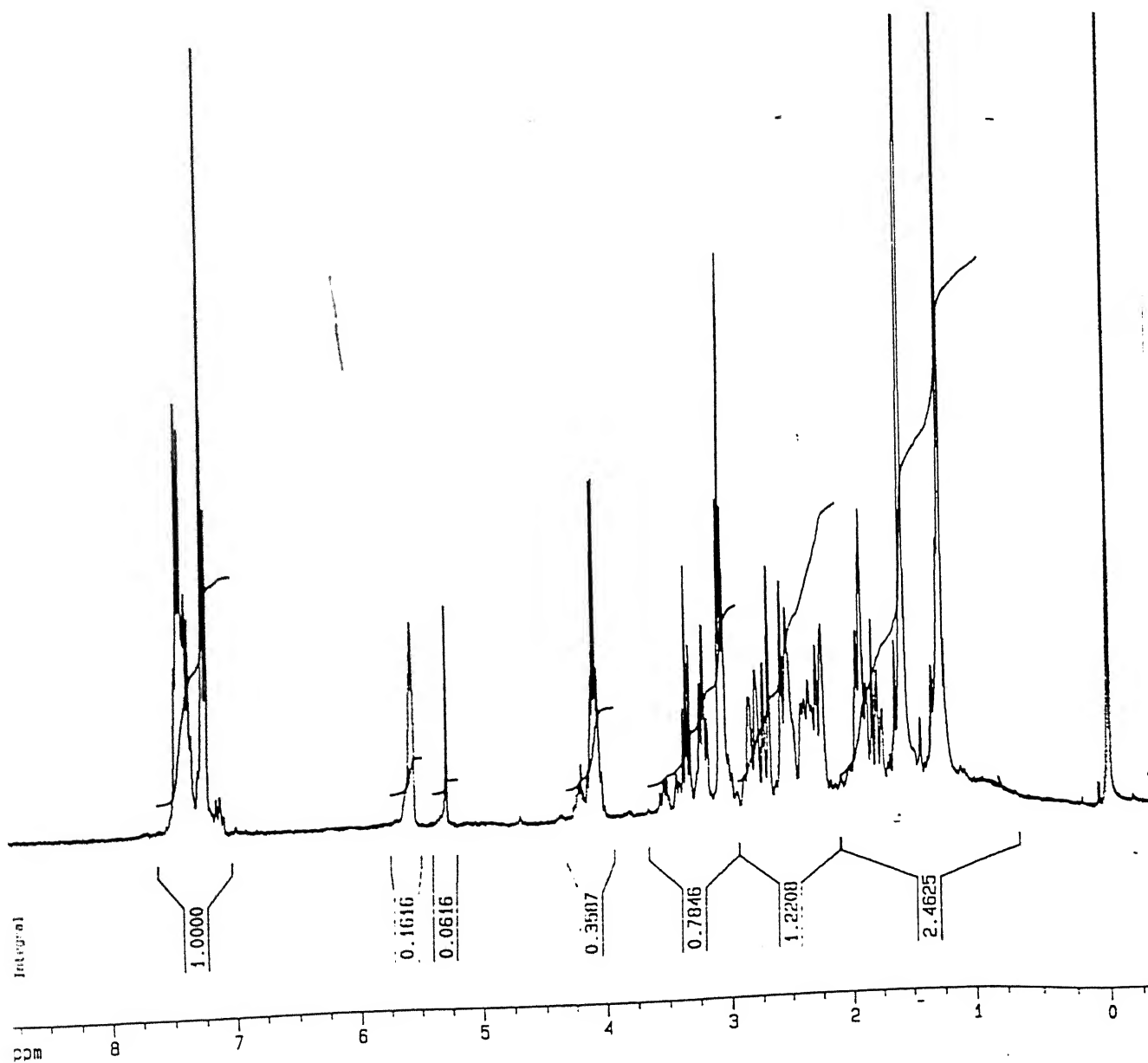


Figure 2.60: 300 MHz  $^1\text{H}$  NMR spectra of more polar isomer isolated from the Diels-Alder reaction of dien **95** with NPM

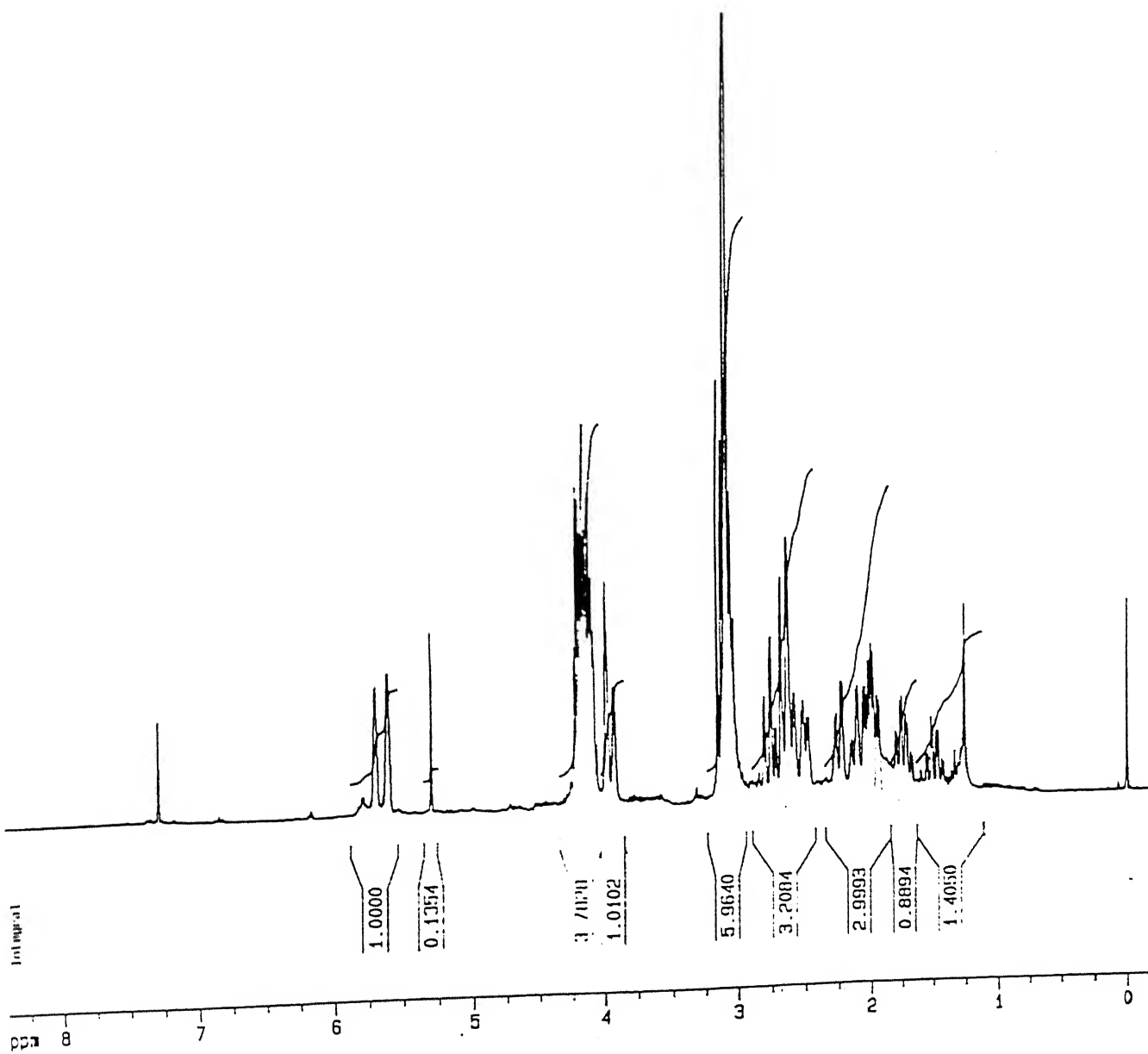


Figure 2.61: 300 MHz  $^1\text{H}$  NMR spectra of a mixture of 98 and 99

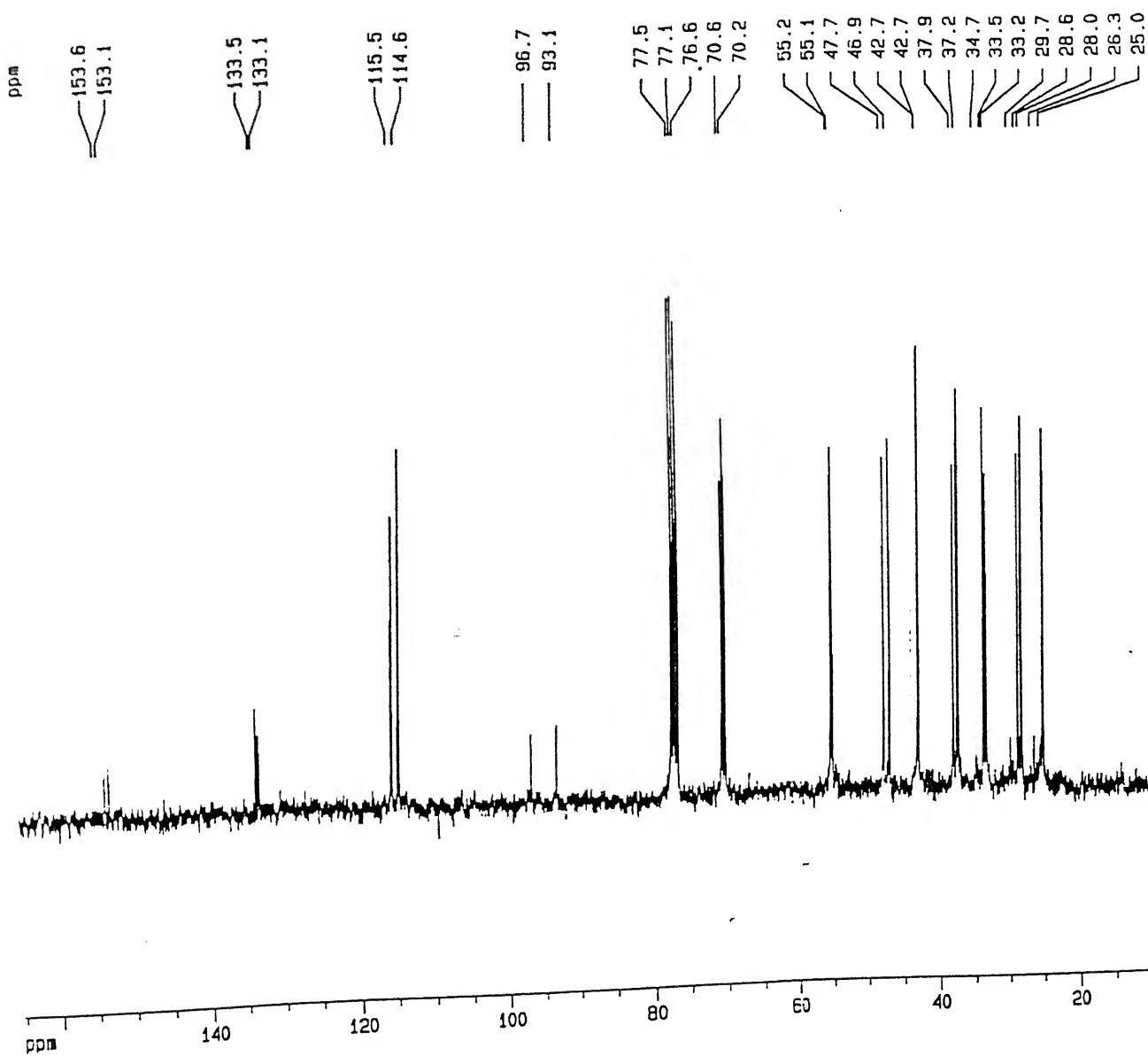
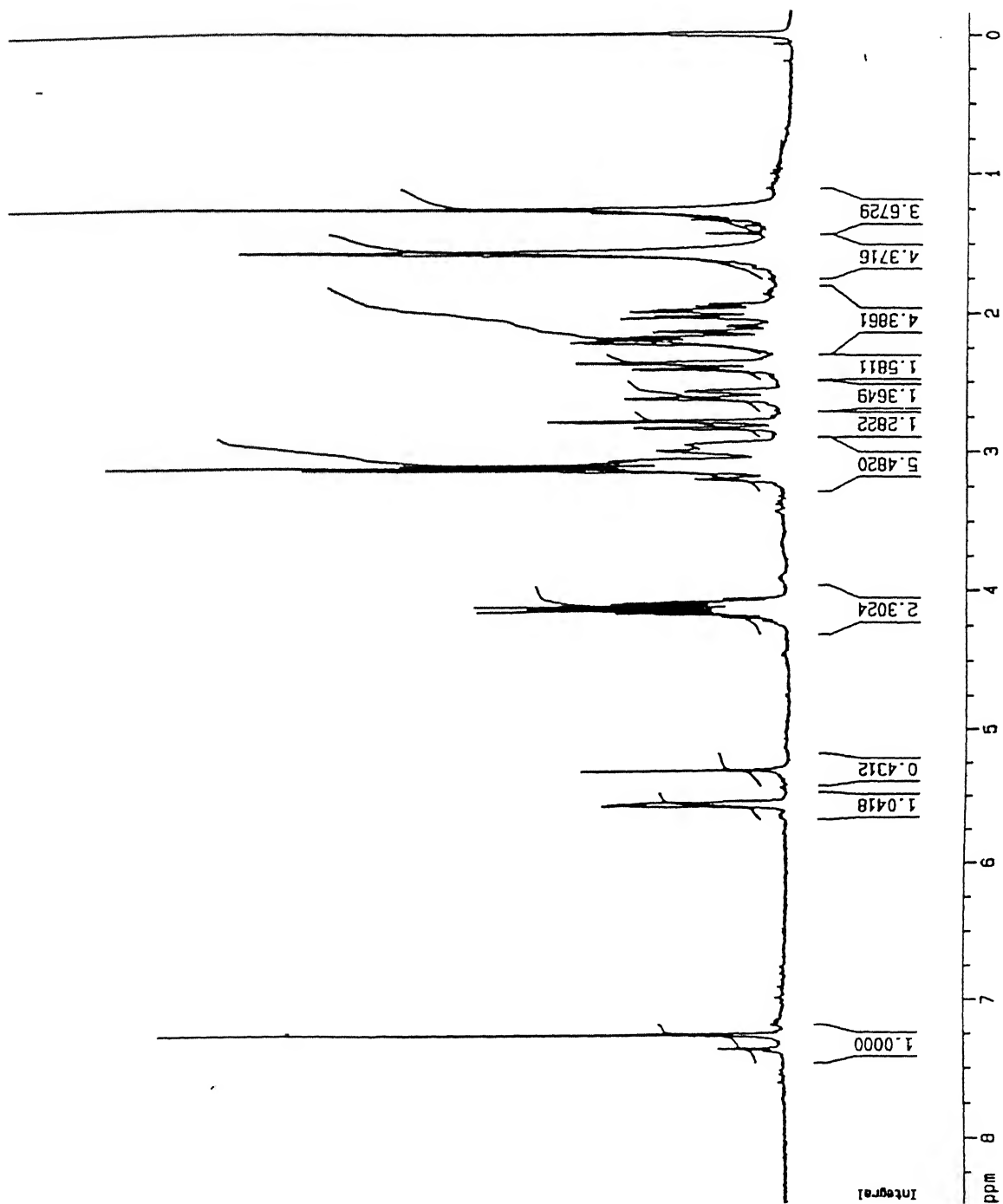


Figure 2.62: 75.5 MHz  $^{13}\text{C}$  NMR spectra of a mixture of 98 and 99

Figure 2.63: 300 MHz  $^1\text{H}$  NMR spectra of minor isomers of 100

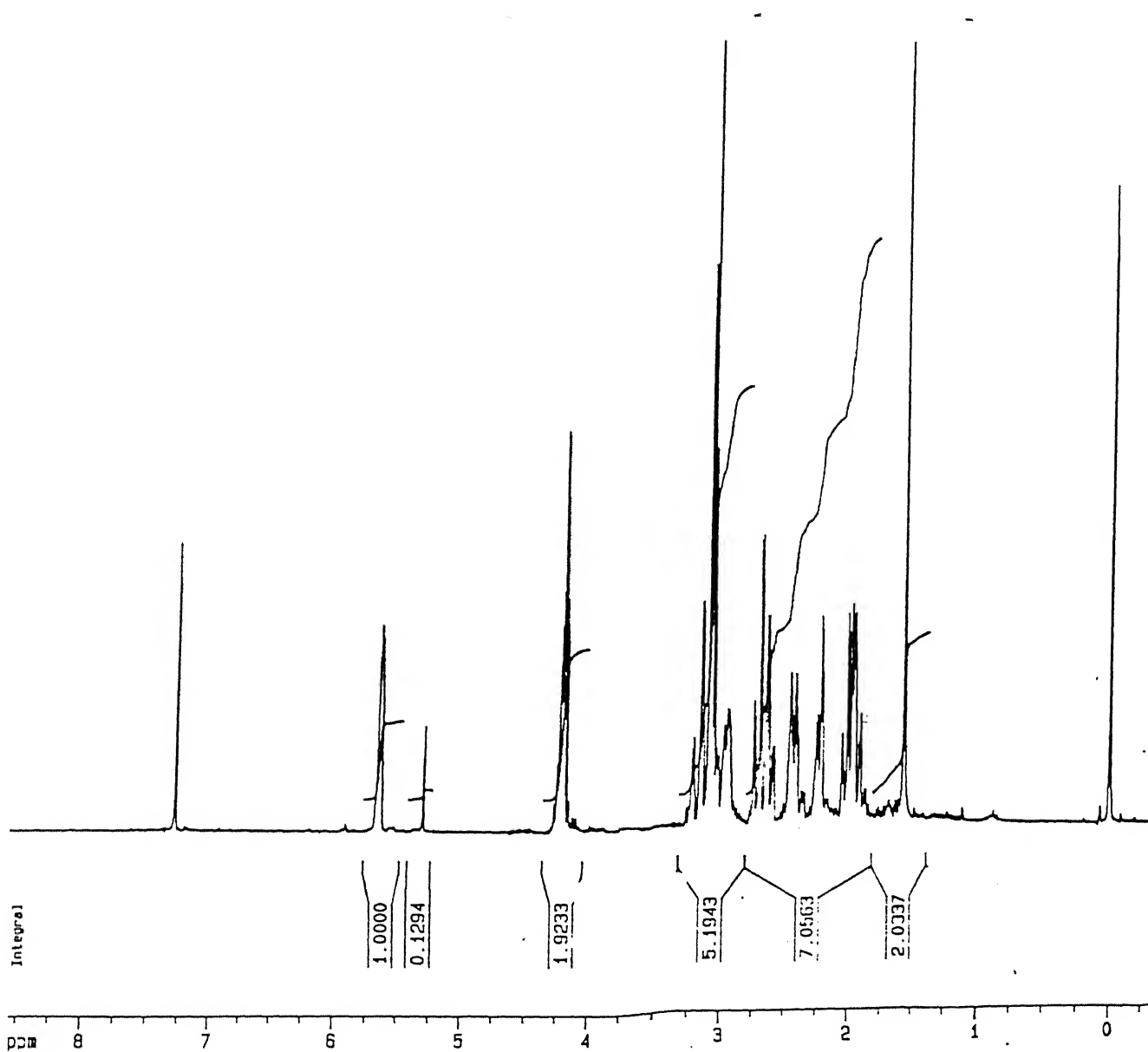


Figure 2.64: 300 MHz  $^1\text{H}$  NMR spectra of major isomer of **100**

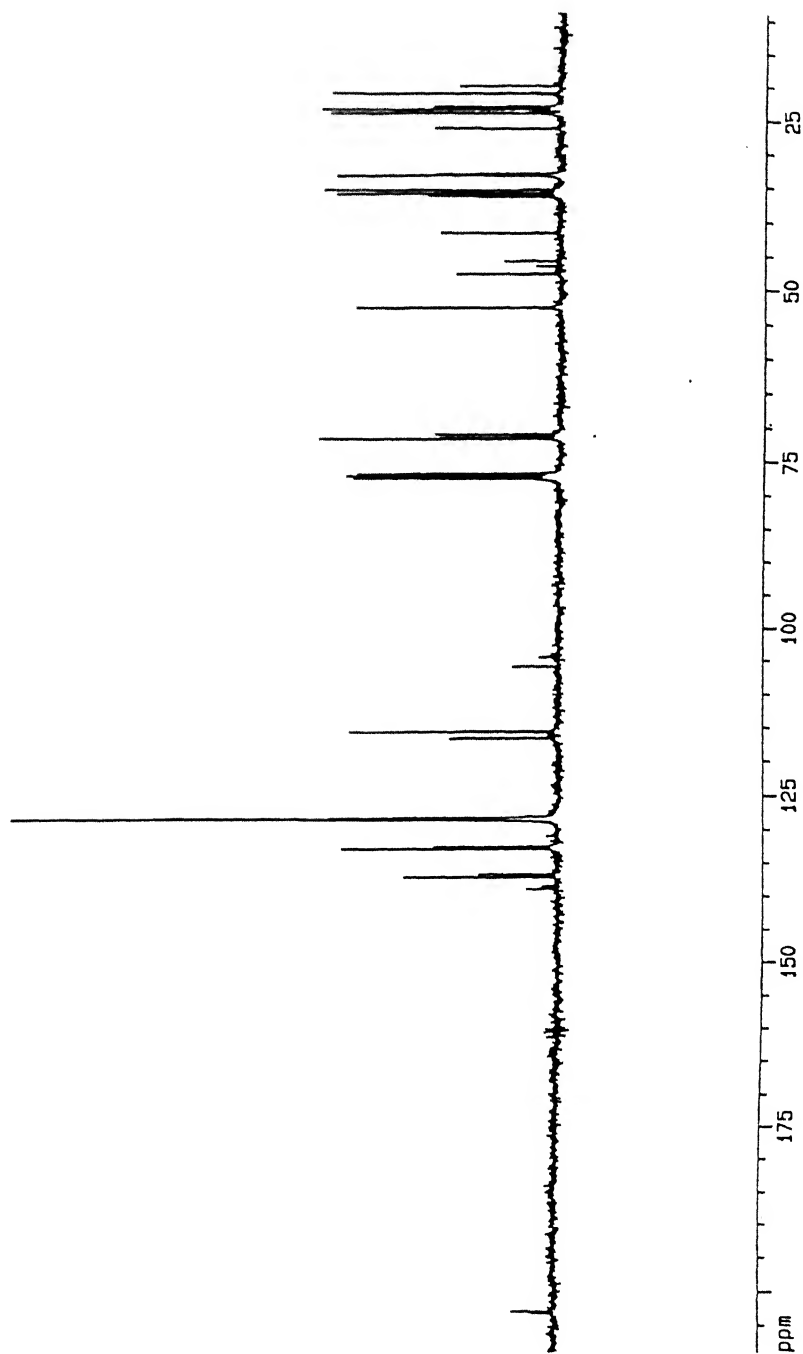


Figure 2.65: 75.5 MHz  $^{13}\text{C}$  NMR spectra of a mixture of 101 and 102



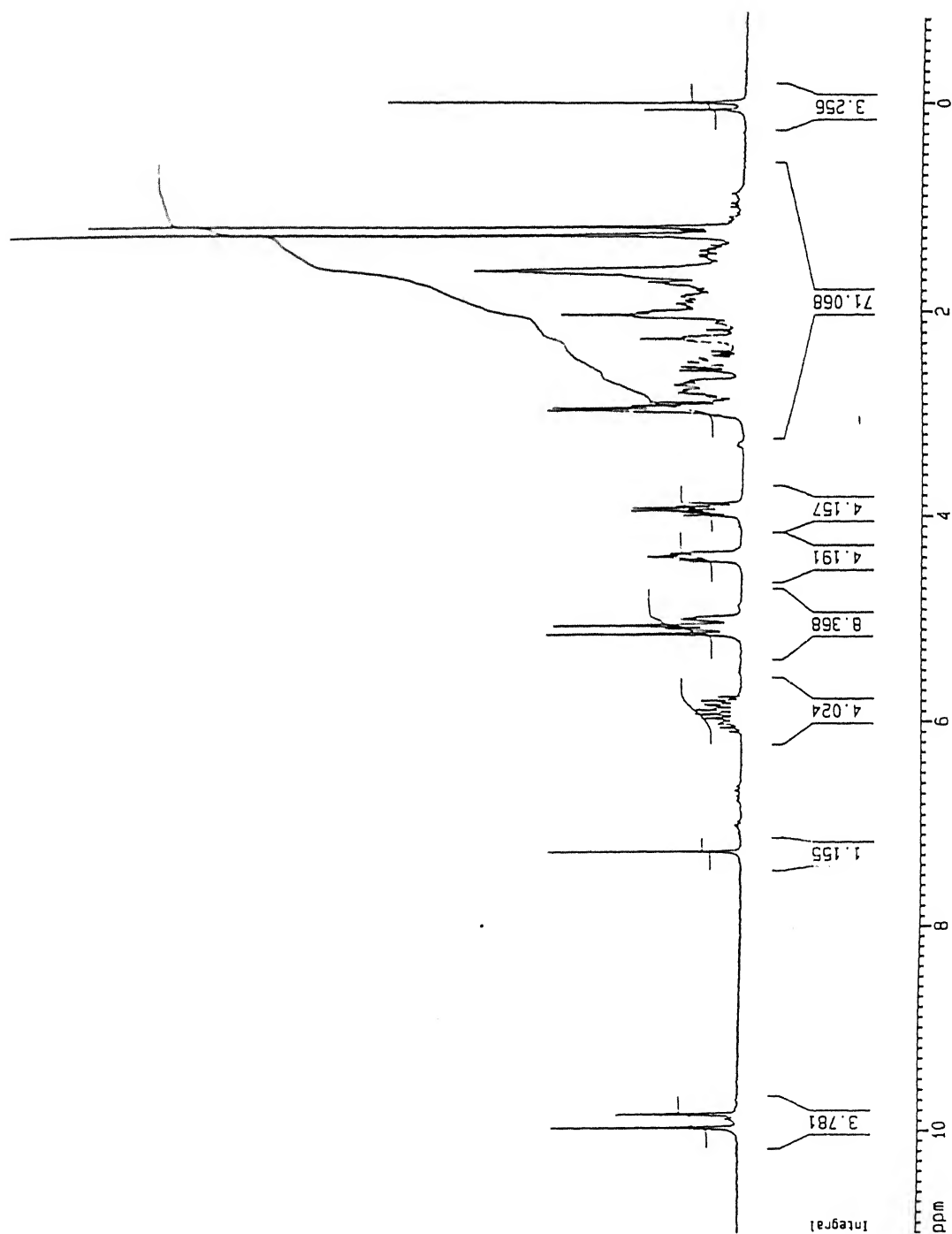
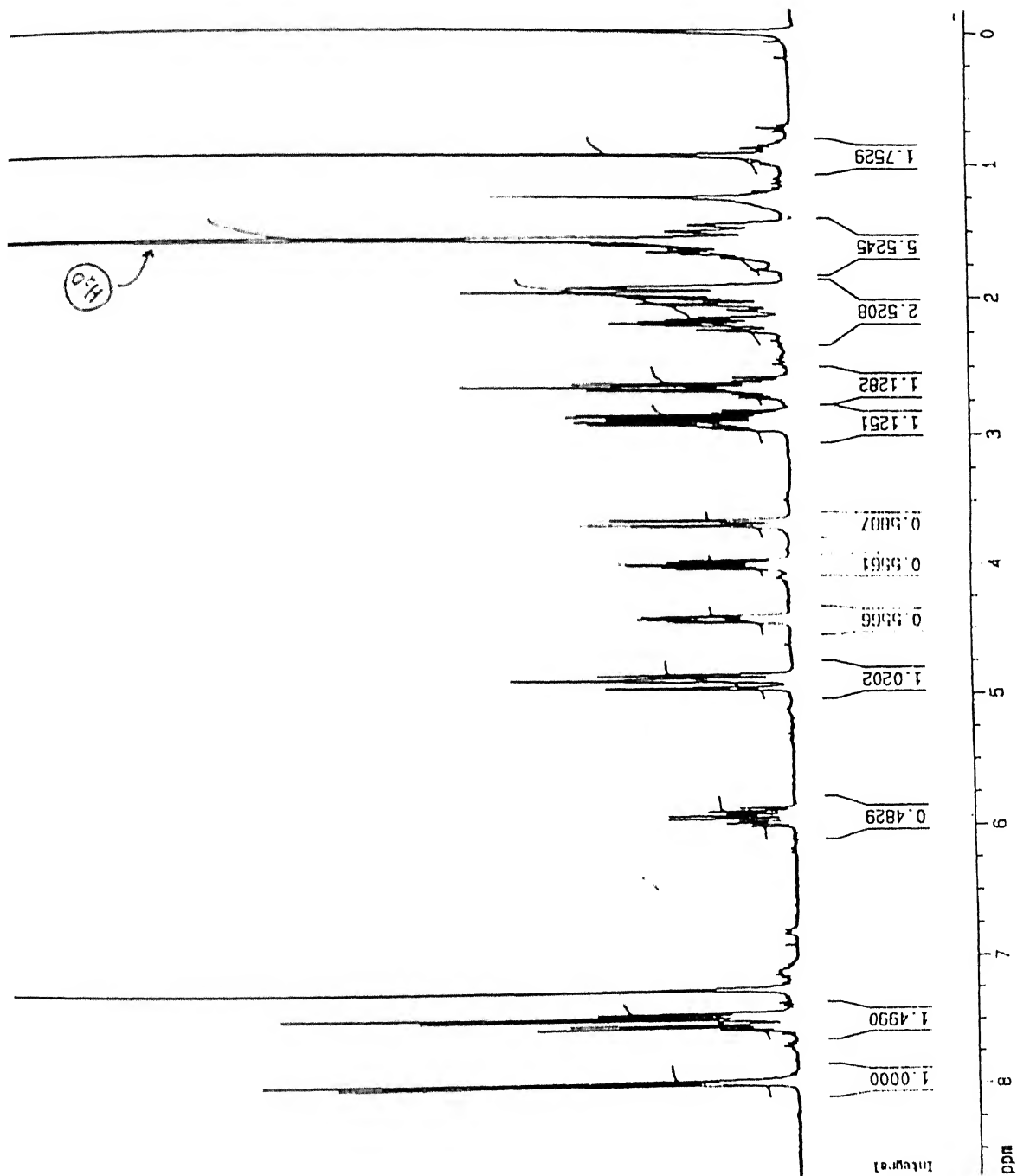


Figure 2.66: 200 MHz  $^1\text{H}$  NMR spectra of a mixture of 103 and 104

Figure 2.67: 300 MHz  $^1\text{H}$  NMR spectra of 101

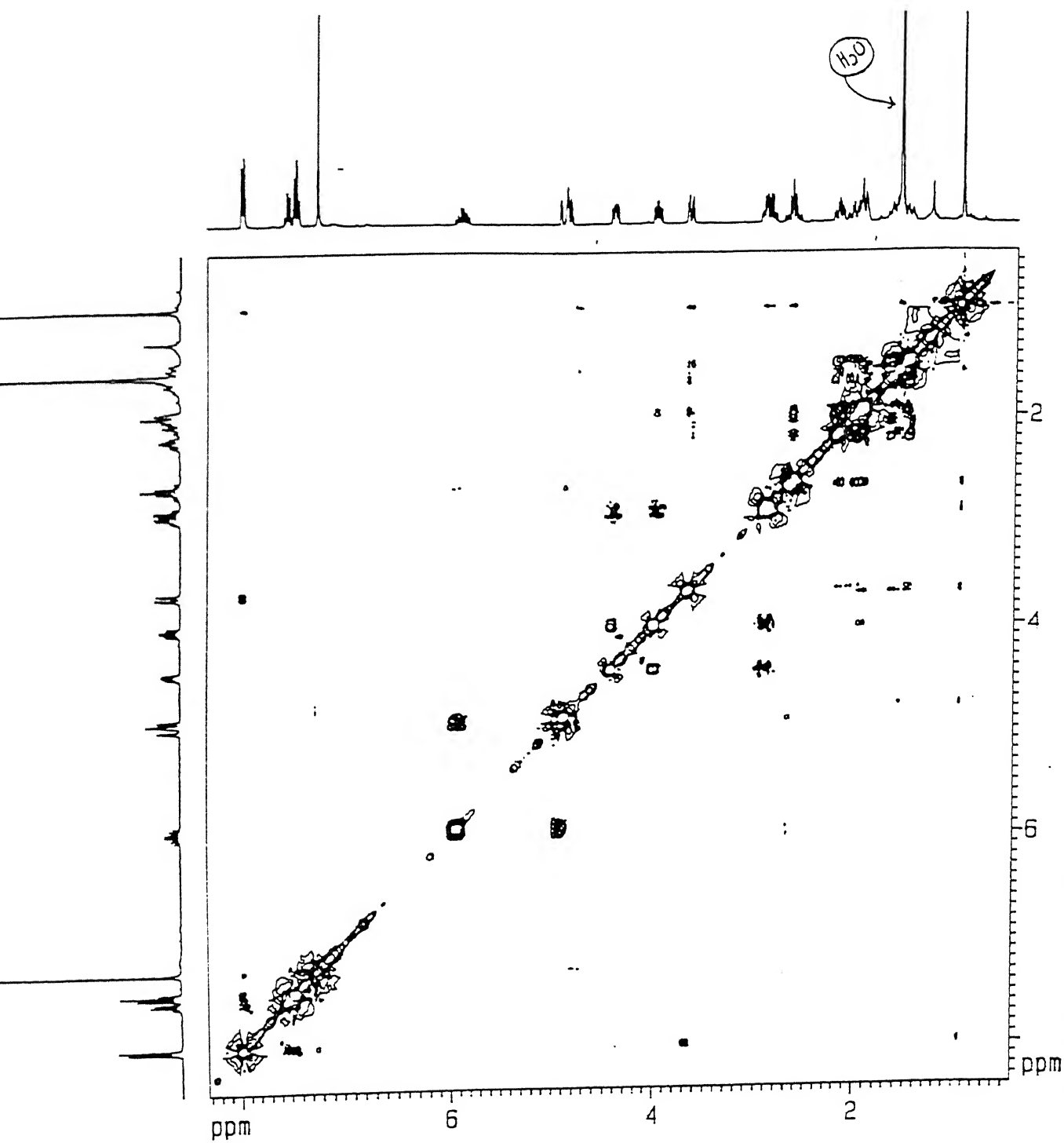
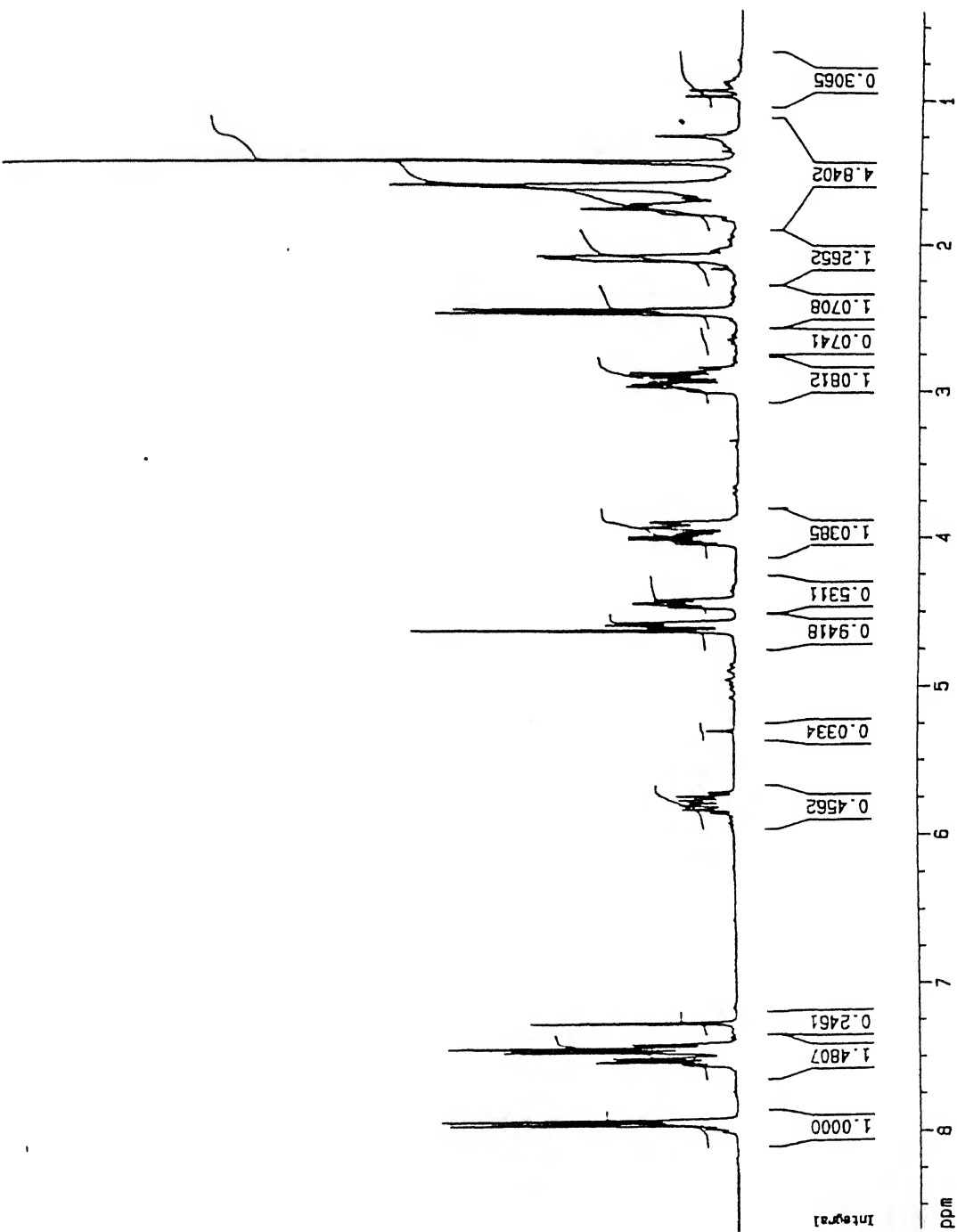


Figure 2.68: 300 MHz ROESY spectra of **101**

Figure 2.69: 300 MHz  $^1\text{H}$  NMR spectra of 102

203



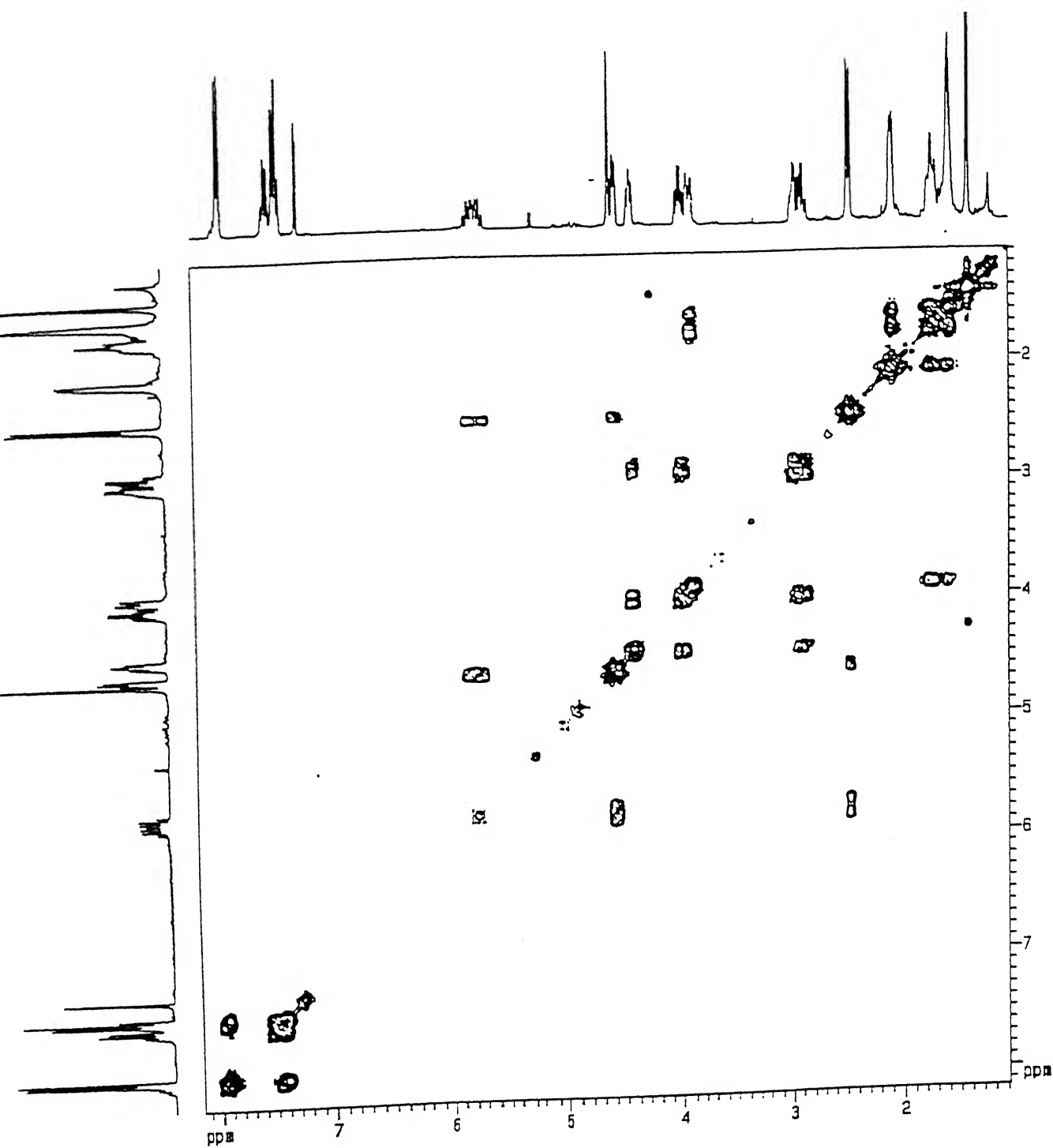


Figure 2.70: 300 MHz COSY spectra of 102

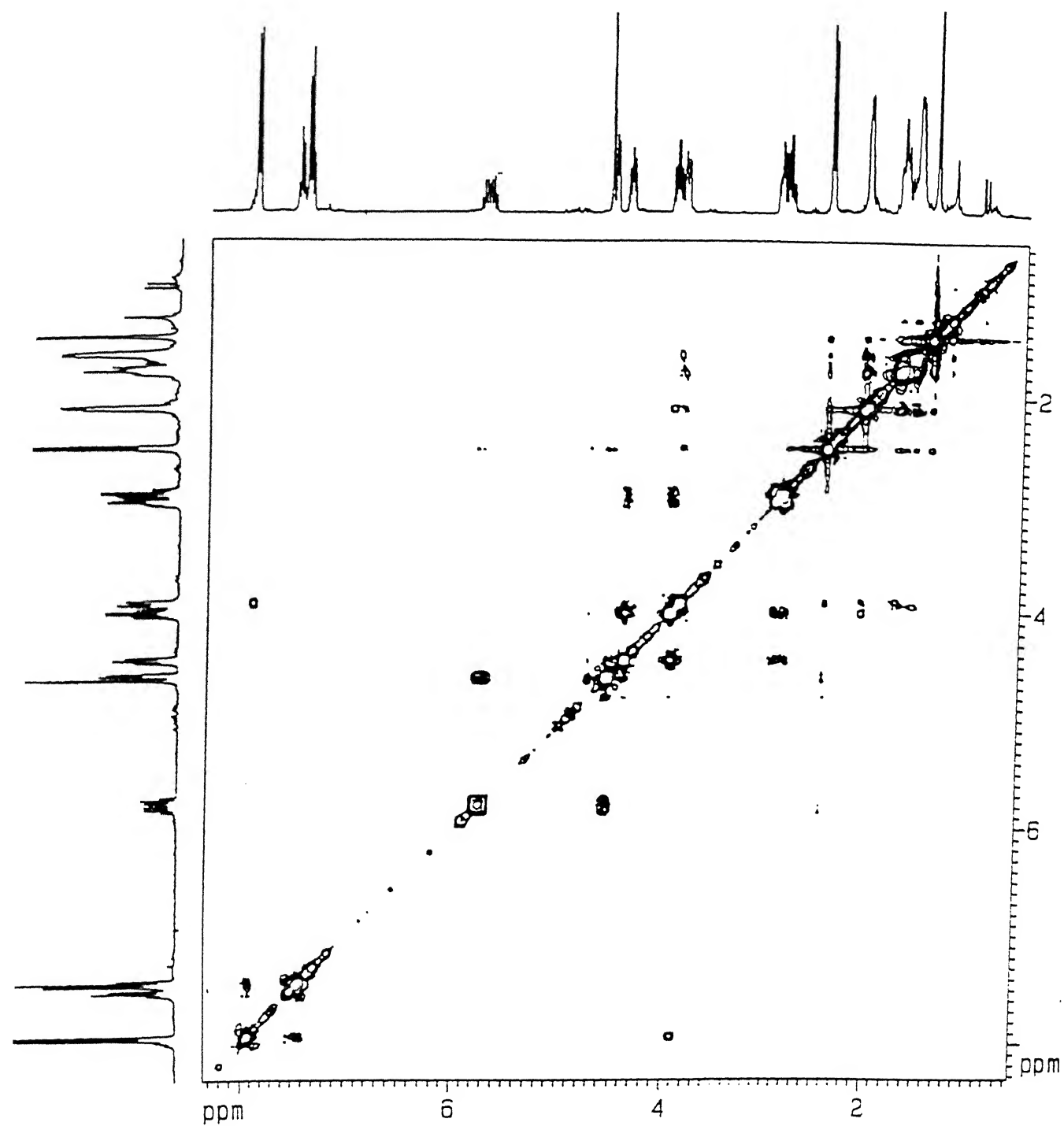


Figure 2.71: 300 MHz ROESY spectra of 102

## Chapter 3

# Synthesis of 2,6-Dioxa-3-oxo-bicyclo[3.3.0]octanes

### 3.1 Introduction

2,6-Dioxa-3-oxobicyclo[3.3.0]skeleton **11** is present in a class of natural products possessing diverse biological activity. Notably, it is present in plumeria and allamanda iridoids such as plumericin (**1**) (Fig. 3.1), allamcin (**2**), and allamandin (**3**) which exhibit cytotoxic, antileukemic, antimicrobial, and antifungal properties,<sup>1, 2</sup> in goniofufurone (**4**) which is an antitumor styryllactone,<sup>1-6</sup> in delessierine (**5**) and dilaspirolactone (**6**) which exhibit anticoagulant properties,<sup>7</sup> and in piptosidin<sup>8</sup> (**7**). Further, certain species of parasitic wasps (in the family of Braconidae) exhibit potential as biological control agents and hence, there has been considerable interest in their morphology and taxonomy. Recently, Williams and coworkers<sup>9</sup> have reported that the Hagen's glands (located in the abdominal tips of the braconid wasps) are rich in  $\gamma$ -lactones including the bicyclic species **8** and **9**.

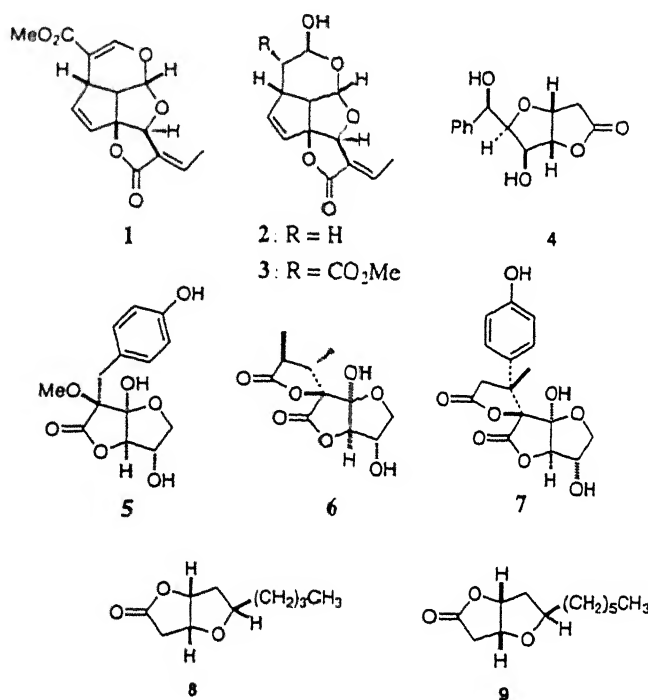
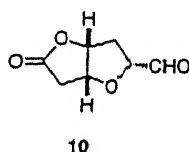


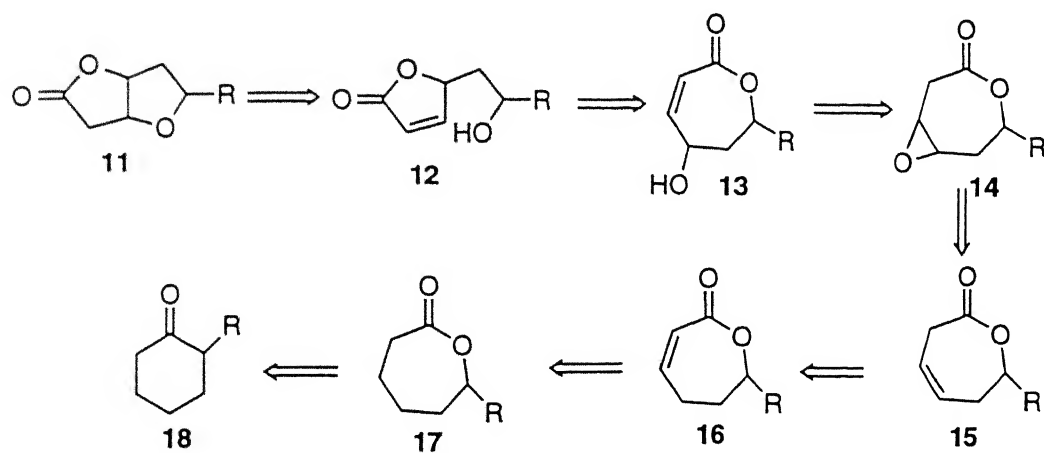
Figure 3.1: Naturally occurring materials containing the 2,6-dioxo-3-oxobicyclo[3.3.0] skeleton

Bicyclic skeleton **10**, which may also serve as an useful synthon in organic syntheses,<sup>10-14</sup> has lately been the focus of attention of several researchers.<sup>5, 15-18</sup>



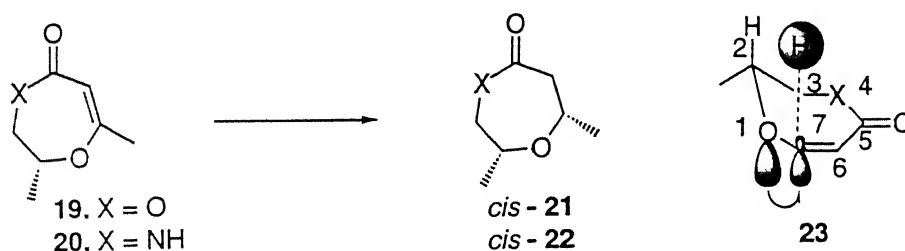
We became interested in the synthesis of the above bicyclic skeleton. Retrosynthetic analysis as shown in the Scheme 3.1 showed that 4,5-dehydro-2-oxepanones **15** could serve as precursors. This was also to give us an opportunity to study the conformational profile and the diastereoface selectivity of these 7-ring systems which have received little attention in the past.





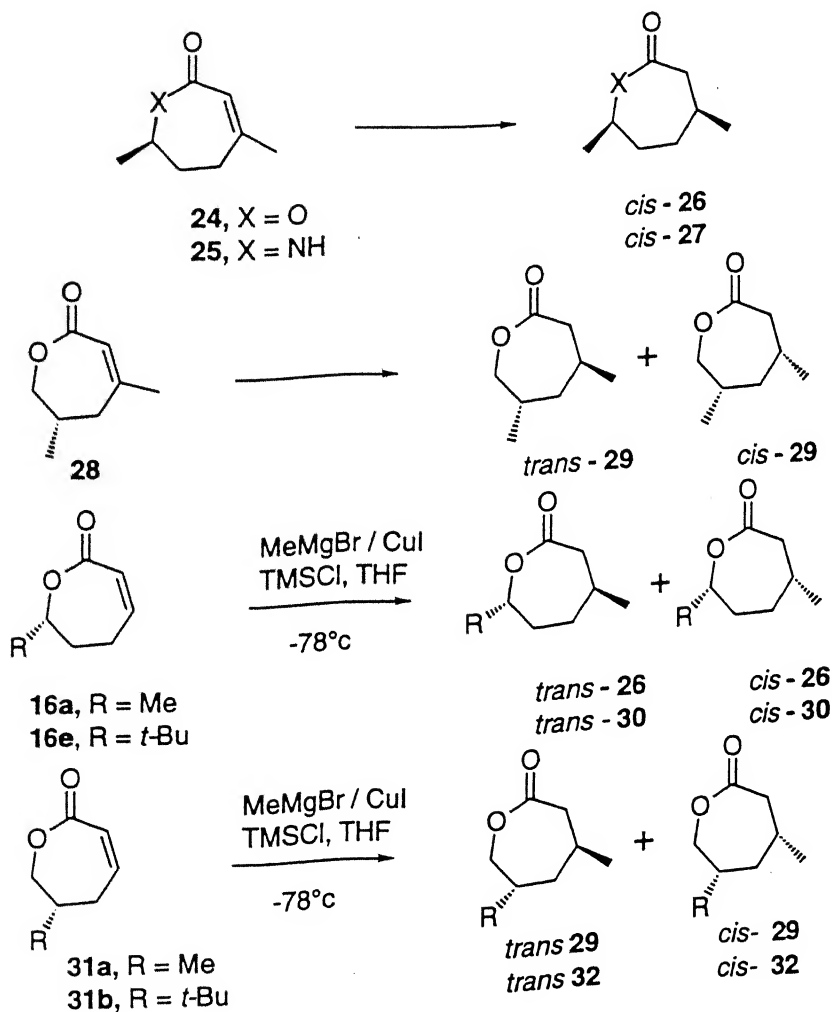
Scheme 3.1:

Sato *et al.*<sup>19</sup> have studied the facial selectivity in addition reactions of 2,3,4,5-tetrahydro-1,4-dioxepin-5-one **19** and the corresponding 1,4-oxazepan-5-one **20**. Catalytic reduction furnished, respectively, the *cis*-**21** and *cis*-**22** as the major products. The observed selectivity was considered due probably to stereoelectronic effects as proposed by Cieplak.<sup>20</sup> The interaction of an oxygen lone pair with the antibonding orbital of the incipient bond [ $\sigma_{C7-H}^*$ ] as shown in **23** favored attack from the  $\beta$ -face.



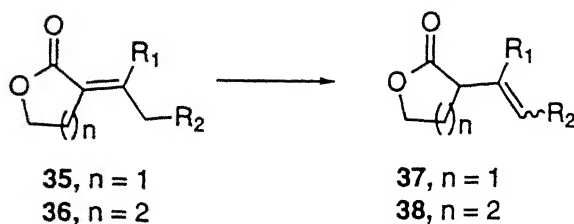
Very recently, Sato and coworkers<sup>21</sup> have also studied the influence of 6- and 7-substituents in addition reactions to dehydrooxepinones. Catalytic reduction of **24** and **25** furnished only the *cis*-products **26** and **27**, respectively. However, **28** gave a mixture of the *trans*- and *cis*-**29** in 1:5 ratio. In the conjugate addition of MeMgBr in the presence of CuI and TMSCl

at  $-78^{\circ}\text{C}$ , **16**( $\text{R}=\text{Me}$ ) gave the *trans*- and *cis*-**26** in a ratio of 4:1. However, **16**( $\text{R}=\text{Bu}^t$ ) gave exclusively the *trans*-**30**. Likewise, whereas **31**( $\text{R}=\text{Me}$ ) gave the *trans*-**29**( $\text{R}=\text{Me}$ ) and the *cis*-**29**( $\text{R}=\text{Me}$ ) in a ratio of 5:1, **31**( $\text{R}=\text{Bu}^t$ ) gave exclusively the *trans*-**32**.



The diastereofacial selectivity of oxepinones **16**( $\text{R}=\text{Me}$ ) in a cycloaddition reaction with 2,4,6-trimethylbenzonitrile-N-oxide gave the *trans*-**33** only. In contrast, **31**( $\text{R}=\text{Me}$ ) gave a 1:1 mixture of the *cis*- and *trans*-**34**. The selectivity is caused mostly by the steric requirements in the transition state. For example, conjugate addition to **16**( $\text{R}=\text{Bu}^t$ ) and **31**( $\text{R}=\text{Bu}^t$ ) occurs preferentially at the less hindered face to give an stable intermediate.

acyclic unsaturated esters in the presence of a catalytic amount of a base. 3-Substituted-8-ring enones have also been studied and shown to undergo photo-induced non-regiospecific deconjugation.<sup>36</sup> Some of these transformation are shown below.

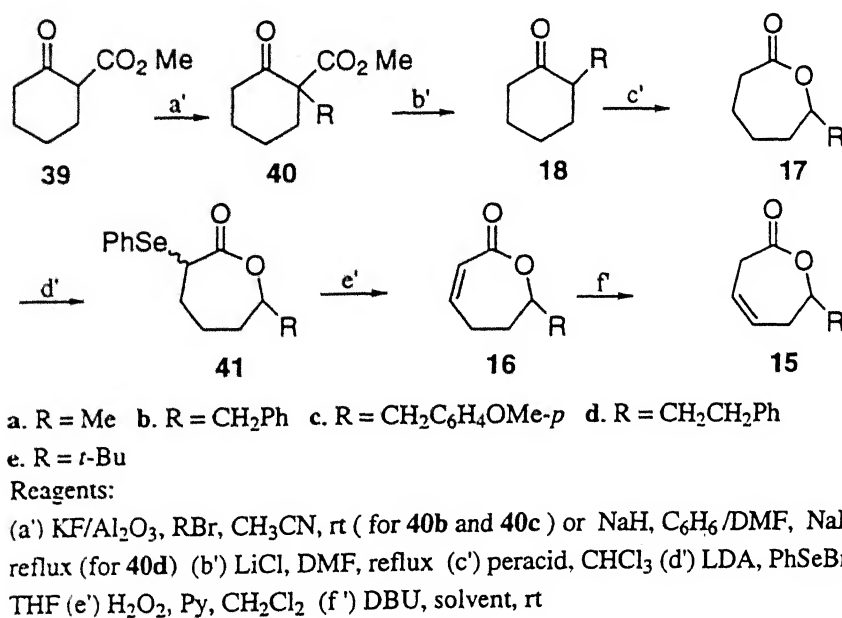


The photo-deconjugation of unsaturated 2-oxepanones **16** appears unreported. However, the requirement of the expensive photochemical equipments and the limitations on the reactant's quantity make the photo-deconjugation less attractive on a preparative scale. We, therefore, set out to explore alternate economical ways to achieve the desired deconjugation. While exploring the epoxidation of  $\alpha,\beta$ -unsaturated carbonyls using  $\text{Bu}^t\text{OOH}$  and DBU, we had isolated, in addition to the expected *cis*- and *trans*-oxiranes, reasonably good amount of the 4,5-dehydro species **15**( $\text{R}=\text{Me}$ ) from the corresponding 3,4-dehydro species **16**( $\text{R}=\text{Me}$ ).<sup>37</sup> This led us to consider using DBU as a base to bring about the requisite deconjugation. In this chapter we describe successful application of DBU (and also DBN) for such deconjugation and the transformation of 7-benzyl-4,5-dehydro-2-oxepanone **15**( $\text{R}=\text{CH}_2\text{Ph}$ ) into the bicyclo[3.3.0] skeleton **11**.

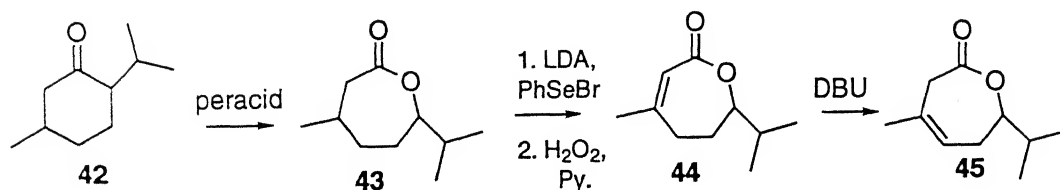
### 3.2.1 Preparation of starting materials

The requisite starting materials **16b-e** were prepared as per the sequence given in the Scheme 3.2. 2-Carbomethoxy cyclohexanone **39** was subjected to alkylation, decarboxylation,<sup>38</sup> Baeyer-Villiger oxidation,<sup>39</sup> selenenation and selenoxide elimination,<sup>22</sup> in that order, to make available the requisite **16b-d**. The 7-methyl derivative **16a** was prepared from the commercially available 2-methyl cyclohexanone (**18**,  $\text{R}=\text{Me}$ ), using a similar protocol and

commencing from the Baeyer-Villiger oxidation. The 3,4-dehydro-7-isopropyl-4-methyl-2-oxepanone **44** was prepared from menthone **42** using a similar sequence of reactions (Scheme 3.3). The requisite 2-*tert*-butylcyclohexanone for the preparation of **16e** was obtained from Lewis acid promoted alkylation of cyclohexanone silylenol ether.<sup>40</sup> The species **18b**,<sup>41</sup> **18c**,<sup>42</sup> **18d**,<sup>43</sup> **17a**,<sup>44</sup> **16a**,<sup>44</sup> and **43**<sup>44</sup> exhibited known <sup>1</sup>H and IR spectral characteristics.



Scheme 3.2:



Scheme 3.3:

The species **16a-e** exhibited vinyl <sup>1</sup>H chemical shifts expected of  $\alpha,\beta$ -unsaturated carbonyls. The carbonyl IR absorptions were also fully supportive of olefin conjugation. The

selenenation reaction furnished, in each instance, a mixture of the two possible isomers of **41** which were not separated because the selenium-containing stereogenic center was soon to be destroyed through selenoxide elimination to generate **16**. DBU and DBN used in the present study were purchased from Fluka and used as received. The  $\text{CDCl}_3$  used for reaction monitoring by  $^1\text{H}$  NMR and for the study of deuterium incorporation in oxepanones was 99.8% in deuterium content and was procured from Sigma, USA.

### 3.2.2 Reaction Monitoring

The transformation of **16** into **15** was monitored by  $^1\text{H}$  NMR in  $\text{CDCl}_3$ . The characteristic absorptions of the olefinic hydrogens in **16** diminished with time and a new set of absorptions characteristic of the olefinic protons in **15** appeared (vide experimental). The relative integrals of these absorptions provided information about the extent of conversion. In the reaction of **44**, a new absorption at  $\delta$  5.44 (br s) appeared at the expense of an absorption at  $\delta$  5.86 (t,  $J=1.2$  Hz) (Fig. 3.16). In the cases of **16b** and **16c**, the reactions were allowed to proceed for 3 h, except when to study equilibration, to achieve 90% conversions when they were quenched with dilute aqueous HCl. The preparative scale isomerizations were carried out in  $\text{CHCl}_3$  for 3 h for **16b** and **16c** (90% conversion) and for 4 h for **16a** and **16d** (quantitative conversion). The deconjugation of **44** was too slow to be preparatively useful.

### 3.2.3 Deconjugative isomerization

7-Benzyl-3,4-dehydro-2-oxepanone **16b** was reacted with one equiv of DBU in  $\text{CDCl}_3$ . There was 90% deconjugation to **15b** in 3 h. Interestingly, in an equilibrium study in  $\text{CDCl}_3$ , a continuous drop in the concentration of **15b** with a corresponding rise in the concentration of **16b** was noticed after the initial 3 h. A 2:3 ratio of **16b**:**15b** was achieved in 25 h. The observation that this ratio did not change afterwards suggested the above to

have constituted the equilibrium point.

Table 3.1: Deconjugative isomerization of the 7-ring lactones

16 into 15 and 44 into 45<sup>a</sup>

substrate	time (h)	conversion <sup>b</sup> (%)	yields <sup>c</sup> (%)	equil. time <sup>d</sup> (h)	equil .ratio <sup>e</sup>
<b>16a</b>	03	100	quant.	no equil.	-
<b>16b</b>	03	90	90	25	2:3
<b>16c</b>	03	90	90	25	2:3
<b>16d</b>	03	100	quant.	no equil.	-
<b>16e</b>	03	100	quant.	no equil.	-
<b>44</b>	24	20	18	na	-

<sup>a</sup> All the reactions were conducted in CHCl<sub>3</sub> at 0.05 mmol scale. <sup>b</sup> Deduced from <sup>1</sup>H spectral integrals of the characteristic signals. <sup>c</sup> The actual isolated yields based on the total conjugated lactone taken. <sup>d</sup> There was no observable change in the ratio after the indicated time. <sup>e</sup> Calculated from <sup>1</sup>H integrals of the products mix after aqueous acidic workup.

The above 2:3 equilibrium composition is indicative of small energy difference between **15b** and **16b**. The observation that the deconjugated species is more abundant than the conjugated counterpart is to show the diminished effectiveness of conjugation between the carbonyl and the double bond in medium ring lactones in comparison to the conjugation in the small ring systems. Whitham<sup>45</sup> and Hirsch<sup>46</sup> have made similar observations and advanced a rationale. In a reaction with only catalytic amount of DBU (10 mol%) in Al<sub>2</sub>O<sub>3</sub>-filtered CDCl<sub>3</sub>, 90% deconjugation took place in 100 h; sustained exposure caused a slow reversal of the reaction. Further, in an experiment in which **15b** was allowed to stand with 10 mol% DBU in Al<sub>2</sub>O<sub>3</sub>-filtered CDCl<sub>3</sub>, the formation of **16b** was detected by <sup>1</sup>H NMR after 60 h. The same reaction with 1 equivalent of DBU was much faster and the equilibrium

16b:15b=2:3 was established in 50 h. The related 7-*p*-methoxybenzyl derivative **16c** behaved in a similar fashion. There was 90% deconjugation with one equivalent of DBU in the first 3 h; the reversal began thereafter to attain 16c:15c=2:3 equilibrium in 25h.

We have also treated the 7-(2-phenethyl) derivative **16d** with DBU in CDCl<sub>3</sub> under similar conditions. Interestingly, the only product obtained even after 50 h was that of deconjugation. This behavior is similar to that of the 7-methyl and 7-*tert*-butyl analogs. All the results on isomerization have been collected in the Table 3.1 for a convenient comparison. The difference in the behaviors of the 7-methyl and the 7-benzyl species in regard to the onset of equilibrium is not understood.

### 3.2.4 Deuterium incorporation

From each of the isomerization experiments with **16a-e** and **44** in CDCl<sub>3</sub>, there was observed a prominent enhancement in the <sup>1</sup>H signal for CHCl<sub>3</sub>. This led us to critically examine the lactones **16b** and **15b** obtained from a full equilibration experiment for a possible deuterium incorporation. From a combination of <sup>1</sup>H and <sup>1</sup>H-decoupled <sup>13</sup>C NMR spectra, partial deuterium incorporation at positions 3 and 5 was deduced. While the absorptions for protons on positions 3 ( $\delta$  5.99-5.95, dd,  $J=12$  and 1.5 Hz) and 5 ( $\delta$  2.54-2.26, m) in **16b** integrated less than the requisite one and two protons (Fig.3.6), respectively, the <sup>13</sup>C spectrum (Fig. 3.7) showed two triplets centred at  $\delta$  122.31 (C3) and 31.15 (C5). These carbons in the undeuterated species absorbed at  $\delta$  122.27 and 31.24, respectively. From the relative integrals, the level of deuterium incorporation at both the positions was computed at approximately 40%. The same set of NMR spectra of **15b** were similarly instructive. The absorptions of the vinyl proton on C5 ( $\delta$  5.69-5.61, m) and that of one proton on C3 ( $\delta$  3.07-2.99, dd,  $J=16.5$  and 8.7 Hz) integrated less than the requisite one full proton each (Fig. 3.8). The extent of deuterium incorporation was calculated, once again, at approximately 40% from the relative <sup>1</sup>H integrals. Interestingly, the other proton at C3

( $\delta$  3.64, bd,  $J=16.5$  Hz) integrated one full proton. This is of conformational significance. Presumably, only the C3-H which is near orthogonal to the  $\sigma$ -plane of the double bond in the chair-like conformation must have undergone the observed deuterium exchange. These findings were confirmed further from the  $^{13}\text{C}$ -D splittings (Fig. 3.9). While a triplet centred at  $\delta$  34.87 ( $\delta$  34.98 in the nondeuterated material) for C3 indicated only one deuterium atom on it, another triplet centred at  $\delta$  118.6 ( $\delta$  118.7 in the nondeuterated material) for C5 confirmed the deuterium incorporation at this position as well. These deuterium incorporations were confirmed from the EIMS of 15c obtained from a full equilibration study in  $\text{CDCl}_3$ ;  $M^+$  signal increased from  $m/z$  232 to  $m/z$  234 (Fig. 3.30).

To investigate the possible role of DBU in the observed deuterium incorporation, it was mixed with  $\text{CDCl}_3$  and the  $^1\text{H}$  spectra recorded at various intervals. With the lapse of time, strong  $\text{CHCl}_3$  absorption appeared. Further, there was a consistent reduction in the intensity of C6-methylene absorption (60 MHz,  $\delta$  2.35, bs). The intensity was reduced to half after 12 d at 30-35°C. Some decomposition (not investigated) commenced thereafter. That the reduction in C6-methylene absorption intensity was necessarily due to the deuterium incorporation was supported from EIMS of such a DBU; the  $M^+$  signal increased from  $m/z$  152 to  $m/z$  153 (100%) (Fig. 3.29). Though the above decomposition is not understood, only one deuterium atom incorporation bears significance.

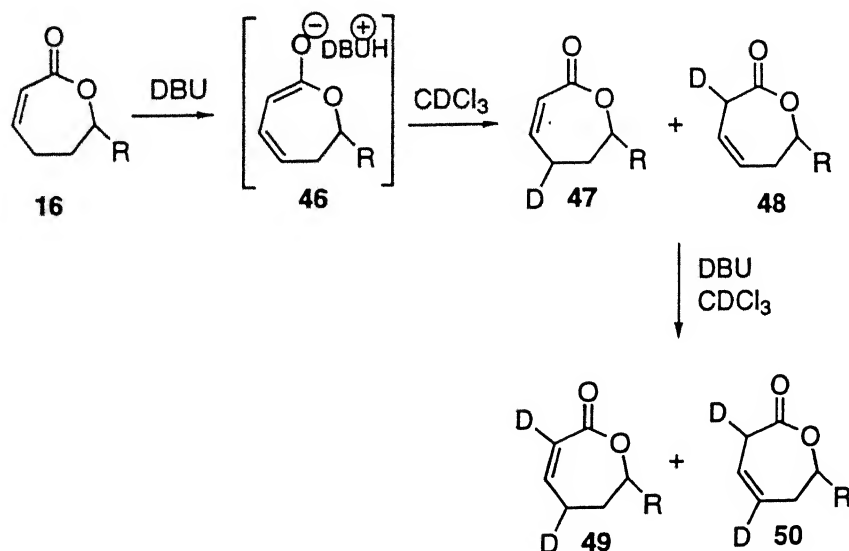
Stereoelectronic considerations suggest that only the C6-methylene hydrogen which is orthogonal to the  $\sigma$  plane of the adjacent  $\text{C}=\text{N}$  double bond in the rigid bicyclic structure of DBU must be exchanged. To determine whether this deuterium came exclusively from  $\text{CDCl}_3$  and not from  $\text{DCl}$  which may be present in samples of  $\text{CDCl}_3$ , and, also, whether the isomerization was indeed base catalysed, two discrete experiments were performed:

- mixing  $\text{DCl}$ -free  $\text{CDCl}_3$  (filtered through basic  $\text{Al}_2\text{O}_3$  of Brockmann grade I) and DBU showed repetition of the facility of deuterium incorporation and the remarkable rise in the  $\text{CHCl}_3$  absorption and



- a reaction of **16b** in THF with one equiv of DBU was as fast as the one in  $\text{CDCl}_3$ .

Thus, while the first experiment confirmed  $\text{CDCl}_3$  as the primary source of deuterium, the second experiment proved, beyond doubt, that all the isomerizations in the present study were only base-catalysed. Both the experiments showed little catalytic role of DCl. Otherwise also, had all the deuterium come only from DCl and none from  $\text{CDCl}_3$ , the enhancement in  $\text{CHCl}_3$  absorption must not have been observed.



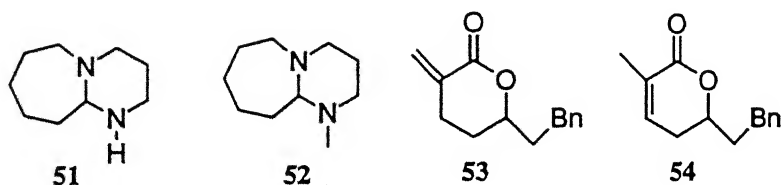
Scheme 3.4:

The dienolate formed on  $\text{H}^+$  abstraction by DBU from C5 of the 3,4-dehydro-2-oxepanones **16** may pick up  $\text{D}^+$  from either  $\text{CDCl}_3$  or  $[\text{DBU-D}]^+$  to result in the observed C5-deuterated-3,4-dehydro-2-oxepanones **47** and the C3-deuterated-4,5-dehydro-2-oxepanones **48**. These species will, of course, react again in an iterative process to generate the eventually observed C3,C5-dideuterated materials **49** and **50** (Scheme 3.4).

### 3.2.5 Significance of the imine double bond

$\text{Pr}_2\text{NEt}$ ,  $\text{Et}_3\text{N}$  and DABCO were also attempted but they all failed to bring about de-

conjugation in **16**. In each instance, the starting material was recovered quantitatively. The success of DBU at the above isomerizations clearly established its superiority over the other common nitrogenous bases and invited for a better understanding of the inherent reasons.



To this end, DBU was reduced<sup>47, 48</sup> to the corresponding fully saturated species **51** and allowed to react with **16b** in  $\text{CDCl}_3$ .  $^1\text{H}$  NMR monitoring confirmed no isomerization even after 24 h. The alternate 1,4-addition of the amine<sup>49-51</sup> to the lactone did not take place either. Identical results were obtained from the related N-methyl derivative **52**. These failures, when taken together with the success of DBU, pointed to a definite positive role of the imine double bond in DBU in the above deconjugations. The structural similarity between DBU and DBN allowed us to consider the latter as well. The material **16b** reacted smoothly with DBN and 90% of **15b** was formed in <2.5 h. Though DBN appears slightly better than DBU, economy approves DBU. Clearly, the positive role of DBU must be ascribed to its enamine character.

### 3.2.6 Attempted deconjugation of systems other than the 7-ring lactones: A comparison

Enthused with the success of DBU-promoted deconjugations, we wished to study the smaller  $\delta$ -valerolactones and acyclic examples. In the event, DBU was added to a  $\text{CHCl}_3$  solution of a mixture of 3-methylidene-6-(2-phenethyl)- $\delta$ -valerolactone (**53**)<sup>37</sup> and 3-methyl-3,4-dehydro-6-(2-phenethyl)- $\delta$ -valerolactone (**54**) to observe a very clean transformation of the former into the latter. The exo-methylene hydrogens in **53** [ $\delta$  6.5 (q,  $J=2$  Hz) and  $\delta$

5.6 (q,  $J=2$  Hz)] disappeared and the signal for the olefinic hydrogen in **54** [ $\delta$  6.6 (1H, m)] intensified. Further deconjugation in **54** did not occur. To the best of our information, this appears to be the first report on such an isomerization. The facility with which this isomerization took place is indeed remarkable. In the cycloalkanone series, similar isomerizations have been reported with the use of  $\text{RhCl}_3 \cdot 3\text{H}_2\text{O}$  in a mixture of  $\text{CHCl}_3$  and  $\text{EtOH}$  under conditions of reflux<sup>52</sup> and with  $\text{Bu}^t\text{OK}$  in  $\text{Bu}^t\text{OH}$  at 50-55 °C,<sup>53</sup> both for several hours. Deprotonation of **53** at C4 by DBU followed by protonation of the resultant allyl anion must constitute the necessary pathway for the observed isomerization.

Acyclic  $\alpha,\beta$ -unsaturated esters were found inert to DBU. The *trans*-methyl 3-benzylacrylate did not react even though the  $\text{C}_\gamma$ -hydrogens will be considered more reactive than the  $\text{C}_5$ -hydrogens in 3,4-dehydro-2-oxepanones for their enhanced acidity due to

- (a) the additional benzylic nature and
- (b) the *transoid* disposition to the ester function.

Ethyl 3,3-dimethylacrylate, which has a methyl replacing the  $\text{C}_5$ -methylenes in the 3,4-dehydro-2-oxepanones, was also inert to DBU.

The inertness of *trans*-methyl 3-benzylacrylate and ethyl 3,3-dimethylacrylate to deconjugative isomerization led us to study a 4-substituted oxepanone to ascertain the site of isomerization (*endo*- vs *exo*-cyclic). Our choice of substrate was **44** which was readily prepared from menthone in an overall 50% yield. In the event **44** was mixed with one equivalent of DBU in  $\text{CDCl}_3$ , there was noted a very slow reaction. Only the product of *endo*-cyclic deconjugation was observed from  $^1\text{H}$  NMR after 30 h. The diminution in the characteristic olefinic  $^1\text{H}$  absorption at  $\delta$  5.86 (t,  $J=1.2$  Hz) in **44** led to a new absorption at  $\delta$  5.44 (br s) (Fig. 3.16). This much slower rate of deconjugation in comparison to the other 7-ring species is due presumably to the steric effects arising from both the ring substituents. Two interesting points, therefore, emerge :

- the *cisoid*  $\text{C}_5$ -methylene is appreciably more susceptible to  $\text{H}^+$  abstraction by DBU

than the *transoid* C5-methyl in 3,4-unsaturated-2-oxepanones.

- while the *cisoid* C5-methylene in 3,4-unsaturated-2-oxepanones is reactive, the *cisoid* C3-methyl in the acyclic 3,3-dimethyl acrylate is not.

In the rigid conformation of **16**, all but C6 ring atoms are nearly coplanar for the requirement of delocalization.<sup>21</sup> This causes considerable strain in the molecule and also fixes one of the two C5-hydrogens orthogonal to the olefin's  $\sigma$  plane for their effective interaction. These two are believed to contribute to the observed lability of the 2-oxepanones to DBU. While the orthogonality factor will raise the acidity of the hydrogen considerably, the relief from ring strain on deconjugation may be equally significant.

### 3.2.7 Application to the synthesis of a pharmacophore

The above deconjugation in the 2-oxepanones is important in synthetic organic chemistry. The favorable economy, the operational simplicity, and the possible further synthetic transformations of the deconjugated materials are noteworthy and worth exploitation in fruitful synthetic endeavors. In demonstration of such an utility, **15b** was reacted with peracid. From the mixture of the two oxiranes produced, the less polar material was the *trans*-**14b** and the more polar the *cis*-**14b** (Scheme 3.5). The *cis/trans* assignment of the oxiranes was made from the X-ray structure of a bicyclic derivative (**11B**) of the *cis* oxirane (*vide infra*).

Since the oxiranes are precursor for the bicyclic derivatives, we have studied the epoxidation of the 4,5-dehydro-2-oxepanones. Both peroxybenzoic acid (PBA) and *m*-chloroperbenzoic acid (*m*-CPBA) were used for the epoxidation. The results are collected in the Table 3.2. The amount of the *trans* oxirane was higher from reaction with *m*-CPBA than that obtained from PBA. The ratios were calculated from the integrals of 300MHz <sup>1</sup>H NMR spectra. When the C7-substituent was Bu<sup>t</sup>, the epoxidation was the most selective; only the *trans* isomer was isolated.

Table 3.2: Epoxidation of 7-substituted-4,5-dehydro-2-oxepanones **15**

R	PBA	<i>m</i> -CPBA
	cis:trans <sup>a</sup>	cis:trans <sup>a</sup>
CH <sub>3</sub>	1.0:2.3	1.0:3.0
PhCH <sub>2</sub>	1.0:1.9	1.0:2.7
PhCH <sub>2</sub> CH <sub>2</sub>	1.0:1.7	1.0:1.8
Bu <sup>t</sup>	0:1	0:1

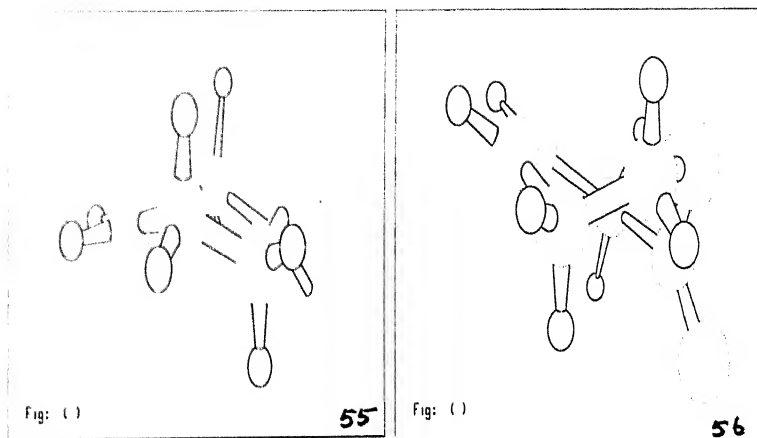
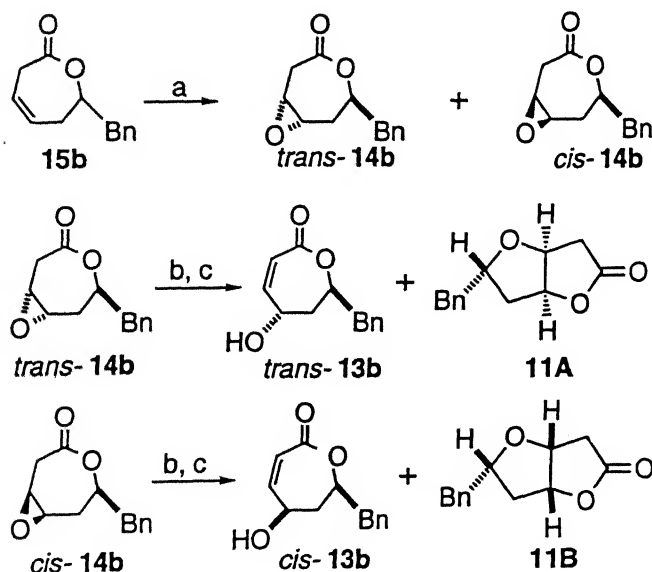


Figure 2.2: Computer generated plot of the chair- and boat-like conformers of the 4,5-dehydro-2-oxepanone.

We have located two minima on the ground state potential energy surface at 6-31G\* level. These are represented by the chair conformer **55** and the boat conformer **56**. The chair conformer is 0.3 kcal/mol more stable than the boat conformer. This energy difference is very small to allow both the conformers to exist in equilibrium at 0 °C to room temperature. However, inclusion of a substituent on C7 will be expected to raise the energy of the boat conformer **56** for the steric interactions of the C7-substituent with the hydrogens on C3 and C5. The observed *trans* epoxidation of **55** can be explained only by a preferential complexation of the peracid with the carbonyl oxygen and, hence, complexation-controlled

delivery of the *per* oxygen. Direct epoxidation will, however, generate the *cis* oxirane. The above complexation of the carbonyl oxygen and peracid in the boat conformer will not be meaningful for the large separation of the former from the site of oxidation. Direct oxidation, once again, will furnish the *cis* oxirane. In the 7-ring lactone bearing a Bu<sup>t</sup> substituent on C7, the substituent is far away from the reaction site and, as such, may not be expected to interfere with the oxidation process. The observation of a single *trans* oxirane appears, therefore, unexpected. However, for the large steric interactions of the Bu<sup>t</sup> butyl group with the hydrogens on C3 and C5, the boat conformer may be raised further in energy, probably to the extent that it is no more present at equilibrium with the chair form. The higher *trans* selectivity in oxidation with *m*-CPBA over that with PBA may be due to the expected slightly better complexing ability of the former oxidant.



Reagents:

(a) peracid, CHCl<sub>3</sub>, rt (b) K<sub>2</sub>CO<sub>3</sub>, DMF (c) 5% aq HCl

The materials 13b, 14b & 11 are mixtures of diastereomers.

For reasons of clarity, only one diastereomer of each is shown.

Scheme 3.5:

The *trans*-14b was reacted further as shown to afford a mixture of *trans*-7-benzyl-3,4-

dehydro-5-hydroxy-2-oxepanone (**13b**) and 7-*exo*-benzyl-2,6-dioxo-3-oxobicyclo[3.3.0]octane (**11A**). The ratio **13b**:**11A** in the mixture was found to be dependent on the duration of the reaction; longer reaction time favored the bicyclic species **11A**. The *cis*-**14b**, on the contrary, furnished predominantly the bicyclic material **11B** under identical conditions. The related *cis*-7-benzyl-3,4-dehydro-5-hydroxy-2-oxepanone (**13b**) was formed, if at all, in small amounts only (TLC) and escaped isolation. That the materials **11A** and **11B** were epimeric was evident from very similar  $^1\text{H}$  absorptions. While a COSY spectrum (Fig. 3.26) helped to locate the various hydrogens in **11A**, a ROESY spectrum (Fig. 3.27) established the *cis* relationship of the benzyl group and the hydrogens on the ring junctions. There were interactions observed between the Ph group and the hydrogen on C5 and between the benzylic methylene and the hydrogen on C8 which is *cis* to the hydrogen on the adjacent ring junction. The stereostructure of its progenitor, the oxirane *trans*-**14b**, must, therefore, be treated as confirmed. Obviously, the stereostructure of the other oxirane must be as in *cis*-**14b** and that of the bicyclic species derived from it as **11B**. This was confirmed further from a single crystal X-ray structure determination of **11B**. An ORTEP plot is presented in Fig. 3.3.

A plausible pathway for the transformation of *trans*-**14b** into **11A** is given in the Scheme 3.6. The intermediacy of the  $\gamma$ -lactone **12b**, produced from the unreacted  $\text{K}^+$  salt on acidification, was confirmed from its isolation and spectral characterization.

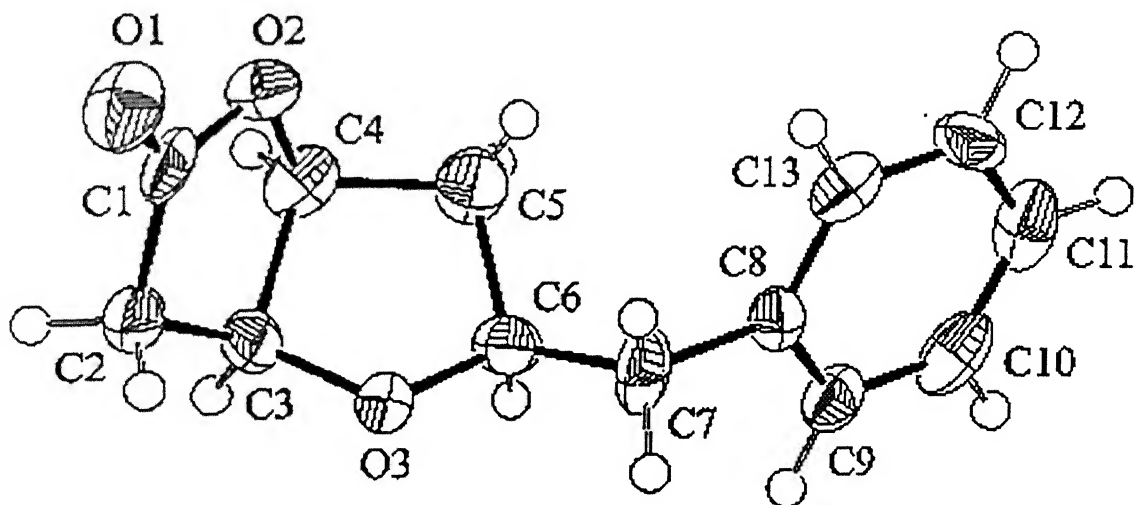
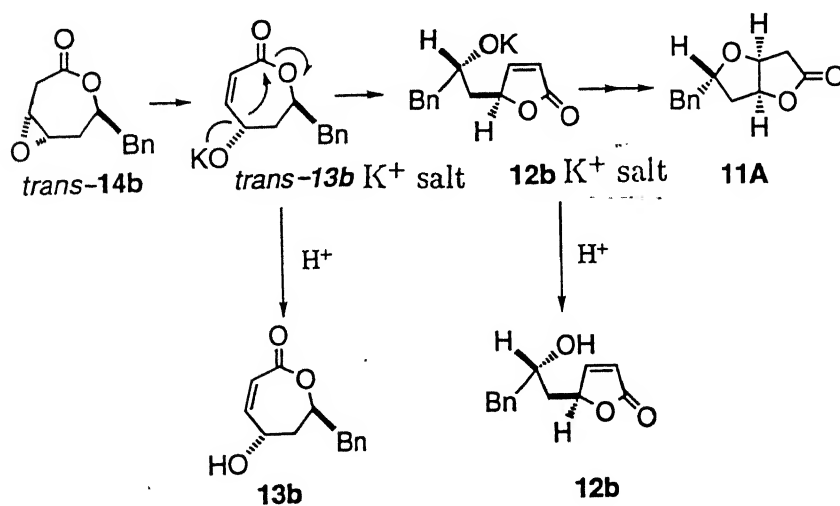


Figure 3.3: An ORTEP plot of **11B**. Selected bond lengths (Å) bond angles (deg), and torsion angles (deg): O2-C4 1.459(7), C1-O2 1.365(7), C1-O1 1.193(7), C3-O3 1.424(7), C6-O3 1.444(7), O1-C1-O2 120.3(6), C1-O2-C4 111.1(5), C3-O3-C6 107.5(5), O2-C4-C5 110.3(6), C7-C6-C5-C4 141.2(6), C3-O3-C6-C7 162.5(5), C8-C7-C6-C5 62.6(8), C9-C8-C7-C6 76.9(9)

### Crystal Data:

MF=C<sub>13</sub>H<sub>14</sub>O<sub>3</sub>, FW=218.25, colourless plate, orthorhombic, Crystal Dimensions= 0.47 X 0.40 X 0.10 mm, a=15.237(2) Å, b=20.217(3) Å, c=7.329(1) Å, V=2257.7(5) Å<sup>3</sup>, Space Group Pbca (#61), Z=8,  $D_{\text{calc}}=1.284\text{g/cm}^3$ ,  $F_{000}=928.00$ ,  $\mu(\text{MoK}\alpha)=0.90\text{cm}^{-1}$ .

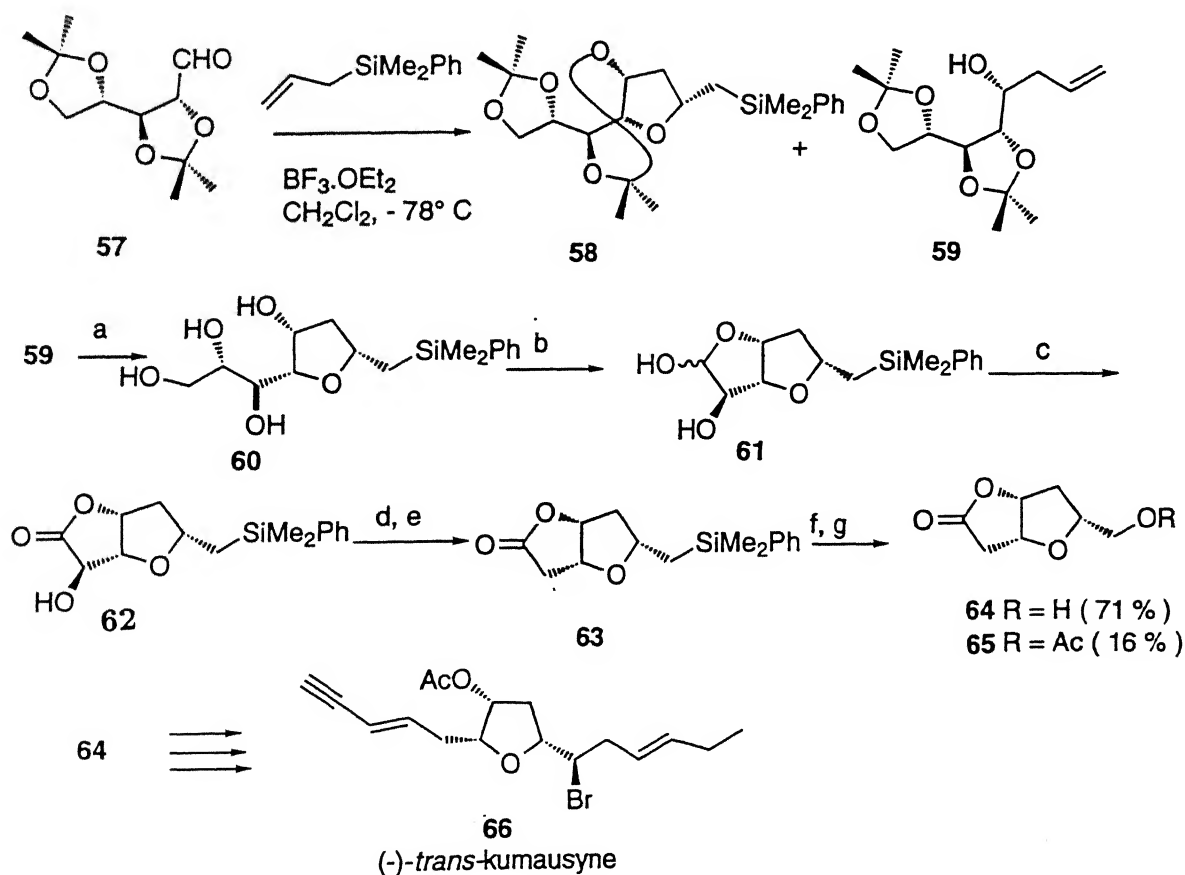


Scheme 3.6:



The significant spectral features are the  $^1\text{H}$  absorptions at  $\delta$  7.57 (1H, dd,  $J=5$  and 1.5 Hz) and  $\delta$  6.10 (1H, dd,  $J=5$  and 2 Hz) for the olefinic hydrogens and at  $\delta$  5.25 (1H, td,  $J=6.5$  and 1.5 Hz) for the hydrogen at C5 (Fig. 3.23). The IR absorption at  $1740\text{ cm}^{-1}$  for the carbonyl supports the assignment. Likewise, the unreacted **13b**( $\text{K}^+$  salt) will produce, on acidification, the observed *trans***13b**. A similar sequence may be considered for the conversion of *cis*-**14b** into **11B**.

Sugimura and Osumi<sup>14</sup> have prepared the key intermediate **64** for the synthesis of (-)-*trans*-Kumausyne **66** from 2,3;4,4-di-O-isopropylidene-*aldehydo*-L-arabinose **57**.

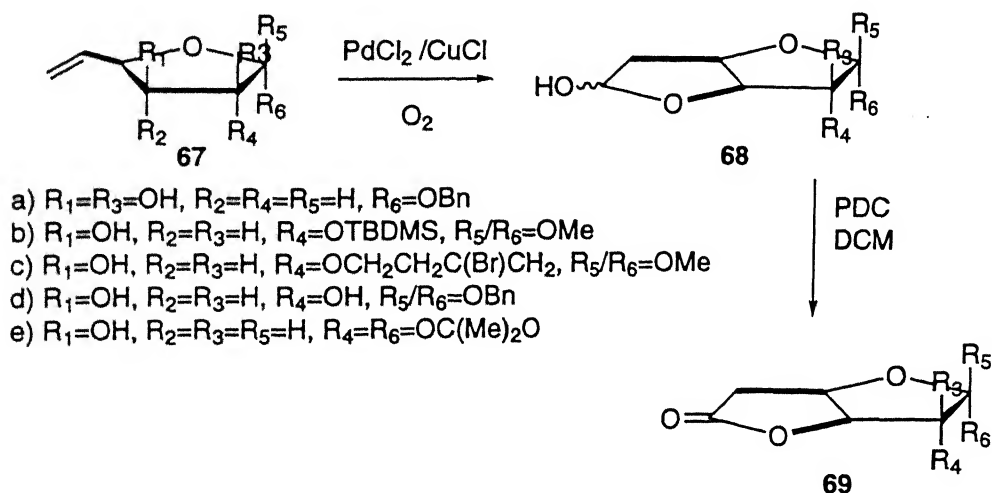


a) Dowex 50W ( $\text{H}^+$ ),  $\text{EtOH} - \text{H}_2\text{O}$  b)  $\text{NaIO}_4$ ,  $\text{EtOH} - \text{H}_2\text{O}$  c) NIS,  $\text{Bu}_4\text{NI}$ ,  $\text{CH}_2\text{Cl}_2$   
 d)  $\text{PhOC(S)Cl}$ , DMAP, MeCN e)  $\text{Bu}_3\text{SnH}$ , AIBN, Toluene, reflux f)  $\text{AcOOH}$ ,  
 $\text{Hg(OAc)}_2$ ,  $\text{AcOH}$

Scheme 3.7:

The species **57** was converted to **58** in a highly stereoselective manner by  $\text{BF}_3 \cdot \text{OEt}_2$ . The isopropylidene group in **58** was removed using an ion exchange resin ( $\text{H}^+$  form). One carbon degradation of the resulting tetrol **60** was carried out with  $\text{NaIO}_4$  to afford the lactol **61** which was converted into the lactone **62** by selective oxidation. Further transformation to the key intermediate **64** involved deoxygenation and Si-C bond cleavage (Scheme 3.7).

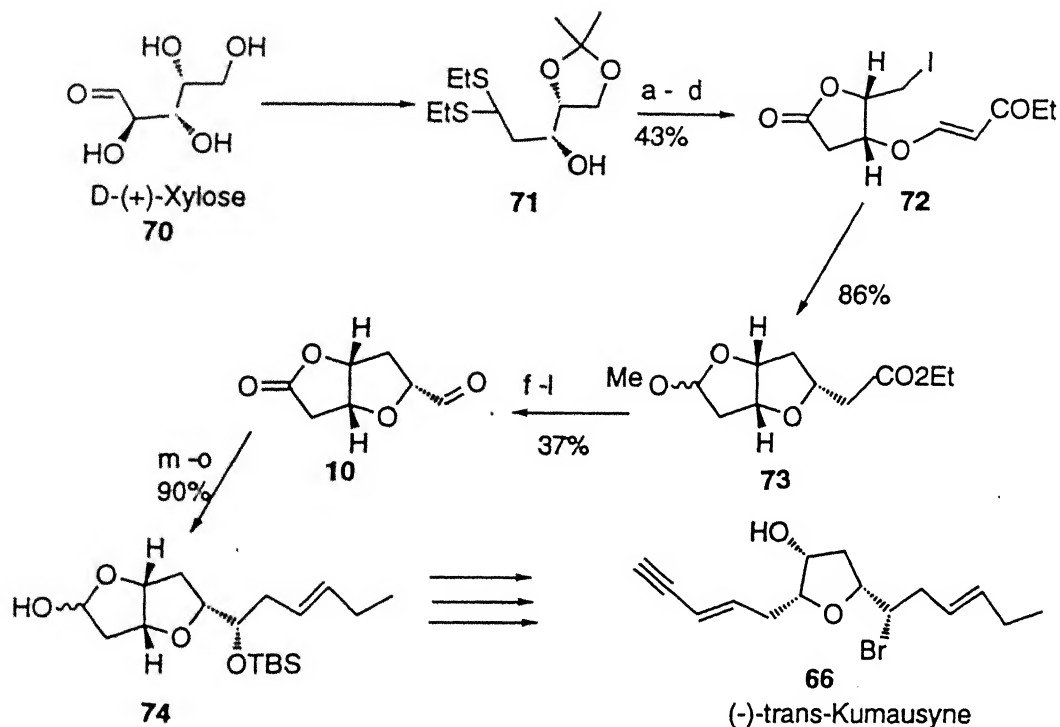
Mereyala and coworkers<sup>54</sup> have prepared the bisfuranosides **69** from Wacker oxidation of the hydroxy vinylfuranoside **67** as shown in the Scheme 3.8.



Scheme 3.8:

Very recently Lee *et al.*<sup>12</sup> have synthesised the aldehydic lactone **10** from D-(+)-xylose **70** as shown in the Scheme 3.9. The bisacetal **71**, prepared from D-(+)-xylose in four steps, was converted into the  $\beta$ -alkoxyacrylate **72** via reaction with ethyl propionate, deprotection with concomitant cyclic acetal formation, tosylation, and iodide substitution. The  $\beta$ -alkoxyacrylate **72** was reacted with tributylstannane under high dilution conditions to yield the bicyclic tetrahydrofuran **73**. The corresponding vinyl derivative obtained from reduction, tosylation, phenylselenide substitution, and selenoxide elimination, in that order, was oxidised to the corresponding lactone. Finally, oxidative removal of one carbon yielded the aldehyde lactone **10** which is a key intermediate in the synthesis of (-)-*trans*-

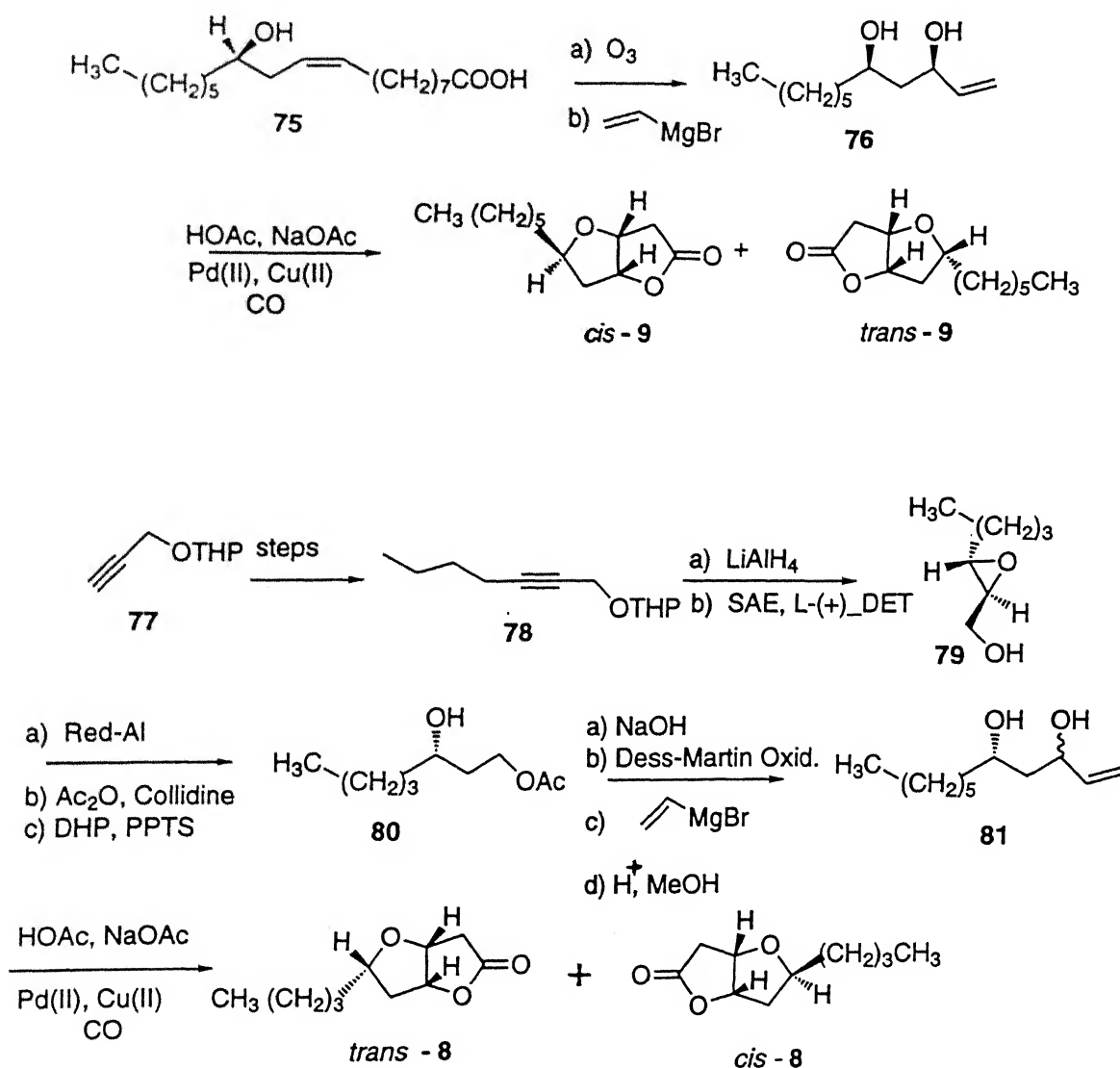
## Kumausyne 66.



- a) HCCCCO<sub>2</sub>Et, NMM, DCM, rt; b) p-TsOH, MeOH, rt, 30 min./1.3eq. PhI(TFA)<sub>2</sub>, rt, 2 h  
 c) p-TsCl, Py., 0 °C; d) 1.5eq. TBAI, Toluene, Reflux  
 e) 1.4eq. Bu<sub>3</sub>SnH, 0.01 eq. AIBN, Benzene (0.02 M), Reflux, 2 h, (Syringe Pump, 3 h).  
 f) LAH, THF, 0 °C; g) p-TsCl, Py., 0 °C h) PhSeNa, EtOH, Reflux; i) H<sub>2</sub>O<sub>2</sub>, EtOH, Reflux  
 j) Jones Reagent, Acetone; k) OsO<sub>4</sub>, NMO, aq. Acetone; l) Pb(OAc)<sub>4</sub>, Na<sub>2</sub>CO<sub>3</sub>, DCM, 0 °C  
 m) 2 eq, CH<sub>2</sub>CHCH(TMS)CH<sub>2</sub>CH<sub>3</sub>, BF<sub>3</sub>·OEt<sub>2</sub>, DCM, -78 °C, r.t.  
 n) TBDMSCl, cat. DMAP, Imidazole, DCM, Reflux; o) DIBAL, Toluene, -78 °C.

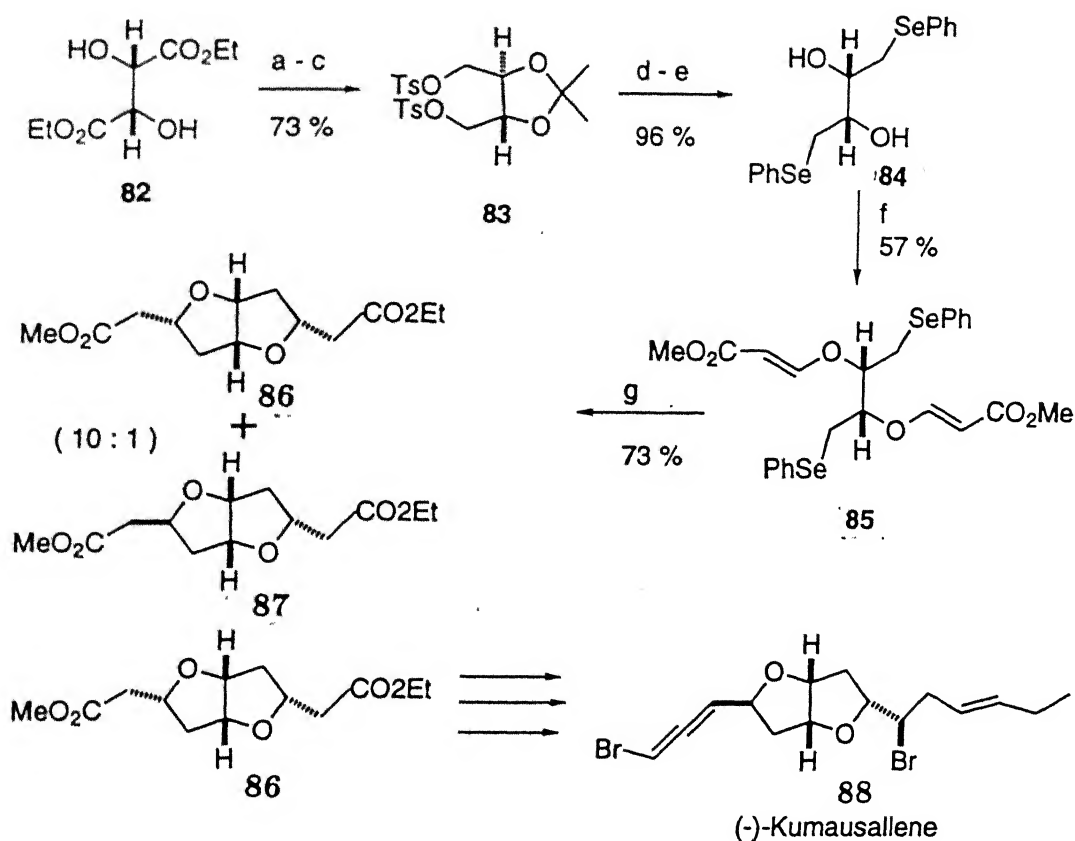
Scheme 3.9:

The first synthesis of the bicyclic lactones 8 and 9 has been reported by Kitching and coworkers.<sup>55</sup> The key step in the synthesis was a palladium(II)-catalysed oxycarbonylation-lactonisation of the unsaturated 1,3-diols 76 and 81 (Scheme 3.10).



Scheme 3.10:

Very recently, Lee *et al.*<sup>56</sup> have reported the synthesis of (-)-Kumausallene 88 from (-)-diethyl D-tartarate 82 as shown in the Scheme 3.11. (-)-Diethyl D(-)-tartarate 82 was converted into the bis(phenylselenide) 84 via the ditosylate 83. Further reaction with methyl propionate produced the bis( $\beta$ -alkoxyacrylate) 85 which, on radical cyclization, proceeded uneventfully to give a 10:1 mixture of the bicyclic products 86 and 87. The material 86 was converted into (-)-Kumausallene 88.



- a)  $\text{Me}_2\text{C}(\text{OMe})_2$ ,  $p\text{-TsOH}$ , Acetone, rt; b) LAH, THF,  $0^\circ\text{C}$   
 c)  $p\text{-TsCl}$ , Py,  $0^\circ\text{C}$ ; d) THF- $\text{H}_2\text{O}$ -TFA (5:2:1), Reflux  
 e)  $(\text{PhSe})_2$ ,  $\text{NaBH}_4$ , EtOH, Reflux; f)  $\text{HCCCCO}_2\text{Me}$ , NMM, DCM, rt  
 g)  $\text{Bu}_3\text{SnH}$ , cat. AIBN, Benzene (0.02 M) Reflux, (Syringe Pump, 4 h)

Scheme 3.11:

### 3.3 Conclusion

In conclusion, we have demonstrated DBU as a base of choice for the deconjugation of 3,4-dehydro-2-oxepanones. Other nitrogenous bases such as  $\text{Pr}_2\text{NEt}$ ,  $\text{Et}_3\text{N}$ , and DABCO failed. LDA and KH, which are much stronger than DBU, also failed. The reactions are base-promoted and cause deuterium incorporation at positions 3 and 5 of 2-oxepanones and position 6 of DBU when conducted in  $\text{CDCl}_3$ . Also, the epoxidation of 4,5-dehydro-2-oxepanones was studied in some detail. That the 4,5-dehydro-2-oxepanones are use-

ful synthetic material has been demonstrated by preparation of 7-exo-benzyl-2,6-dioxo-3-oxobicyclo[3.3.0]octane **11**. This bicyclic skeleton is an important pharmacophore present in several natural products of medicinal significance.

## 3.4 Experimental

### 2-Benzyl-2-carbomethoxycyclohexanone (**40b**).

This material was prepared using KF-Al<sub>2</sub>O<sub>3</sub> as a base.<sup>57, 58</sup> In the event, KF-Al<sub>2</sub>O<sub>3</sub> (4.80 g, 30.0 mmol of KF) was added to a solution of 2-carbomethoxycyclohexanone (1.56 g, 10.0 mmol) and PhCH<sub>2</sub>Br (2.10 g, 12.0 mmol) in dry CH<sub>3</sub>CN (30 mL). The mixture was stirred at rt for 5 h. Filtration and purification furnished the pure product ; 2.26 g, 92%.

<sup>1</sup>H NMR (60 MHz):

δ 7.0 (5H, s), 3.5 (3H, s), 3.2 (1H, d, *J*=14 Hz), 2.7 (1H, d, *J*=14 Hz), 2.5-2.0 (m, 2H), 2.0-1.2 (m, 4H).

IR (film): 1720, 1700 cm<sup>-1</sup>.

### 2-Benzylcyclohexanone (**18b**).

A solution of **40b** (1.132 g, 4.6 mmol) in anhyd DMF (18.5 mL) was mixed with anhyd LiCl (0.39 g, 9.2 mmol) and heated to 145-150 °C under N<sub>2</sub> for 7 h. The mixture was cooled to rt and poured into cold 5% aqueous NaHCO<sub>3</sub> (75 mL) and extracted with ether (3 x 30 mL). The combined extracts were washed with brine (1 x 25 mL), dried, filtered, and concentrated. A chromatographic purification furnished **18b** (0.778 g, 90%) as an oil. This material exhibited the earlier reported <sup>1</sup>H and IR spectral characteristics.<sup>41, 59</sup> For the above decarboxylation with LiCl in DMF, we have discovered that 4 mL of DMF for every mmol of the substrate constituted the optimum. With lower volumes of DMF, considerably large amounts of the corresponding carboxylic acids were formed.<sup>60</sup>

### 7-Benzyl-2-oxepanone (**17b**).

To an ice-cold solution of **18b** (0.376 g, 2.0 mmol) in CHCl<sub>3</sub> (10 mL) was added *m*-

CPBA (70%, 0.740 g, 4.0 mmol). The mixture was allowed to come to rt and stirred for 50 h. This was poured into 20% aqueous  $\text{Na}_2\text{SO}_3$  (10 mL), stirred for 30 min and diluted with  $\text{CHCl}_3$  (10 mL). The layers were separated and the aqueous layer extracted with  $\text{CHCl}_3$  (2 x 5 mL). The combined extracts were washed with 10% aq  $\text{NaHCO}_3$  (2 x 10 mL) and brine (1 x 10 mL), in that order. The organic solution was dried, filtered, and concentrated to furnish a residue which was chromatographed to afford **17b**; 0.40 g, 98%.

$^1\text{H}$  NMR (60 MHz):

$\delta$  7.15 (5H, s), 4.6-4.0 (1H, m), 3.0-2.3 (4H, m), 2.0-1.1 (6H, m).

IR (film) :  $1720\text{ cm}^{-1}$

Anal. Calcd for  $\text{C}_{13}\text{H}_{16}\text{O}_2$ : C, 76.44; H, 7.90. Found: C, 76.58; H, 7.71.

*Trans- and cis-7-benzyl-3-selenophenyl-2-oxepanones (41b).*

*n*-BuLi (1.6 M, 0.75 mL, 1.2 mmol) was added to a solution of  $\text{Pr}_2\text{NH}$  (0.122 g, 1.2 mmol) in THF (1.5 mL) at  $-80^\circ\text{C}$ . This was stirred for 15 min and a solution of **17b** (0.204 g, 1.0 mmol) in THF (2 mL) added dropwise. After 20 min, a THF solution of PhSeBr (1.0 mL, 1.2 mmol) [a solution of PhSeBr in THF was prepared by mixing, for 10 s, a solution of  $\text{Br}_2$  (96 mg, 0.6 mmol) in THF (0.5 mL) with a solution of diphenyl diselenide (188 mg, 0.6 mmol) in THF (0.5 mL)] was added, all in one portion. The reaction was allowed to come to rt and worked up. The mixture was diluted with  $\text{Et}_2\text{O}$  (10 mL) and acidified with 5% aqueous HCl (5 mL). The layers were separated and the organic layer washed successively with  $\text{H}_2\text{O}$  (2 x 5 mL) and 10% aq  $\text{NaHCO}_3$ . The organic solution was dried, filtered, and concentrated to furnish a residue which was purified for **41b** by chromatography; 0.274 g, 76%. Both the *cis*-**41b** and the *trans*-**41b** were isolated and characterized separately.

*Cis-7-benzyl-3-selenophenyl-2-oxepanones (41b)*

$^1\text{H}$  NMR (400 MHz), (Fig. 3.4):

$\delta$  7.60-7.20 (10H, m), 4.50 (1H, m), 4.20 (1H, dd,  $J=12$ , 2 Hz), 3.1 (1H, dd,  $J=12$ , 6 Hz), 2.82 (1H, dd,  $J=12$ , 6 Hz), 2.12 (1H, bd,  $J=14$  Hz), 2.00-1.82 (3H, m), 1.65-1.55 (1H, m), 1.48-1.35 (1H, m).

IR (film) : 1710, 1600  $\text{cm}^{-1}$ .

***Trans*-7-benzyl-3-selenophenyl-2-oxepanones (41b)**

$^1\text{H}$  NMR (400 MHz); (Fig. 3.5):

$\delta$  7.55-7.20 (10H, m), 5.25 (1H, m), 4.25 (1H, t,  $J=4$  Hz), 3.10 (1H, dd,  $J=12$ , 6 Hz), 2.85 (1H, dd,  $J=14$ , 6 Hz), 2.10 (2H, m), 2.00 (1H, td,  $J=12$ , 3 Hz), 1.90-1.75 (2H, m), 1.65-1.55 (1H, m).

IR (film) : 1710, 1600  $\text{cm}^{-1}$ .

**7-Benzyl-3,4-dehydro-2-oxepanone (16b)**

$\text{H}_2\text{O}_2$  (350  $\mu\text{L}$  of a 30% aq solution mixed with 700  $\mu\text{L}$  of  $\text{H}_2\text{O}$ , 3.0 mmol) was added dropwise to a solution of **41b** (0.359 g, 1.0 mmol) and pyridine (0.158 g, 2.0 mmol) in  $\text{CH}_2\text{Cl}_2$  (5 mL) at 0 °C. The solution was stirred for 20 min at 0 °C and at rt for 20 min. This was poured into a mixture of  $\text{CH}_2\text{Cl}_2$  (10 mL) and 5% aqueous  $\text{NaHCO}_3$  (10 mL) and stirred for 5 min. The layers were separated and the aqueous solution extracted with  $\text{CH}_2\text{Cl}_2$  (2 x 5 mL). The combined organic extracts were washed successively with cold 5% aqueous HCl (1 x 10 mL),  $\text{H}_2\text{O}$  (1 x 10 mL), and brine (1 x 10 mL). Drying and solvent removal furnished a residue which was chromatographed to give **16b**; 0.162 g, 80%.

$^1\text{H}$  NMR (300 MHz); (Fig. 3.6):

$\delta$  7.34 (5H, m), 6.41-6.34 (1H, td,  $J=12$ , 4.5 Hz), 5.99-5.95 (1H, td,  $J=12$ , 1.8 Hz), 4.57-4.49 (1H, dq,  $J=7.5$ , 1.8 Hz), 3.19-3.12 (1H, dd,  $J=14$ , 6.5 Hz), 2.91-2.84 (1H, dd,  $J=14$ , 7.0 Hz), 2.54-2.26 (2H, m), 2.15-1.90 (2H, m).

IR (film) : 1700, 1630  $\text{cm}^{-1}$ .

Anal. Calcd for  $\text{C}_{13}\text{H}_{14}\text{O}_2$ : C, 77.20; H, 6.93. Found: C, 77.33; H, 7.05.



**3,4-Dehydro-7-(*p*-methoxybenzyl)-2-oxepanone (16c)**

The above protocol for the transformation of **40b** into **16b** was adopted. The material **18c**, which has earlier been prepared by allowing N-(1-cyclohexenyl)pyrrolidine to combine with 4-methoxybenzyl chloride,<sup>24, 25</sup> was prepared in 88% yield from **40c** and **40c**, itself, was prepared from 2-carbomethoxy cyclohexanone in 90% yield. The yields of the other purified intermediates and **16c** itself and their spectral characteristics are as follows:

**2-Carbomethoxy-2-*p*-methoxybenzyl cyclohexanone (40c):** 90% yield.

<sup>1</sup>H NMR (60 MHz):

δ 7.1-6.8 (4H, m), 3.8 (3H, s), 3.7 (3H, s), 3.3-2.7 (2H, 2d, *J*=14 Hz), 2.6-2.2 (4H, m), 2.0-1.4 (4H, m).

**7-*p*-Methoxybenzyl-2-oxepanone (17c):** 95% yield.

<sup>1</sup>H NMR (60 MHz):

δ 7.2-6.6 (4H, m), 4.5-3.9 (1H, m), 3.7 (3H, s), 3.1-2.4 (2H, 2 dd, *J*=13, 5 Hz), 2.6-2.3 (2H, m), 2.1-1.1 (6H, m).

IR (film) : 1710, 1600 cm<sup>-1</sup>.

Anal. Calcd for C<sub>14</sub>H<sub>18</sub>O<sub>3</sub>: C, 71.77; H, 7.74. Found: C, 71.58; H, 7.90.

***Trans*- and *cis*-7-*p*-methoxybenzyl-3-phenylselenenyl-2-oxepanone (41c)**

This was a 2:1 mixture of the expected *trans*- (δ 5.13, C7-H) and *cis*- isomers (δ 4.40, C7-H) (75% yields), respectively. The chromatographic separation was difficult for the very little difference in the polarities (TLC). However, a small sample of *trans*-**41c** was obtained in a state of purity.

***Trans*-7-*p*-methoxybenzyl-3-phenylselenenyl-2-oxepanone (41c)**

<sup>1</sup>H NMR (300 MHz):

δ 7.55-6.80 (4H, m), 5.13 (1H, m), 4.19 (1H, m), 3.78 (3H, s), 3.03-2.97 (1H, dd, *J*=15 and 6 Hz), 2.81-2.74 (1H, dd, *J*=15 and 6 Hz), 2.12-2.05 (2H, m), 2.05-1.50 (4H, m).

IR (film) : 1705, 1600  $\text{cm}^{-1}$ .

7-*p*-Methoxybenzyl-3,4-dehydro-2-oxepanone (16c): 82% yield.

$^1\text{H}$  NMR (300 MHz); (Fig. 2.10):

$\delta$  7.16 (2H, d,  $J=9$  Hz), 6.84 (2H, d,  $J=9$  Hz), 6.41-6.33 (1H, td,  $J=12$ , 4.5 Hz), 6.00-5.94 (1H, td,  $J=12$ , 1.8 Hz), 4.51-4.43 (1H, m), 3.79 (3H, s), 3.12-3.05 (1H, dd,  $J=14$ , 6 Hz), 2.85-2.78 (1H, dd,  $J=14$ , 6 Hz), 2.60-2.25 (2H, m), 2.07-1.90 (2H, m).

IR (film) : 1695, 1600  $\text{cm}^{-1}$ .

Anal. Calcd for  $\text{C}_{14}\text{H}_{16}\text{O}_3$ : C, 72.39; H, 6.94. Found: C, 72.24; H, 7.20.

### 2-Carbomethoxy-2-(2-phenethyl)cyclohexanone (40d)

2-Carbomethoxy cyclohexanone (0.78 g, 5 mmol) was added dropwise to an oil free suspension of NaH (0.24 g of a 60% oil dispersion, 6.0 mmol) in dry DMF (5 mL) and  $\text{C}_6\text{H}_6$  (15 mL) and the resulting mixture stirred until the gas evolution ceased (10 min). NaI (75 mg, 0.5 mmol) and 2-phenethyl bromide (0.93 g, 5 mmol) were added and the contents refluxed for 1 h. The reaction mixture was cooled to rt, mixed with saturated aqueous  $\text{NH}_4\text{Cl}$  (20 mL) and extracted with ether (2 x 15 mL). The organic extracts were washed with  $\text{H}_2\text{O}$  (2 x 15 mL) and brine (1 x 15 mL), dried, and concentrated. The crude material was purified by chromatography to furnish the desired 40d, 0.94 g, 72%.

$^1\text{H}$  NMR (60 MHz):

$\delta$  7.1 (5H, s), 3.7 (3H, s), 3.0-1.2 (12H, m).

Anal. Calcd for  $\text{C}_{16}\text{H}_{20}\text{O}_3$ : C, 73.82; H, 7.74. Found: C, 73.68; H, 7.86.

### 3,4-Dehydro-7-(2-phenethyl)-2-oxepanone (16d)

This material was prepared from 40d by following the reaction sequence and the experimental procedures given above for the transformation of 40b into 16b. The synthesis of 18d has earlier been accomplished in 15% yield by allowing palladium-assisted coupling of styrene with the Li-enolate of cyclohexanone<sup>43</sup> The yields of 17d, 41d and 16d and their spectral characteristics are as follows:

**7-(2-Phenethyl)-2-oxepanone (17d):** 75% yield.

$^1\text{H}$  NMR (300 MHz); (Fig. 3.12):

$\delta$  7.32-7.17 (5H, m), 4.21-4.16 (1H, m), 2.88-2.50 (4H, m), 2.12-1.4 (8H, m).

IR (film) :  $1710\text{ cm}^{-1}$ .

Anal. Calcd for  $\text{C}_{14}\text{H}_{18}\text{O}_2$  C, 77.03; H, 8.31. Found: C, 77.23; H 8.50.

**Trans- and cis-7-(2-phenethyl)-3-phenylselenenyl-2-oxepanone (41d):** 82% yield.

$^1\text{H}$  NMR (60 MHz):

$\delta$  5.4-4.9 and 4.9-4.5 (1H, m), 4.3-3.8 (1H, m), 3.0-2.6 (2H, m).

IR (film):  $1700\text{ cm}^{-1}$ .

**3,4-Dehydro-7-(2-phenethyl)-2-oxepanone (16d):** 80% yield.

$^1\text{H}$  NMR (300 MHz); (Fig. 3.13):

$\delta$  7.32-7.17 (5H, m), 6.42-6.35 (1H, td,  $J=12$ , 4.5 Hz), 6.02-5.96 (1H, td,  $J=12$ , 2 Hz), 4.32-4.24 (1H, m), 2.86-2.72 (2H, m), 2.58-2.32 (2H, m), 2.17-2.1.95 (3H, m), 1.90-1.80 (1H, m).

IR (film):  $1685\text{ cm}^{-1}$ .

Anal. Calcd for  $\text{C}_{14}\text{H}_{16}\text{O}_2$ : C, 77.75; H, 7.45. Found: C, 77.87; H 7.60.

**3-Phenylselenenyl-7-methyl-2-oxepanone (41a):** 70% yield (isomeric mixture)

$^1\text{H}$  NMR (60 MHz):

$\delta$  7.7-7.2 (5H, m), 5.2-4.7 (1H, m), 4.3-4.0 (1H, bt), 1.3 (3H, d,  $J=6$  Hz).

IR (film) :  $1705\text{ cm}^{-1}$ .

**3,4-Dehydro-7-methyl-2-oxepanone (16a)**

This material was synthesized from 2-methyl cyclohexanone by following the protocol used for the transformation of 18b into 16b. The material 17a<sup>44</sup> was obtained from 18a in 80% yield. The species 41a was transformed into the known 16a<sup>44</sup> in 76% yield.

**3,4-Dehydro-7-isopropyl-4-methyl-2-oxepanone (44)**

Like the synthesis of **16a** from **18a**, the synthesis of **44** commenced from menthone (**42**). The oxidation of **42** proceeded in 70% yield to generate the known **43**.<sup>44</sup> The yield and the spectral characteristic of **44** is given below:

**3,4-Dehydro-7-isopropyl-4-methyl-2-oxepanone (44): 60% yield**

<sup>1</sup>H NMR (300 MHz); (Fig. 3.15):

$\delta$  5.86 (1H, t,  $J=1.2$  Hz), 4.06-4.01 (1H, ddd,  $J=2.7$  Hz), 2.54-2.44 (1H, td,  $J=18, 6$  Hz), 2.33-2.22 (1H, m), 1.94 (3H, s), 1.00-0.97 (6H, 2d,  $J=6.6$  Hz).

Anal. Calcd for C<sub>10</sub>H<sub>16</sub>O<sub>2</sub>: C, 71.38; H, 9.59. Found: C, 71.59; H, 9.85

**7-tert-butyl-2-oxepanone (16e)**

<sup>1</sup>H NMR (60 MHz):

$\delta$  4.0-3.6 (d, 1H), 2.7-1.2 (m, 7H), 1.0 (s, 9H).

**Trans-3-phenylselenenyl-7-tert-butyl-2-oxepanone (41e)**

<sup>1</sup>H NMR (300 MHz):

$\delta$  7.63-7.60 (m, 2H), 7.32-7.27 (m, 3H), 4.56-4.53 (d, 9.6 Hz, 1H), 4.23-4.20 (t, 4.5 Hz), 2.18-1.46 (m, 6H), 1.01 (s, 9H).

**3,4-Dehydro-7-tert-butyl-2-oxepanone (16e)**

<sup>1</sup>H NMR (60 MHz):

$\delta$  6.7-5.8 (m, 2H), 4.1-3.8 (m, 1H), 2.7-1.8 (m, 4H), 1.0 (s, 9H).

**General procedure for isomerization:**

The lactones **16a-e** and **44** (0.05 mmol) and DBU (0.076 g, 0.05 mmol) were mixed together in CHCl<sub>3</sub> (2 mL) [or CDCl<sub>3</sub> (0.4 mL) if the reaction were to be monitored by <sup>1</sup>H NMR] and kept aside for 3 h for **16a-e** and for 30 h for **44** while monitoring the progress by TLC. The workup involved dilution with Et<sub>2</sub>O (10 mL), washing with cold 2% aqueous HCl (2 x 5 mL), water (1 x 5 mL) and brine (1 x 5 mL). The organic solution was dried, concentrated to furnish a residue, and purified. The material balance was near

quantitative.

**7-Benzyl-4,5-dehydro-2-oxepanone (15b)**

$^1\text{H}$  NMR (300 MHz); (Fig. 3.8):

$\delta$  7.34-7.22 (5H, m), 5.69-5.61 (1H, m), 5.58-5.48 (1H, m), 4.93-4.85 (1H, m), 3.67-3.60 (1H, md), 3.13-3.06 (1H, dd,  $J=14$ , 6.8 Hz), 3.07-2.99 (1H, dd,  $J=16.5$ , 8.7 Hz), 2.88-2.81 (1H, dd,  $J=14$ , 6 Hz), 2.45-2.41 (2H, m).

IR (film) : 1720, 1650  $\text{cm}^{-1}$ .

Anal. Calcd for  $\text{C}_{13}\text{H}_{14}\text{O}_2$ : C, 77.20; H, 6.93. Found: C, 77.30; H, 7.10.

**7-*p*-Methoxybenzyl-4,5-dehydro-2-oxepanone (15c)**

$^1\text{H}$  NMR (300 MHz); (Fig. 3.11):

$\delta$  7.17 (2H, d,  $J=8.5$  Hz), 6.85 (2H, d,  $J=8.5$  Hz), 5.69-5.62 (1H, td,  $J=11$ , 3.6 Hz), 5.52 (1H, m), 4.88-4.79 (1H, q,  $J=6$  Hz), 3.79 (3H, s), 3.07-3.00 (1H, dd,  $J=14$ , 6.6 Hz), 2.82-2.75 (1H, dd,  $J=14$ , 6.3 Hz), 2.42-2.40 (2H, m).

Anal. Calcd for  $\text{C}_{14}\text{H}_{16}\text{O}_3$ : C, 72.39; H, 6.94. Found: C, 72.20; H 7.18.

**7-(2-Phenethyl)-4,5-dehydro-2-oxepanone (15d)**

$^1\text{H}$  NMR (300 MHz); (Fig. 3.14):

$\delta$  7.29-7.14 (5H, m), 5.66-5.47 (2H, m), 4.61-4.54 (1H, m), 2.86-2.69 (2H, m), 2.51-2.41 (1H, m), 2.32-2.26 (1H, d,  $J=18$  Hz), 2.07-2.00 (1H, m), 1.86-1.77 (1H, m).

IR (film) : 1715  $\text{cm}^{-1}$ .

Anal. Calcd for  $\text{C}_{14}\text{H}_{16}\text{O}_2$ : C, 77.75; H, 7.45. Found: C, 77.94; H, 7.65.

**4,5-Dehydro-7-isopropyl-4-methyl-2-oxepanone (45)**

$^1\text{H}$  NMR (300 MHz); (Fig. 3.16):

$\delta$  5.44 (1H, bs), 4.46-4.39 (1H, ddd,  $J=2.7$  Hz), 3.80 (1H, bd,  $J=16$  Hz), 2.86 (1H, d,  $J=16$  Hz), 2.44-2.23 (2H, m), 1.93-1.82 (1H, m), 1.79 (3H, s), 1.00-0.96 (6H, 2d,  $J=6.6$  Hz).

Anal. Calcd for  $C_{10}H_{16}O_2$ : C, 71.38; H, 9.59. Found: C, 71.53; H, 9.83.

**7-*tert*-butyl-4,5-dehydro-2-oxepanone (15e)**

$^1H$  NMR (60 MHz):

$\delta$  6.0-5.4 (m, 2H), 3.8-3.4 (m, 1H), 3.1-2.2 (m, 4H), 1.0 (s, 9H).

**1,8-Diazabicyclo[5.4.0]undecane (51)**

Glacial AcOH (0.395 g, 6.5 mmol) was added to an ice-cold solution of DBU (1.0 g, 6.5 mmol) in EtOH (20 mL). To the stirred solution was then added  $NaBH_4$  (0.25 g, 6.5 mmol) in small portions. The reaction was stirred at rt for 2 h whereupon some white solid separated out. The EtOH was removed and the residue taken with EtOAc (20 mL) and  $H_2O$  (2 mL). This resulted in a clear biphasic solution to which was added enough anhyd  $Na_2SO_4$  to absorb the water. Filtration and solvent removal furnished **51**; 0.80 g, 80%. Absence of the broad multiplet at  $\delta$  2.0 for the allylic  $CH_2$  in DBU indicated a complete reduction.

$^1H$  NMR (60 MHz):

$\delta$  3.8-2.9 (1H, br m), 2.9-2.3 (7H, m), 1.9-1.2 (10H, br m).

Anal. Calcd for  $C_9H_{18}N_2$ : C, 70.08; H, 11.76; N, 18.16. Found: C, 69.76; H, 12.00; N, 18.48.

**N-Methyl-1,8-diazabicyclo[5.4.0]undecane (52)**

MeI (2.0 g, 14 mmol) was added to a stirring solution of DBU (1.52 g, 10 mmol) in dry benzene (25 mL) at rt. A white precipitate separated out immediately. The stirring was continued for 30 min and then the solvent was evaporated. The white solid thus received was taken in EtOH (20 mL) and treated with, in portions and under stirring,  $NaBH_4$  (0.38 g, 10 mmol). After 2 h, the EtOH was evaporated and the residue was dissolved in EtOAc (20 mL) and  $H_2O$  (3 mL). Enough  $Na_2SO_4$  was added to absorb  $H_2O$ . Filtration and solvent removal furnished **52**; 1.52 g, 90%.

$^1H$  NMR (300 MHz):

$\delta$  2.85-2.54 (7H, m), 2.47 (3H, s), 1.80-1.59 (10H, m).

Anal. Calcd for  $C_{10}H_{20}N_2$ : C, 71.38; H, 11.98; N, 16.64. Found: C, 71.15; H, 12.24; N, 16.88.

*Trans- and cis-7-benzyl-4,5-epoxy-2-oxepanones (14b)*

To a stirred solution of **15b** (44 mg, 0.22 mmol) in  $CHCl_3$  (0.4 mL) at 5 °C was added  $PhCO_3H$  (0.56 mL of a 0.5 M solution in  $CHCl_3$ ). The mixture allowed to come to rt and stirred for 15 h. Saturated aqueous  $Na_2SO_3$  (3 mL) was added and the contents stirred for 30 min. The reaction was partitioned between  $CHCl_3$  (15 mL) and  $H_2O$  (5 mL). The layers were separated and the aqueous layer extracted with  $CHCl_3$  (2 x 5 mL). The combined organic extracts were washed with 10% aqueous  $NaHCO_3$  (2 x 7 mL) and brine (7 mL). Drying, removal of solvent, and chromatography furnished *trans*-**14b** (28 mg, 60%, mp 78-79 °C) and *cis*-**14b** (14 mg, 30%, mp 86-87 °C), both as powdery solids.

*Trans-7-benzyl-4,5-epoxy-2-oxepanones (14b)*

$^1H$  NMR (400 MHz); (Fig. 3.17):

$\delta$  7.35-7.15 (5H, m), 4.30 (1H, m), 3.30 (1H, m), 3.20-3.10 (2H, m), 3.05 (1H, dd,  $J=12.6$  Hz), 2.96 (1H, dd,  $J=15, 3$  Hz), 2.85 (1H, dd,  $J=12.6$  Hz), 2.45 (1H, d,  $J=15$  Hz), 2.16 (1H, ddd,  $J=15, 10, 2$  Hz).

IR (KBr): 1720, 1590  $cm^{-1}$ .

Anal. Calcd for  $C_{13}H_{14}O_3$ : C, 71.54; H, 6.47. Found: C, 71.61; H, 6.37.

*Cis-7-benzyl-4,5-epoxy-2-oxepanones (14b)*

$^1H$  NMR (400 MHz); (Fig. 3.18):

$\delta$  7.35-7.20 (5H, m), 4.66 (1H, m), 3.41 (1H, unsym d,  $J=15$  Hz), 3.30 (1H, dd,  $J=15, 6$  Hz), 3.2 (2H, m), 3.05 (1H, dd,  $J=15, 6$  Hz), 2.78 (1H, dd,  $J=15, 6$  Hz), 2.37 (1H, dd,  $J=18, 12$  Hz), 2.18 (1H, ddd,  $J=15, 4, 2$  Hz).

IR (KBr) : 1730, 1590  $cm^{-1}$ .

Anal. Calcd for  $C_{13}H_{14}O_3$ : C, 71.54; H, 6.47. Found: C, 71.64; H, 6.58.

*Trans*-7-methyl-4,5-epoxy-2-oxepanone (14a)

The procedure used for the transformation of **15b** into **14b** was followed. The mixture of *trans*-**14a** and *cis*-**14a** was obtained in 95% yield. These were separated into the individual components. The *cis*-**14a**, however, was found unstable and decomposed.

<sup>1</sup>H NMR (200 MHz); (Fig. 3.19):

δ 4.38-4.24 (m, 1H), 3.34-2.96 (m, 3H), 2.42-2.11 (m, 2H), 1.4-1.38 (d, 4.2 Hz, 3H), 1.36-1.25 (m, 1H).

*Trans*-7-(2-phenethyl)-4,5-epoxy-2-oxepanone (14d)

The procedure used for the transformation of **15b** into **14b** was followed. The mixture of *trans*-**14d** and *cis*-**14d** was obtained in 92% yield. These were separated into the individual components. The *cis*-**14d**, however, was found unstable and decomposed.

<sup>1</sup>H NMR (200 MHz); (Fig. 3.20):

δ 7.37-7.05 (m, 5H), 4.08-3.97 (m, 1H), 3.30-3.25 (m, 1H), 3.20-3.08 (m, 2H), 2.90-2.67 (m, 3H), 2.39-2.00 (m, 3H), 1.9-1.72 (m, 1H).

*Trans*-7-*tert*-butyl-4,5-epoxy-2-oxepanone (14e)

The procedure used for the transformation of **15b** into **14b** was followed. The material **14e** was obtained in 97% yield.

<sup>1</sup>H NMR (200 MHz); (Fig. 3.21):

δ 3.76-3.70 (d, 10.8 Hz, 1H), 3.32-3.06 (m, 4H), 2.5-2.42 (dd, 16.15, 0.95 Hz, 1H), 2.16-2.02 (dddd, 2.32 10.85 Hz, 1H), 0.98 (s, 9H).

*Trans*-3,4-Dehydro-5-hydroxy-7-benzyl-2-oxepanone (**13b**) and 7-*exo*-benzyl-2,6-dioxo-3-oxo-bicyclo [3.3.0]octane (**11A**)

K<sub>2</sub>CO<sub>3</sub> (90 mg, 0.66 mmol) was added to a solution of *trans*-**14b** (48 mg, 0.22 mmol) in DMF (1.0 mL). The mixture was stirred at rt for 2 h and then 5 mL H<sub>2</sub>O was added. This was extracted thoroughly with EtOAc (3 x 10 mL). The combined extracts were washed



with brine (10 mL), dried, and concentrated. The residue was chromatographed to afford *trans*-**13b** (36 mg, 75%) and **11A** (10 mg, 20%).

*Trans*-3,4-Dehydro-5-hydroxy-7-benzyl-2-oxepanone (**13b**)

$^1\text{H}$  NMR (60 MHz); (Fig. 3.22):

$\delta$  7.2 (5H, s), 6.3 (1H, dd,  $J=12, 3$  Hz), 5.7 (1H, dd,  $J=12, 1$  Hz), 4.9-4.2 (2H, m), 2.9 (2H, dd,  $J=14, 6$  Hz), 2.3-1.9 (2H, m).

IR (film): 3420, 1695, 1625, 1490  $\text{cm}^{-1}$ .

Anal. Calcd for  $\text{C}_{13}\text{H}_{14}\text{O}_3$ : C, 71.54; H, 6.47. Found: C, 71.41; H, 6.29.

7-*Ero*-benzyl-2,6-dioxa-3-oxo-bicyclo [3.3.0]octane (**11A**)

$^1\text{H}$  NMR (300 MHz); (Fig. 3.24):

$\delta$  7.33-7.18 (5H, m), 5.09-5.06 (1H, t,  $J=5$  Hz), 4.82-4.79 (1H, t,  $J=5$  Hz), 4.40-4.31 (1H, sextet,  $J=6$  Hz), 2.95 (1H, dd,  $J=12, 6$  Hz), 2.85 (1H, dd,  $J=12, 6$  Hz), 2.75 (1H, dd,  $J=18, 6$  Hz), 2.65 (1H, d,  $J=18$  Hz), 2.35-2.29 (1H, dd,  $J=12, 4$  Hz), 1.80-1.71 (1H, ddd,  $J=12, 9, 4$  Hz).

$^{13}\text{C}$  NMR (300 MHz); (Fig. 3.25):

$\delta$  175.7, 137.3, 129.1, 128.3, 126.4, 84.5, 78.6, 77.6, 40.5, 38.1, 36.4.

IR (film) : 1770, 1590  $\text{cm}^{-1}$ .

Anal. Calcd for  $\text{C}_{13}\text{H}_{14}\text{O}_3$ : C, 71.54; H, 6.47. Found: C, 71.48; H, 6.60.

7-*Endo*-benzyl-2,6-dioxa-3-oxobicyclo[3.3.0]octane (**11B**)

This material was prepared from the *cis*-oxirane **14b** (48 mg, 0.22 mmol) by treatment with  $\text{K}_2\text{CO}_3$  (90 mg, 0.66 mmol) in dry DMF for 2 h. Usual workup as above for the transformation of *trans*-**14b** into *cis*-**13b** and **11A** and purification furnished **11B**: 46 mg, 96%. This was recrystallized from a mixture of  $\text{CCl}_4$  and pet-ether; mp 64  $^\circ\text{C}$ .

$\delta$  7.33-7.19 (5H, m), 5.04-4.99 (1H, m), 4.56-4.53 (1H, m), 4.26-4.17 (1H, q,  $J=7$  Hz), 3.04-2.97 (1H, dd,  $J=14$ , 7.2 Hz), 2.86-2.80 (1H, dd,  $J=14$ , 6.3 Hz), 2.75 (2H, d,  $J=4.5$  Hz), 2.44-2.34 (1H, q,  $J=7.2$  Hz), 2.07-1.99 (1H, ddd,  $J=14.4$ , 7.5, 2.1 Hz).

### 3,4-Dehydro-5-(2-hydroxy-3-phenylpropyl)- $\gamma$ -butyrolactone (12b)

On one occasion only, we were able to isolate a small amount of **12b** from the reaction of *trans*-**14b** with  $K_2CO_3$  in DMF (*vide supra*).

$^1H$  NMR (80 MHz); (Fig. 3.23):

$\delta$  7.64-7.50 (1H, dd,  $J=5$ , 1.5 Hz), 7.50-7.10 (5H, m), 6.15-6.05 (1H, dd,  $J=5$ , 2 Hz), 5.40-5.17 (1H, td,  $J=6.5$ , 1.5 Hz), 4.28-3.90 (1H, m), 2.95-2.71 (2H, m), 2.14-1.8 (3H, t,  $J=5$  Hz)

IR (film): 3340, 1740, 1590  $cm^{-1}$ .

Anal. Calcd for  $C_{13}H_{14}O_3$ : C, 71.54; H, 6.47. Found: C, 71.61; H, 6.36.

EIMS  $m/z$  218 ( $M^+$ ).

# References

- [1] Trost, B.M.; Mao, M.K.-T.; Balkovec, J.M.; Buhlmyer, P. *J. Am. Chem. Soc.* **1986**, *108*, 4965.
- [2] Trost, B.M.; Balkovec, J.M.; Mao, M.K.-T. *J. Am. Chem. Soc.* **1986**, *108*, 4974.
- [3] Surivet, J.P.; Vatele, J.M. *Tetrahedron Lett.* **1997**, *38*, 819.
- [4] Mukai, C.; Hirai, S.; Kim, I.J.; Kido, M.; Hanaoka, M. *Tetrahedron*. **1996**, *52*, 6547.
- [5] Gracza, T.; Hasenohrl, T.; Stahl, U.; Jager, V. *Synthesis*. **1991**, 1108.
- [6] Gracza, T.; Jager, V. *Synthesis*. **1994**, 1359, We are thankful to Prof. V.Jager for his reprint.
- [7] Poss, A.J.; Belter, R.K. *Tetrahedron Lett.* **1987**, *28*, 2555.
- [8] Poss, A.J.; Symth, M.S. *Tetrahedron Lett.* **1987**, *28*, 5469.
- [9] Williams, H.J.; Wong, M.; Wharton, R.A.; Vinson, S.B. *J. Chem. Ecology*. **1988**, *14*, 1727.
- [10] Cha, J.K.; Cooke, R.J. *Tetrahedron Lett.* **1987**, *28*, 5473.
- [11] Rossin, R.; Jones, P.R.; Murphy, P.J.; Worsley, W.R. *J. Chem. Soc., Perkin Trans. I*. **1996**, 1323.
- [12] Lee, E.; Yoo, S.; Choo, Y.S.; Cheon, H.S.; Chong, Y.H. *Tetrahedron Lett.* **1997**, *38*, 7757.
- [13] Grese, T.A.; Hutchinson, K.D.; Overman, L.E. *J. Org. Chem.* **1993**, *58*, 2468.
- [14] Osumi, K.; Sugimura, H. *Tetrahedron Lett.* **1995**, *36*, 5789.
- [15] Krishnudu, K.; Krishna, P.R.; Mereyala, H.B. *Tetrahedron Lett.* **1996**, *37*, 6007.
- [16] Surivet, J.P.; Vatele, J.M. *Tetrahedron Lett.* **1996**, *37*, 4373.
- [17] P.-Jones, G.C.; Moore, C.J.; Brecknell, D.J.; Konig, W.A.; Kitching, W. *Tetrahedron Lett.* **1997**, *38*, 3479.
- [18] Grese, T.A.; Hutchinson, K.D.; Overman, L.E. *J. Org. Chem.* **1993**, *58*, 2468.
- [19] Sato, M.; Kuroda, H.; Kaneko, C.; Furuya, T. *J. Chem. Soc., Chem. Commun.* **1994**, 687.

- [20] Cieplak, A.S. *J. Am. Chem. Soc.* **1981**, *103*, 4540.
- [21] Sato, M.; Uehara, F.; Aizawa, K.; Kaneko, C.; Satosh, S.; Furuya, T. *Tetrahedron Lett.* **1996**, *37*, 633.
- [22] Reich, H.J.; Renga, J.M.; Reich, I.L. *J. Am. Chem. Soc.* **1975**, *97*, 5434.
- [23] Ikeda, Y.; Ukai, J.; Ikeda, N.; Yamamoto, H. *Tetrahedron Lett.* **1984**, *25*, 5177.
- [24] Krebs, E.P. *Helv. Chimica Acta.* **1981**, *64*, 1023.
- [25] Hermann, J.L.; Kieczkowski, G.R.; Schlessinger, R.H. *Tetrahedron Lett.* **1973**, 2433.
- [26] Rathke, M.W.; Sullivan, D. *Tetrahedron Lett.* **1972**, 4249.
- [27] Ringold, H.J.; Malhotra, S.K. *tetrahedron Lett.* **1962**, 669.
- [28] Birch, A.J. *J. Chem. Soc.* **1950**, 1551, 2325.
- [29] Gammill, R.B.; Bryson, T.A. *Synthesis.* **1976**, 401.
- [30] Henin, F.; Mortezaei, R.; Pete, J.-P. *Synthesis.* **1983**, 1019.
- [31] Henin, F.; Mortezaei, R.; Muzart, J.; Pete, J.-P. *Tetrahedron Lett.* **1985**, *26*, 4945.
- [32] Pete, J.-P.; Henin, F.; Mortezaei, R.; Muzart, J.; Piva, O. *Pure & Appl. Chem.* **1986**, *58*, 1257.
- [33] Mortezaei, R.; Henin, F.; Muzart, J.; Pete, J.-P. *Tetrahedron Lett.* **1985**, *26*, 6079.
- [34] Skinner, I.A.; Weedon, A.C. *Tetrahedron Lett.* **1983**, *24*, 4299.
- [35] Lombardo, D.A.; Weedon, A.C. *Tetrahedron Lett.* **1986**, *27*, 5555.
- [36] Majetich, G.; Lowery, D.; Khetani, V.; Song, J.-S.; Hull, K.; Ringold, C. *J. Org. Chem.* **1991**, *56*, 3988 and references cited therein.
- [37] Unpublished results.
- [38] Krapcho, A.P. *Synthesis.* **1982**, 893.
- [39] Alphand, V.; Furstoss, R.; Moreau, S.P.; Roberts, S.M.; Willetts, A.J. *J. Chem. Soc., Perkin Trans. 1.* **1996**, 1867.
- [40] Reetz, M.T. *Angew. Chem. Int. Ed. Engl.* **1982**, *21*, 96.
- [41] House, H.O.; Gall, M.; Olmstead, H.D. *J. Org. Chem.* **1971**, *36*, 2361.
- [42] Wimmer, Z.; Romanuk, M. *Collect. Czech. Chem. Commun.* **1981**, *46*, 2573.
- [43] Hegedus, L.S.; Williams, R.E.; McGuire, M.A.; Hayashi, T. *J. Am. Chem. Soc.* **1980**, *102*, 4973.
- [44] Fougne, E.; Rousseau, G. *Synthesis.* **1989**, 661.
- [45] Heap, N.; Whitham, G.H. *J. Chem. Soc. B.* **1966**, 164.

- [46] Hirsch, J.A.; Mease, R.C. *J. Org. Chem.* **1984**, *49*, 2925.
- [47] Anderson, P.S.; Lyle, R.E. *Tetrahedron Lett.* **1964**, 153.
- [48] Anderson, P.S.; Kruenger, W.E.; Lyle, R.E. *Tetrahedron Lett.* **1965**, 4011.
- [49] Stork, G.; White, W.N. *J. Am. Chem. Soc.* **1956**, *78*, 4609.
- [50] Stork, G.; A.F., Kreft; III. *J. Am. Chem. Soc.* **1977**, *99*, 3850,8773.
- [51] Danishefsky, S.; McKee, R.; Singh, R.K. *J. Am. Chem. Soc.* **1977**, *99*, 4783.
- [52] Andrieux, J.; Barton D.H.R. Patin, H. *J. Chem. Soc., Perkin Trans. 1.* **1977**, 359.
- [53] Barton, D.H.R.; Bateson, J.H.; Datta, S.C; Magnus, P.D. *J. Chem. Soc., Perkin Trans. 1.* **1976**, 503.
- [54] Krishnudu, K.; Krishna, P.R.; Mereyala, H.B. *Tetrahedron Lett.* **1996**, *37*, 6007.
- [55] Paddon-Jones, G.C.; Moore, C.J.; Brecknell, D.J.; Konig, W.A.; Kitching, W. *Tetrahedron Lett.* **1997**, *38*, 3479.
- [56] Lee, E.; Yoo, S.; Choo, H.; Song, H.Y. *Tetrahedron Lett.* **1998**, *39*, 3197.
- [57] Yadav, V.K.; Kapoor, K.K. *Tetrahedron.* **1996**, *52*, 3659.
- [58] Yadav, V.K.; Kapoor, K.K. *Tetrahedron Lett.* **1994**, *35*, 9481.
- [59] Henderson, D.; Richardson, K.A.; Taylor, R.J.K.; Saunders. J. *Synthesis.* **1983**, 996.
- [60] Yadav, V.K.; Kapoor, K.K. *Ind. J. Chem.* **1996**, *35B*, 8.

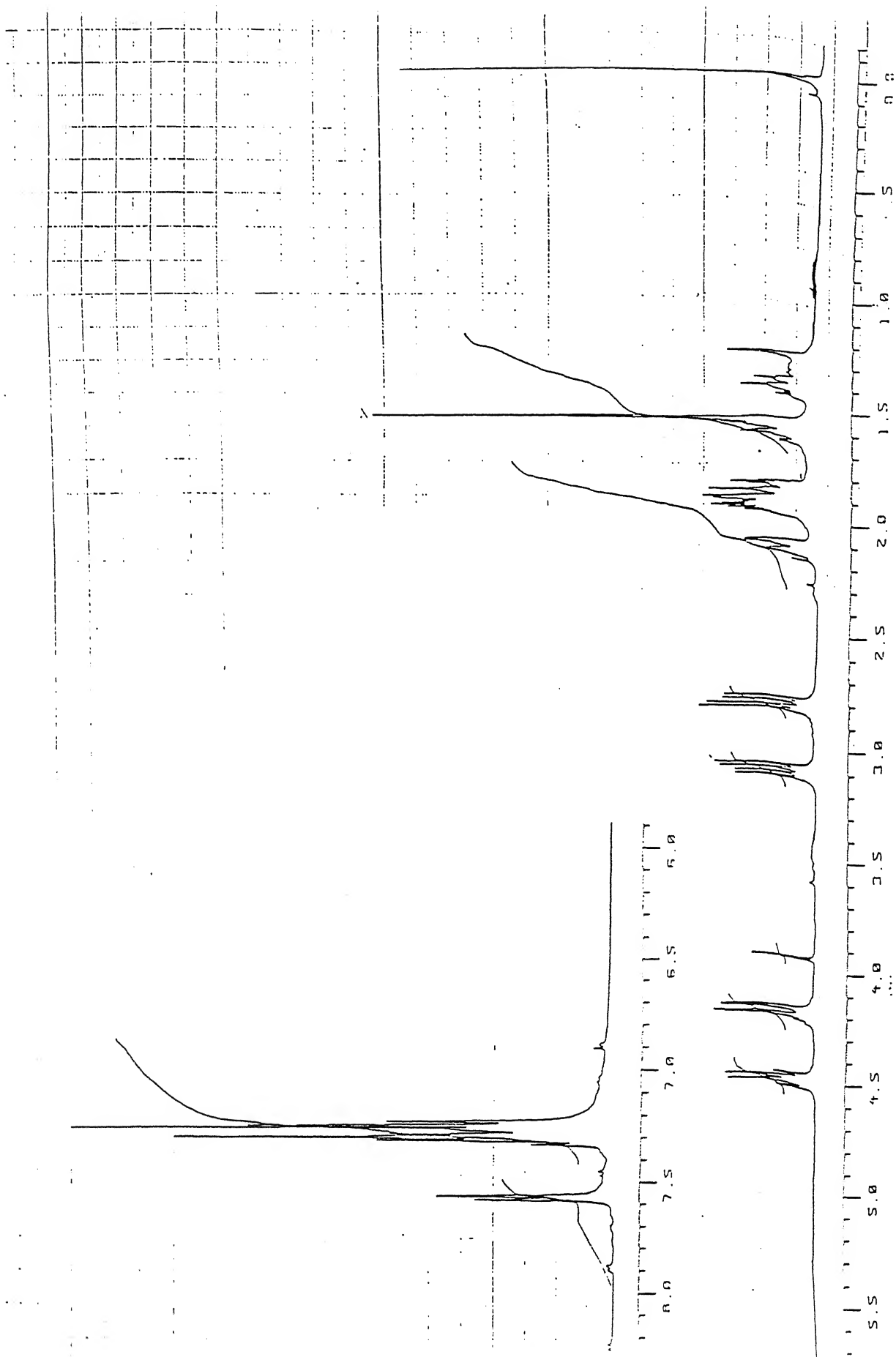


Figure 3.4: 400 MHz  $^1\text{H}$  NMR spectra of *cis*-41b

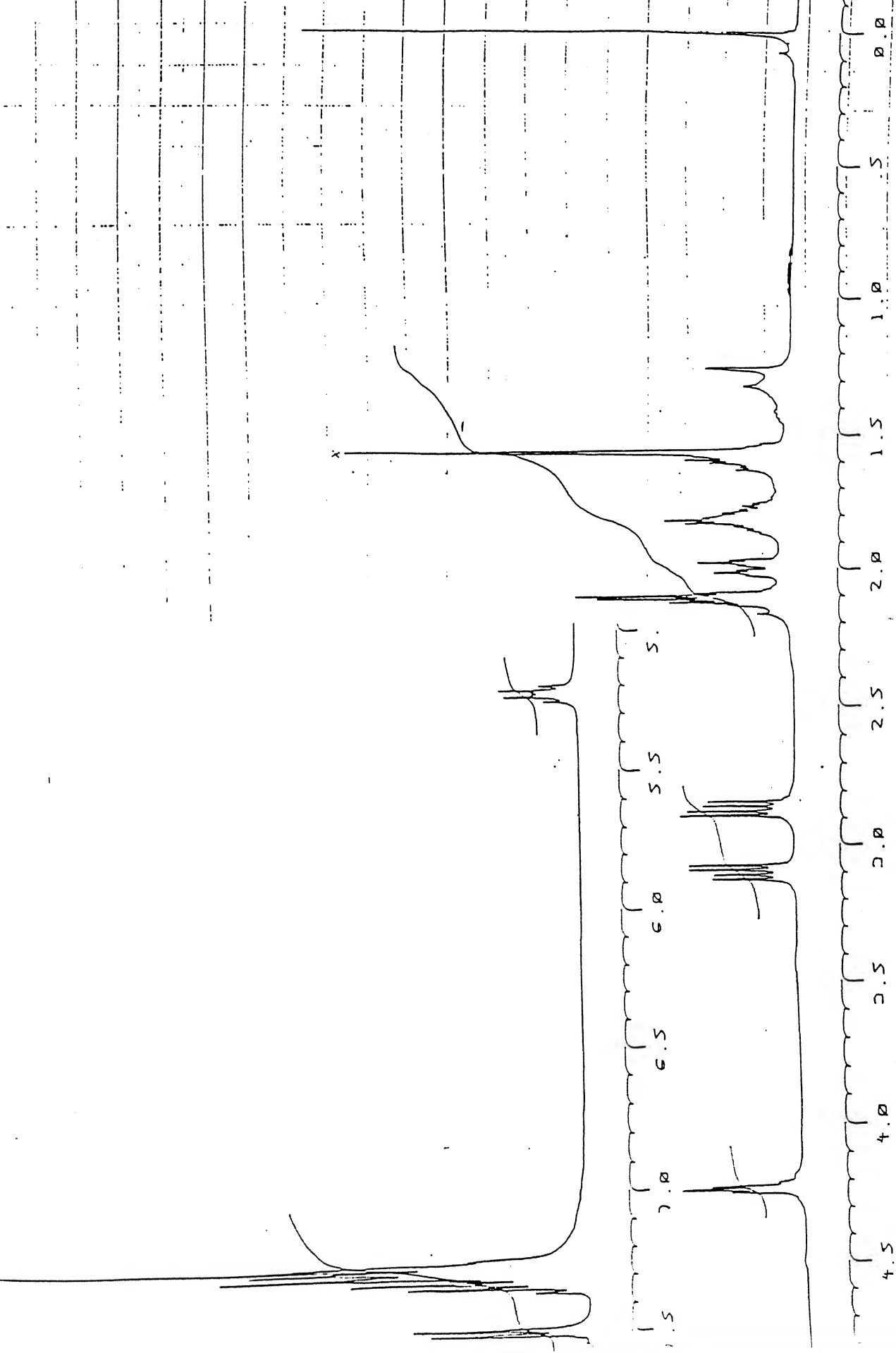


Figure 3.5: 400 MHz  $^1\text{H}$  NMR spectra of *trans*-41b

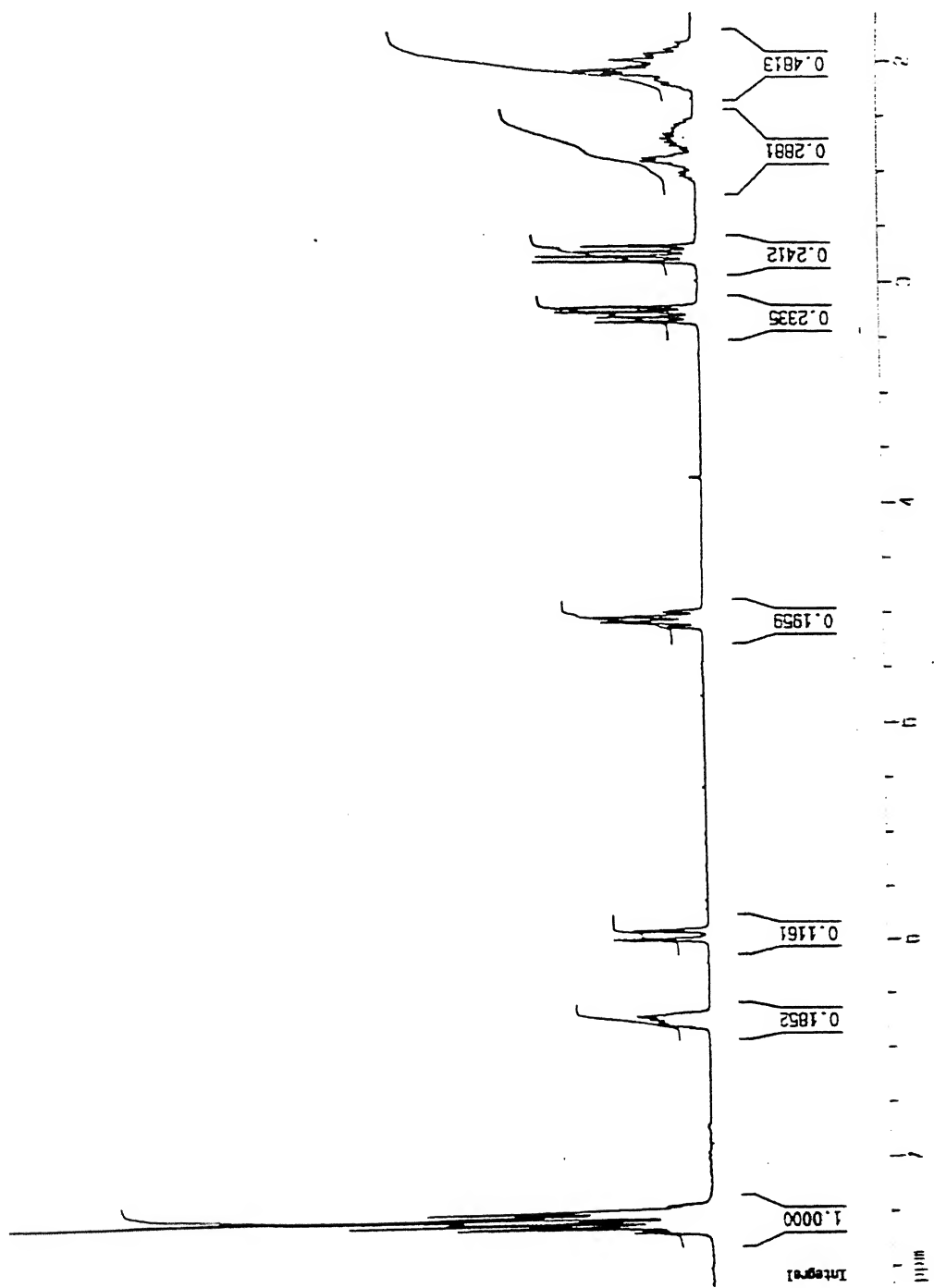


Figure 3.6: 300 MHz  $^1\text{H}$  NMR spectra of 16b (from equilibration experiment)



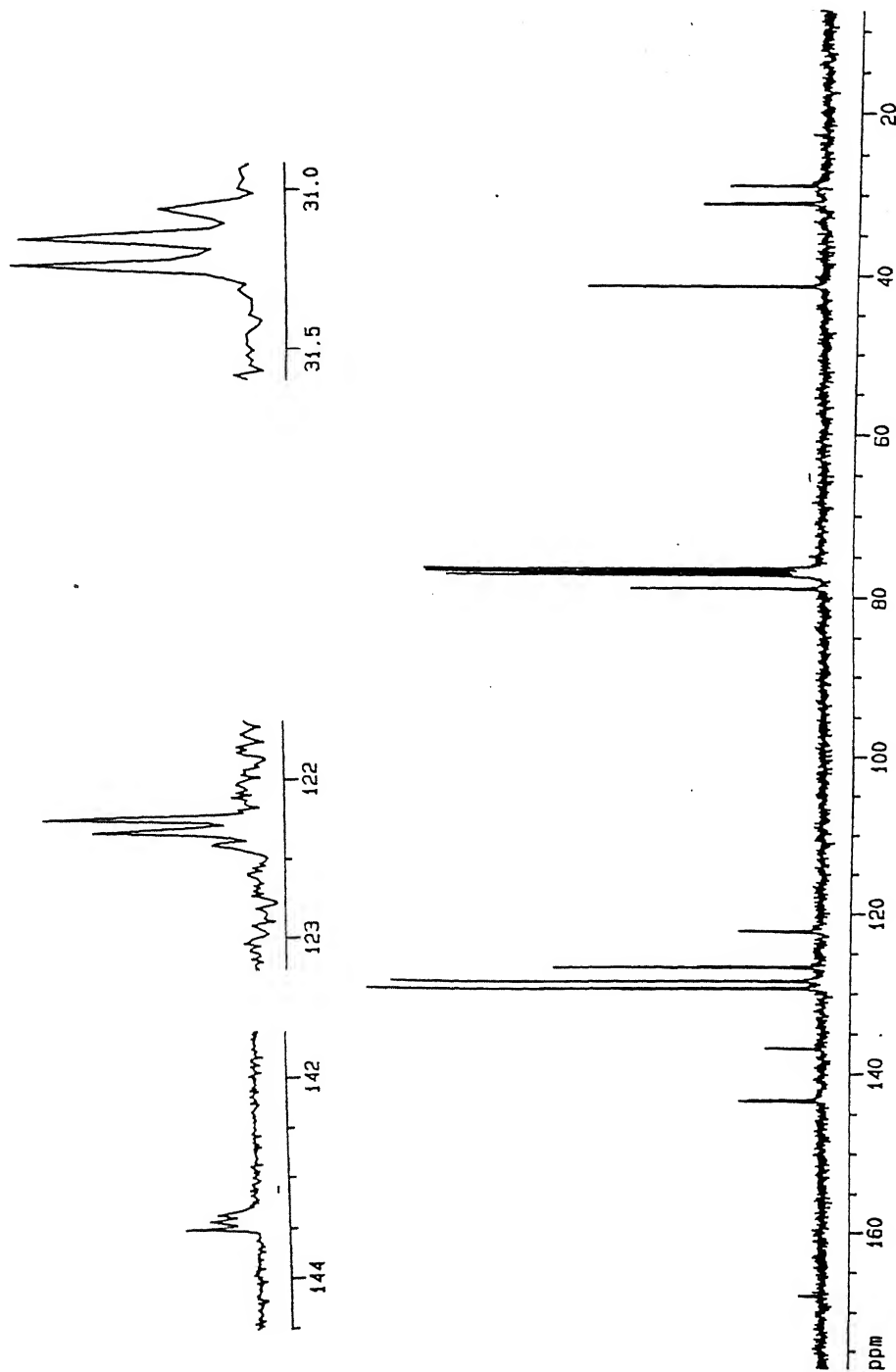


Figure 3.7: 75.5 MHz  $^{13}\text{C}$  NMR spectra of 16b (from equilibration experiment)

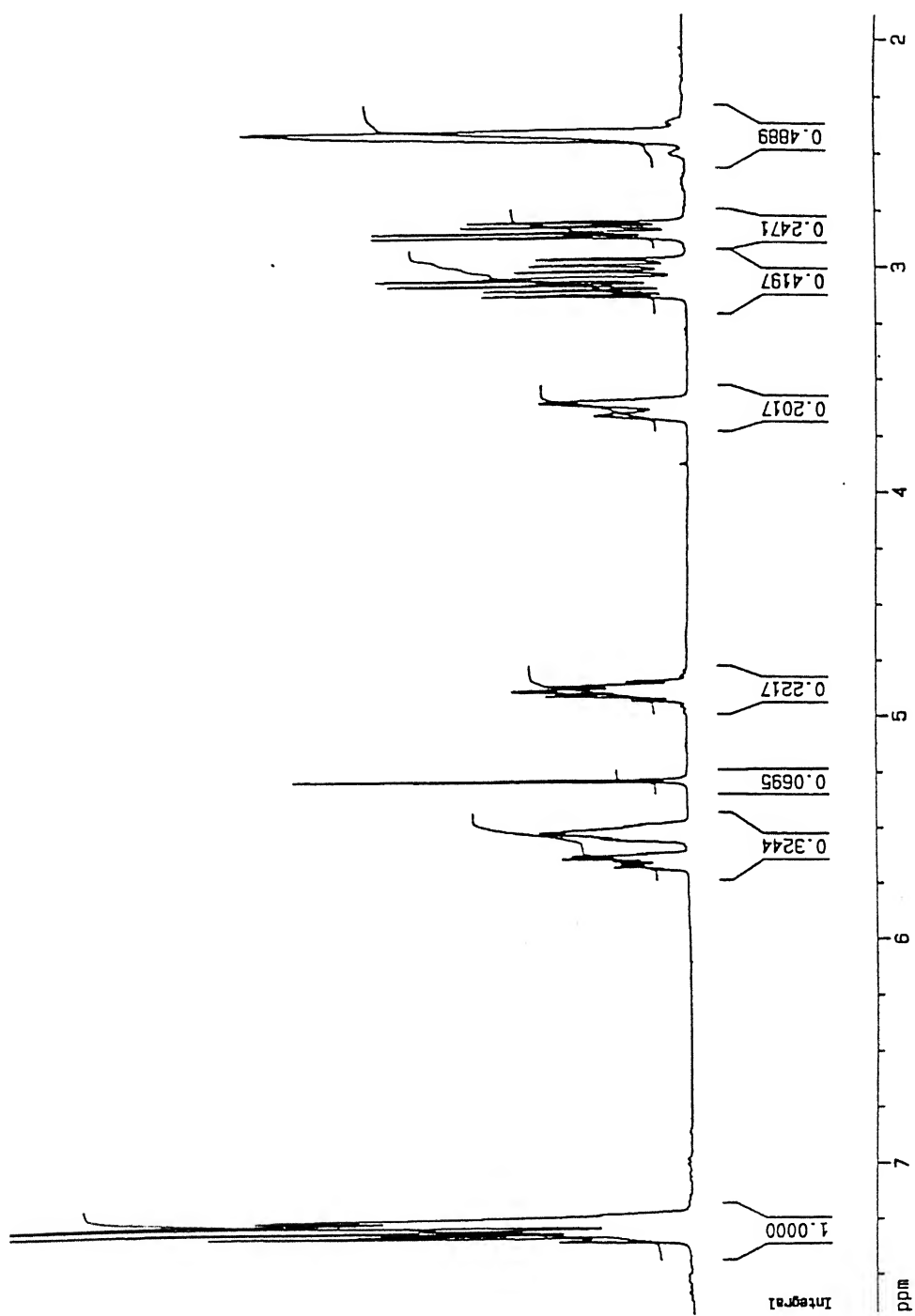


Figure 3.8: 300 MHz  $^1\text{H}$  NMR spectra of 15b (from equilibration experiment)

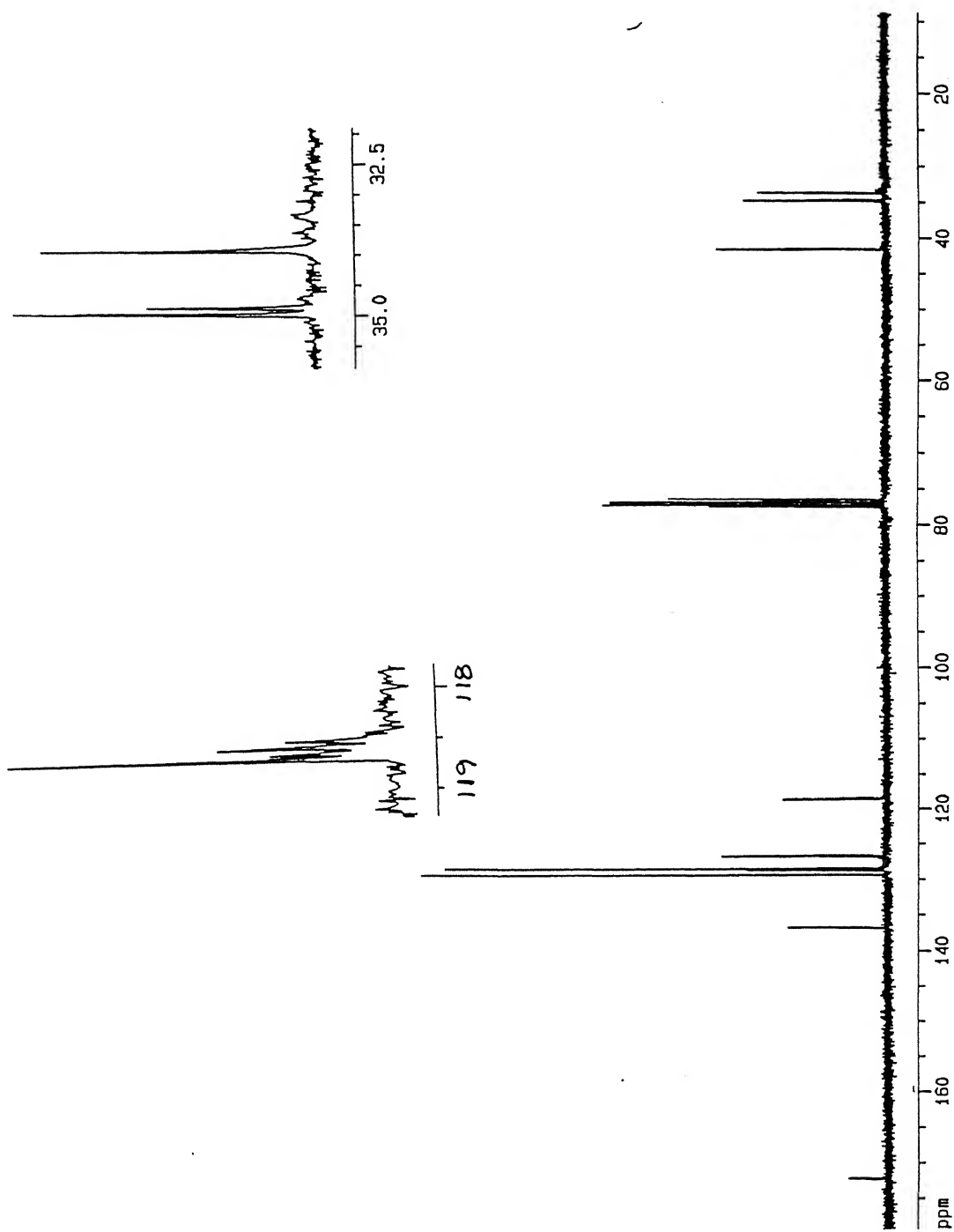


Figure 3.9: 75.5 MHz  $^{13}\text{C}$  NMR spectra of 15b (from equilibration experiment)

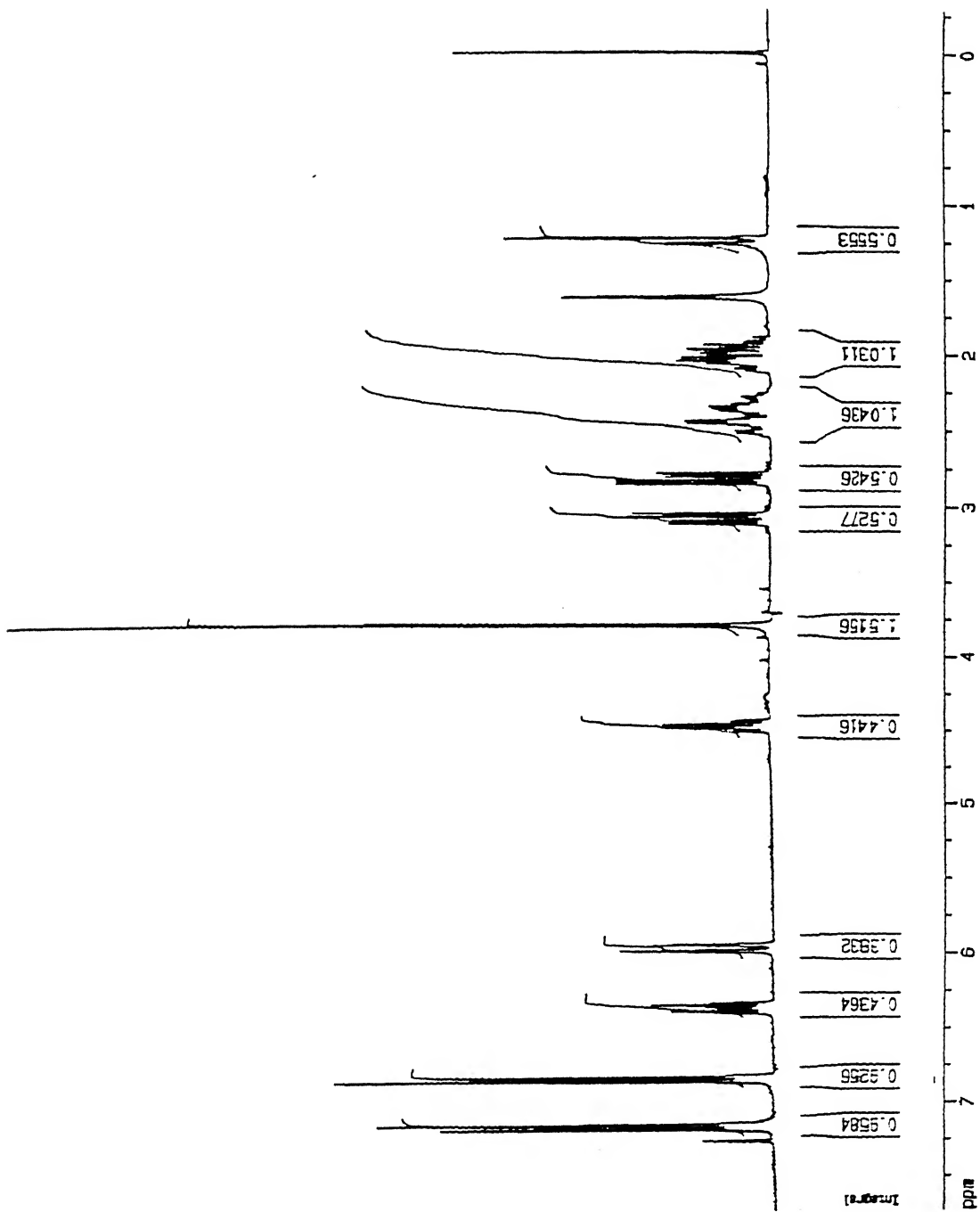
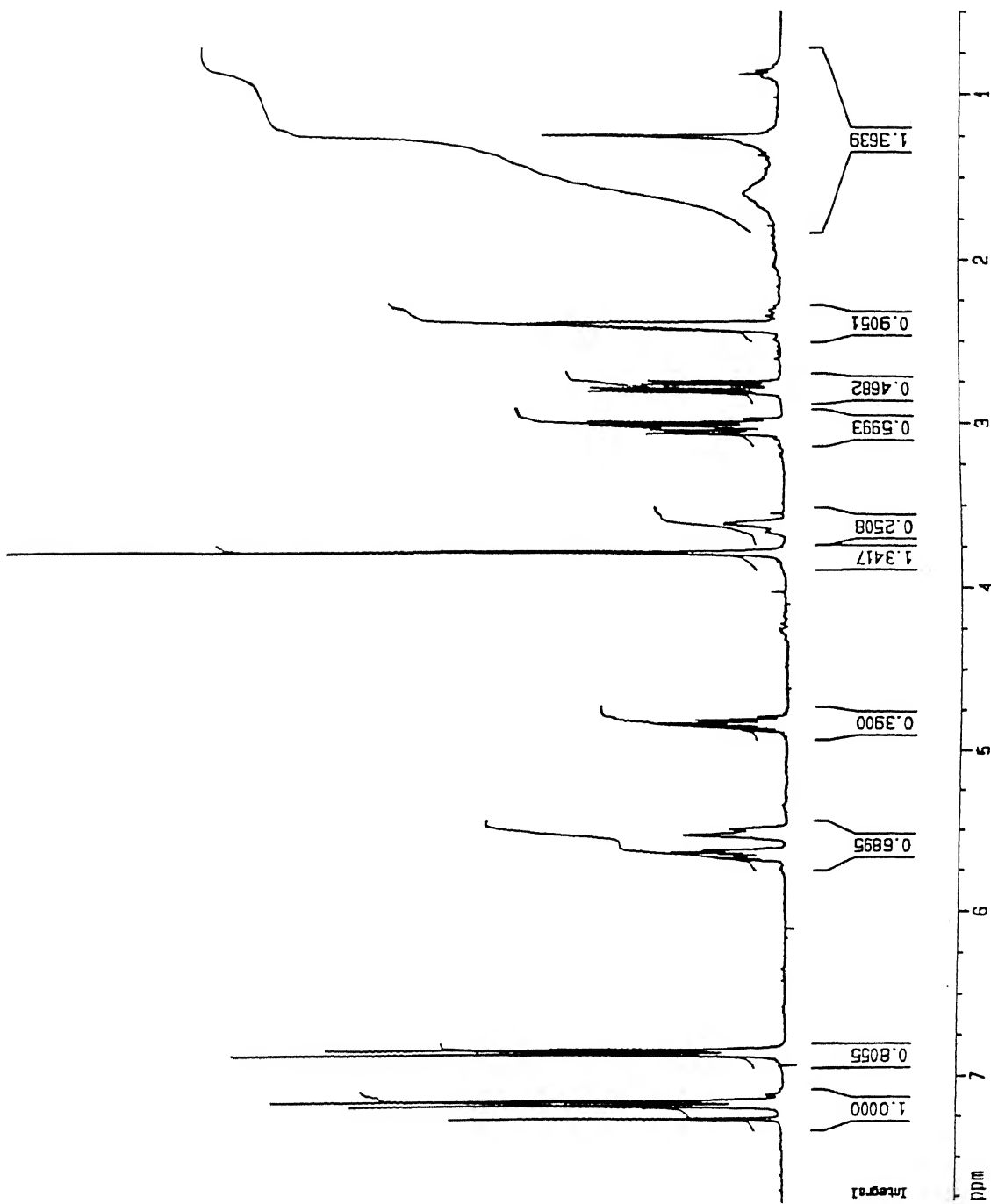
Figure 3.10: 300 MHz  $^1\text{H}$  NMR spectra of 16c

Figure 3.11: 300 MHz  $^1\text{H}$  NMR spectra of **15c**

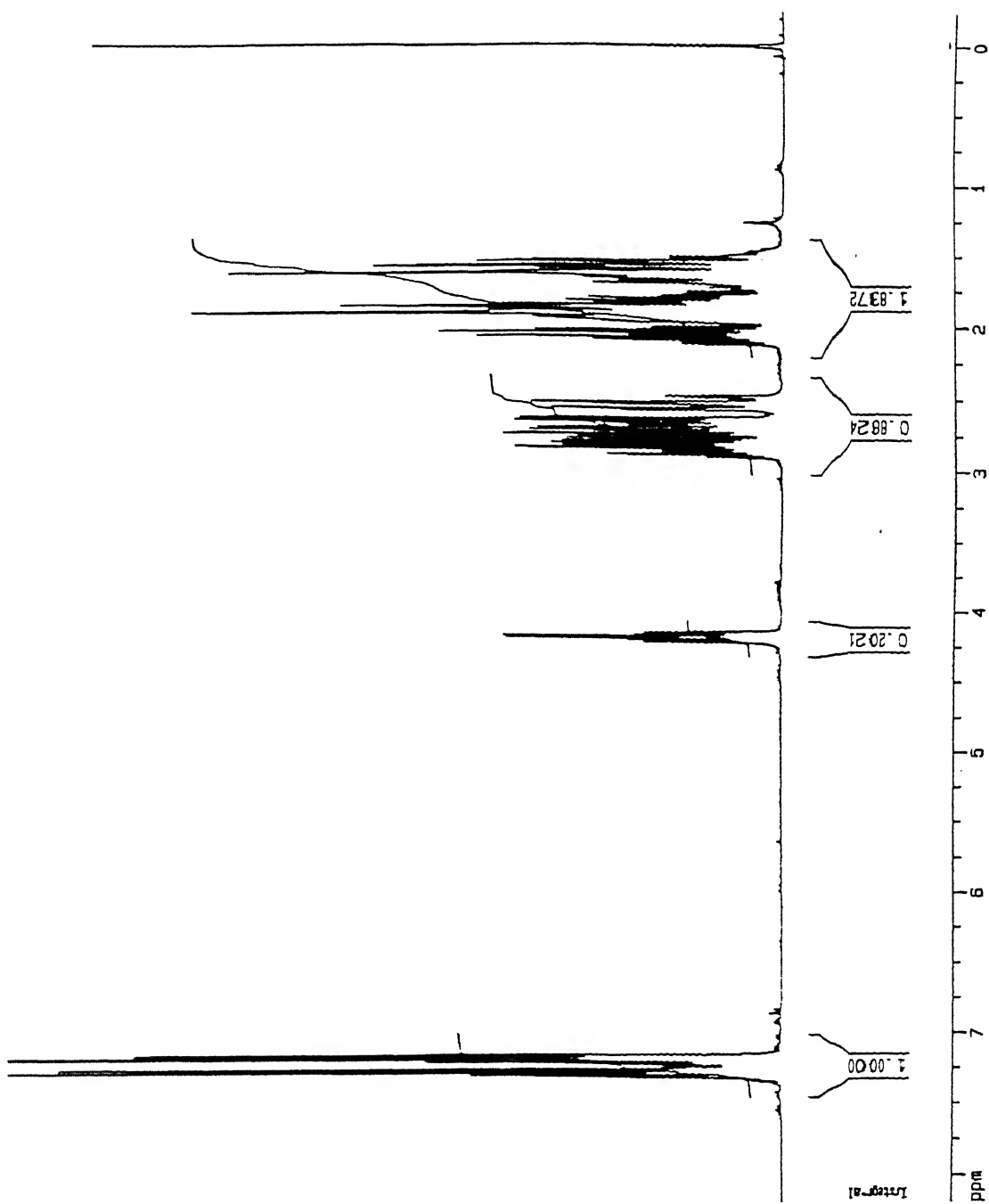
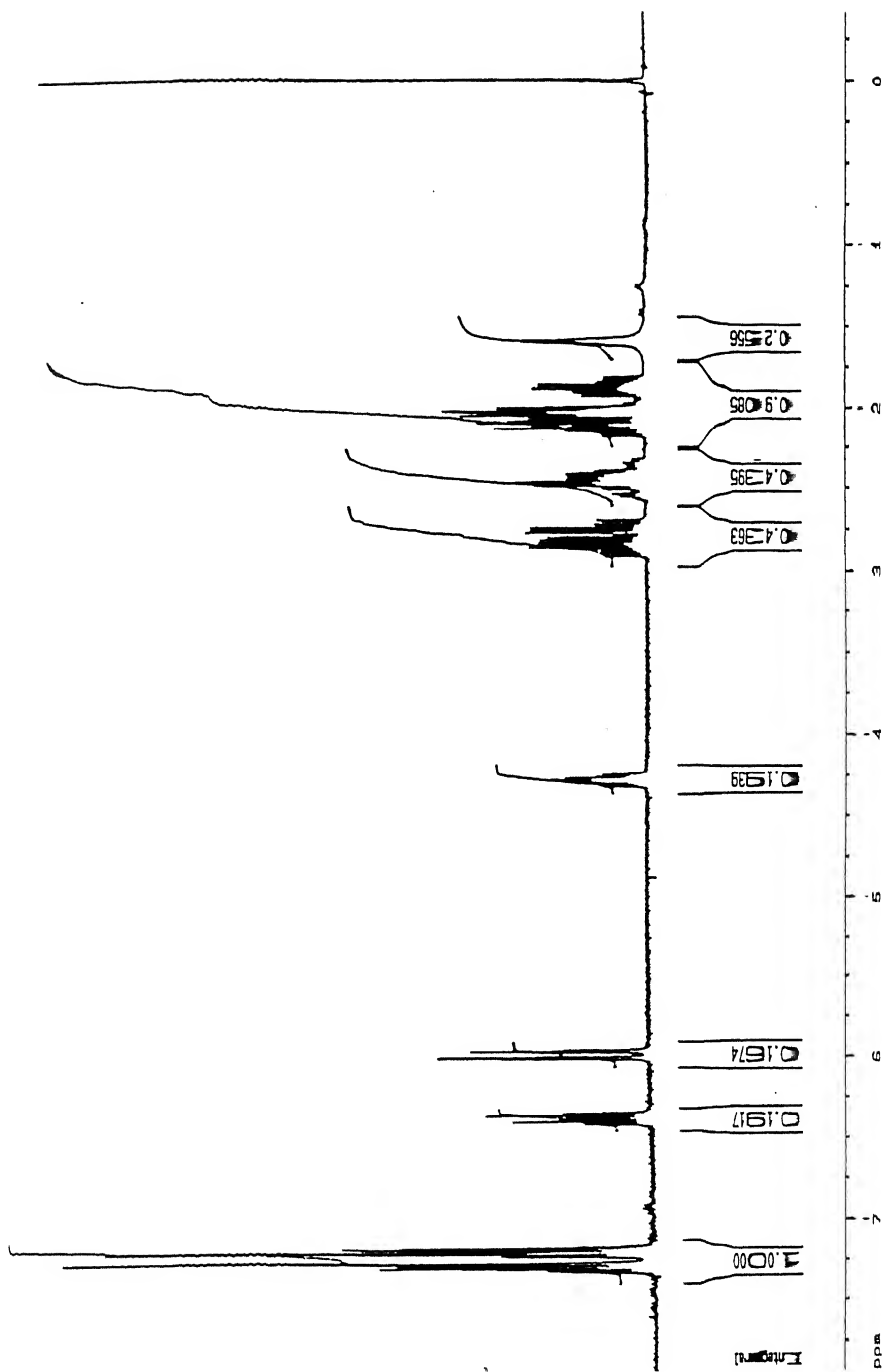
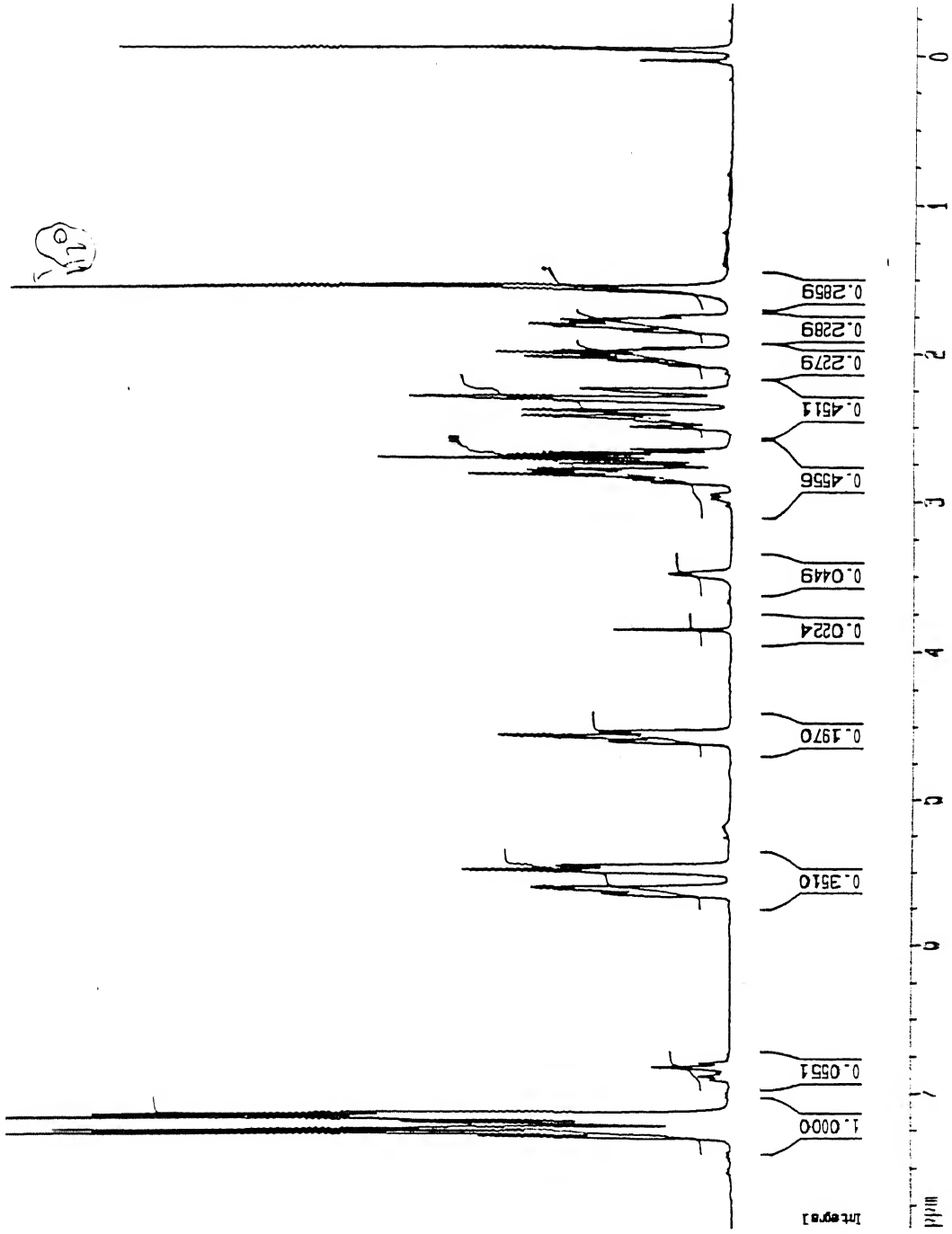
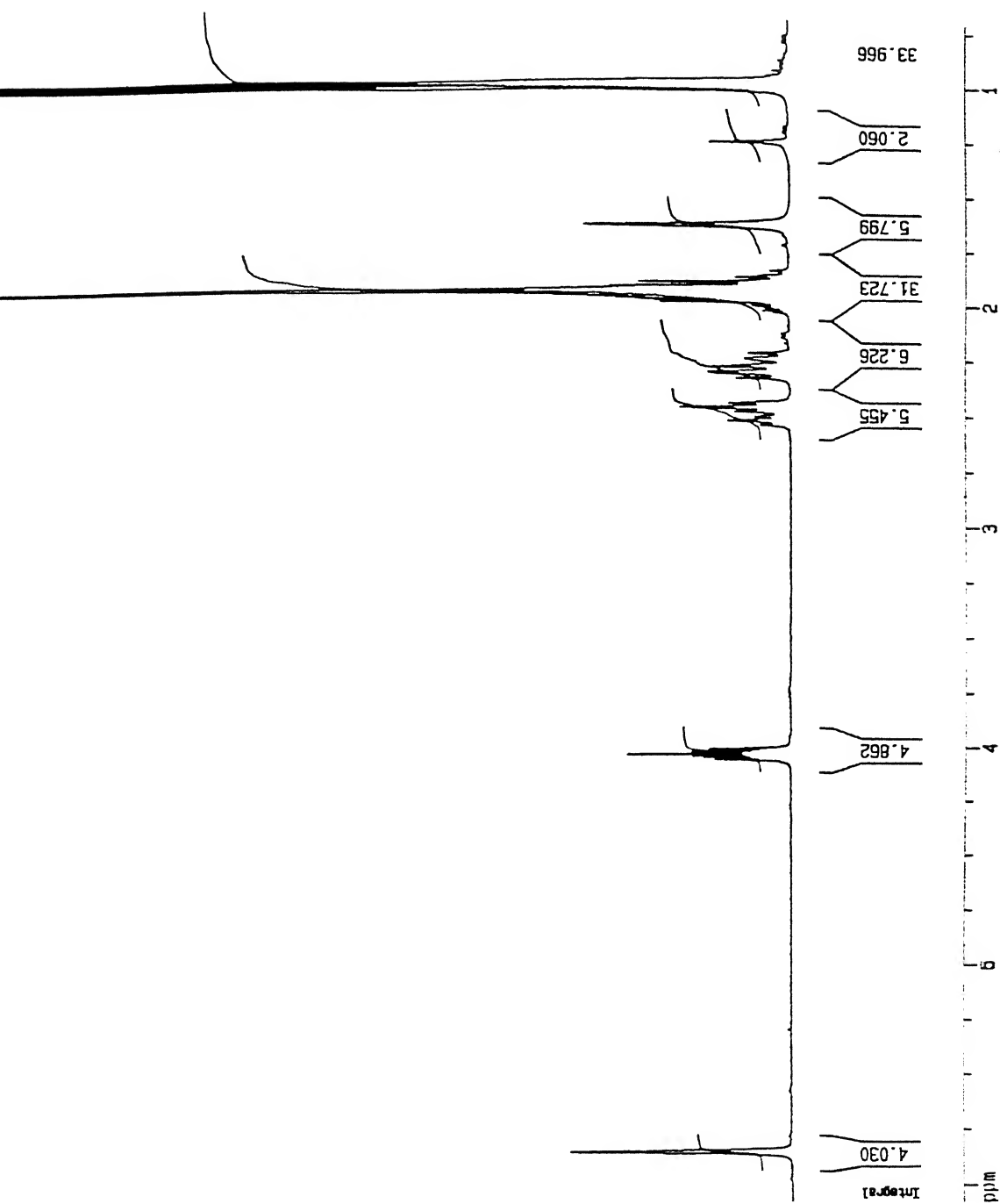
Figure 3.12: 300 MHz  $^1\text{H}$  NMR spectra of 17d

Figure 3.13: 300 MHz  $^1\text{H}$  NMR spectra of 16a



Figure 3.14: 300 MHz <sup>1</sup>H NMR spectra of 15d



Figure 3.15: 300 MHz <sup>1</sup>H NMR spectra of 44

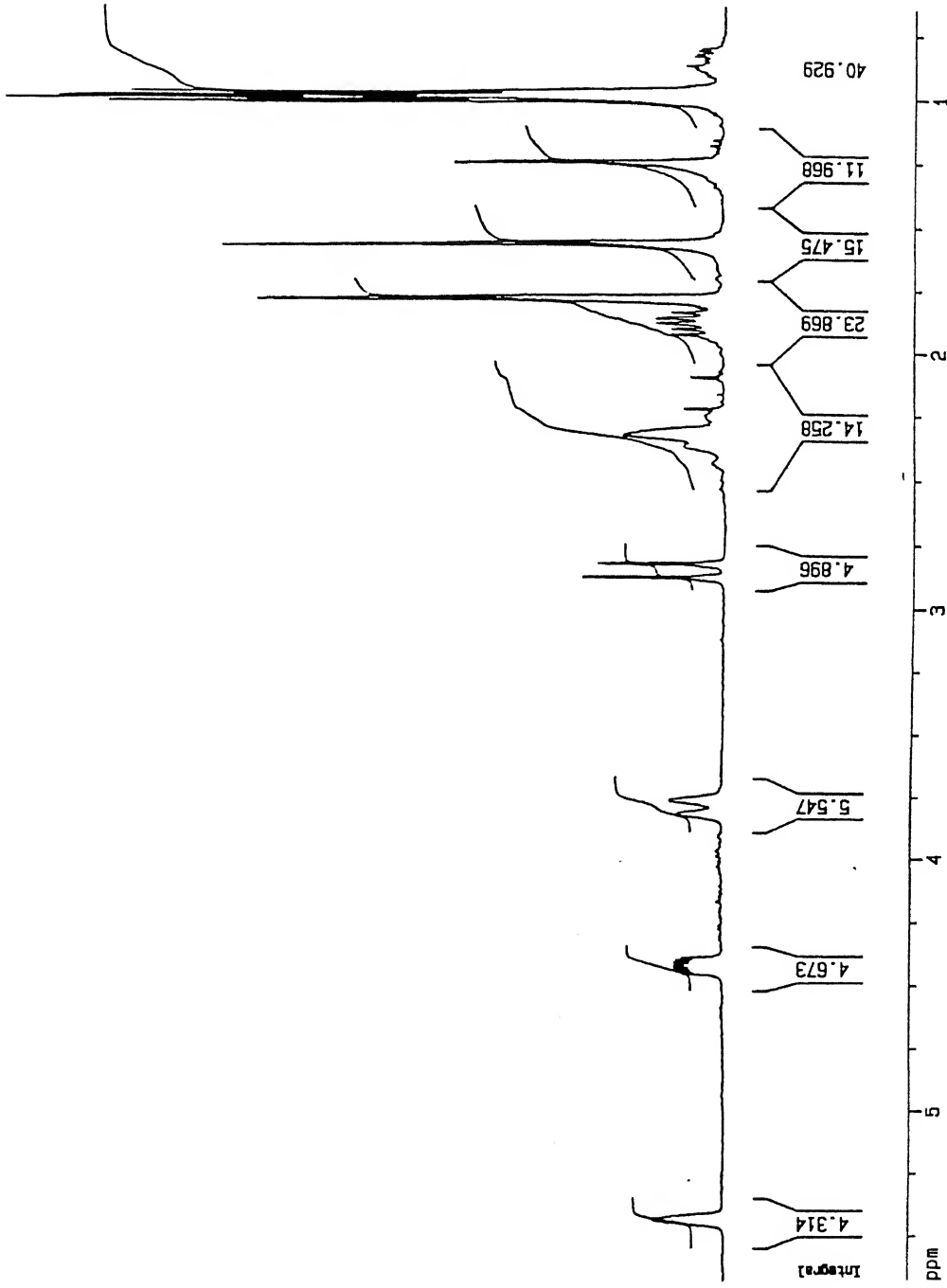
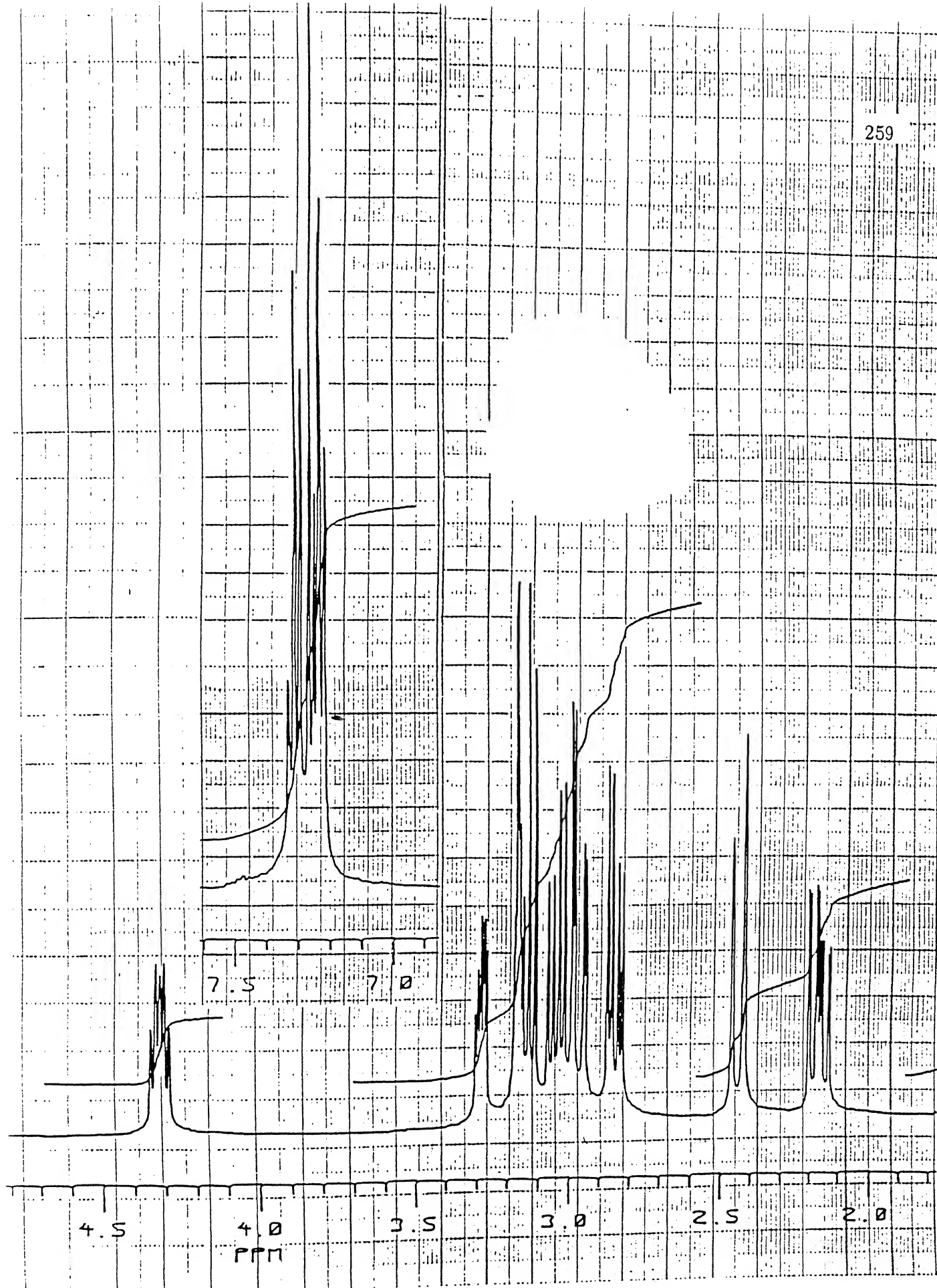
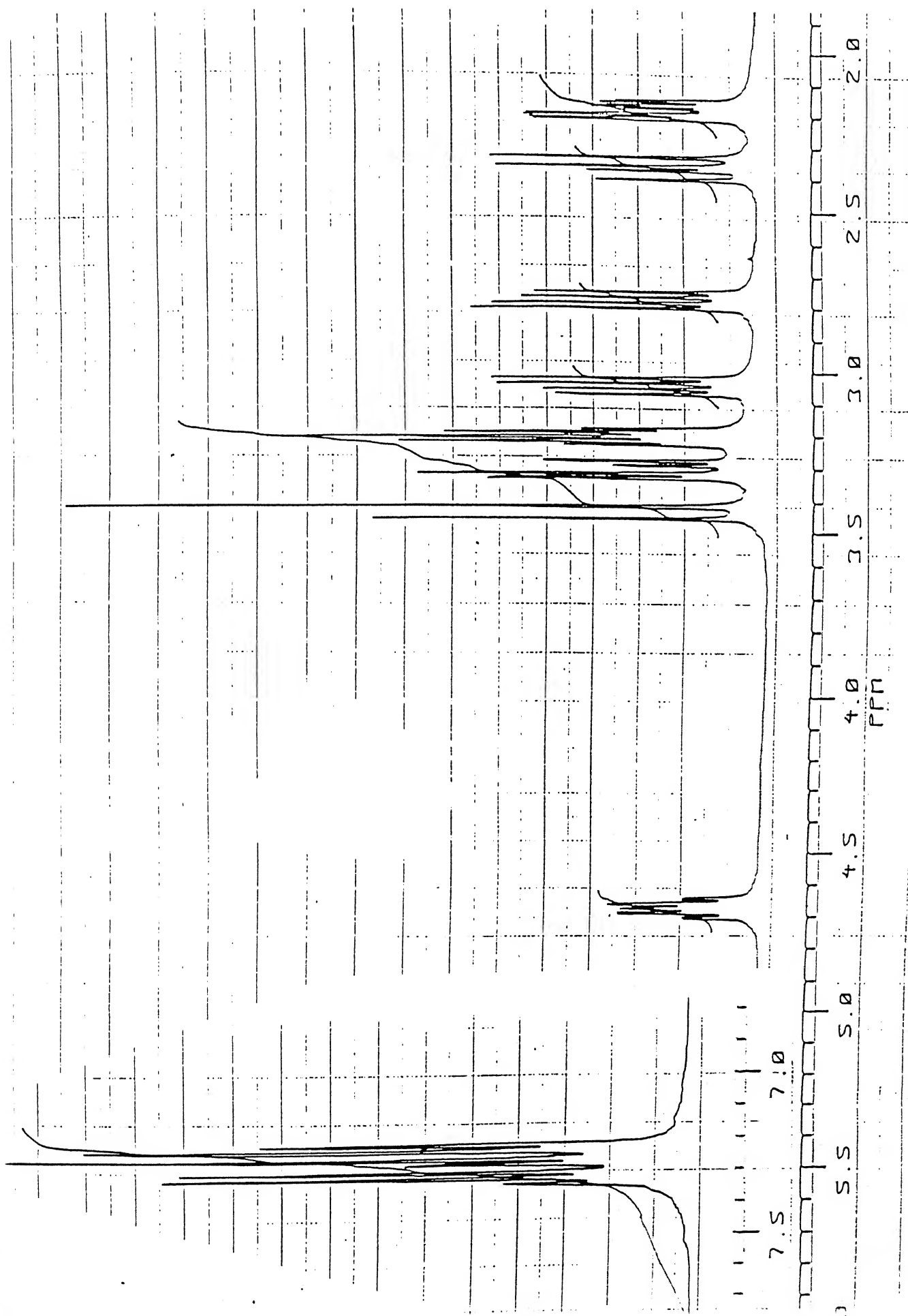


Figure 3.16: 300 MHz  $^1\text{H}$  NMR spectra of 45



Figure 3.18: 400 MHz  $^1\text{H}$  NMR spectra of *cis*-14b

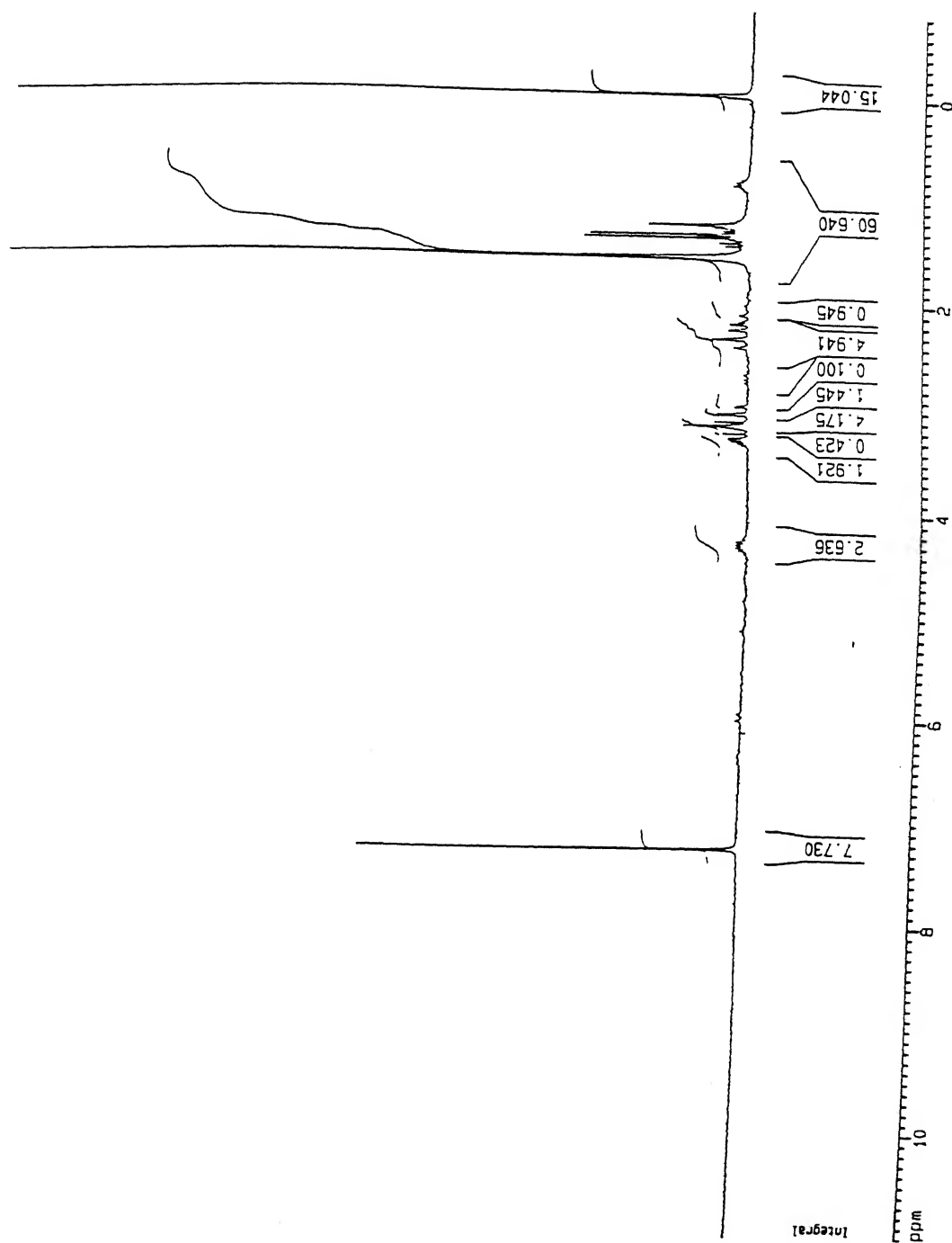


Figure 3.19: 200 MHz  ${}^1\text{H}$  NMR spectra of *trans*-14a

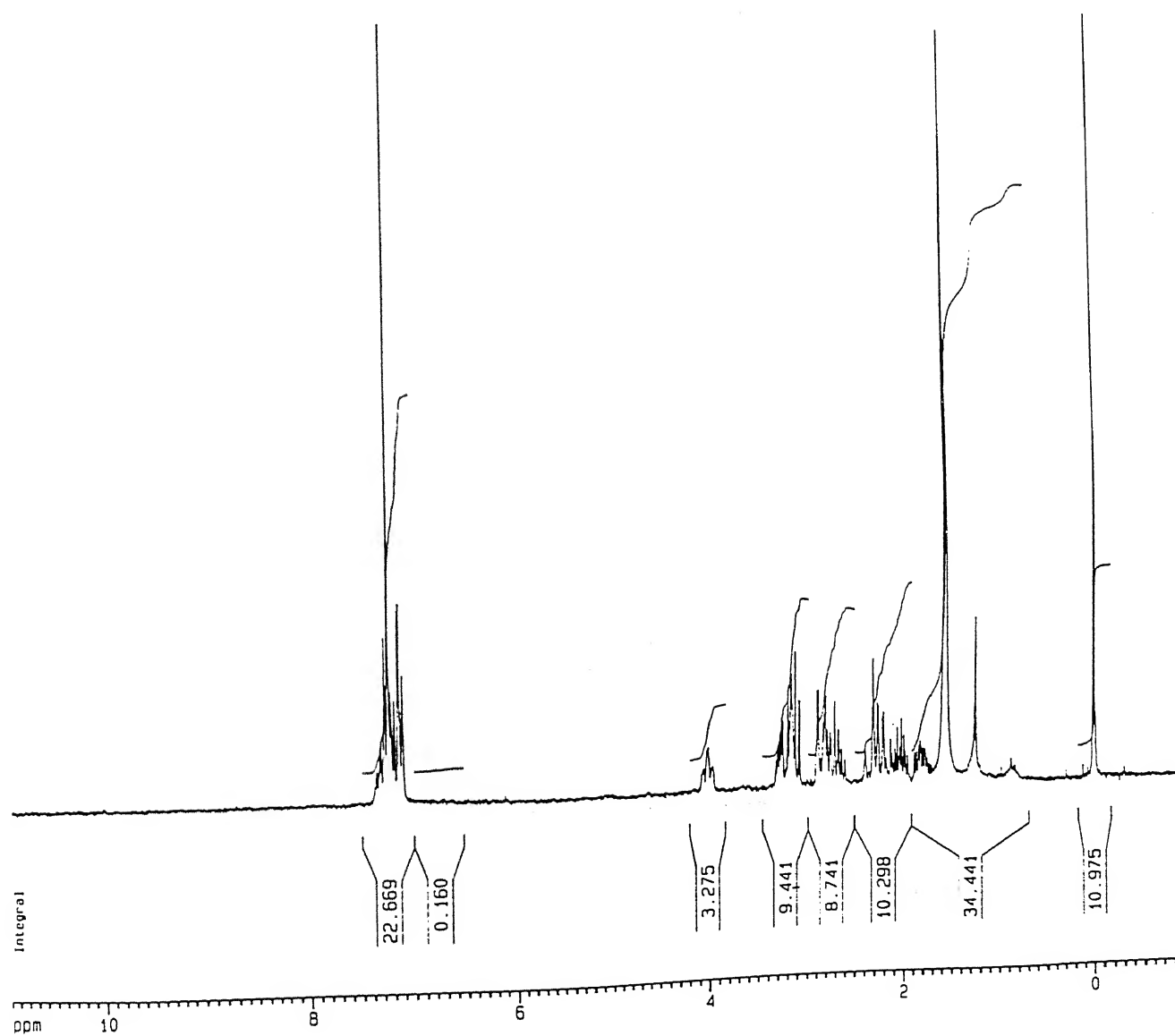


Figure 3.20: 200 MHz  $^1\text{H}$  NMR spectra of *trans*-14d

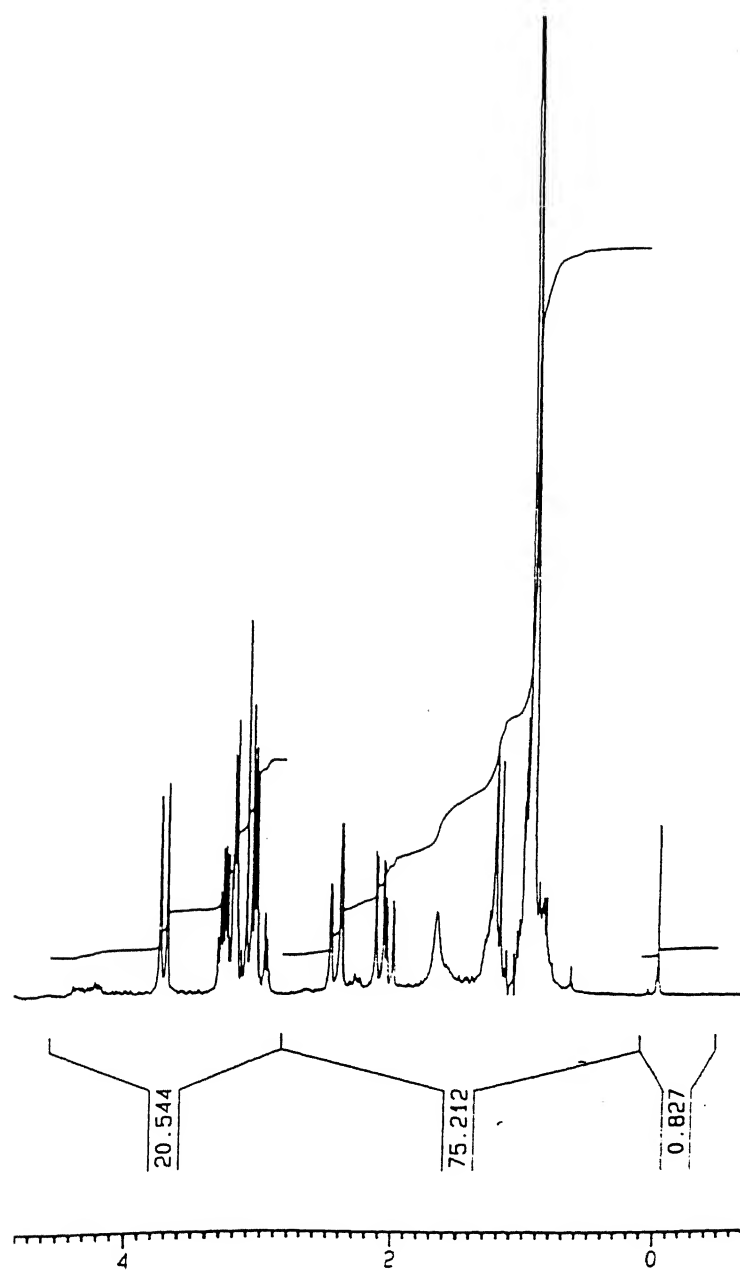


Figure 3.21: 200 MHz  $^1\text{H}$  NMR spectra of *trans*-14e

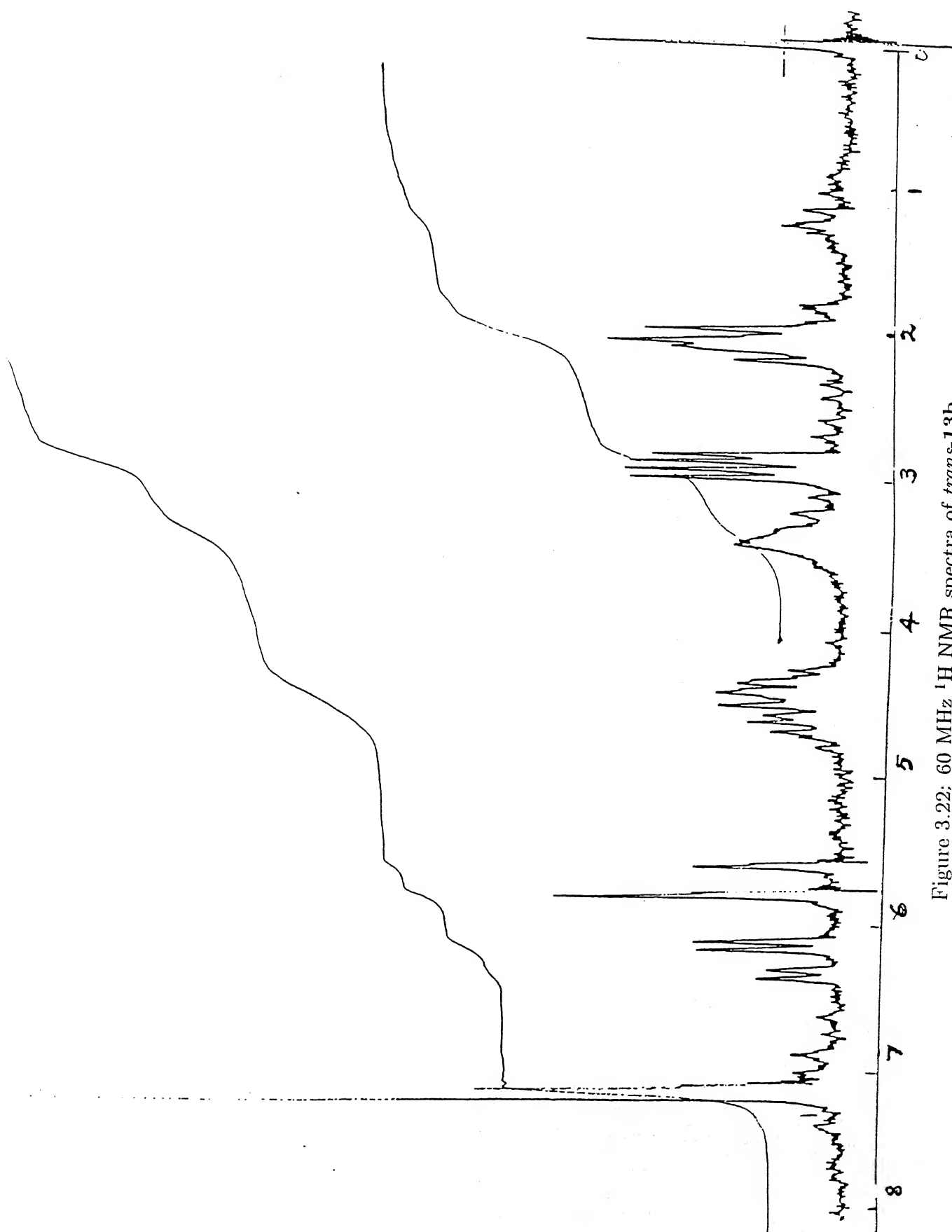


Figure 3.22: 60 MHz  $^1\text{H}$  NMR spectra of *trans*-13b



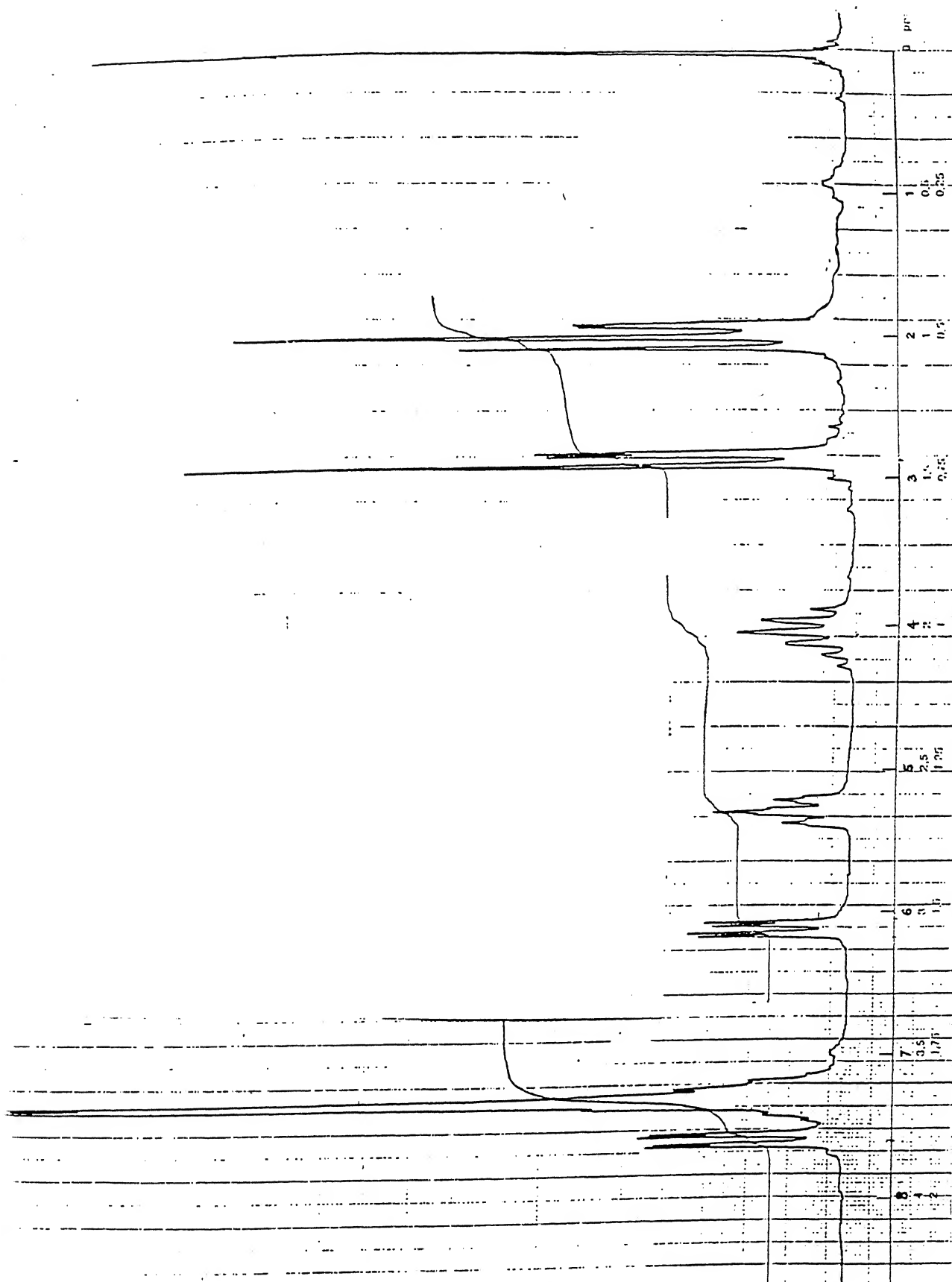


Figure 3.23: 80 MHz  $^1\text{H}$  NMR spectra of *trans*-12b

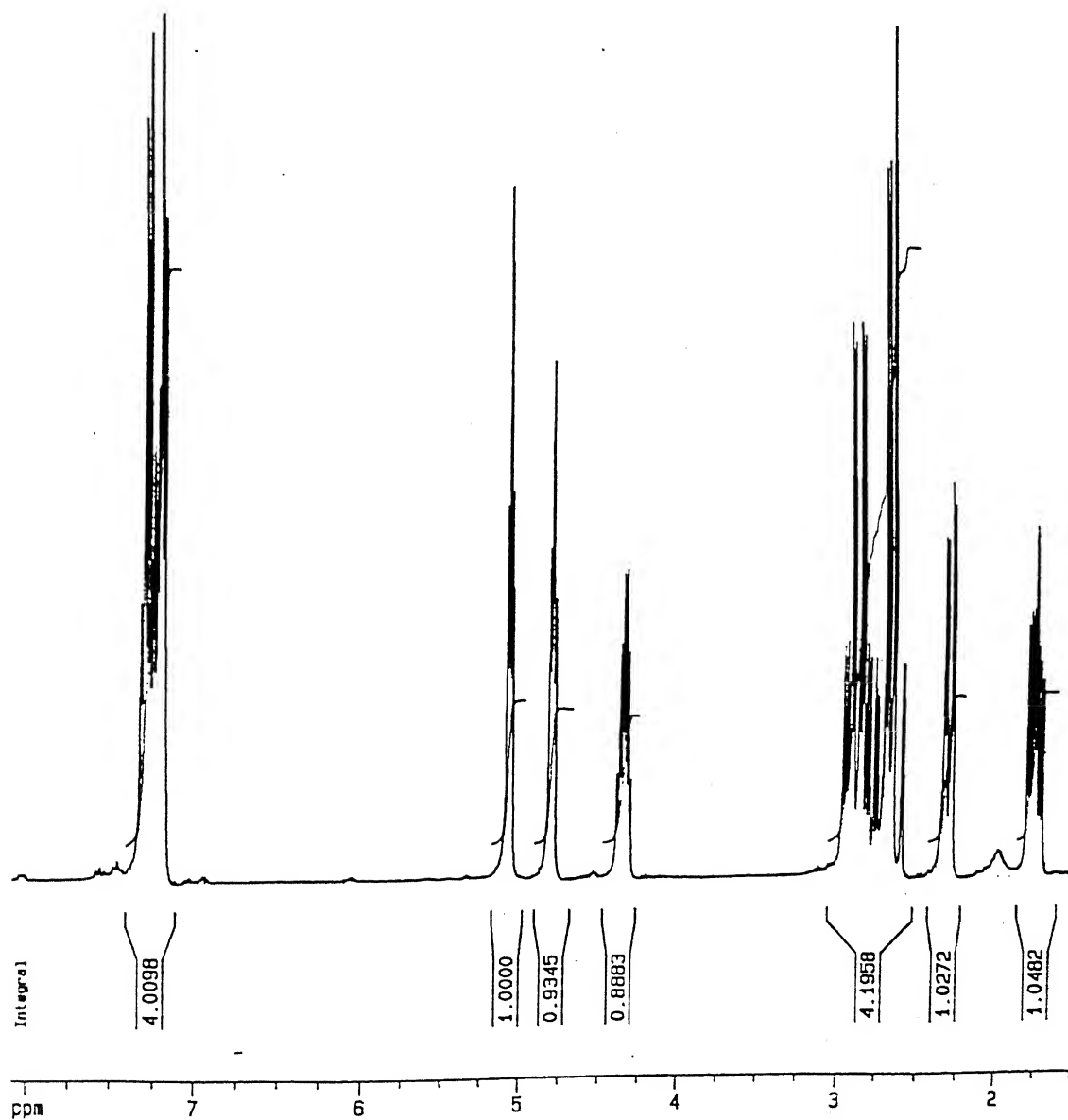


Figure 3.24: 300 MHz  $^1\text{H}$  NMR spectra of 11A

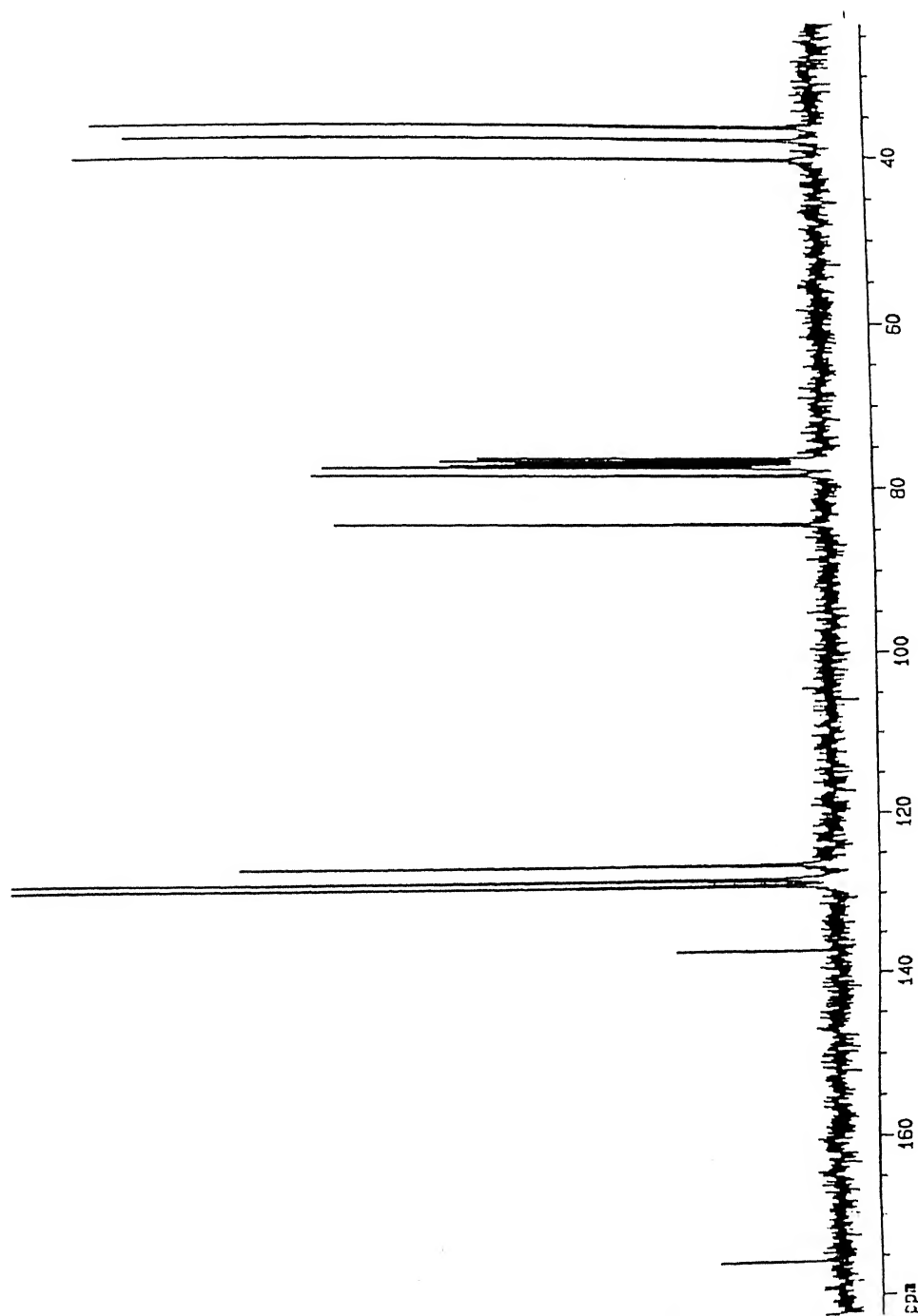


Figure 3.25: 75.5 MHz  $^{13}\text{C}$  NMR spectra of 11A



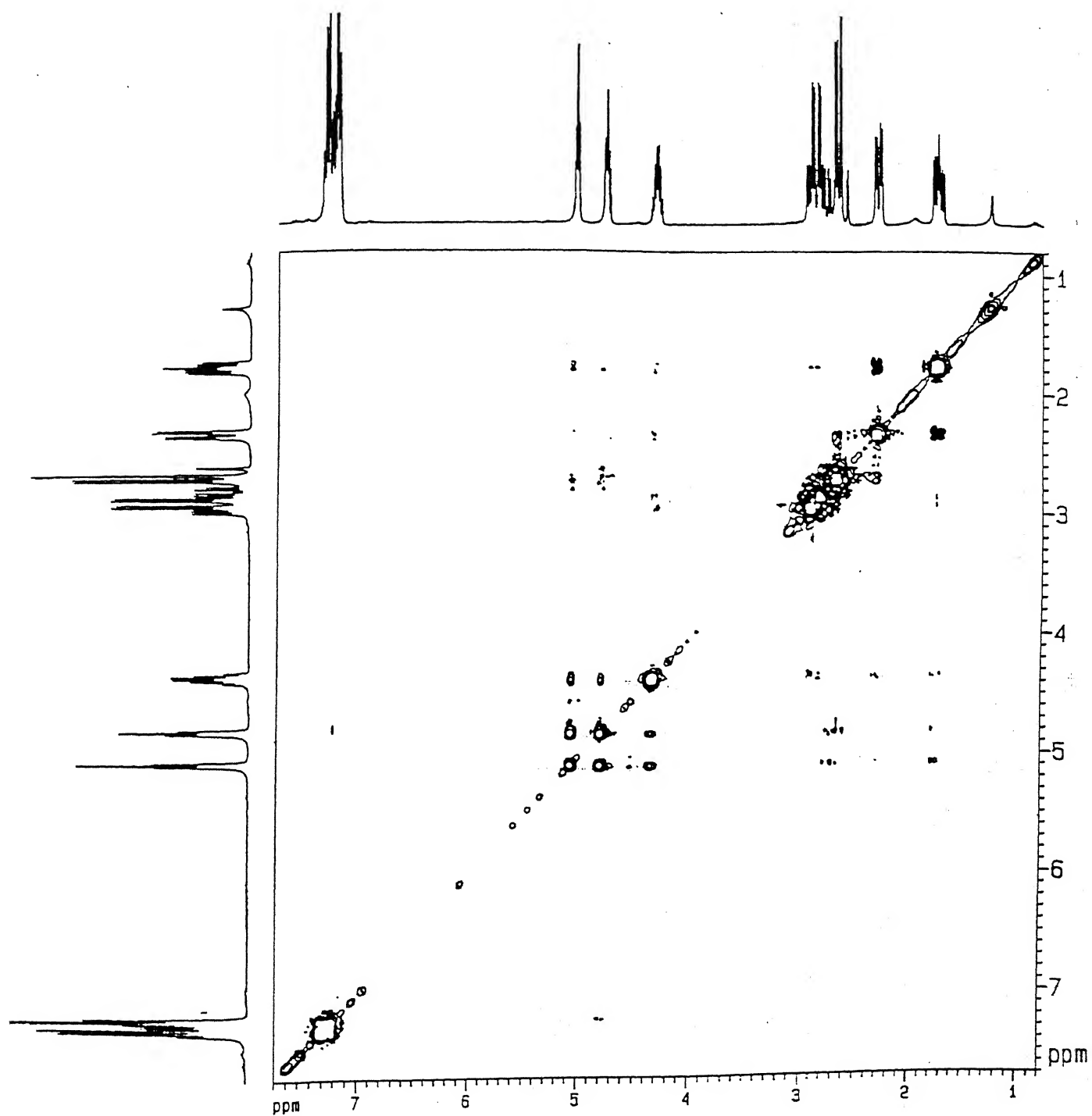
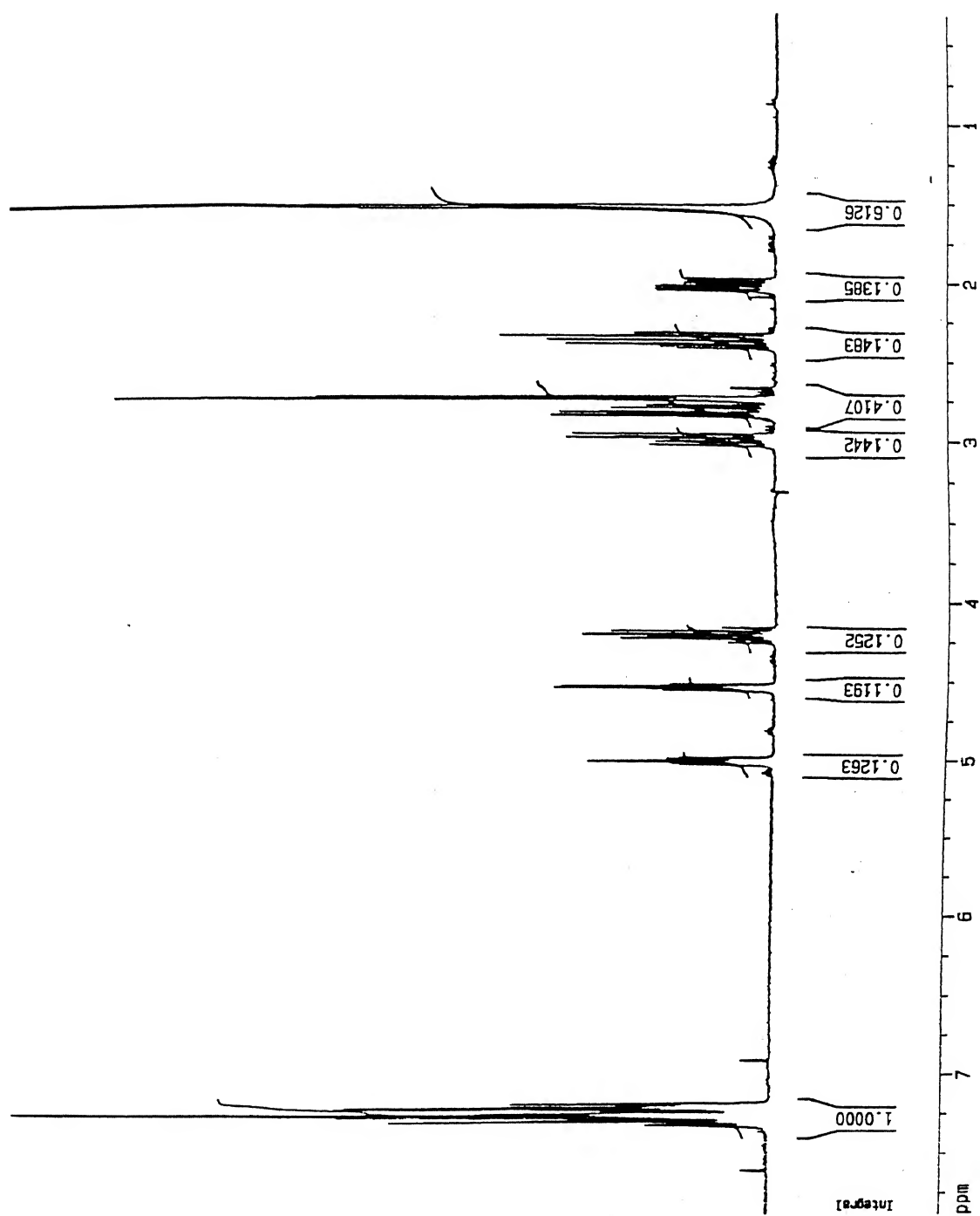


Figure 3.27: 300 MHz ROESY spectra of 11A

Figure 3.28: 300 MHz  $^1\text{H}$  NMR spectra of 11B

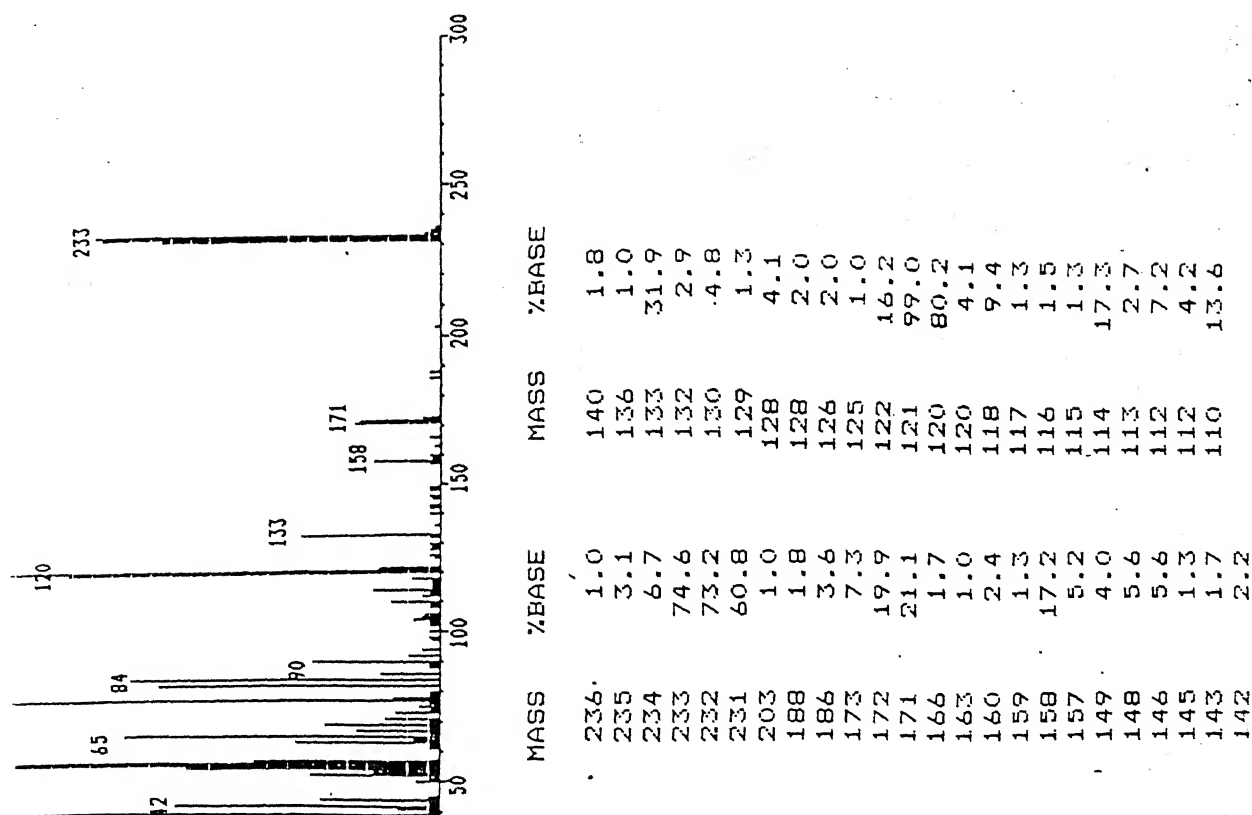


Figure 3.30: EIMS of 15c with deuterium (from equilibration experiment)

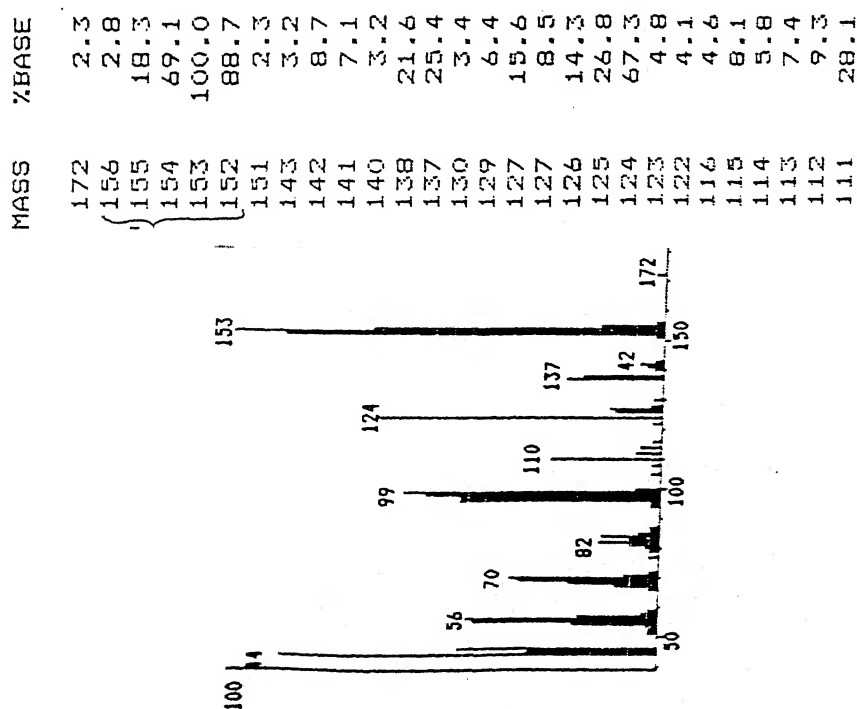


Figure 3.29: EIMS of Deuterated DBU